Role of MYB Transcription Factors During Phellem Differentiation

Dissertation

der Mathematisch-Naturwissenschaftlichen Fakultät

der Eberhard Karls Universität Tübingen

zur Erlangung des Grades eines

Doktors der Naturwissenschaften

(Dr. rer. nat.)

vorgelegt von

David Sebastián Molina Garcés

aus Quito - Ecuador

Tübingen

2023

Gedruckt mit Genehmigung der Mathematisch-Naturwissenschaftlichen Fakultät der Eberhard Karls Universität Tübingen.

Tag der mündlichen Qualifikation:	14.12.2023
Dekan:	Prof. Dr. Thilo Stehle
1. Berichterstatter/-in:	Prof. Dr. Laura Ragni
2. Berichterstatter/-in:	Prof. Dr. Marja Timmermans

Contents

1. Summary

The periderm is a crucial protective barrier that plays a vital role in secondary growth. It is a multi-layered tissue composed anatomically of three layers: the phellem or cork, the phellogen or cork cambium, and the phelloderm. The phellogen, a meristematic layer, undergoes bifacial divisions, generating the phellem outward and the phelloderm inward. The phellem comprises specialized cells that accumulate substantial amounts of suberin and lignin, providing it with an exceptional protective capacity. This accumulation holds significant potential for plant breeding and biotechnological applications. However, there is still very little knowledge regarding the regulatory mechanisms governing phellem differentiation and the specific accumulation of apoplastic barriers. Arabidopsis root has emerged as a significant model for studying the periderm, facilitating the understanding of this process. In our research, we explore the role of the MYB68 clade transcription factor in regulating phellem differentiation in the Arabidopsis periderm. Our findings reveal that overexpression of MYB68 in the periderm triggers phellem differentiation. This differentiation process involves an increase in suberin deposition, facilitated by the upregulation of genes related to suberin polymerization and biosynthesis. Additionally, our study demonstrates that aside from regulating apoplastic barriers, MYB68 deactivates the meristematic activity of the phellogen. Notably, in certain loss-of-function mutants of this clade, we observe a delay in phellem differentiation. As a complementary aspect of our research, we seek to gain a better understanding of the significance of apoplastic barrier establishment in the periderm. Firstly, we explore whether the periderm can respond to issues affecting the apoplastic barrier. In our research, we suggest that the Schengen pathway plays two pivotal roles: first, in the specific polymerization of the apoplastic barrier in the phellem, and second, in serving as a part of a surveillance system that monitors barrier integrity. Secondly, we demonstrate the importance of the aromatic monomers produced in the phenylproanoid pathway for the proper establishment of apoplastic barriers in the phellem. This work contributes to our understanding of the molecular mechanisms underlying periderm development, particularly in relation to phellem differentiation and the establishment of apoplastic barriers. We aim to provide useful tools and concepts that will aid in the design of new biotechnological tools to improve agricultural activities and offer sustainable alternatives for production.

2.Zusammenfassung

Die Periderm ist eine entscheidende Schutzbarriere, die eine wesentliche Rolle im sekundären Wachstum spielt. Es handelt sich dabei anatomisch um ein mehrschichtiges Gewebe, bestehend aus drei Schichten: dem Phellem oder Kork, dem Phellogen oder Korkkambium und dem Phelloderm. Das Phellogen, eine meristematische Schicht, durchläuft bifaziale Teilungen, wobei er das Phellem nach außen und das Phelloderm nach innen erzeugt. Das Phellem besteht aus spezialisierten Zellen, die erhebliche Mengen an Suberin und Lignin ansammeln und ihm außergewöhnliche Schutzeigenschaften verleihen. Diese Anreicherung birgt erhebliches Potenzial für Pflanzenzüchtung und biotechnologische Anwendungen. Es gibt jedoch noch sehr wenig Wissen über die regulatorischen Mechanismen, die die Differenzierung des Phellems und die spezifische Anhäufung apoplastischer Barrieren steuern. Die Arabidopsis-Wurzel hat sich als ein bedeutendes Modell für die Erforschung der Periderm herausgestellt, was das Verständnis dieses Prozesses erleichtert. In unserer Forschung untersuchen wir die Rolle des MYB68-clade-Transkriptionsfaktors bei der Regulation der Phellem-Differenzierung in der Arabidopsis-Periderm. Unsere Ergebnisse zeigen, dass die Überexpression von MYB68 in der Periderm die Phellem-Differenzierung auslöst. Dieser Differenzierungsprozess umfasst eine Zunahme der Suberin-Ablagerung, erleichtert durch die Hochregulation von Genen, die mit der Suberin-Polymerisation und -Biosynthese zusammenhängen. Darüber hinaus zeigt unsere Studie, dass MYB68 neben der Regulation apoplastischer Barrieren auch die meristematische Aktivität des Phellogen deaktiviert. Bemerkenswert ist, dass in bestimmten loss-of-function-Mutanten dieser Klade eine Verzögerung der Phellem-Differenzierung beobachtet wird. Als ergänzenden Aspekt unserer Forschung streben wir ein besseres Verständnis der Bedeutung der apoplastischen Barrieren im Periderm an. Zunächst untersuchen wir, ob das Periderm auf Probleme mit der apoplastischen Barriere reagieren kann. In unserer Forschung schlagen wir vor, dass der Schengen-Weg zwei entscheidende Rollen spielt: erstens bei der spezifischen Polymerisation der apoplastischen Barriere im Phellem und zweitens als Teil eines Überwachungssystems, das die Integrität der Barriere überwacht. Zweitens zeigen wir die Bedeutung der im Phenylproanoid-Weg produzierten aromatischen Monomere für die ordnungsgemäße Bildung apoplastischer Barrieren im Phellem ist es notwending. Diese Arbeit trägt zu unserem Verständnis der molekularen Mechanismen der Periderm-Entwicklung bei, insbesondere in Bezug auf die Phellem-Differenzierung und die Bildung apoplastischer Barrieren. Wir streben danach, nützliche Werkzeuge und Konzepte bereitzustellen, die die Gestaltung neuer

biotechnologischer Instrumente zur Verbesserung landwirtschaftlicher Aktivitäten ermöglichen und nachhaltige Alternativen für die Produktion bieten sollen.

3. Introduction

3.1 Apoplastic barriers in plants

Apoplastic barriers are identified as evolutionary adaptations which help plants in surviving and thriving in demanding environments. These are located within the apoplast, which is defined as the intercellular spaces between cell membranes, separating plant tissues and shield them from the external environment. (Nawrath et al., 2013; Farvardin et al., 2020). In this context, apoplastic barriers could also be identified as diffusion barriers because they reinforce the polysaccharide-based cell wall with hydrophobic materials such as suberin and lignin blocking the movement of hydrophilic substances (Franke & Schreiber, 2007). Apoplastic barriers could be found in many plant organs and at different developmental stages. For instance, during primary growth stage, the surface of epidermal cells is protected by the cuticle. In the root's primary tissues, the most well-known examples include Casparian strips and suberin lamellae in the endodermis and exodermis. These are recognized as dynamic hydrophobic modifications of the cell wall during plant development capable of responding to specific environmental cues (Nawrath et al., 2013; Barberon & Geldner, 2014). In secondary growth, apoplastic barriers reinforce the phellem of the periderm in both root and shoots. In contrast to the endodermis, there is little information available on how these diffusion barriers are specifically produced and accumulated in the periderm. Recent studies have contributed to a better understanding of the significant importance of these barriers within the periderm. For instance, in Arabidopsis, the specific repression of the phenylpropanoid pathway, responsible for producing lignin monomers and the aromatic fraction of suberin, leads to the collapse of the phellem and results in a dramatic reduction in salt stress tolerance (Andersen et al., 2021; Franke & Schreiber, 2007). Moreover, apoplastic barriers can seal tissues and create structures that aid in the effective separation of organs, like the abscission zone of siliques, as well as after wounding. Furthermore, specialized diffusion barriers, such as cutin or suberin, have been reported to play a role in the protection of pollen and seeds. (Coen et al., 2019; Lee et al., 2018a).

3.1.1 Suberin and lignin

Suberin and lignin are biopolymers present in nearly all plants and they have a significant impact on the planet. In fact, after cellulose, lignin is the second-largest carbon sink in plants, representing 30% of the total biomass produced on Earth (Boerjan et al., 2003; Weng & Chapple, 2010). From a chemical perspective, lignin and suberin share both similarities and

differences. Both contain aromatic compounds in their structures, produced by the phenylpropanoid pathway, but they require different monomers. (Graça, 2015; Serra & Geldner, 2022). One crucial distinction is that suberin has an aliphatic polyester portion, whereas lignin is primarily composed of monolignols. Although the structure of suberin is not entirely clear, some research utilizing several approaches and technologies has provided valuable insights that help us speculate on its structure (Serra & Geldner, 2022). Briefly, suberin is believed to consist of two domains: aromatic and aliphatic domains. The aliphatic domain contains oxygenated long chain fatty acid (C16-C24) derivatives such as fatty acids, ω-hydroxyacids and α,ω -diacids and fatty alcohols, and glycerol, which is the main component of suberin polyester. The final large macromolecule is formed by the creation of ester linkages among them (Franke & Schreiber, 2007; Graça, 2015; Serra & Geldner, 2022). On the other hand, the aromatic portion suberin is mostly composed of ferulic acid as the primary aromatic monomer in suberin, along with hydroxycinnamic acids. The organization of these monomers is still a mystery, and further exploration in this aspect is needed (Bernards, 2002; Kolattukudy, 1980; Pollard et al., 2008; Serra & Geldner, 2022). While the debate about the structure remains ongoing, several molecular suberin genes have been identified in recent years. For instance, GPAT5 was the first suberin biosynthetic gene to be discovered. This enzyme transfers a very long-chain aliphatics (C20–C24) to a glycerol based receptor during suberin biosynthesis (Belsson et al., 2007; Vishwanath et al., 2015). The *gpat5* mutants show a significant decrease of very long fatty acids (C20-C24) in roots and seed coats (Belsson et al., 2007; Yonghua Li et al., 2007). Following the discovery of GPAT5, a significant number of enzymes and transcriptional regulators have been identified as suberin-related genes. Recent research has highlighted the essential role of GDSL-motif esterase/acyltransferase/lipase (GDSLs/GELPs) alongside biosynthetic enzymes, transporters, and transcriptional regulators in suberin polymerization within cell walls. These GDSLs/GELPs are active in the process and play a pivotal role. For instance, in the *gelp22 gelp38 gelp51 gelp49 gelp9* quintuple mutant, it has been observed that the suberin lamella cannot be established in the endodermis. (Ursache et al., 2021). All this has provided us with a robust genetic framework, enhancing our understanding of how suberin aliphatic monomers are produced and transported to the apoplast (Figure X) (Serra & Geldner, 2022).

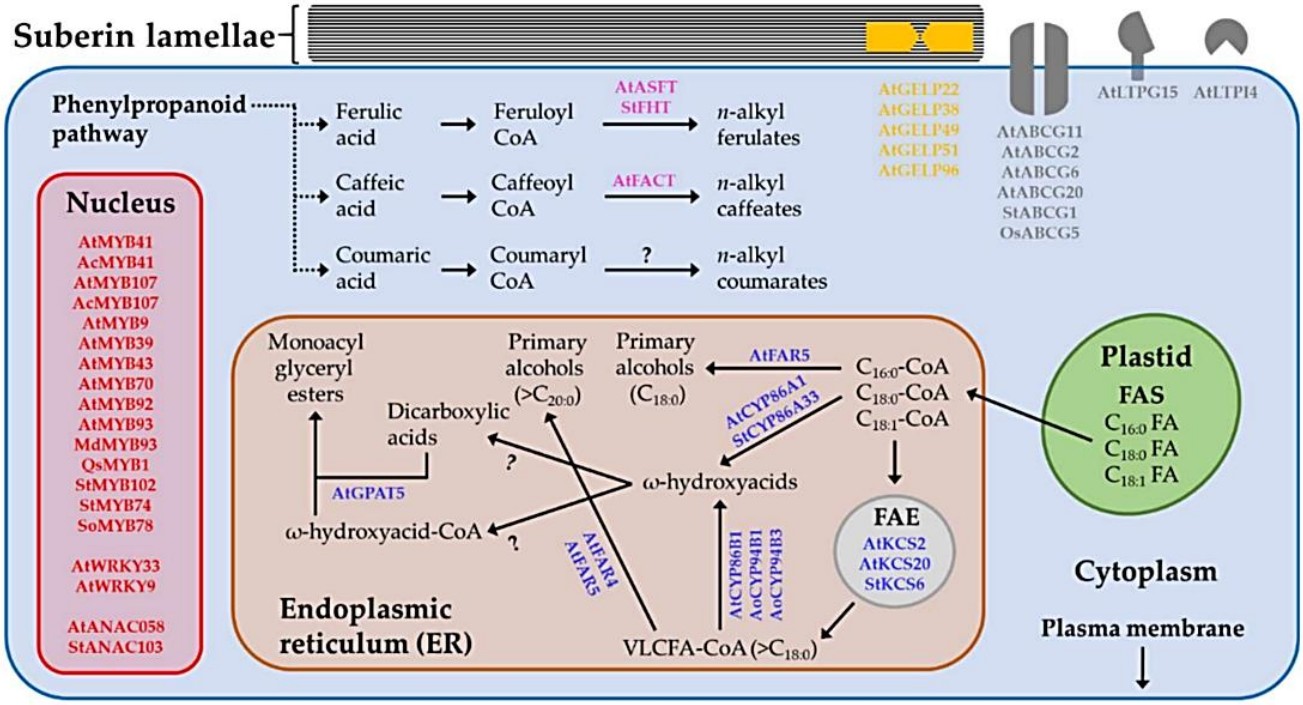

Figure X: It shows the suberin biosynthesis pathway including genes/enzymes involved in suberin polyaliphatic monomers (blue), suberin polyphenolic monomers (pink), suberin monomer polymerization (orange), suberin monomer transport (gray) and regulation of the suberin pathway (red) (Nomberg et al., 2022).

On the other hand, the lignin is a biopolymer formed primarily from monolignols especially hydroxycinnamyl alcohols, characteristically p-coumaryl, coniferyl, and sinapyl alcohols. Lignins derived from these hydroxycinnamyl alcohols are commonly classified as hydroxyphenyl (H), guaiacyl (G) and syringyl (S) lignin (Weng & Chapple, 2010). These monolignols are synthesized in the cytoplasm and transported across the cell membrane to the apoplast as building blocks. In the final step, two major groups of enzymes, laccases and peroxidases, play a pivotal role. These enzymes facilitate the oxidative radical-radical coupling of monolignols in the apoplastic spaces, leading to the final lignification (Sangha et al., 2012). The biosynthesis of lignin is entirely dependent on the phenylpropanoid pathway. This pathway not only produces primary metabolites for lignin and the aromatic portion of suberin biosynthesis but also serves as a precursor for certain secondary metabolites, including flavonoids, coumarins, and lignans (Vogt, 2010). The phenylpropanoid pathway starts with three reactions leading to the synthesis of 4-coumaroyl CoA. Alterations in these reactions result in dramatic phenotypes characterized by strong changes in lignin and suberin deposition and composition (Andersen et al., 2021; Fraser & Chapple, 2011). For instance, PAL gene

family (PAL1,2,3 and 4) catalyzes the initial step in which phenylalanine undergoes deamination to produce trans-cinnamic acid. In Arabidopsis, *pal1 pal2* mutant plants exhibit a considerable reduction in lignin, and overaccumulation of phenylalanine (Raes et al., 2003; Rohde et al., 2004). Although the Phenylpropanoid pathway has been elucidated for many years and is relatively well understood, important questions still remain open. For instance, the polar specificity polymerization, or the oxidation step in the final stages of polymerization is unknown. Nevertheless, some information has been provided, especially regarding the Casparian strip formation in the endodermis. For instance, SHORT-ROOT (SHR) has been identified as a Casparian strip master regulator via the activation of MYB36 and SCARECROW (SCR). MYB36 in turn directly and positively regulates Casparian strip genes (Casparian strip machinery) such as transmembrane Casparian strip membrane domain proteins (CASPs), peroxidases (i.e PER64) and the dirigent-like protein ESB1 (Kamiya et al., 2015a; Li et al., 2018). The formation of Casparian strips begins with the specific subcellular localization of CASPs proteins in the plasma membrane where the final lignin barrier will be constructed. CASPs establish a highly scaffolded transmembrane protein platform that recruits NADPH oxidase RBOH (SGN4), certain peroxidases, very likely PER64, and ESB1, which co-localize for the polymerization of lignin (Fujita et al., 2020; Kamiya et al., 2015; Rojas-Murcia et al., 2020). Very recently, dirigent proteins (DIR) such as DIR9, DIR24, DIR16, and DIR18 have been described, along with ESB1, as pivotal proteins in the specific initiation of lignin polymerization. Casparian strip analysis in double and higher-order mutants of this family showed defective Casparian strip formation, with a different phenotype shown in the *esb1* single mutant. All of this indicates the cooperative activity of MYB36 regulation, which initiates Casparian strip formation, and the pivotal role of the Schengen pathway in enhancing the polymerization of lignin to close the gap in the developing Casparian strip (Gao et al., 2023).

3.1.2 Schengen-pathway for monitoring and building the diffusion barrier

The protective capacity of the diffusion barrier relies on the integrity of the apoplastic barrier. The plant's ability to monitor the integrity of the apoplastic barrier was initially observed in the endodermis of Arabidopsis. Researcher were able to demonstrate using genetic, microscopic, and chemical methods, that in *myb36* plants, Casparin strip polymerization is diminished, resulting in early accumulation of suberin and ectopic lignification in the endodermis. In concordance with this, *esb1* and *casp1casp3*, downstream targets of MYB36, also exhibited similar phenotype that *myb36* (Kamiya et al., 2015a; Reyt et al., 2021).

Additionally, significant defects in Casparian strips were observed in a knockout mutant of the receptor kinase SGN3, which exhibits strong expression in the endodermis. Interestingly, in this case, no early compensatory suberization was detected in the endodermis (Pfister et al., 2014). Based on this and other evidence, researchers have proposed the existence of a barrier surveillance system known today as the 'Schengen pathway,' which monitors the integrity of Casparian strips and suberin lamella in the endodermis. In the endodermis, this pathway serves not only as a surveillance system but is also essential for the formation of contiguous Casparian strips in roots (Doblas et al., 2017; Nakayama et al., 2017). This surveillance system relies on the tightly regulated interaction of the ligand peptides CASPARIAN STRIP INTEGRITY FACTORS 1 and 2 (CIF1 and CIF2), and a leucine-rich repeat receptor like kinase SCHENGEN3 (SGN3, also called GSO1). The perception of the peptide is mediated by SCHENGEN3 (SGN1) kinase protein, and it triggers a signalling cascade that includes the activation of NADPH oxidase RBOHF (SGN4) leading to the production of ROS necessary for lignin polymerization (Figure Y) (Doblas et al., 2017; Fujita et al., 2020a; Nakayama et al., 2017; Reyt et al., 2021). In the endodermis, single mutant versions of these components disrupt Casparian strip formation without triggering suberin compensation, indicating the collaborative nature of this pathway (Fujita et al., 2020a). The ligand peptides CIF1 and CIF2 are produced in the stele and then transported through the apoplast to reach the permeable endodermis, where they bind to the SGN3 receptor. In contrast, the receptor, along with the SGN1 kinase, exhibits highly precise sub-cellular localization. SGN3 is localized to the endodermal plasma membrane, occupying positions on both sides of the Casparian strip, while SGN1 is polarly located on the outer plasma membrane facing the cortex. All of these processes including the MYB36 activation of the Casparian strip machinery induce its formation, ultimately blocking peptide diffusion and deactivating the Schengen pathway. This phenomenon also explains the excessive accumulation of suberin in the endodermis of mutants with impaired Casparian strip formation (Alassimone et al., 2016; Doblas et al., 2017; Fujita et al., 2020a; Kamiya et al., 2015c; Pfister et al., 2014; Reyt et al., 2021)

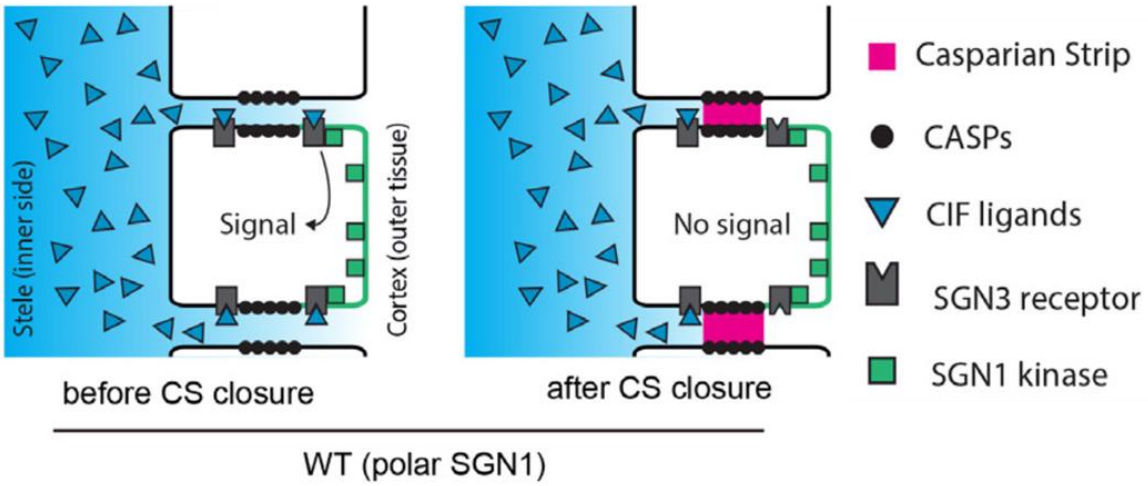

Figure Y: Schengen pathway illustration in the endodermis, shows the activation of the SGN3 receptor after the diffusion of the ligand peptides CIF from the stele through the apoplast for the formation of Casparian strips. (modified from Fujita et al., 2020)

It's important to note the receptors' ability to sense the ligand peptides. The affinity is based on the large spiral-shaped ectodomain of SGN3 and GSO2. CIF peptides are tyrosine-sulfated peptides, and their unsulfated form shows a dramatic reduction in affinity (Doblas et al., 2017; Doll et al., 2020; Komori et al., 2009). For instance, nonsulfated CIF2^{nsY64} exhibits significantly reduced binding affinity, approximately 100- to 1,000-fold, in its interaction with the GSO1/SGN3 ectodomain (Komori et al., 2009). In this context, the tyrosyl-protein sulfotransferase (TPST/SGN2) plays a pivotal role in tyrosine sulfation, which, along with proline hydroxylation and hydroxyproline arabinosylation, is a common posttranslational modification found in ligand peptides (Doblas et al., 2017; Komori et al., 2009). For example, *tpst* / *sgn2* mutant displays a similar phenotype than *sgn3* and *sgn1* in the endodermis. Therefore, TPST/SGN2 is recognize as an important component for the activation of the Schengen pathway.

This pathway is not exclusive to the endodermis, and new roles and components have been described in various plant tissues and environmental contexts. For instance, the formation of the plant embryonic cuticle requires two kinase receptors, SGN3 (GSO1) and GSO2, along with another SGN3 binding peptide, TWISTED SEED1 (TWS1), in collaboration with ALE1, a protease from the subtilase family, and TPST. Loss of function plants such as *gso1 gso2* and *ale1*, exhibit a permeable cuticle that is unable to protect the plant from water loss, compromising its survival (Creff et al., 2019; Doll et al., 2020; Fiume et al., 2016). Another example of the importance of Schengen components is observed in the pollen grains. In this

context, SGN3 (GSO1) and GSO2 bind to CIF3 and CIF4 peptides to ensure proper tapetum function. This is crucial for the formation of the pollen wall, which is rich in the biopolymer sporopollenin, and serves to protect the developing pollen (Truskina et al., 2022).

3.2 Phellem, phellogen and phelloderm: the periderm

Vascular plants undergo through secondary growth in addition to primary growth. Secondary growth can be simply defined as an increase in the thickness of the roots and stems. It is thought that secondary growth arose as an evolutionary fine-tuning adaptation in some seed plants, allowing them to better adapt to land environments. For instance, vascular tissues facilitate the transport of water, nutrients, and signalling molecules throughout the plant while also providing mechanical support (Fischer et al., 2019;De Rybel et al., 2016). Secondary growth is characterized by the increase of thickness of stems and roots, as well as the presence of specialized cell types with thickened cell walls. The increase of plant thickness is primarily facilitated by two meristematic layers: the vascular cambium and the phellogen, also known as cork cambium. The vascular cambium develops from the procambium, located between the differentiated xylem and phloem. In the end, this process results in the formation of a ring of meristematic cells that have the capability to divide and generate secondary xylem inward and secondary phloem outward (Nieminen et al., 2015). The secondary xylem and secondary phloem cells are the primary specialized cell types originated from the vascular cambium at the onset of secondary growth. In general, it is well-known that phloem plays a crucial role in the transport of photo-assimilates, solutes, signalling molecules, and plant hormones from shoots to roots, while xylem is responsible for water transport from roots to shoots and provides structural support (Fischer et al., 2019). On the other hand, the phellogen is the second meristematic layer that enters the scene during secondary growth. It gives rise to the periderm, which not only contributes to the plant's expansion but also, owing to its highly specialized cells, provides protection against water loss, potential pathogen attacks, and wounding (Ragni & Greb, 2018). The periderm is a protective tissue that plays a crucial role in secondary growth. It replaces the epidermis in roots, stems, and other plant organs in tight coordination with the plant's expansion. The periderm is anatomically divided into three layers: the phellem or cork, the phellogen or cork cambium, and the phelloderm (Barra-Jiménez & Ragni, 2017; Campilho et al., 2020; Evert, 2006). The middle layer of the periderm is the phellogen or cork cambium. This is a meristematic ring that divides bifacially to form outward the phellem and inward the phelloderm. The phellem consists of specialized cells that accumulate very high amounts of

suberin and lignin. This high degree of specialization gives the phellem its protective capacity and has drawn the attention of researchers due to its economic importance as a raw material and its potential biotechnological benefits (Campilho et al., 2020; Serra et al., 2022) . For instance, a variety of potato with more phellem layers and high rate if suberization is resistant to common scab (Thangave et al., 2016). Lastly, little information exists regarding the phelloderm, which is likely composed of parenchymatous tissue responsible for nutrient transport and storage.

In stems, the periderm does not have a unique origin and can develop from several tissues, including the epidermal layers, subepidermal layers, or phloem (Fischer et al., 2019; Serra et al., 2022a). In contrast, in roots, periderm (developmental periderm), as lateral roots, develops from the pericycle, the layer between endodermal cells and the vasculature in primary growth (Beeckman & De Smet, 2014; Wunderling et al., 2018). Another type of periderm, called the wound periderm, can be develop under specific conditions typically after wounding to repair and seal the affected plant tissue (Serra et al., 2022a). Periderm development has been pioneered studied in Arabidopsis roots, and we can define some key developmental stages. It begins with the first anticlinal divisions in the pericycle cells close to the xylem pole pericycle. These divisions continue throughout all the pericycle cells, establishing one ring of periderm cells. Then periclinal divisions continue subsequently in some periderm cells until a second layer of new periderm cells is form. Initially, these second layer can be identified as developing phellem cells, which do not yet contain suberin and lignin. As these new developing phellem cells mature and accumulate suberin and lignin, the cortex and epidermis detach from the same positions. Ongoing periclinal divisions of the phellogen result in the formation of phelloderm cells inward stablishing the three characteristic layers of the periderm. Finally, the cortex and the epidermis are completely detached, and a single functional mature layer of phellem will be stablish. The phellogen and the cambium continue to divide, generating new layers of cells and expanding the plant's girth(Serra et al., 2022a; Wunderling et al., 2018).

Periderm development, as we have seen, is a highly coordinated process that involves the orchestration of phellogen division, the deposition of diffusion barriers, specialized polymers that block apoplastic spaces, the detachment of primary tissue, and the continuous production of new cells in coordination with the cambium. In comparison with the cambium, there is limited information available about the key regulators of periderm development. Nevertheless, recent efforts have identified some molecular players with a pivotal role in the periderm. For instance, auxin, a plant hormone reported in most growth and developmental processes (Weijers et al., 2018), plays a crucial role in the establishment of the first phellogen cells and

the maintenance of their meristematic activity. For example, blocking polar auxin transport using N-1-naphthylphthalamic acid (NPA) significantly reduces periderm development compared to mock plants (Xiao et al., 2020). Furthermore, it was shown that specific auxin response factors (ARFs) independently regulate periderm and lateral root formation. For instance, ARF5 and ARF8 control phellogen activity through the activation of WUSCHEL-RELATED HOMEOBOX 4 (WOX4) and KNAT1/BREVIPEDICELLUS (BP) (Serra et al., 2022a; Xiao et al., 2020). Finally, periderm development can be influenced by environmental conditions, depending on the plant species. Factors such as water availability, temperature, and light intensity all affect the timing of periderm development (Evert, 2006). For example, in Arabidopsis, it is suggested that short light and continuous light conditions influence the timing of phellogen development (Wunderling et al., 2018) .

3.2.1 Phellem establishment and development

Phellem is a specialized tissue originate from the outer side of the phellogen (Serra et al., 2022a). One of the main characteristics is the significant presence of suberin, lignin, and waxes. These play a crucial role as they ensure the periderm's protective function. For instance, suberin acts as a physical barrier against pathogens and dehydration. This is because suberin makes the apoplastic spaces hydrophobic, rendering cell walls impermeable and preventing excessive water loss from the root. The differentiation of the phellem involves the establishment of apoplastic barriers, together with cell expansion and the accumulation of polar and nonpolar soluble compounds. In the final stage of development, phellem cells remodel the chromatin and activate programmed cell death (PCD) as part of their developmental process (Inácio et al., 2018; Wunderling et al., 2018; Serra et al., 2022). Interestingly, genes related to programmed cell death (PCD), suberin and lignin biosynthesis, and proanthocyanidin biosynthesis were found in both developing periderm and wound periderm, but with some specific differences. For example, the wound periderm tends to accumulate proanthocyanidins earlier and in different cellular compartments. In contrast, developing phellem undergoes strict developmental PCD. All of these differences between developing phellem and wound phellem can result in variations in their barrier properties (Inácio et al., 2018, 2021).

3.2.2 Molecular regulators for phellem differentiation

Phellem development requires the participation of molecular regulators to coordinate the cell changes. Little is known about regulatory networks that enhance the change of identity of phellem cells (Serra et al., 2022). Transcriptomic analysis in different plant species has revealed a limited number of putative regulators. For instance, in Arabidopsis, it was shown

that ANAC046 is expressed in the periderm and can induce suberization in the periderm when overexpressed (Mahmood et al., 2019) In addition, transcriptomic datasets often provide a significant number of characterized suberin or lignin-related genes that are not exclusive to the phellem but also have a role in the endodermis and seed coat. For example, characterized suberin genes such as the suberin biosynthetic FERULOYL TRANSFERASE (FHT), HYDROXYLASE OF ROOT SUBERIZED TISSUE (HORST/ CYP86A1), or ALIPHATIC SUBERIN FERULOYL TRANSFERASE (ASFT) (Boher et al., 2013; Höfer et al., 2008; Molina et al., 2009). Other research approaches, such as chromatin immunoprecipitation (ChIP) followed by high-throughput DNA sequencing (ChIP-Seq) in Cork oak, found that QsMYB1 directly regulates genes necessary for suberin and lignin biosynthesis, as well as presumably cork formation and differentiation (Capote et al., 2018). Recently, ribosome affinity purification followed by mRNA sequencing (TRAP-SEQ) was conducted to monitor the initiation and progression of phellem differentiation in Arabidopsis roots. Putative regulators were identified, including genes associated with suberin and lignin, as well as WOX, NAC, and MYB transcription factors. Additionally, the identified genes are involved in various metabolic processes, such as the synthesis and transport of cell wall components, response to stresses, and energy production (Leal et al., 2022).

3.4.2 Apoplastic barriers in the phellem

In the periderm, the deposition of suberin and lignin is crucial for the development and function of the tissue. Both polymers reinforce the phellem, where they accumulate and envelop the entire phellem cell. Suberization process occurs quickly in phellem cells. In fact, the feruloyl transferase (FHT) protein accumulates already in the phellogen (Boher et al., 2013)

While the amount of suberin deposited in the phellem varies depending on plant organs, plant species, and environmental conditions, suberin remains a crucial component in all scenarios, constituting a substantial portion of periderm mass (Serra et al., 2022). For instance, in the potato periderm, suberin could represent up to 50% of the total dried weight (Mattinen et al., 2009). On the other hand, lignin also constitutes a significant portion of the periderm's composition. Primarily, the monolignol units, guaiacyl (G), and to a lesser extent, syringyl (S), are the principal components of lignin. Interestingly, the lignin present in the phellem cells differs in monolignol composition from the lignin found in the xylem (Fagerstedt et al., 2015). In addition of suberin and lignin, aliphatic waxes are also present in the periderm. They have an important role in the formation of diffusion barriers in the periderm and cuticle (Nawrath et al., 2013; Schreiber et al., 2005). Interestingly, the amount of suberin and lignin found in the

periderm of Arabidopsis roots is much greater than that found in the endodermis (Ranathunge & Schreiber., 2011) This contrast highlights the limited available data regarding the regulation, deposition, and response of apoplastic barriers in the periderm when compared to the endodermis.

3.3 MYB transcription factors, potential regulators of the periderm

Transcriptional regulation is a critical biological process that orchestrates gene activities, defining cell and tissue identity during development, and coordinating many cellular activities in response to a diversity of intra- and extracellular signals. One of the largest families of transcription factors in plants is the V-myb myeloblastosis viral oncogene homolog (MYB) proteins, and they are represented in all major eukaryotic lineages (Dubos et al., 2010). Initially, MYB transcription factors were associated with the regulation of cell proliferation and differentiation, but today it is known that they are involved in various aspects of development such as stress responds and metabolic regulation (Kranz et al., 1998; Stracke et al., 2001; Dubos et al., 2010; Liu et al., 2015) . The main characteristic of MYB transcription factors is the highly conserved MYB domain, which consists of up to four imperfect amino acid sequence repeats (R) of approximately 52 amino acids each, with each forming three α-helices. MYB transcription factors have been classified into four groups based on the organization of their repeated sequences, or MYB domains, adjacent to each other. For instance, R2R3-MYB class is characterized by possessing two repeats (R2 and R3) of the prototypic MYB protein c-Myb (Dubos et al., 2010). In plants, the majority of MYBs belong to the R2R3-MYB group. Generally, this group is characterized by having a DNA binding domain (MYB domain) in the N-terminal part of the proteins and an activation or repression domain in the C-terminus (Dubos et al., 2010; Wu et al., 2022). Based on the high conservation of the MYB domain and amino acid motifs in the C-terminal domains, 25 sub-groups (or clades) have been defined. (Dubos et al., 2010; Stracke et al., 2001). The initial classification was primarily based on Arabidopsis MYB proteins, but new evidence indicates that these groups can be conserved in other angiosperms. Interestingly, in some cases, these clades are extended and even exclusive to certain plant species with potentially putative specialized functions (Dubos et al., 2010; Jiang et al., 2004). For instance, in *Populus trichocarpa*, the comprehensive characterization of the R2R3-MYB family has revealed some exclusive new subgroups not found in Arabidopsis. These subgroups may contribute to lineage-specific phenotypic innovations. (Wilkins et al., 2009). The number of members of this type of R2R3-MYB transcription factors, in some cases exceeding hundred members, is in line with their

pivotal role in plant-specific processes. These processes encompass cell fate identity, primary and secondary metabolism, developmental regulation, and stress responses (Dubos et al., 2010).

3.3.1 MYB68 transcription factor clade

In cork oak (*Quercus suber L.*), it was previously described that QsMYB1, the closest homologue of Arabidopsis MYB68 and MYB84, had a putative role in periderm developmental regulation, including activities related to lignin and suberin deposition (Almeida et al., 2013; Capote et al., 2018). The MYB68 clade (clade 14 in Kranz et al., 1998 and Stracke et al.,2001), or at least some of its members, has been studied for approximately 20 years in many plant species, and some roles have been designated to them. This clade is composed of six members in Arabidopsis: MYB36, MYB37, MYB38, MYB68, MYB84, and MYB87 (Stracke et al., 2001). Phylogenetic analysis of the members of this clade shows that all of them are homologous to the tomato (*Solanum lycopersicum*) BlIND, and they are characterized by an additional amino acid between the first and the second conserved Trp residues of the R2 repeat. Interestingly, only MYB68 and MYB84 show conservation outside the MYB domain. Furthermore, transcriptional analysis reveals that MYB37, MYB38, MYB84, and MYB87 transcripts can be detected in different plant organs. In contrast, MYB36 and MYB68 expression is mostly limited to the root (Müller et al., 2006). MYB68 and its closest homologue, MYB84, were postulated to share overlapping expression in the pericycle cells. The initial evidence suggested possible redundant roles in root development and responses to environmental cues, especially related to temperature changes (Feng et al., 2004). New evidence suggests that MYB68 and MYB84 have different, or at least additional, functions and localization in the root regulating development in both primary and secondary growth. For example, it has shown that MYB84 is expressed in the root and hypocotyl periderm of Arabidopsis (Wunderling et al., 2018).

MYB37, MYB38, and MYB84 were the first members of this clade to be postulated as specific developmental regulators. These MYBs were initially defined based on their first identified functions as REGULATORS OF AXILLARY MERISTEMS (RAX) (Müller et al., 2006) Among these, evidence shows that MYB37 (RAX1) and CUP-SHAPED COTYLEDON (CUC) genes promote the early stages of axillary meristem formation (Keller et al., 2006). Later on, double and triple mutants of MYB37 (RAX1), MYB38 (RAX), and MYB84 (RAX3) show that they have redundant functions in the formation of axillary meristems, with some specificity depending on the phases of vegetative development (Dubos et al., 2010; Müller et

al., 2006). Recently, it has been proposed that AtMYB2 diminishes the formation of axillary meristems by directly downregulating MYB37 (RAX1), especially in specific environmental contexts. For instance, it has been shown that salt stress and drought stress enhance the expression of MYB92. (Jia et al., 2020). In secondary growth, using vascular cambium cell-specific transcript profiling and genetic analyses, it has been shown that MYB87, together with other transcription factors such as WUSCHEL-RELATED HOMEOBOX 4 (WOX4), KNOTTED-like from Arabidopsis thaliana 1 (KNAT1; also known as BREVIPEDICELLUS or BP), NAC DOMAIN CONTAINING PROTEIN 15 (ANAC015), LOB DOMAIN-CONTAINING PROTEIN 3 (LBD3), SHORT VEGETATIVE PHASE (SVP), PETAL LOSS (PTL), RESPONSE TO ABA AND SALT 1 (RAS1), regulates cambial activity. On one side, WOX4, ANAC015, BP, and LBD3 promote cambial division, while SVP, PTL, RAS1, and MYB87 repress this activity. For instance, Overexpression of MYB87 in the vascular cambium dramatically reduces its division, thereby truncating the expansion of the root (J. Zhang et al., 2019).

The most well-known member of this clade is MYB36, recognized as a master regulator of Casparian strips (Kamiya et al., 2015). MYB36 is directly activated by SCARECROW (SCR) downstream of SHORTROOT (SHR) activation. In this context, MYB36 not only activates the Casparian strip formation machinery but also regulates the developmental switch from a proliferative state to differentiation. This developmental switch is based on the repression of genes involved in controlling the specificity and division of new cells, such as SCR, JACKDAW (JKD), MAGPIE (MGP), and NUTCRACKER (NUC), which pattern the cortical and endodermal progeny. (Liberman et al., 2015). We further explore the role of MYB36 in Casparian strip regulation and formation in the apoplastic barrier section.

3.3.2 Other MYBs of interest

In the periderm, considering the numerous processes involved in the establishment of the phellem and its maturation, it is likely that other transcription factor may play a role. The activity of these MYBs could be related with a generic function in specific pathway regardless of the plant organ involved. For example, MYB41 regulates suberin biosynthesis in different plant organs. MYB41 was the first transcription factor suggested to play a role in the molecular regulation of suberin biosynthetic genes. It was initially reported as a cuticle regulator in response to abiotic stress, and its overexpression was found to alter cuticle conformation (Cominelli et al., 2008). Subsequently, MYB41 was identified as a master regulator of suberin biosynthesis, capable of coordinating the expression of numerous genes involved in the

synthesis of both aromatic and aliphatic suberin monomers. This is not the case for GPAT5, which only slightly increases the accumulation of some suberin monomers. Furthermore, ectopic overexpression of MYB41 in Nicotiana leaves can lead to a significant increase in suberin monomers, surpassing the proportion of cuticle monomers (Kosma et al., 2014). After further investigation, researchers using several approaches were able to identify a set of MYB transcription factors that can activate suberin biosynthetic genes. This set includes MYB41, MYB9, MYB39, MYB41, MYB53, MYB92, MYB93, and MYB107. Briefly, MYB39 is expressed in the endodermis and is identified as a regulator of endodermis suberization during development (Cohen et al., 2020). Although its upregulation promotes the expression of suberin biosynthetic, transport, and regulatory genes, the single mutant version of MYB39 shows a mild phenotype, suggesting the existence of redundant regulators (Shukla et al., 2021). MYB53, MYB92, and MYB93 form an independent subgroup of MYB transcription factors, and together with MYB9 and MYB107, they are able to directly activate the BIOTIN CARBOXYL CARRIER PROTEIN2 (BCCP2) and other fatty acid biosynthetic genes. (To et al., 2020). This initial evidence and further research suggest that these transcription factor could have a role in suberin regulation. Furthermore, it was demonstrated that MYB9 and MYB107 coordinate the biosynthesis, transport, and polymerization of suberin in the seed's outer integument layer. Single versions of *myb9* or *myb107* show a significant reduction in suberin monomers, increased permeability, reduced stress resistance, and reduced germination under osmotic and salt stress (Gou et al., 2017; Lashbrooke et al., 2016). Furthermore, the *myb41 myb53 myb92 myb93* quadruple mutant demonstrates the pivotal role of these genes in endodermis suberization during development and in response to stress. In addition, it is worth noting that these transcription factors act downstream of either the Schengen pathway or ABA signalling response, two independent processes, to activate suberin biosynthetic genes without altering the formation of Casparian strips (Shukla et al., 2021).

4. Objectives

Secondary growth is a dynamic process that integrates various developmental mechanisms and responds to physiological, molecular, and environmental cues (Groover and Robischson, 2006). One of the most distinctive tissues in secondary growth is the periderm, a multilayer barrier capable of protecting plant roots and stems against abiotic and biotic stresses while simultaneously regulating plant growth expansion. The central layer of the periderm, called the phellogen or cork cambium, possesses a meristematic nature and divides in both directions. Outward, it forms the phellem, also called cork, while inward, it forms the phelloderm. The phellem functions as the protective layer and undergoes dramatic cell wall modifications generally characterized by the presence of suberin, lignin and aliphatic waxes. Together, they grant the protective barrier properties to the phellem. Problems with the integrity of the phellem can negatively impact plant growth especially if the barrier is not established or repaired.

Understanding the regulation of the periderm is complex due to the distinct characteristics of each layer, and the limited number of identified regulators. Until today it was shown the pivotal role of auxin in phellogen formation and maintenance. In addition, few suberin related genes involved in biosynthesis and polymerization have been identified, although their functions are not exclusive to the periderm and could express in other tissues as the endodermis. Therefore, our central scientific question focuses on identifying and characterizing molecular regulators of the phellem differentiation. Previous research has suggested that QsMYB1, homolog of MYB84 and MYB68 transcription factors in Arabidopsis, control phellem establishment in Quercus. Using Arabidopsis roots as a model, we investigate the role of the MYB68 clade in controlling phellem differentiation, which includes accumulating apoplastic barriers and reducing the meristematic capacity of the phellogen. We utilize a range of approaches, including suberin staining combined with confocal or fluorescence microscopy and chemical analysis of suberin using gas chromatography–mass spectrometry (GCMS), to investigate root suberinization. Our goal is to develop new, easily replicable methods for analyzing phellem differentiation, with a focus on gaining a better understanding of the spatiotemporal polymerization and deposition of apoplastic barriers along the Arabidopsis root during phellem differentiation. Additionally, we aim to investigate the importance of phellem integrity and whether a surveillance system exists to monitor periderm integrity.

All things considered, this work will help us investigate further the ways in which environmental and physiological signals positively influence phellem establishment as barrier. The importance of this research is not restricted to Arabidopsis; the knowledge gained also extends to other plant species, including trees, and environmental contexts, which may have implications for agriculture and sustainable production.

5. Results in Form of Manuscripts

5.1 Draft manuscript 1: A Cluster of MYB Transcription Factors Regulate Stem Cell Proliferation and Cork Differentiation During Periderm Development.

D.M. and L.R. planned the majority of the experiments. N.R, X.Z, WX conducted preliminary experiments. D.M conducted the majority of the experiments. D.R. made the vibratome sections. D.M and L.R. acquired the confocal images. D.M, L.R., D.R, N.R, W.X, T.A, XZ did the molecular cloning and generated the plant lines. D.M. performed the Fluorol Yellow (FY) experiments. D.M and S.H. conduct the plant embedding and characterized pPXY:MYB87-GR. D.M. measured the number of phellogen and periderm. D.M. conducted the RNA related experiments. D.R. and D.M helped in generating the T3 lines. L.R. wrote the paper with the help of D.M and T.A.

Title: A cluster of MYB transcription factors regulate stem cell proliferation and cork differentiation during periderm development.

Authors: David Molina[1], Sara Horvath[1], Xudong Zhang[1, §], Wei Xiao[1,†], Noah Ragab[1], Dagmar Ripper[1], Tonni Grube Andersen[2] Laura Ragni[1,3*]

[1] ZMBP-Center for Plant Molecular Biology, University of Tübingen, Auf der Morgenstelle 32, D-72076 Tübingen, Germany.

[2] Max Planck Institute for Plant Breeding Research, Carl-Von-Linné-weg 10, 50829, Cologne, Germany.

[3] University of Freiburg, Institute of Biology II, Schänzlerstr 1, 79104 Freiburg, Germany.

* Corresponding/Lead contact: laura.ragni@biologie.uni-freiburg.de

§ Present address: University of Hohenheim, Institute of Crop Science, Quality of Plant Products (340e), Stuttgart, Germany

† Present address: Ghent University, Department of Plant Biotechnology and Bioinformatics, 9052 Ghent, Belgium; VIB Center for Plant Systems Biology, 9052 Ghent, Belgium.

David Molina: 0000-0001-5858-3331; david.molina@zmbp.uni-tuebingen.de

Sara Horvath: sara.horvath@zmbp.uni-tuebingen.de

Xudong Zhang: xudong.zhang@uni-hohenheim.de

Wei Xiao: 0000-0002-6392-5866; wei.xiao@psb.vib-ugent.be

Noah Ragab: noah.ragab@student.uni-tuebingen.de

Dagmar Ripper: dagmar.ripper@zmbp.uni-tuebingen.de

Tonni Grube Andersen: 0000-0002-8905-0850; tandersen@mpipz.mpg.de

Laura Ragni : 0000-0002-3651-8966; laura.ragni@biologie.uni-freiburg.de

Abstract :

Plants have developed specialized barriers to protect and isolate the inner tissues from the environment while maintaining plant homeostasis. Different barriers are present in various plant organs and at different growth stages. During secondary growth, the periderm acts as the protective tissue, covering roots, stems, and branches while they get thicker. The periderm is a dynamic barrier comprising a stem cell niche known as cork cambium, which bifacially divides to generate phelloderm inward and cork outward. Cork cells have a unique cell well impregnated with suberin and lignin polymers, essential for the barrier function.

The differentiation process that forms new cork cells from the cork cambium is largely unknown despite its importance. In this work, we identify members of the MYB36-subclade transcription factors, such as MYB68, as master regulators of cork differentiation. On the one hand, this set of MYBs promotes suberin deposition by inducing the expression of enzymes involved in all the steps of suberin biosynthesis, including the recently discovered suberin polymerizing enzymes GDSLipases; on the other hand, it represses cork cambium proliferation, possibly by interfering with WOX4 and BP activity. Furthermore, we demonstrated that suberin deposition in the cork is a robust process regulated by a complex network of transcription factors, including other MYB transcription factors that promote suberin deposition in the endodermis. However, only members of the MYB36 subclade can repress cell proliferation in different developmental contexts, highlighting general and specific functions for MYB transcription factors in the cork. Finally, tissues specific manipulation of MYB activity can be used to obtain thicker periderms and more suberized cork layers, traits of biotechnological interest, and to asses how these traits affect plant performance in response to stresses.

Introduction:

Plant barriers, like our skin, protect and isolate the vasculature from the environment, regulating nutrient assimilation, gas exchange, water loss, and pathogen penetration (Serra *et al.*, 2022b). Depending on the plant family/species and developmental stages, different barriers occur in roots. During primary growth, the endodermis, present in all vascular plants, and the exodermis, present in many flowering plants, are the central protective tissues of roots (Barberon *et al.*, 2016; Doblas *et al.*, 2017; Enstone *et al.*, 2002; Serra *et al.*, 2022b). The periderm replaces the endodermis in the older part of the roots, undergoing extensive radial thickening. This is typical of trees, but it also occurs in many herbaceous plants, such as Arabidopsis (Kosma *et al.*, 2015; Serra *et al.*, 2022b). The periderm, in contrast to the other barriers, comprises a stem cell niche, the cork cambium, that allows the barrier to follow the radial growth of the organs. The cork cambium can remain active for many years or throughout plant life, producing the cork tissue toward the environment and the phelloderm toward the vasculature (Campilho *et al.*, 2020; Evert, 2006; Serra *et al.*, 2022b)

Common to all root barriers is the presence of specialized polymers such as suberin and lignin that impregnate the cell walls (Serra *et al.*, 2022b). The endodermis is characterized by localized lignin depositions, “the Casparian strips,” and a suberin lamella, which accumulates later in development(Doblas *et al.*, 2017; Naseer *et al.*, 2012). Similarly, the exodermis is a ligno-suberized layer in which lignin deposition in a U-shaped fashion precedes suberin accumulation (Cantó-Pastor *et al.*, 2022; Manzano *et al.*, 2022). The cork cell wall is also impregnated with both polymers (Kosma *et al.*, 2015; Serra *et al.*, 2022b). Plants with lower suberin contents in the endodermis and or periderm are less resistant to abiotic stresses, highlighting these polymers' protective function, while periderm thickness correlates with the ability to withstand wildfire and pathogen penetration (Andersen *et al.*, 2021; Barberon *et al.*, 2016; Graves *et al.*, 2014).

The recalcitrant nature of suberin, which is even more resistant than lignin in soil, has sparked a great interest in the molecular regulation of polymer accumulation in root barriers for biotechnological purposes (Harman-Ware *et al.*, 2021). The molecular network underlying the different steps of endodermis differentiation is well characterized, and different transcription factors regulate the specific steps. MYB36 is the key regulator of Casparian strip formation, and it directly activates PEROXIDASES, scaffold proteins such as CASPs and ESB1 and RBOH required for polar lignin deposition (Kamiya *et al.*, 2015; Liberman *et al.*, 2015; Wang *et al.*, 2022). Suberin deposition in the endodermis is promoted by a large array of MYB TFs belonging to different subclades(Dubos *et al.*, 2010), such as the S10 (MYB9, MYB39, MYB107), the S11 (MYB41, MYB74) and S24 subclade (MYB53, MYB92, MYB93), (Cohen *et al.*, 2020; Kosma *et al.*, 2014; Lashbrooke *et al.*, 2016; Shukla *et al.*, 2021; Wang *et al.*, 2020; Xu *et al.*, 2022). Suberin is highly dynamic, and several hormones such as Abscisic acid (ABA), Ethylene, and Gibberellins and nutrient status determine suberin homeostasis (Barberon *et al.*, 2016; Binenbaum *et al.*, 2023; Wei *et al.*, 2019). For

instance, ABA is well known to trigger suberin deposition via the activation of MYBs and suberin biosynthesis enzymes (Shukla *et al.*, 2021; Wei *et al.*, 2019), while Ethylene application and iron deficiency have a repressive effect in suberin deposition (Barberon *et al.*, 2016).

Less is known about periderm ontogenesis and cork differentiation. Recently, we showed that auxin is required for the first formative divisions in the pericycle, which gives rise to the cork cambium; in addition, auxin is necessary to maintain an active cork cambium (Xiao *et al.*, 2020). Downstream of auxin act, the transcription factors WOX4 and BP, to promote cork cambium proliferation(Xiao *et al.*, 2020). However, how the stem cells of the cork cambium differentiate into the cork cell and what regulates suberin deposition in the cork is still largely unknown. QsMYB1 (ortholog of MYB84/MYB68) has been proposed to control cork differentiation (Almeida *et al.*, 2013; Capote *et al.*, 2018). However, functional characterization is still missing due to limitations in working with cork oak trees. Interestingly, MYB84 has been previously employed as a periderm marker in Arabidopsis root (Wunderling *et al.*, 2018; Xiao *et al.*, 2020) MYB84 and MYB68 belong to the S14 subclade of R2-R3 MYB transcription factors (from now on referred to as the MYB36 subclade)(Dubos *et al.*, 2010), which included the master regulator of Casparian strips MYB36.

Here, we explored the role of the MYB36 clade transcription factors during cork differentiation. We showed that MYB68 and, to a lesser extent, other members of the clade regulated suberin deposition in the cork via the activation of suberin polymerizing and biosynthesis genes. Moreover, induction of MYB68 in the cork is sufficient to increase suberin levels, while induction in the periderm results in plants with an extra cork layer, traits of biotechnological interest in programs aiming to improve soil carbon sequestration. Interestingly this set of MYBs also represses cork cambium proliferation. This stem cell repressive differentiation behavior is limited to the MYB36 subclade, while MYBs of neighboring clades also contribute to regulating cork suberin levels, highlighting that suberin deposition in the cork is a robust process controlled by multiple sets of MYB transcription factors.

Results :

All members of the MYB36 subclade are expressed during periderm development

MYB36 subclade comprises six members: MYB36, MYB37, MYB38, MYB68, MYB84 and MYB87. We first focused on MYB68 and MYB84, which represent the closest orthologs of QsMYB1 in Arabidopsis, and mapped their expression pattern during the early and late steps of periderm development by employing promoter-fluorophore reporter lines. Both MYBs were expressed during periderm formation (Fig. S1A), and their expression is maintained in the periderm of old roots (Fig. 1A and S1A). MYB68 was expressed predominantly in the cork cambium and a few cork cells, whereas the expression of MYB84 was broader toward the cork (Fig1.A S1A,C). Both MYB68 and MYB84 expression overlaps with PEROXIDASE 15, a

marker for early cork differentiation/ cork cambium, and partially with WOX4 in the cork cambium (a regulator of cork cambium proliferation) and GPAT5 in the cork (a suberin biosynthesis gene) (S1C)(Wunderling *et al.*, 2018; Xiao *et al.*, 2020). Notably, this expression pattern is consistent with a role for MYB68 and MYB84 in the early steps of cork differentiation.

Interestingly, we found that the other members of the S14 subclade were also expressed during periderm formation in overlapping and distinct domains. *MYB37/RAX1* and *MYB38/RAX2* expression encompassed all periderm layers, whereas *MYB36* was more restricted to the mature cork, while *MYB87* was predominantly expressed in the cork cambium suggesting that MYB S14 subclade contributes to periderm formation and differentiation with distinct and overlapping roles (FigS1A-B).

A set of MYB TFs promotes suberin deposition in the cork

The hallmark of cork differentiation is suberin deposition, which can be easily imaged by fluorescent staining. Fluorol yellow (FY) staining, compared to analytical approaches, is a quick method to quantify suberin deposition and allows spatial resolution (Lux *et al.*, 2005; Ursache *et al.*, 2018; Wunderling *et al.*, 2018). Thus, to investigate the role of S14-subclade MYBs in suberin deposition, we employed FY.staining in *myb* loss of function mutants. In the mature cork of roots of *myb68*, *myb84*, *myb87*, *myb36* single mutants, *myb68 myb87* double mutant, and *myb37 myb38 myb84* triple mutants, we observed normal suberin deposition (Figure S1D) suggesting redundancy among the different members of clade S14. In agreement, the inactivation of both *MYB68* and *MYB84* led to a mild reduction of suberin, while only in the *myb37 myb38 myb68 myb84* quadruple mutant (*myb quadr.*) we detected a drastic decrease in suberin deposition in the cork (Figure 1B).

Interestingly, when we explored the suberin deposition pattern in the whole cork (Andersen *et al.*, 2021), we noticed a reduction of the relative-mature-cork region compared to the developing-cork region in *myb68* single mutants, while *myb87*, *myb84*, *myb37 myb38 myb84*, and *myb36* do not show any phenotypes (Figure S2A). *myb68 myb87* double mutants were indistinguishable from *myb68* single mutants, whereas *myb68 myb84* double mutants and the *myb* quadruple mutants showed a stronger reduction (Figure 1C, S2A). Importantly, these observations cannot be explained by impaired primary root growth or delay in periderm development in *mybs* mutants as these mutants display a root length comparable to WT (or even slightly longer) and a slightly higher cork ratio, suggesting normal primary growth and periderm development (Figure S2B-C). Altogether, the analysis of MYB loss of function mutants suggests that MYB68 and, to a lesser extent, MYB84, MYB37, and MYB38 contribute to cork differentiation. Consistent with a major role for MYB68 in promoting suberin deposition, cork-specific induction of MYB68 (*pGPAT5:MYB68-GR*) was sufficient to rescue the *myb68 myb84* suberin phenotypes (Fig S2D-E).

Suberin is a complex polymer based on ester-bond linked glycerol, fatty acids, their oxidized derivates, and ferulic acid (Serra and Geldner, 2022). Recent work showed that although ferulic acid

represents only a tiny fraction of the total components, it is crucial for de novo suberin deposition (Andersen *et al.*, 2021). We performed GS-MS analysis to investigate whether suberin chemical composition is affected in the *myb37 myb38 myb68 myb84* quadruple mutants. In the *myb37 myb38 myb68 myb84* quadruple mutant, we observed a reduction of most of the aliphatic components compared to WT, while aromatic acids, such as ferulic acid, were unchanged or slightly increased, indicating that MYB68, MYB84, MYB37, and MYB38 regulate the core suberin biosynthesis pathway (Figure 1D). In agreement with this, we did not observe any decrease of lignin accumulation in the cork of the *myb68 myb84* double mutants and myb quadruple mutants as quantified by basic fuchsin staining (Figure S2F). Next, we wondered if MYB68 is sufficient to promote suberin deposition in the cork. To tackle this, we generated tissue-specific inducible lines using the pGPAT5 promoter, which is strongly expressed in the cork during periderm development. Upon induction of MYB68 in the cork, we detected an increase of FY signal in the cork, proving that MYB68 is sufficient to trigger suberin accumulation (Figure 1E, S2G).

It is known that reduced suberin deposition impacts barrier functionality and permeability, and thus, suberin mutants are less resistant to salt stress (Andersen *et al.*, 2021; Ursache *et al.*, 2021). We assessed the physiological impact of reduced suberin deposition of *myb quadr*. mutants, by exposing the root region encompassing the periderm to salt stress (by employing split plates). This is a fundamental requirement to study periderm-specific responses as salt stress strongly impacts primary root growth and suberin accumulation in the endodermis (Andersen *et al.*, 2021; Barberon *et al.*, 2016; Duan *et al.*, 2015; Julkowska *et al.*, 2014; Ursache *et al.*, 2021), which may lead to indirect effects in the periderm. Primary root length in treated or untreated plants was comparable (Figure 1F and S2G; however, the shoots of the *myb37 myb38 myb68 myb84* quadruple mutants were smaller and more compact in the salt-treated plants, showing that impaired cork differentiation affects tolerance to salt (Figure 1) (Figure 1F and S2H).

Overall, we showed that members of the MYB36 clade, except for MYB36, promote suberin deposition in the cork, with MYB68 playing a major role.

MYB68 **promotes the expression of suberin biosynthesis and polymerizing enzymes**

To explore how MYBs promote suberin deposition, we investigated the transcript profiling of *myb68 my84* double mutants. To avoid developmental heterogeneity, we sampled only the uppermost two cm of 18-day-old roots, representing a uniform growth stage with a fully established periderm. Among the downregulated genes in *myb68 myb84*, we found many suberin biosynthesis enzymes, such as *CYTOCHROME P450 FAMILY 86* (*CYP86A1)/HORST, CYP86B1/RALPH, GLYCEROL-3-PHOSPHATE-SN-2-ACYLTRANSFERASE 5* (*GPAT5*), *FATTY ACID REDUCTASEs* (*FARs), 3-KETOACYL-COENZYME A SYNTHASE (KCSs)(*Figure S3A*)*, which are expressed in the cork (Leal *et al.*, 2022; Serra *et al.*, 2022a; Wunderling *et al.*, 2018). In this group, we also noticed the recently characterized endodermal GDSL-type esterase/lipase proteins (GELP38, GELP51, GELP49, and GELP96), which polymerize suberin in the

apoplast (Ursache *et al.*, 2021). In accordance with the idea that GELPs may also act in the cork, many GELPS that were downregulated in *myb68 myb84* are enriched in cork tissue *versus* whole-root tissues (Leal *et al.*, 2022), and we could confirm that *GELP38*, *GELP51*, and *GELP96* and *GELP49* are expressed in the cork by employing fluorescent reporters (Figure 2A). Furthermore, the loss of function of five GELPs (*gelp22 gelp38 gelp51 gelp49 gelp96: gelp q.*) resulted in roots that almost lacked FY signal (Figure 2B-C), pointing out that GELPs are also required for suberin polymerization in the cork. Notably, the expression of *GELP51* under a cork-specific promoter (*pGPAT5:GELP51*) in *myb68 myb84* could totally rescue suberin deposition in the mature cork (Figure 2D) and partially the cork differentiation quantified as (developing versus mature cork region) (Figure 2E), highlighting the importance of GELP in suberin deposition.

Interestingly, the expression of other MYB TFs belonging to the MYB41 and MYB39 subgroups (subcade S11 and subclade S10), which are known to control suberin deposition in the root endodermis and in the seed coat (Cohen *et al.*, 2020; Kosma *et al.*, 2014; Lashbrooke *et al.*, 2016; Shukla *et al.*, 2021), was unchanged or increased in *myb68 myb84* with exception for MYB53, indicating that MYB68 acts directly on suberin biosynthesis and or that compensatory regulatory mechanism occurs.

To confirm that MYB68 activates the expression of suberin-associated genes in the cork, we exploited a complementary approach: we induced the expression of MYB68 in the periderm (*pPER15:MYB68-GR*) and checked the expression of a set of genes by qPCR. FAR4, HORST/CYP86A1, GPAT5, GELP8, GELP51, GELP96, GELP38 and MYB53 were upregulated upon MYB68 induction indicating that MYB68 activates the suberin pathway at multiple steps (Figure 2F). In agreement, the expression of MYB68 in tobacco leaves triggered the activation of luminescent reporters for suberin biosynthesis enzymes (*pGPAT5:nnLUX*, *pFAR4:nnLUX*; FiG S3B-C), suberin polymerizing enzymes (p*GELP8:nnLUX*, *pGELP38:nnLUX*, pGELP51*:nnLUX*; FIG2 G) and suberin regulatory genes (*pMYB53:nnLUX*; FigS3E) suggesting that MYB68 directly activate them. Interestingly, MYB36 was able to promote the expression of *pFAR4:nnLUX* and *pCASP2:nnLUX* (CASP2 is a known MYB36 target (Kamiya *et al.*, 2015)) only (FigS3E), while MYB68 could not activate the expression of *pCASP2:nnLux* (FigS3E) highlighting the specificity among these TFs.

Altogether, these results show that MYB68 and, to a lesser extent, other members of the subclade with the exception of MYB36, regulate suberin deposition in the cork.

A specific set of MYBs represses stem cell proliferation in the cork cambium

The fact that MYB68, MYB84, MYB37, MYB38, and MYB87 expression pattern encompasses the cork cambium (Figure S1A-C), prompted us to investigate whether these TFs play additional roles in the periderm. First, we quantified cambium proliferation and differentiation rate in loss of function mutants by measuring the number of periderm cells per cross-section and ratio of cork cells per number of peridermal

cells (Cork ratio), respectively. *myb84*, *myb87,* and *myb37 myb38 myb84* triple mutant do not display any difference in the total number of periderm cells and cork ratio compared to WT (FigSA-F), whereas *myb68* single mutants, *myb68 myb87,* and *myb68 myb84* double mutants showed reduced cork cells number per total periderm cell number ratio. In *myb68 myb84*, we observed a trend toward more periderm cells (significant in 6 experiments out 8), and this phenotype was stronger in *myb37 myb38 myb68 myb84* quadruple mutants, indicating that MYB68 and, to a lesser extent, MYB84, MYB37 and MYB38 repress stem cell proliferation in the cork cambium. Interestingly, in *myb68 myb84* and *myb37 myb38 myb68 myb84* mutants, we observed gaps (Fig S4G; red arrowheads) in the autofluorescent signal coming from the aromatic components of differentiated cork cells compared to WT (Figure 5), further highlighting the role of these MYBs in promoting cork differentiation and repressing stem cell proliferation.

In agreement, periderm-specific induction of *MYB68* (*PER15:MYB68-GR*) resulted in a decrease in the total number of periderm cells, a higher cork cells per total periderm cells ratio, and the formation of an extra suberized cork layer, confirming a dual role for MYB68 in promoting differentiation and repressing proliferation of the cork cambium (Figure 3D). To exclude that the effect of MYB68 on stem cell proliferation is an indirect consequence of altered suberin content in the cork, we analyzed lines with reduced suberin deposition in the cork for cell proliferation phenotypes. The suberin biosynthesis mutants *ralph horst* (Salas-González *et al.,* 2021), which mimic *myb68 myb84* mutants regarding FY staining (Figure S4H-I), were undistinguishable from WT in terms of periderm cell number and cork per total number of periderm cells (FiG3G-H). In addition, *gelp quintuple* mutants, which almost lack suberin in the cork, displayed an increase of cork per periderm cell ratio and reduced periderm cell number (FiG3G-H), which is the opposite phenotype of *myb37 myb38 myb68 myb84* mutants supporting the idea that this group of MYBs plays a specific function in regulating stem cell proliferation.

MYB68 and MYB84 regulate stem cell proliferation via WOX4 and BP.

Auxin plays a pivotal role in orchestrating cork cambium initiation and maintenance (Xiao *et al.,* 2020), which begs the question of whether MYB68, MYB84, MYB37 and MYB38 converge on the auxin signaling network of the periderm. To tackle this, we took advantage of the fact that blocking polar auxin transport via pharmacological interference (NPA treatment) results in delayed periderm formation/growth (Xiao *et al.,* 2020) and tested whether NPA treatment suppresses the periderm overproliferation phenotype of *myb37 myb38 myb68 myb84* quadruple mutants. NPA treatment in WT decreased periderm cell numbers, while in *myb quadruple* mutants, no effect was visible. Mechanistically, there could be two alternative explanations: these MYBs act in a totally independent pathway, or crosstalk with auxin-induced periderm program occurs downstream of the auxin signaling perception machinery. To disentangle this, we tested whether MYB68 and MYB84 genetically interact with WOX4 and BP, two known downstream of auxin cork cambium regulators (Xiao *et al.*, 2020). For this purpose, we obtained *wox4 myb68 my84* and *bp myb68 myb84* triple

mutants.

Wox4 and *bp* mutants showed a reduction of total periderm cell number compared to WT, confirming previous findings. The inactivation of BP in *myb68 myb84* resulted in a reduction of the total number of periderm cells compared to *myb68 my84* double mutants. Similarly, the loss of function of *WOX4* in *myb68 my84* led to a decrease in periderm cell number. These results showed that WOX4 and BP are necessary for the increased proliferation rate/periderm cell number of the *myb68 myb84*. Interestingly, WOX4 expression was unchanged in *myb68 myb84* double mutant, and BP was only mildly upregulated, suggesting that MYB68 and MYB84 do not directly repress WOX4 and BP expression.

Several groups of MYBs regulate suberin deposition in the cork, but stem cell repression is restricted to MYB36 clade.

We next wondered whether MYBs belonging to other subclades, which regulate suberin in other developmental contexts (Cohen *et al.*, 2020; Kosma *et al.*, 2014; Lashbrooke *et al.*, 2016; Shukla *et al.*, 2021; Wang *et al.*, 2020; Xu *et al.*, 2022), also act in the cork. Interestingly, MYB39 has been reported to be expressed in the cork (Cohen *et al.*, 2020), and by exploiting available transcriptomic data for cork-enriched expression (Leal *et al.*, 2022) and fluorescent reporters, we could show that *MYB41*, *MYB53*, *MYB92* and *MYB93* are expressed in the cork (Fig5A and S3A). Thus, we analyzed suberin deposition in the *myb41 myb53 myb92 myb93* quadruple mutants. Loss of function in *MYB41*, *MYB53*, *MYB92*, and *MYB93* resulted in decreased suberin accumulation in the cork, and in a reduction of the relative-mature-cork region compared to the developing-cork region (FIG5B-C), highlighting that suberin deposition in the cork is regulated by several groups of MYBs belonging to different subclades. However, *myb41 myb53 myb92 myb93* quadruple mutant did not show an increased number of periderm cells, reduced cork to periderm cell ratio, and gaps of undifferentiated cork as observed in *myb quadr*. mutants, suggesting that they do not repress stem cell proliferation in the cork cambium (FIG5D-F).

Finally, we investigate whether MYB68 can promote differentiation/repress cell proliferation in other developmental contexts. As MYB87 has been previously described as a repressor of vascular cambium activity, and overexpression of MYB87 leads to reduced radial growth (Zhang *et al.*, 2019), we tested whether MYB68 can repress vascular cambium proliferation.

Vascular cambium-specific overexpression of both MYB87 and MYB68 (*PXY:MYB68-GR* and *PXY:MYB87-GR*) resulted in an increase of xylem vessel numbers due to enhanced differentiation and reduced proliferation of the vascular cambium, showing that MYB68 can repress vascular cambium activity (FIG5G-H; S4J). Altogether, these findings showed that suberin deposition in the cork is a robust process that is regulated by multiple MYBs transcription factors belonging to different subclades, while only MYBs of the MYB36-sub clade represses stem cell proliferation.

Discussion

The plant body is covered and protected from biotic and abiotic stress by different protective/barrier tissues depending on the organ, plant species, and age. The periderm, the protective tissue of the organs undergoing radial thickening, has been extensively described in many plant species; however, only recently it has started to be characterized at the molecular level thanks to advances in omics technologies and the establishment of the Arabidopsis as a model for studying periderm development and cell biology (Wunderling *et al.*, 2018). The periderm is a dynamic barrier, including a stem cell population, which can remain active for many years or throughout the entire plant life. Auxin and vascular cambium initiation are critical signals for the establishment and maintenance of the cork cambium, and the transcription factors WOX4 and BP/KNAT1 act downstream of auxin, regulating cork cambium proliferation (Xiao *et al.*, 2020). However, how cork cells differentiate from the stem cells of the cork cambium and become highly suberized and lignified is largely unknown. Suberin and lignin depositions in the cork are important for barrier function and cork cell integrity, as plants with reduced suberin and lignin levels have collapsed cork cells and are more susceptible to salinity stress (Andersen *et al.*, 2021).

Our findings revealed that MYB68 and other members of its subclade orchestrate cork differentiation by repressing the proliferation of the cork cambium and promoting suberin deposition of the cork. MYB68 regulates suberin deposition at many levels: it promotes the expression of other transcription factors, such as MYB53, known to regulate suberin deposition (Shukla *et al.*, 2021), and of enzymes important in the synthesis of the aliphatic suberin components and in suberin polymerization in the apoplast such as GDSL lipases/GELPs. Ursache and colleagues have recently shown that five GELPs are required for suberin deposition in the endodermis (Ursache *et al.*, 2021). Interestingly, our genetic analysis revealed that the same GELPs are essential for suberin accumulation in the cork and are the major targets of MYB68. Surprisingly, the expression of a single GELP was sufficient to restore the suberin phenotype of *myb68 myb84* double mutants, highlighting redundancy in the family and their importance in suberin deposition. In contrast to MYB36, MYB68 is able to trigger the expression of the suberin network and induce extra accumulation of suberin in the cork, revealing specificity among closely related transcription factors. However, we could show that other MYBs that belong to different subclades and promote suberin in other developmental contexts, such as MYB39, MYB41, MYB92, and MYB93, also act in the cork, implying that suberin deposition is a robust process controlled by a complex network of transcription factors.

Unique to the MYB36 subclade is the role of supporting differentiation by repressing cell proliferation. In fact, only combined loss of function of MYB68, MYB84, MYB37, and MYB38 and not of other MYBs promoting suberin results in extra not differentiated periderm layers and, in general, in more peridermal cells. In addition, overexpression of MYB68 in the periderm triggers the exhaustion of the cork cambium and the production of more cork differentiated layers, a trait of agroeconomic interest as extra cork layers correlate with resistance to common scab disease in potato tuber and periderm thickness to wildfire survival

in trees (Graves *et al.*, 2014; Thangavel *et al.*, 2016). The cell proliferation repression is not restricted to MYB68, but it encompasses the whole subclade as MYB87 has been show to restrain vascular cambium activity (Zhang *et al.*, 2019), while *myb36* mutants are characterized by extra ground tissue layers at the root tip (Kamiya *et al.*, 2015; Liberman *et al.*, 2015). Ectopic expression of MYB68 in the vascular cambium mimics MYB87 overexpression: consumption to the vascular cambium and extra xylem vessels, suggesting that MYB68 can replace the function of MYB87, highlighting their conserved function. In the cork cambium, MYB68 represses proliferation in parallel/ downstream of auxin, which is required for cork cambium maintenance and initiation, as interfering with auxin accumulation does not impede the formation of a thick periderm in *myb qudr.* mutants. However, WOX4 and BP genetically interact with MYB68 and MYB84 as they are required for the extra periderm layers that are produced by the cork cambium of *myb68 myb84* double knock-outs. Interestingly, MYB68 does not seem to regulate the expression of WOX4 and BP directly. Possible explanations are that MYBs interact at the protein level with regulators of WOX4 and BP or that MYB68 and MYB84 bind to WOX4 and BP, interfering with normal WOX4 and BP transcriptional outputs. This is a likely scenario as MYB transcription factors are known to form homodimers heterodimers and to interact with other classes of transcription factors to regulate developmental processes such as stomata formation and trichome differentiation (Pattanaik *et al.*, 2014) (Refs).

In conclusion, our work illustrates the importance of MYB transcription factors in orchestrating the different steps of cork differentiation, highlighting subclade-specific and unspecific functions. The notion that orthologs of MYB68 are expressed in cork cells of the stems of several trees and during wound potato supports the idea that there are conserved mechanisms between root, stem, and wound-induced cork differentiation. Supporting even a broader role for MYB68, it has been recently proposed to regulate suberin deposition in the endodermis and during fruit russeting (Xu *et al.*, 2022; Xu *et al.*, 2023).

In conclusion, our work provides novel targets to engineer and manipulate barrier properties, such as the number of barrier cell layers and polymer deposition. Moreover, it will pave the way to dissect how the different barrier traits affect plant performance during development and in specific stress conditions.

Acknowledgments

This work was supported by the Deutsche Forschungsgemeinschaft (DFG) with grant RA2590/4-1 and SFB1101 project B10 to LR. The LSM780 and the Arabidopsis walk in chamber used in this study were acquired via a DFG investition grants (**INST 37/965-1 FUGG**).

Materials and Methods

Plant Material and Growth

Unless stated otherwise, plants were grown in vitro in 1/2MS media at 22C in continuous light. All Arabidopsis thaliana lines are in the Columbia background. Details of mutant alleles and transgenic lines are described in Supl file S1. For DEX (Sigma, Cat# D1756) induction, plants were initially grown and then, after either 9 or 14 days, transferred to 1/2MS media supplemented with 10μM DEX. For NPA (Duchefa Cat# N0926) treatments, plants were grown for 9 days on 1/2MS and then transferred to 1/2MS media supplemented with 10μM NPA. For salt stress experiments, plants were grown for 12 days on 1/2MS, then transferred to four-well split plates supplemented with 100mM NaCl in one of the chambers. For all pharmacological treatments, unless specified otherwise, plants were treated for 5 days. For the qPCR experiments, 17-day-old plants were treated for 24 hours on 1/2MS media supplemented with 10μM DEX.

Histological Techniques.

For the analysis of root suberin, Fluorol Yellow (Santa Cruz Cat# sc-215052) was employed. Complete roots (for assessing root suberin coverage) or root periderm sections (for confocal suberin analysis) were first collected and placed in water. Subsequently, they were incubated in a solution of Fluorol Yellow 088 (0.01% dissolved in lactic acid) in the dark for 30 minutes at 70°C. The stained material was subsequently washed twice with water and incubated in a solution of aniline blue (0.5% in water) for counterstaining. After staining, plant material was mounted with 10% glycerol on glass slides for analysis using epifluorescence or confocal microscopy. As for plastic sections, the procedure remained the same, except in this case, Fluorol Yellow was dissolved in water, and the FY incubation was carried out at room temperature in the dark.

For periderm lignin studies, roots were collected in water and then stained in a solution of Basic Fuchsin (Sigma, 857343-100G) (0.5% in water) for 5 minutes. Afterward, they were washed three times with water, mounted with water on glass slides, and observed under the microscope.

For periderm anatomy studies, 1 cm root samples from the root junction were collected in water. Thin plastic cross-sections were obtained following the protocol described in (de Reuille and Ragni, 2017) using Technovit 7100 (Heraeus Kulzer Cat# 64709003). 5-7 mm. Plastic sections were stained with 0.1% toluidine blue and imaged with a Zeiss Axio M2 imager microscope.

For gene expression analysis, we employed two approaches: vibratome cross-sections and whole-mounts. First, in the case of vibratome cross-sections, 1cm-root sample (0.5 cm below the root junction) were collected in water and then fixed using a 4% PFA solution (in 1xPBS) following the protocol described in (Ursache *et al.*, 2018). The fixation was performed under vacuum for 1-2 hours, and after this, the root parts were rinsed twice for 1 min in 1xPBS. The root samples were embedded in agarose blocks to obtain cross-

sections with the vibratome. Approximately 20 vibratome cross-sections were collected in water, and then transfer to clearing solution (ClearSee), as described in (Ursache *et al.*, 2018). Staining of vibratome cross-sections was prepared following the protocol described in (Wunderling *et al.*, 2018). The cross-sections were collected in water and stained with either Direct Red or Calcoflour White for subsequent examination. For Calcoflour White staining, vibratome cross-sections were stained with a 0.05% Calcoflour White solution (in ClearSee) for 5 minutes. As for Direct Red staining, vibrotome sections were incubated for 30 minutes in a 0.05% Direct Red solution (in ClearSee). In both cases, the cross-sections were subsequently washed three times for 5 minutes each with the clearing solution and mounted on a glass slide using ClearSee. For whole-mounts, root sections were directly mounted on a solution of Propidium Iodide (PI, 10-20 mg/ml) for subsequent analysis.

Confocal Laser Scanning Microscopy Imaging

Confocal pictures were obtained using a Zeiss LSM 880 CLS microscope. Whole mount roots, roots virbratome sections, plastic cross-sections or clear sections cross-sections were imaged with a Zeiss LSM880 with the following settings: cork autofluorescence (ex.405 nm; em. 420-460 nm), Basic Fuchsin (ex.566 nm; em.570-630 nm). FY (ex.488nm, em. 490- 540 nm), GFP (488nm, 490 -510 nm), Venus and Citrine: (ex. 514 nm; em. 520–540 nm) and Calcofluor white (ex.475 nm, em 405-425nm). 3D reconstructions and Orthogonal views of a Z stack were obtained using the ZEN Black software.

Suberin quantification

For the determination of suberin content in the periderm, GC-MS (Gas Chromatography-Mass Spectrometry) was employed. Sample collection and the suberin extraction were conducted following the protocol described in (Andersen *et al.*, 2021). In brief, root sections of approximately 2 cm from the root junction were collected from 19-day-old plants. Most lateral roots were removed from the samples. Enzymatic treatment was utilized for cell wall degradation, followed by Soxhlet extraction with a chloroform: methanol mixture (1:1; v/v) for 2 days to remove unbound lipids. In order to quantify (µg/mg dried sample) the suberin monomers detected by GC-MS, 25 µl of C32 alkane internal standard (13,5 mg/50 ml) was added to each sample.

Image Analyses

In periderm anatomy studies, plastic cross-sections were used to quantify the number of periderm and cork cells. Initially, bright-field cross-section images were used to determine the total count of periderm cells. Subsequently, fluorescent microscopy was applied to the same plastic cross-sections to ascertain the number of cork cells. Cross-sections were exposed to UV excitation through a 365 nm DAPI filter to observe the intrinsic autofluorescence of mature cork cells. The total number of periderm cells and the ratio of phellem

cells to the total number of periderm cells are presented in the results. Three independent experiments were conducted, and only one was presented. The cork ratio: cork length in cm / total root length in cm was measured as described in (Wunderling *et al.*, 2018).

Molecular Cloning

Green gate cloning system, described in (Lampropoulos *et al.*, 2013), was used to create the majority of constructs used in this study. Promoters were amplified from genomic DNA and the coding sequences from root c-DNA. Primers used for the cloning are listed in Data S5. All modules and vectors used in this study are described in Data S3. The module assembly strategy is described in Data S4. The promoter of MYB87 was cloned using Gateway technology in pDNOR207 and then introduced into a final destination vector containing NLS-GFP. All final constructs were transformed into Agrobacterium tumefaciens GV3101 together with pSoup for final transformation via floral dipping or transactivation assays

Genome editing

The cloning of plasmids used for genome editing of MYB87 via CRISPR-Cas9 was conducted following the procedure outlined in (Fauser *et al.*, 2014). The following gRNA was used: attgACCGTGCTGCGACAAGATGG. MYB87 sgRNA primers are listed in Data5. In brief, oligos were annealed and subsequently ligated into BbsI-linearized Gateway-entry plasmid pEn-Chimera. Finally, MYB87 sgRNA was introduced into the Crispr-Cas9 using a Gateway reaction. The final constructs were introduced into Col-0 plants using floral dipping. Positive Fast-red-T1 seeds were selected, cultivated in soil, and genotyped. T2 seeds without the Crispr-Cas9 construct were selected (no red fluorescent seeds), propagated, and genotyped to obtain homozygous MYB87 mutant plants. For genotyping, we amplified the region of interest with the primers described in DataS5 and analyzed it by sequencing.

Sample preparation for RNA-seq and qPCR experiments

RNA was extracted from root sections of approximately 2 cm from the root junction. Lateral roots were excised, and the samples were promptly collected in a tube submerged in liquid nitrogen to preserve RNA integrity. To create one single RNA sample, between 40 and 50 root sections were pooled together. The RNA extraction was done using the Universal RNA Purification Kit (Roboklon, E3598-02) according to the manufacturer's protocol.

RNAseq data processing and analysis.

RNA sequencing (pair-end 150bp) was performed at Novogene. Raw data sequences will be available after publishing. Data processing and data analysis were performed using the Galaxy platform (https://usegalaxy.eu/)(Afgan *et al.*, 2018). Adaptors were removed with Trim Galore using default

parameters, and read quality was assessed with FastQC. Reads were aligned to the TAIR10 genome using HISAT2 using default parameters. Reads were counted using featureCounts, and differential gene expression analysis was performed using DESeq2 and can be queried in DataS6.

qPCR analysis

C-DNA was synthesized using AMV Reverse Transcriptase Native (Roboklon, E1372-01). qPCR was performed using MESA blue (Eurogentec, RT-SYS2X-03- +NRWOUB) in a CFX96 Real-Time System machine (BIO-RAD). Primers used for qPCR are listed in Table S5. The relative expression was calculated using CFX Maestro software (BIO-RAD), and the samples were normalized against EF1. qPCR experiments were repeated at least 3 times, and one experiment was shown.

Transient Transactivation Studies in Nicotiana benthamiana Leaves

Using the GreenGate cloning system, we constructed a vector containing the 35s promoter and our transcription factor of interest, tagged with mCherry at the C-terminus. Subsequently, we generated additional GreenGate vectors where the fungal luciferase (*N. nambi* luciferase, nnLuz) was expressed downstream of our promoter of interest. These vectors were then transformed into GV3101 Agrobacterium strains and cultured overnight until reaching an OD 600 of 0.8. To transiently express both the luciferase and transcription factor, we infiltrated 3-week-old N. benthamiana leaves via co-infiltration with the P336-FBP_11 vector from (Khakhar *et al.*, 2020) (Available from AddGene (#139702)), which contains the luciferin production and recycling pathway. For co-infiltration, the Agrobacterium culture of each vector was diluted to an OD of 0.250, resulting in a total OD of 0.750 for each leaf. The mixture was washed with water twice and then resuspended in an infiltration medium composed of 10mM MgCl2, 1mM MES, and 100µM Acetosyringone. The resuspended solution was incubated for 1 hour and subsequently infiltrated into tobacco leaves.

After 3 days post-infiltration (dpi), the infiltrated leaves were evaluated for luminescence using a CCD camera (Amersham 600 gel imager) following a 3-minute exposure.

Quantitative Analysis

No statistical method was emplyed to predetermine the sample size. The experiments were not randomized. IBM SPSS Statistics version 24-25-26 (IBM) was used to make statistical analysis. The number of periderm and phellem cells, the root length, and the root suberin coverage was determined using imageJ / Fiji5. The Root length and Root Suberin Coverage were measured according to (Andersen *et al.*, 2021). For the suberin root coverage quantification in old roots that comprised the periderm, the statistic was performed separately for each root zone.

For multiple sample comparisons, a oneway ANOVA with Tukeys's post hoc (equal variance not assumed)

test was performed unless otherwise stated. For GC-MS and periderm experiments, statistical analyses were performed with IBM SPSS Statistics version 25 (IBM). First, the datasets were tested for the homogeneity of variances using the Levene's Test. The significant differences between the two datasets were calculated using a Welch's two-tailed t-test in case of a non-homogeneous variance or a Student's two-tailed t test if the variance was homogeneous. For the detailed suberin quantification of each compound/category of compounds via GC-MS, the statistic was performed separately for each compound/category (indicated by the absence or presence of ';'' close to the letter).

Figures:

Figure 1: (A) Schematics drown of a periderm, the different tissue layers are highlighted in distinct colors: cork; green: cork cambium; beige: phelloderm. (B) Confocal microscopy images of vibratome cross-sections of 19-day-old roots showing the expression of MYB68 (*pMYB68: NLS-3xGFP*; Green) and MYB84 *(pMYB84:NLS-3xGFP*; Green) in the cork (white arrows) the cells are outlined by Calcofluor White staining (magenta). (C and D) Suberin quantification by Fluorol yellow (FY) staining and suberin coverage in the cork of wild type (WT), *myb68 myb84*, and *myb quad* (*myb37 myb38 myb84 myb68*) roots. (C) Representative images showing fluorescence relative intensities of cork cells stained with FY (14-day-old plants). (D) Suberin deposition in the Arabidopsis root periderm can be divided into two distinct stages. In the Developing cork (light orange) region, only a few cork cells are suberized, while in the mature cork (dark orange) region, all cork cells are already differentiated. Relative quantification of developing and mature cork suberin regions in 19-day-old plants. (E) Quantification of suberin constituents (µg/ mg dry sample) via GC-MS in the cork of WT and *myb quadr*. Suberin constituents include DCA (α,ω-dicarboxylic acids), ω-OH (ω-hydroxy fatty acids), Alcohol (fatty alcohols), Acid (fatty acids) and aromatic compounds (cis-ferulic acid, p-coumaric acid and trans-ferulic acid). (F) Representative images showing fluorescence relative intensities of FY signal in the cork of pGPAT5:MYB68-GR, induced and not induced roots. 9-day-old plants were treated for 5 days with mock or 10µM DEX. (G and H) NaCl effect on *myb quadr.* and WT growth. (G) Plants were grown for 9 days prior to transfer to split plates (Most upper part is supplemented with 150 mm NaCl or mock) for 5 days**.** H) Quantification of the rosette area (cm^2) of (G). In (D) One-way ANOVA (95% CI, post hoc: Tukey HSD, n = 10–14). In (E) Student T-Test (*: $P<0.05$, n:3-4). In (H) Two-way ANOVA, G*T: Genotype (WT or *myb quadr*.) treatment (mock or Wt) (95% CI, *:$P<0.05$, n = 16-18). Black bars: 1cm, white scale bars: 20µM, yellow scale bars: 10µM

Figure 1

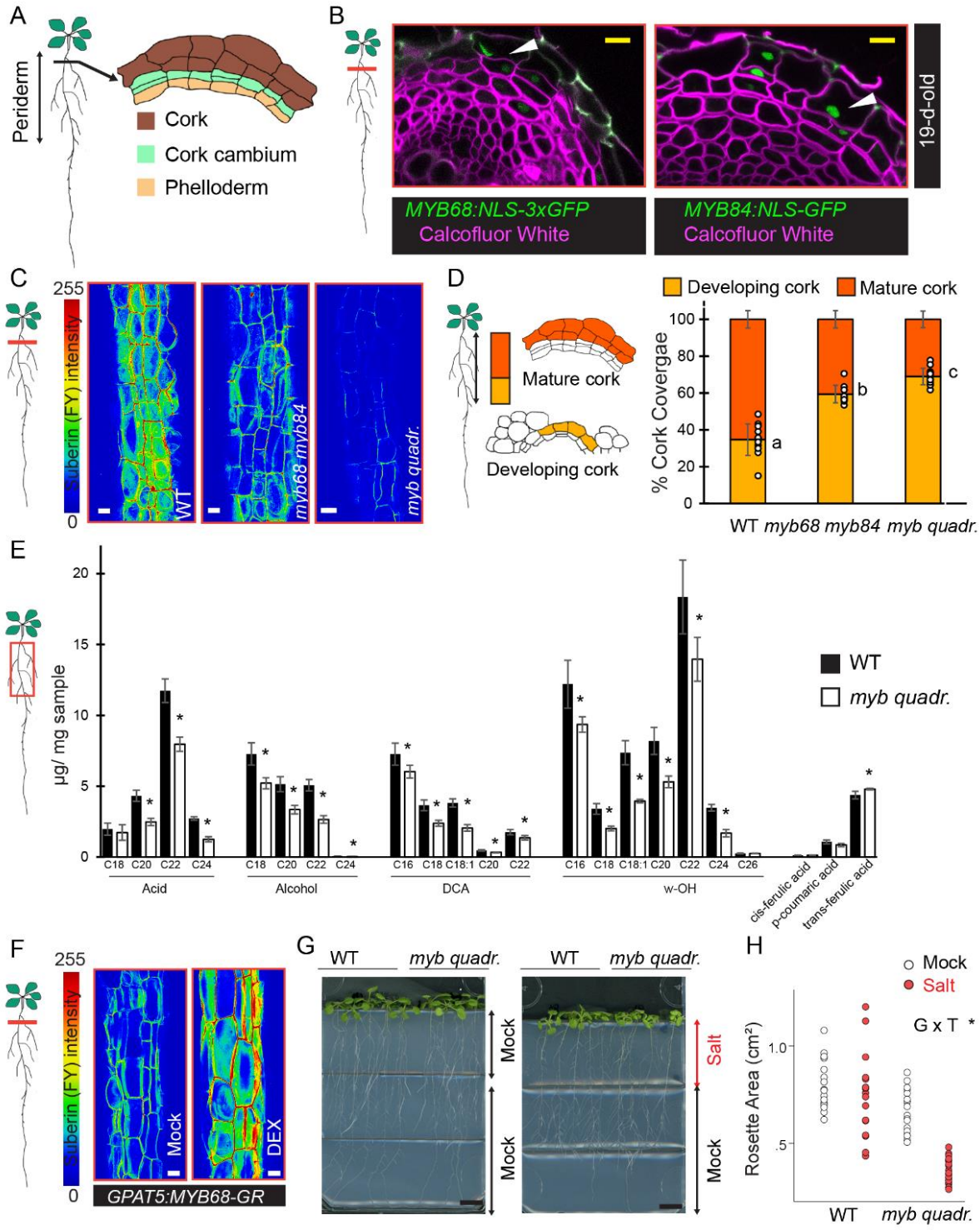
A
Periderm
Cork
Cork cambium
Phelloderm
B
19-d-old
MYB68:NLS-3xGFP
Calcofluor White
MYB84:NLS-GFP
Calcofluor White
C
255
Suberin (FY) intensity
0
WT
myb68 myb84
myb quadr.
D
Mature cork
Developing cork
Developing cork
Mature cork
% Cork Covergae
100
80
60
40
20
0
a
b
c
WT myb68 myb84 myb quadr.
E
µg/ mg sample
20
15
10
5
0
WT
myb quadr.
C18 C20 C22 C24
Acid
C18 C20 C22 C24
Alcohol
C16 C18 C18:1 C20 C22
DCA
C16 C18 C18:1 C20 C22 C24 C26
w-OH
cis-ferulic acid
p-coumaric acid
trans-ferulic acid
F
255
Suberin (FY) intensity
0
Mock
DEX
GPAT5:MYB68-GR
G
WT
myb quadr.
WT
myb quadr.
Mock
Mock
Salt
Mock
H
Mock
Salt
G x T *
Rosette Area (cm²)
1.0
.5
WT
myb quadr.

Figure 2: (A) Orthogonal view of z stacks showing the expression of GELP38 (*pGELP38:NLS-3xVenus*), GELP96 (*pGELP96:NLS-3xVenus*), GELP51(*pGELP51:NLS-3xVenus*) and GELP49 (*pGELP49:NLS-3xVenus*) in the cork (white arrows) (14 day- old plants). (B) Representative images showing fluorescence relative intensities of FY signal in the cork of WT, *gelp q1* and *gelp q2* (*gelp38 gelp51 gelp49 gelp96 gelp22*) (14-day-old-plants). (C) Relative quantification of developing and mature cork suberin regions of WT, *gelp q1* and *gelp q2* 19-day-old roots. (D) Representative images showing fluorescence relative intensities of FY signal of 14-day-old WT, *myb68 myb84* and *pGPAT5:GELP51 myb68 myb84* roots. (E) Relative quantification of developing and mature cork suberin regions of 19-day-old WT, *myb68 myb84* and *pGPAT5:GELP51 myb68 myb84* plants. (F) Log2 Fold Change of relative expression of selected suberin biosynthesis, polymerizing, and regulating genes, upon induction of MYB68 in the periderm (*pPER15:MYB68-GR;* plants were grown 17 days prior to treatment with mock or 10 µM DEX for 24h.). Data were obtained by qPCR as described in the methods section. p values (P val.) are based on Student's t test mock vs DEX. (G) Transactivation studies in *N. benthamiana* leaves using luciferase reporting system. Upper panels show the luminescence intensities of leaves co-infiltrated with an effector construct (*p35S:mCherry*, *p35S:MYB68-mCherry*, *p35S:MYB84-mCherry*), a reporter construct (promoter of interest fused with LUZ reporter (*pGELP8:LUX, pGELP38:LUX* and *pGELP51:LUX*), and the FBP12 construct (encoding the fungal bioluminescent pathway. Lower panels show the RGB images of the same leaves. (C and E) One-way ANOVA (95% confidence interval [CI], post hoc: Tukey HSD, n = 10-14). Black scale bars: 1cm and white scale bars: 20µm.

Figure 2

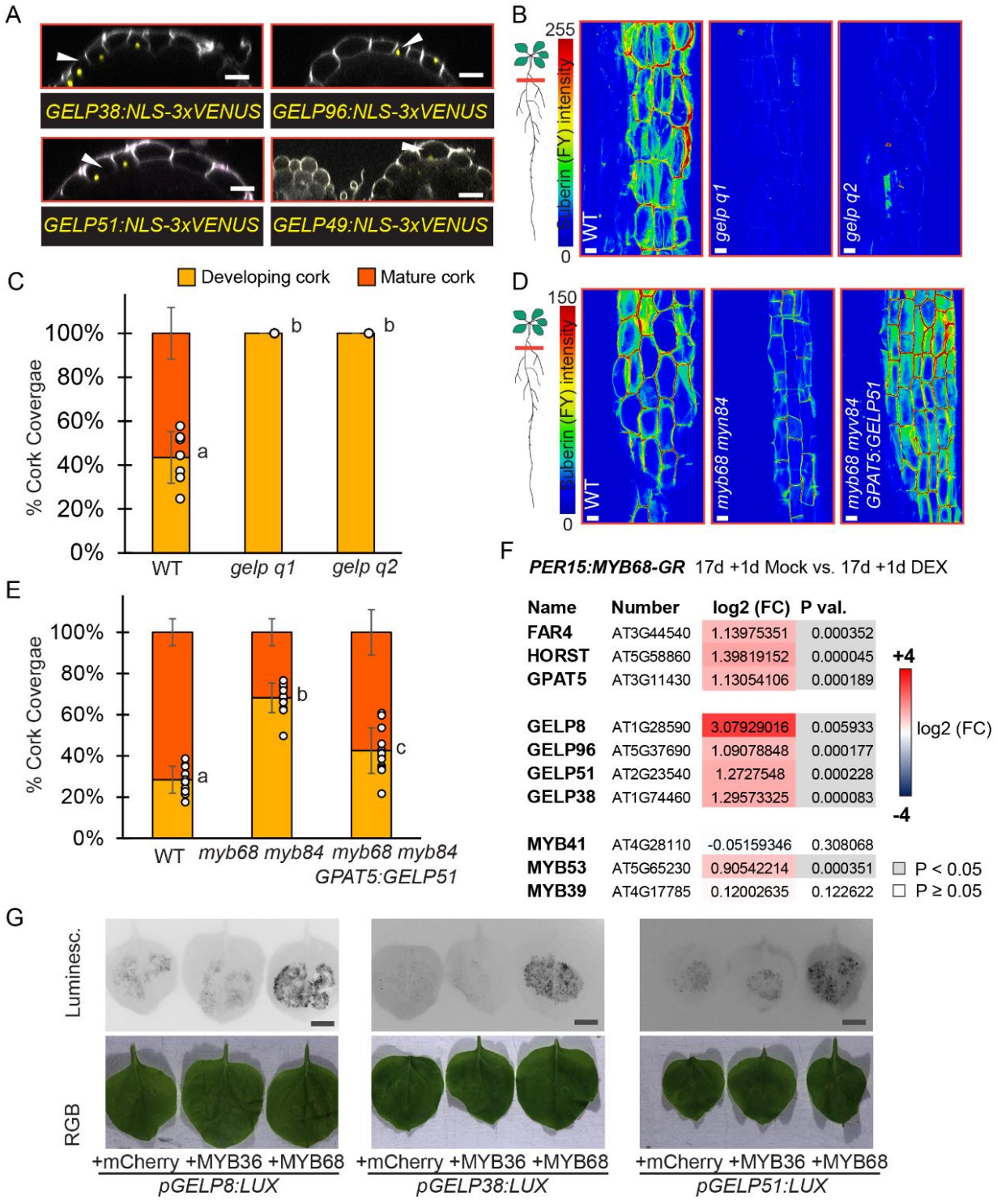
A
GELP38:NLS-3xVENUS
GELP96:NLS-3xVENUS
GELP51:NLS-3xVENUS
GELP49:NLS-3xVENUS
B
255
Suberin (FY) intensity
0
WT
gelp q1
gelp q2
C
Developing cork
Mature cork
% Cork Covergae
100%
80%
60%
40%
20%
0%
a
b
b
WT
gelp q1
gelp q2
D
150
Suberin (FY) intensity
0
WT
myb68 myn84
myb68 myv84
GPAT5:GELP51
E
% Cork Covergae
100%
80%
60%
40%
20%
0%
a
b
c
WT
myb68 myb84
myb68 myb84
GPAT5:GELP51
F
PER15:MYB68-GR 17d +1d Mock vs. 17d +1d DEX
Name Number log2 (FC) P val.
FAR4 AT3G44540 1.13975351 0.000352
HORST AT5G58860 1.39819152 0.000045
GPAT5 AT3G11430 1.13054106 0.000189
GELP8 AT1G28590 3.07929016 0.005933
GELP96 AT5G37690 1.09078848 0.000177
GELP51 AT2G23540 1.2727548 0.000228
GELP38 AT1G74460 1.29573325 0.000083
MYB41 AT4G28110 -0.05159346 0.308068
MYB53 AT5G65230 0.90542214 0.000351
MYB39 AT4G17785 0.12002635 0.122622
+4
log2 (FC)
-4
P < 0.05
P ≥ 0.05
G
Luminesc.
RGB
+mCherry +MYB36 +MYB68
pGELP8:LUX
+mCherry +MYB36 +MYB68
pGELP38:LUX
+mCherry +MYB36 +MYB68
pGELP51:LUX

Figure 3: (A) Cross-sections (plastic embedding) of the uppermost part of 14-day-old WT, *myb68 myb84*, and *myb quadr*. roots. (B) Quantification of the total number of periderm cells of the experiment is presented in (A). (C) Quantification of the ratio of the number of cork cells/number of periderm cells in the experiment presented in (A). (D) Cross-sections and fluorol yellow staining of the uppermost part of 14-day-old *pPER15:MYB68-GR* roots. 9-day-old plants were treated for 5 days with mock or 10 µM DEX. The white arrows highlight the two layers of cork. (E and F) Ratio of the number of cork cells/number of periderm cells and the total number of periderm cells of the experiment presented in (D). (G) Cross-sections of the uppermost part of 14-day-old WT, *ralph horst*, and *gelp q1* roots. (H) Quantification of the ratio of the number of cork cells/number of periderm cells in the experiment presented in (G). (B, C and H). One-way ANOVA (95% confidence interval [CI], post hoc: Tukey HSD, n = 15-20). (E and F) Student T-Test (*: $P<0.05$, n:15-20). Black and yellow scale bars: 20µm. Red dots indicate cork cells, and the whole periderm is highlighted in green.

Figure 3

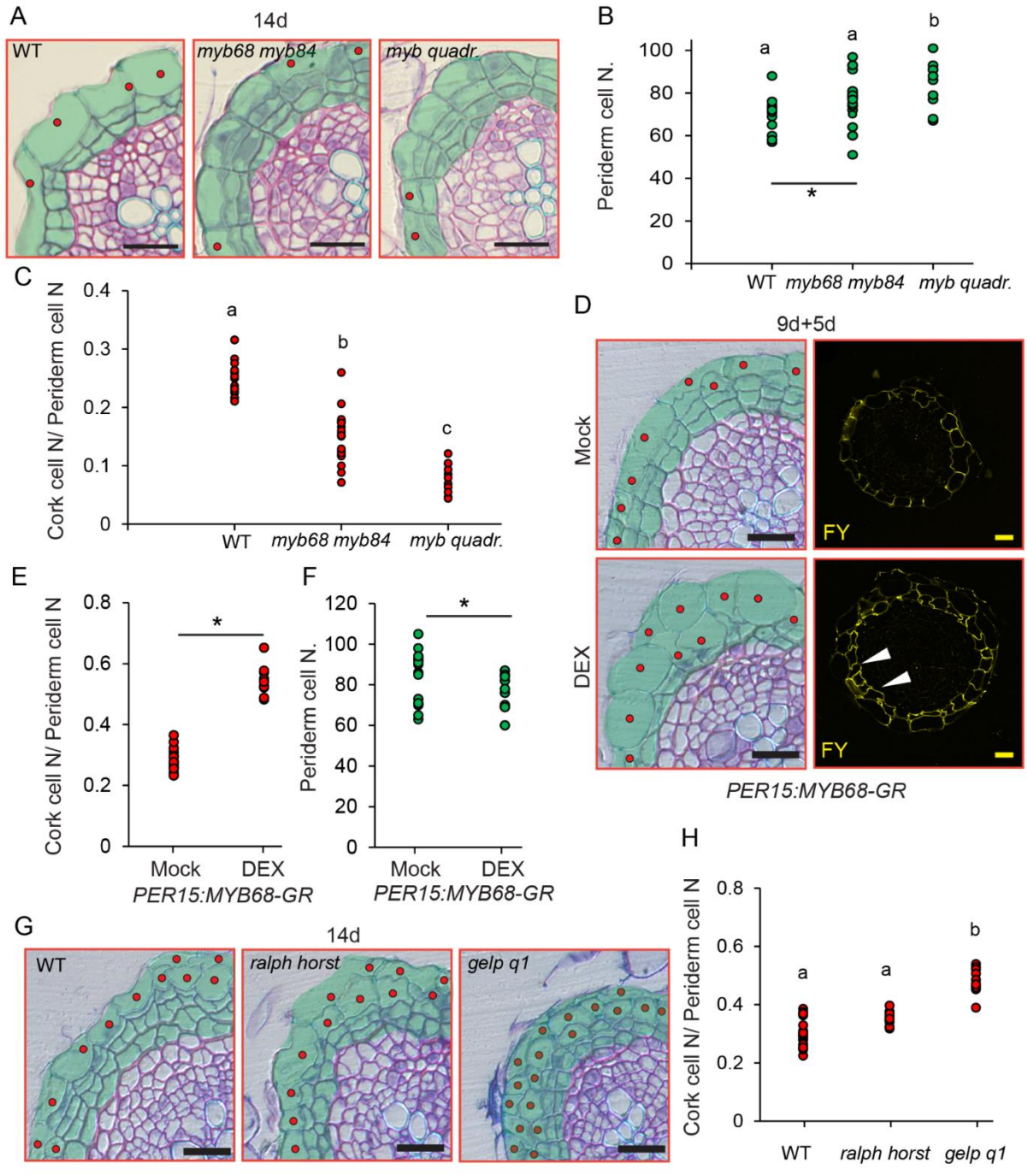
A
14d
WT
myb68 myb84
myb quadr.
B
Periderm cell N.
100
80
60
40
20
0
a
a
b
*
WT
myb68 myb84
myb quadr.
C
Cork cell N/ Periderm cell N
0.4
0.3
0.2
0.1
0
a
b
c
WT
myb68 myb84
myb quadr.
D
9d+5d
Mock
DEX
FY
FY
PER15:MYB68-GR
E
Cork cell N/ Periderm cell N
0.8
0.6
0.4
0.2
0
*
Mock
DEX
PER15:MYB68-GR
F
Periderm cell N.
120
100
80
60
40
20
0
*
Mock
DEX
PER15:MYB68-GR
G
14d
WT
ralph horst
gelp q1
H
Cork cell N/ Periderm cell N
0.8
0.6
0.4
0.2
0
a
a
b
WT
ralph horst
gelp q1

Figure 4: (A) Cross-sections (plastic embedding) of the uppermost part of 14-day-old WT and *myb quadr*. roots treated with N-1-naphthylphthalamic acid (NPA). 9-day-old plants were treated for 5 days with mock or 10µM NPA. (B and C) Quantification of the ratio of the number of cork cells/number of periderm cells and the total number of periderm cells in the experiment presented in (A). (D) Cross-sections of the uppermost part of 14-day-old WT, *myb68 myb84*, *wox4* and *wox4 myb68 myb84.* (E) Quantification of the total number of periderm cells of the experiment presented in (D). (F) Cross-sections of the uppermost part of 14-day-old WT, *myb68 myb84*, *bp* and *bp myb68 myb84.* (G) Quantification of the total number of periderm cells of the experiment presented in (F). In (B, C, E, and F) Two-tailed Students T-Test (*: $P<0.05$, n:15-20). Black scale bars: 20µm. The whole periderm is highlighted in green.

Figure 4

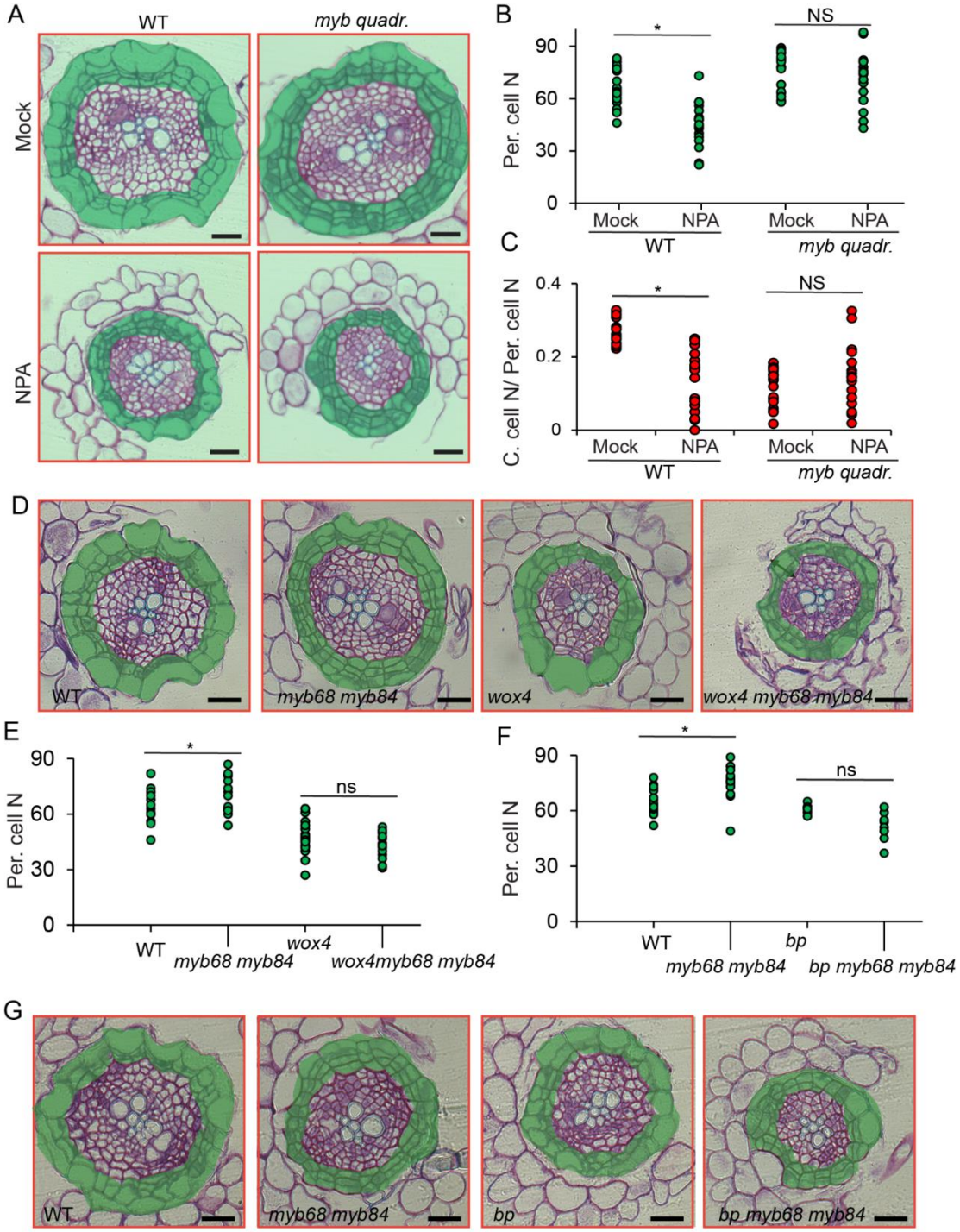
A
WT
myb quadr.
Mock
NPA
B
Per. cell N
90
60
30
0
*
NS
Mock
NPA
Mock
NPA
WT
myb quadr.
C
C. cell N/ Per. cell N
0.4
0.2
0
*
NS
Mock
NPA
Mock
NPA
WT
myb quadr.
D
WT
myb68 myb84
wox4
wox4 myb68 myb84
E
Per. cell N
90
60
30
0
*
ns
WT
myb68 myb84
wox4
wox4myb68 myb84
F
Per. cell N
90
60
30
0
*
ns
WT
myb68 myb84
bp
bp myb68 myb84
G
WT
myb68 myb84
bp
bp myb68 myb84

Figure 5 (A) Orthogonal view of z stacks showing the expression of MYB41 (*pMB41:NLS-3xVenus*), MYB53 (*pMYB53:NLS-3xVenus*), and MYB93 (*pMYB93:NLS-3xVenus*) in the cork (red arrowheads) of 14 day-old plants. (B and C) Suberin quantification by Fluorol yellow (FY) staining and suberin coverage in the cork of WT, *myb41myb53 myb92 myb93,* and *myb quadr*. roots. (B) Relative quantification of developing and mature cork suberin regions of 19-day-old plants. (C) Representative images of the relative intensity of FY signal c (14-day-old plants). (D) Cross-sections (plastic embedding) of the uppermost part of 14-day-old WT and *myb41 myb53 myb92 myb93* and *myb quadr*. roots. The upper panels show bright field pictures and the lower panels show autofluorescence (DAPI filter) in response to UV radiation of cork cells. The red arrowheads indicate the absence of differentiated cork cells. (E and F) Quantification of the ratio of the number of cork cells/number of periderm cells and the total number of periderm cells of the experiment presented in (D). (G) Quantification of the number of xylem vessels upon induction of MYB68 and MYB87 in the vascular cambium (*pPXY:MYB68-GR* and *pPXY:MYB87-GR*; 9-day-old plants were treated for 5 days with mock or 10µM DEX) in the cross-sections shown in (H and S). (H) Cross-sections of the uppermost part of 14-day-old pPXY:MYB68-GR roots. (B, E and F) One-way ANOVA (95% confidence interval [CI], post hoc: Tukey HSD, (B) n = 10-14, (E and F) n=15-20. (G) Student T-Test (*: $P<0.05$, n:15-20). Black scale bars: 20µm. The whole periderm is highlighted in green.

Figure 5

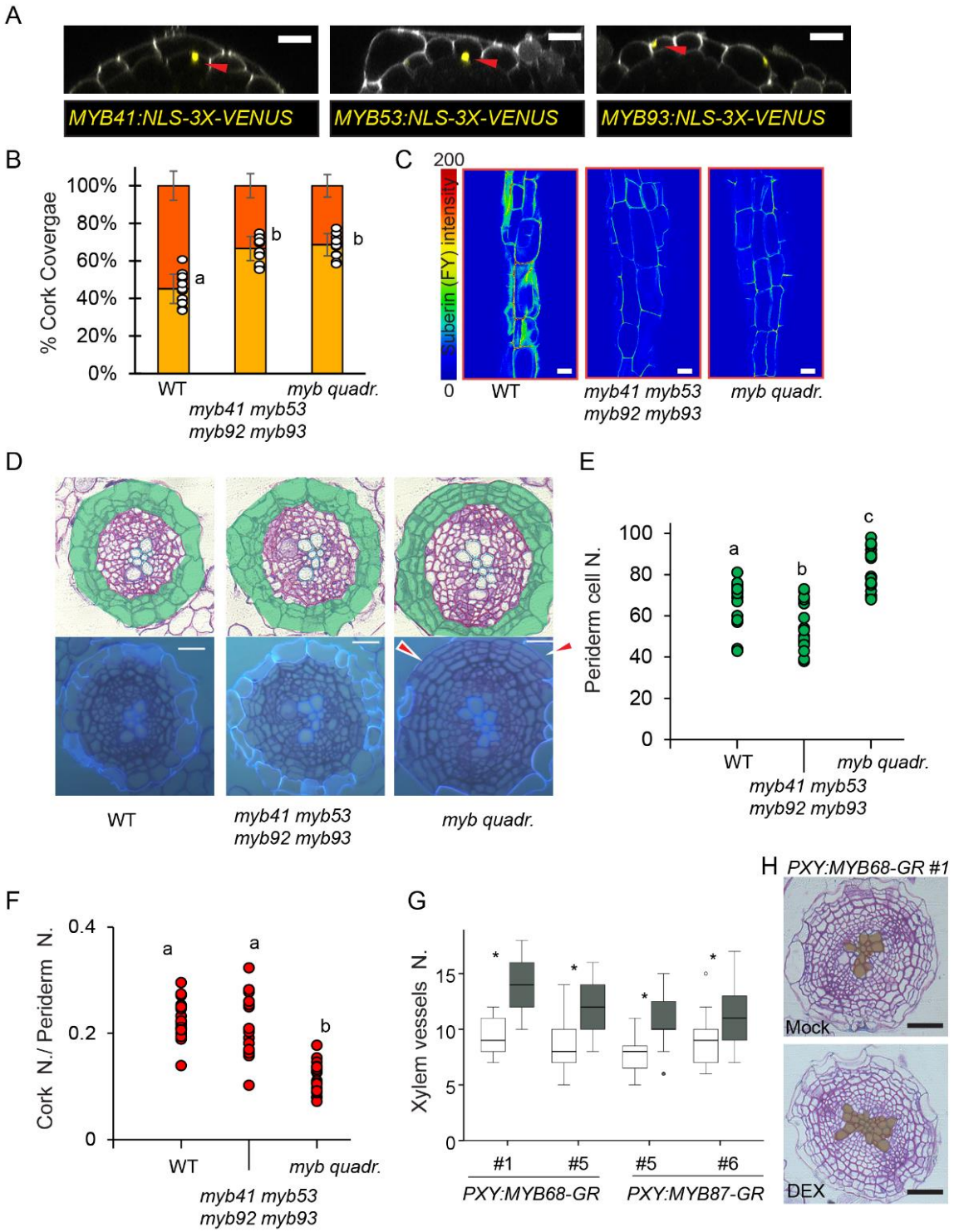
A
MYB41:NLS-3X-VENUS
MYB53:NLS-3X-VENUS
MYB93:NLS-3X-VENUS
B
% Cork Covergae
100%
80%
60%
40%
20%
0%
a
b
b
WT
myb quadr.
myb41 myb53
myb92 myb93
C
200
Suberin (FY) intensity
0
WT
myb41 myb53
myb92 myb93
myb quadr.
D
WT
myb41 myb53
myb92 myb93
myb quadr.
E
Periderm cell N.
100
80
60
40
20
0
a
b
c
WT
myb quadr.
myb41 myb53
myb92 myb93
F
Cork N./ Periderm N.
0.4
0.2
0
a
a
b
WT
myb quadr.
myb41 myb53
myb92 myb93
G
Xylem vessels N.
15
10
5
0
#1
#5
#5
#6
PXY:MYB68-GR
PXY:MYB87-GR
H
PXY:MYB68-GR #1
Mock
DEX

Supplemental figures:

Figure S1 (A) Orthogonal view of z stacks showing the expression of MYB68 (pMYB68:NLS-3xGFP W13Y), MYB84 (MYB84:NLS-3xGFP W13Y), MYB87 (pMYB87:NLS-GFP), MYB37(pMYB37:NLS-GFP), MYB38 (pMYB38:NLS-Scarlet) and MYB36 (pMYB36g:NLS-GFP *myb36*) at two periderm developmental stages (14-day-old roots). W131Y (a ubiquitous plasma membrane marker), Pi, or the intrinsic autofluorescence of cork cells was employed to outlay cells. The white arrows indicate the expression in the cork. (B) Confocal microscopy images of vibratome cross-sections of 19-day-old roots showing the expression of MYB37, MYB38, MYB36, and MYB87 in the periderm using the same lines used in (A). The white arrowheads indicate the expression in the cork. (C) Orthogonal view of z stacks showing the expression of MYB68 and MYB84 together with Cork (*GPAT5:mCitrine-SYP122)* differentiating cork/cork cambium (*PER15:mCherry-SYP122*), and cork cambium/phelloderm WOX4 (*WOX4:YFPer*) cambium and phelloderm) reporters. (D and E) Representative images of the relative intensity of FY signal in the cork. (D) WT, *myb68*, *myb84*, *myb87* and *myb37 myb38 myb84*. (E), WT and *myb36.* White scale bars: 20µm.

Supplemental figure 1

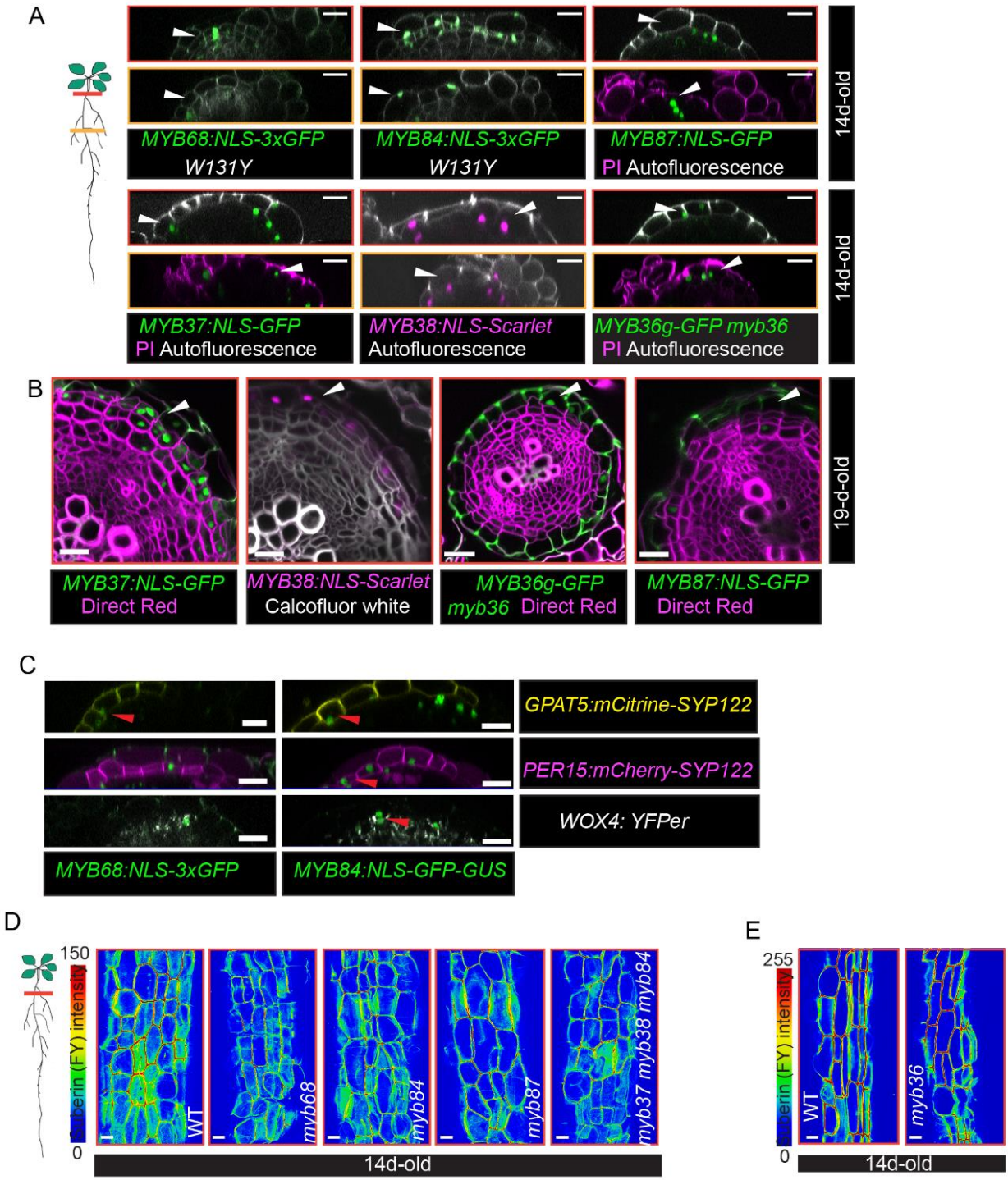

Figure S2 (A) Representative images of the fluorescence relative intensities of fluorol yellow signal in the periderm of 14-day-old WT, *myb68 myb87*, *myb68 myb84*, and *myb quadr*. roots. (B, C, and D) Quantification of percentage coverage of developing and mature cork of 19-day-old WT, *myb36*, *myb68*, *myb84*, *myb87*, *myb68 myb87*, *myb68 myb84*, *myb37 myb38 myb84* and *myb quadr*. roots. (E) Root length (cm) of 14-day-old WT, *myb68 myb84*, and *myb quadr*. roots (F) Quantification of cork ratio of 14-day-old WT, *myb68 myb84*, and *myb quadr*. roots. Data were obtained as described in the methods section (G) Relative quantification of developing and mature cork suberin regions of 19-day-old WT and pGPAT5:MYB68-GR *myb68 myb84* roots. 9-day-old plants were treated for 5 days with mock or 10µM DEX. (H) Representative images of the fluorescence relative intensities of fluorol yellow signal in the periderm of 14-day-old WT and pGPAT5:MYB68-GR *myb68myb84* roots. 9-day-old plants were treated for 5 days with mock or 10µM DEX. (I) Representative images of the fluorescence relative intensities of basic fuchsin signal of 14-day-old WT, *myb68myb84*, and *myb quadr* roots. (C, E, F and G) One-way ANOVA (95% confidence interval [CI], post hoc: Tukey HSD, (n = 10-14) (B and D) Two-tailed Students T-Test (*: $P<0.05$, n:15-20) White scale bars: 20µm.

Supplemental figure 2

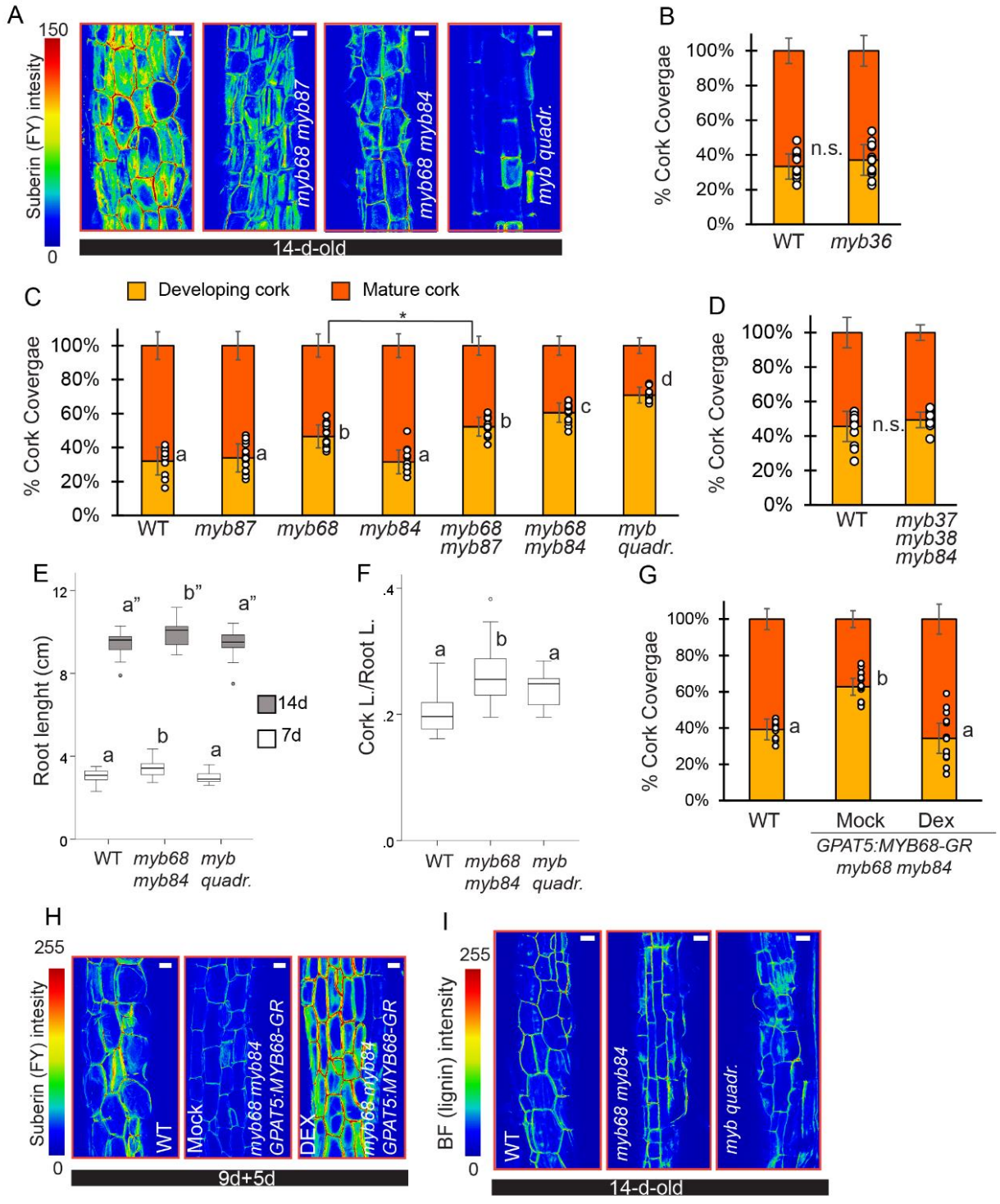

Figure S3 (A) Set of differentially expressed genes in WT vs. *myb68 myb84*, and Cork enriched gene vs All tissues (data from (Leal *et al.*, 2022)). The log 2 fold changes and adjusted P value are highlighted by a color code. (B,C, D and E). Transactivation studies in *N. benthamiana* leaves using luciferase reporting system. Upper panels show the luminescence intensities of leaves co-infiltrated with an effector construct (p35S:mCherry, p35S:MYB68-mCherry, p35S:MYB84-mCherry), a reporter construct (promoter of interest fused with LUZ reporter pFAR4:LUX, pGPAT5:LUX, pMYB53:LUX and pCASP2:LUX), and the FBP11 construct (encoding the fungal bioluminescent pathway). Lower panels show the RGB images of the same leaves. Black scale bars: 1cm

Supplemental figures 3

A

Gene Name	Gene Number	WT *vs* *myb68 myb84* log2 (FC)	WT *vs* *myb68 myb84* Padj	Cork *vs* All tissues log2 (FC)	Cork *vs* All tissues Padj
KCS2	AT1G04220	-0.2096	3.2E-01	2.77535	2.8E-108
FAR1	AT5G22500	-0.46373	5.2E-08	4.02325	6.2E-217
FAR4	AT3G44540	-0.55878	4.0E-06	2.91422	3.4E-127
FAR5	AT3G44550	-0.5692	1.5E-05	3.01793	3.9E-141
HORST	AT5G58860	-0.52038	1.3E-08	2.39351	2.9E-68
KCS20	AT5G43760	-0.5495	7.0E-08	0.71423	1.8E-07
GPAT5	AT3G11430	-0.4574	8.3E-04	2.09063	4.5E-41
RALPH	AT5G23190	-0.35883	7.2E-03	1.96528	1.2E-41
FACT	AT5G63560	-0.44276	2.2E-07	2.96926	3.6E-172
GELP8	AT1G28590	-1.68939	7.3E-21	2.02028	1.5E-10
GELP49	AT2G19050	-1.07764	7.8E-07	-0.35252	NA
GELP16	AT1G29670	-1.02618	9.3E-09	-1.03629	4.3E-03
GELP20	AT1G53940	-0.87642	1.8E-08	-0.90834	2.7E-01
GELP100	AT5G45670	-0.71291	8.6E-05	-0.53723	3.8E-01
GELP102	AT5G45950	-0.61461	1.2E-02	-1.24362	5.7E-02
GELP69	AT3G27950	-0.59009	1.4E-02	1.42546	8.9E-02
GELP67	AT3G16370	-0.58804	1.2E-05	-2.21072	1.5E-37
GELP103	AT5G45960	-0.57349	3.4E-02	1.43564	4.4E-02
GELP63	AT3G14210	-0.56307	2.5E-02	1.16349	1.9E-01
GELP96	AT5G37690	-0.54612	1.0E-06	2.09176	2.0E-65
GELP51	AT2G23540	-0.48493	4.0E-08	1.82549	2.6E-49
GELP41	AT1G75900	-0.4468	1.2E-01	-1.36994	1.0E-03
GELP73	AT3G50400	-0.43842	6.8E-03	1.28259	9.5E-15
GELP38	AT1G74460	-0.43497	1.5E-04	1.73705	1.6E-39
GELP22	AT1G54000	-0.26539	4.7E-02	0.29083	1.4E-01
MYB41	AT4G28110	0.16726	7.3E-01	0.98029	1.7E-02
MYB93	AT1G34670	-0.05159	8.6E-01	1.59116	4.0E-31
MYB53	AT5G65230	-0.38532	1.6E-01	1.24628	1.1E-09
MYB92	AT5G10280	0.17894	2.9E-01	1.89528	2.9E-29
MYB39	AT4G17785	0.01933	9.7E-01	1.92438	3.2E-06
MYB107	AT3G02940	0.23685	0.4895	1.57173	2.8E-21
MYB74	AT4G05100	0.80997	8E-06	2.39236	1.1E-40
MYB9	AT5G16770	0.03333	0.956	1.35888	1.1E-14
MYB102	AT4G21440	0.58926	2.6E-02	3.20486	3.5E-27
ANAC46	AT3G04060	-0.11147	5.9E-01	0.42101	1.9E-01
WOX4	AT1G46480	0.04027	9.2E-01		
BP	AT4G08150	0.47762	6.5E-05		

-2 log2 (FC)+2

-4 log2 (FC)+4

Padj < 0.01

Padj ≥ 0.01

B

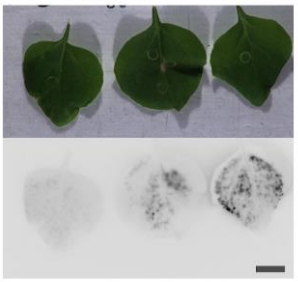

+mCherry +MYB36 +MYB68

pFAR4:LUX

C

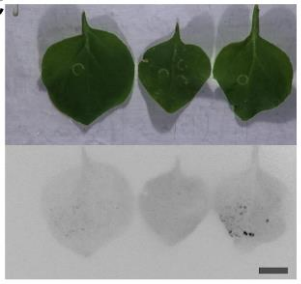

+mCherry +MYB36 +MYB68

pGPAT5:LUX

D

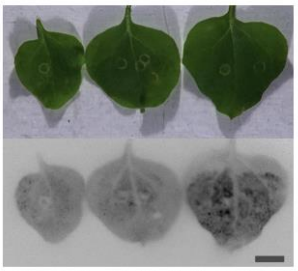

+mCherry +MYB36 +MYB68

pMYB53:LUX

E

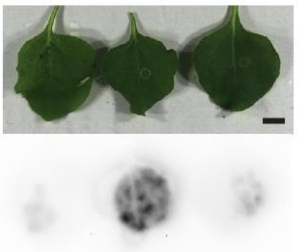

+mCherry +MYB36 +MYB68

pCASP2:LUX

Figure S4 (A) Cross-sections (plastic embedding) of the uppermost part of 14-day-old WT and *myb37 myb38 myb84.* Black double-headed arrows show the periderm area. (B and C) Quantification of the ratio of the number of cork cells/number of periderm cells and the total number of periderm cells of the experiment is presented in (A). (D) Cross-sections of the uppermost part of 14-day-old WT, *myb87*, *myb68*, *myb84*, *myb68myb87*, *myb68myb8*4, *myb quadr*. Black double-headed arrows show the periderm area. (E and F) Quantification of the ratio of the number of cork cells/number of periderm cells and the total number of periderm cells of the experiment presented in (D). (G) Cross-sections of 14-day-old WT, *myb68myb84*, and *myb quadr*. roots. It shows autofluorescence in response to UV radiation excitation of phellem cells. Red arrows show the developing cork characterized by the lack of fluorescence. (H and I) Fluorol Yellow (FY.) Staining and Cork suberin coverage of WT and *ralph horst* roots. (H) Relative quantification of developing and mature cork suberin regions of 19-day-old plants. (I) Fluorescence relative intensities of fluorol yellow signal in the periderm of 14-day-old plants. (J) Cross-sections of the uppermost part of 14-day-old *pPXY:MYB68-GR* and *pPXY:MYB87-GR*. Two independent lines of *pPXY:MYB87-GR* are shown. 9-day-old plants were treated for 5 days with mock or 10µM DEX. (B, C, and H) Two-tailed Students T-Test (*: $P<0.05$, (B and C) n:15-20, (H) n:10-15). (E and F) One-way ANOVA (95% confidence interval [CI], post hoc: Tukey HSD, (n = 15-20) Scale bars (black and white) in cross sections 20µm.

Supplemental figures 4

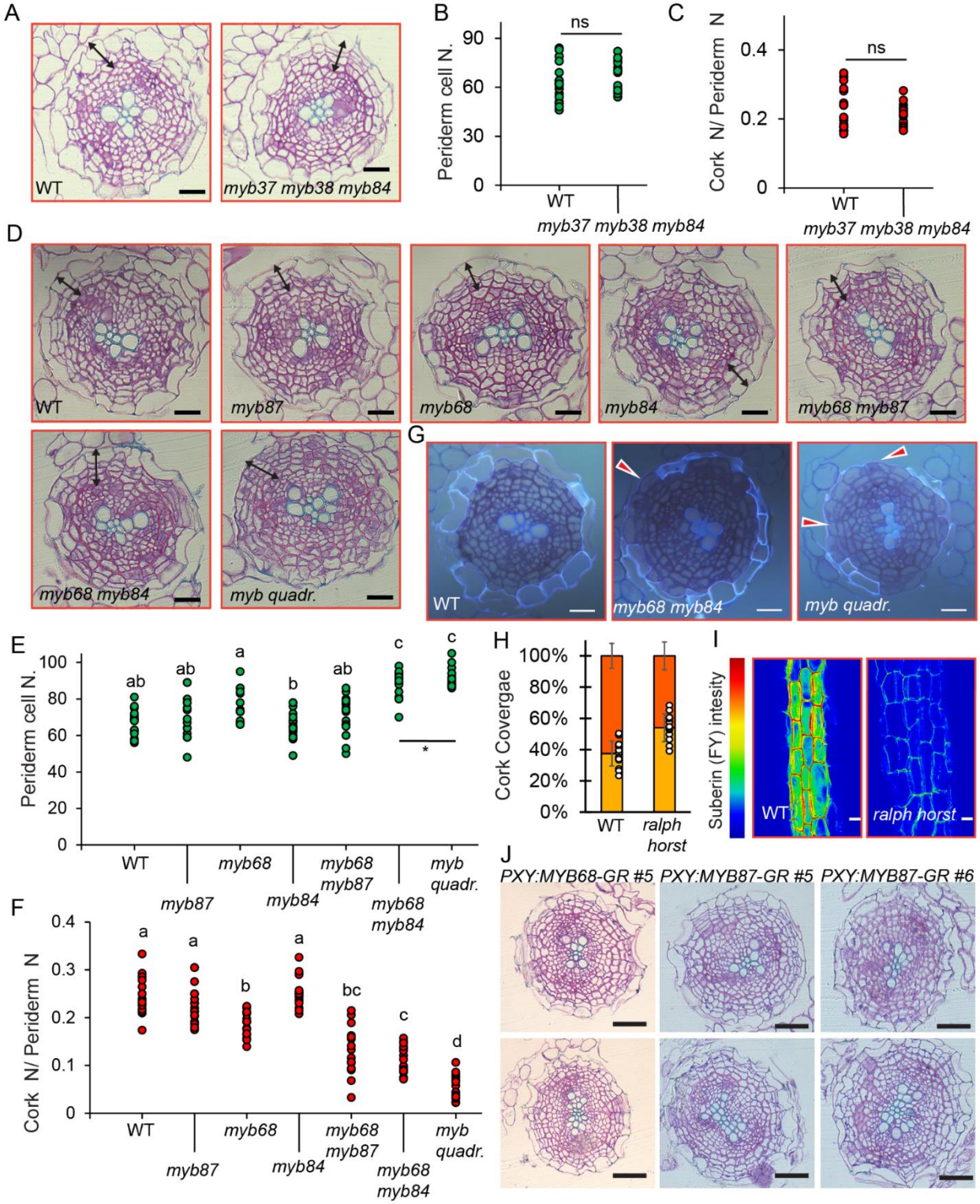

Supplemental tables:

Table S1 Transgenic lines used in this study

Arabidopsis Lines	**Obtained from/by**	**Described in**
MYB84:NLS-3xGFP	Our work	(Wunderling et al. 2018)
MYB68:NLS-3xGFP	This study	This study
MYB87:NLS-GFP	This study	This study
MYB37:NLS-3xGFP	This study	This study
MYB38:NLS-3xScarlet	This study	This study
MYB36g-GFP in myb36-1	N69051	
MYB68:NLS-3XGFP WOX4:ER-YFP	Crossing	This study (Suer et al. 2011)
MYB68:NLS-3XGFP GPAT5:mCitrine-SYP122	Crossing	(Wunderling et al. 2018) (Barberon et al. 2016)
MYB84:NLS-GFP-GUS WOX4:ER-YFP	Crossing	(Wunderling et al. 2018) (Suer et al. 2011)
MYB84:NLS-GFP-GUS GPAT5:mCitrine-SYP122	Crossing	(Wunderling et al. 2018) (Barberon et al. 2016)
GPAT5:MYB68-GR in MYB84:NLS-GFP GUS GPAT5:mCitrine-SYP122 PER15:mCherry-SYP122	This study	This study
GPAT5:MYB87-GR in MYB84:NLS-GFP GUS GPAT5:mCitrine-SYP122 PER15:mCherry-SYP122	This study	This study
GPAT5:MYB84-GR	This study	This study
GPAT5:MYB36-GR	This study	This study
GPAT5:MYB37-GR	This study	This study
GPAT5:MYB38-GR	This study	This study
GPAT5:MYB68-GR in myb68-2-4 myb84-1	This study	This study
PER15:MYB68-GR	This study	This study
PER15:MYB36-GR	This study	This study
PER15:MYB84-GR	This study	This study

GPAT5:GELP51 in myb68-2-4 myb84-1	This study	This study
GELP22:NLS-3xmVenus	Robertas Ursache	(Ursache et al. 2021)
GELP38:NLS-3xmVenus	Robertas Ursache	(Ursache et al. 2021)
GELP49:NLS-3xmVenus	Robertas Ursache	(Ursache et al. 2021)
GELP51:NLS-3xmVenus	Robertas Ursache	(Ursache et al. 2021)
GELP96:NLS-3xmVenus	Robertas Ursache	(Ursache et al. 2021)
MYB41:NLS-3xmVenus	Marie Barberon	(Shukla et al. 2021)
MYB93:NLS-3xmVenus	Marie Barberob	(Shukla et al. 2021)
ELTP:MYB41	Marie Barberob	(Shukla et al. 2021)

Table S2 Mutant alleles used in this study

Name used in the paper	**Allele**	**Atg**	**Type**	**Obtained from/by**	**Described in**
myb84	myb84-1	AT3G49690	Salk_141918C	N653820	(Feng et al. 2004)
myb68	myb68-2-4	AT5G65790	CRISPR	CRISPR in Col	This study
myb87	myb87-3a	AT4G37780	CRISPR	CRISPR in Col	This study
myb36	myb36-1	AT5G57620	EMS		
myb37 myb38 myb84	rax1-3 rax2-1 rax3-1	AT3G49690 AT5G23000 AT5G65790	SALK_071748C Wisconsin line; rax3 En-1	Sonia Gosalves	(Muller et al. 2006)
myb68 myb84	myb68-2-4 myb84-1	AT3G49690 AT5G65790	CRISPR Salk_141918C	Crossing	This study
myb68 myb87	myb68-2-4 myb87-3b	AT3G49690 AT5G65790	CRISPR	CRISPR in myb68-2-24	This study
myb quad.	rax1-3 rax2-1 rax3-1 myb68-2-4	AT3G49690 AT5G23000 AT5G23000 AT5G65790	SALK_071748C Wisconsin line; rax3 En-1 CRISPR	Crossing	This study

horst ralph	horst-1 ralph-1	At5g58860/CYP86A1 At5g23190/ CYP86B1	SALK_107454 SM.37066	Rochus Franke	(Salas-González et al. 2021)
gelp q1	gelp22-c1 gelp38-c3 gelp49-c1 gelp51-c1 gelp96-c1	AT1G54000 AT1G74460 AT2G19050 AT2G23540 AT5G37690	CRISPR	Robertas Ursache	(Ursache et al. 2021)
gelp q2	gelp22-c1 gelp38-c3 gelp49-c1 gelp51-c1 gelp96-c1	AT1G54000 AT1G74460 AT2G19050 AT2G23540 AT5G37690	CRISPR	Robertas Ursache	(Ursache et al. 2021)
wox4	wox4-1	AT1G46480	GK_462GO1	Thomas Greb	(Suer et al. 2011)
bp	bp-9	AT4G08150	Transposon insertion	Pautot Veronique	(Mele et al. 2003)
myb68 myb84 bp	myb68-2-4 myb84-1 bp-9	AT3G49690 AT5G65790 AT4G08150	CRISPR Salk_141918C Transposon insertion	Crossing	This study
myb68 myb84 wox4	myb68 2-4 myb84-1 wox4-1	AT3G49690 AT5G65790 AT1G46480	CRISPR Salk_141918C GK_462GO1	Crossing	This study
myb41 myb53 myb92 myb93	myb41_c2-myb53_c1-myb92_c1-myb93_c1	AT4G28110 AT5G65230 AT5G10280 AT1G34670	CRISPR	Marie Barberon	(Shukla et al. 2021)

Table S3 Greengate cloning mudles used in this study

GG modules/vectors used in this study	Ref.	Obtained
pGG-A0	(Lampropoulos et al. 2013)	Jan Lohmann
pGG-C0	(Lampropoulos et al. 2013)	Jan Lohmann
pZ03	(Lampropoulos et al. 2013)	Jan Lohmann
pGG-A-pGPAT5	This study	This study
pGG-A-pPER15	(Xiao et al. 2020)	Our group
pGG-A-pMYB68	This study	This study
pGG-A-pMYB84	This study	This study
pGG-A-pMYB37	This study	This study
pGG-B03 (B-dummy)	(Lampropoulos et al. 2013)	Jan Lohmann
pGG-B05 (NLS)	(Lampropoulos et al. 2013)	Jan Lohmann
pGG-C25 (3xGFP)	(Lampropoulos et al. 2013)	Jan Lohmann
pGG-C-*MYB68*	This study	This study
pGG-C-*MYB36*	This study	This study
pGG-C-GELP51	This study	This study
pGG-D-GR	(Ramakrishna et al. 2019)	Thomas Greb
pGG-D2 (D-dummy)	(Lampropoulos et al. 2013)	Jan Lohmann
pGG-E1 (pea RBCS terminator)	(Lampropoulos et al. 2013)	Jan Lohmann
pGG-F5 (Hygro R)	(Lampropoulos et al. 2013)	Jan Lohmann
pGG-F12 (Sulfo R)	(Lampropoulos et al. 2013)	Alexis Maizel
pGG-F-FR (FASTRED)	(Vilches Barro et al. 2019)	Alexis Maizel

Table S4 GreenGate assembly of final constrcuct used in this study

Final vector (in pZO2)	A	B	C	D	E	F
MYB68:NLS-3xGFP	*pMYB68*	B5	*C25*	D2	E1	F5
MYB84:NLS-3xGFP	*pMYB84*	B3	*C25*	D2	E1	F5
MYB37:NLS-3xGFP	*pMYB37*	B5	*C25*	D2	E1	F5
GPAT5:MYB68-GR	*pGPAT5*	B3	MYB68	GR	E1	FR
GPAT5:MYB36-GR	*pGPAT5*	B3	MYB36	GR	E1	FR
PER15:MYB68-GR	*pPER15*	B3	MYB68	GR	E1	FR
GPAT5:GELP51	*pGPAT5*	B3	GELP51	D2	E1	FR

Table S5 Oligos used in this study

Element	Primer for cloning	Sequence
pMYB68	A-pMYB68 F	AACAGGTCTCAACCTAATACGATGCTACTCTGTTGTT
	Br-pMYB68 R	AACAGGTCTCATGTTAGGAGGATGGTGTATGATAATG
pMYB84	A-pMYB84 F	AACAGGTCTCAACCTCGTGGACTTGGACTTGTTTA
	Br-pMYB84 R	AACAGGTCTCATGTTACTTGTACTCCTAGTGAAGTCTTG
pMYB37	A-pMYB37 F	AACAGGTCTCAACCTGTACTTCACATGATAACACG
	Br-pMYB37 R	AACAGGTCTCATGTTTCTCGTTAGTGAATTGAAG
pGPAT5	A-pGPAT5 F	AACAGGTCTCAACCTTCGCAAACGTCAATGGTCTAT
	Br-pGPAT5 R	AACAGGTCTCATGTTTTCTTTTGTTTTTTGCTCGAATATT A
MYB68	C-MYB68 F	AACAGGTCTCAGGCTCAATGGGAAGAGCACCGTGTTGT
	Dr-MYB68P R	AACAGGTCTCACTGACACATGATTTGGCGCATTGAA
MYB36	C-MYB36 F	AACAGGTCTCAGGCTCAATGGGAAGAGCTCCATGCT
	Dr-MYB36 R	AACAGGTCTCACTGAAACACTGTGGTAGCTCATCTGAG
GELP51	C-GELP51 F	AACAGGTCTCAGGCTCAATGGCCACAAGAGCTTCTA
	Dr-GELP51 R	AACAGGTCTCACTGATCACATATCTCTAAGTTTGC
pMYB38		
pMYB87	1/2B1pMYB87 F	AAAAAGCAGGCTGGGTATAAGTACAGCCCAAGT
	1/2B2pMYB87 R	AGAAAGCTGGGTATCTTGTTCTCTAGGTATTTATC
gRNA	MYB87 gRNA B F	
		ATTGGAAAGGGCCATGGTCGACGG
MYB87	MYB87 gRNA B R	
		AAACCCGTCGACCATGGCCCTTTC
gRNA MYB68		

Allele	**Primer for genotyping**	**Sequence**
myb84-1	WT :	AACAGGTCTCAACCTAATACGATGCTACTCTGTTGTT
	Mut:	AACAGGTCTCATGTTAGGAGGATGGTGTATGATAATG
rax1-3	WT :	AACAGGTCTCAACCTCGTGGACTTGGACTTGTTTA
	Mut:	AACAGGTCTCATGTTACTTGTACTCCTAGTGAAGTCTTG
rax2-1	WT :	
	Mut:	
rax3-1	WT :	AACAGGTCTCAACCTTCGCAAACGTCAATGGTCTAT
	Mut:	AACAGGTCTCATGTTTTCTTTTGTTTTTTGCTCGAATATT A
Wox4-1	WT :	AACAGGTCTCAGGCTCAATGGGAAGAGCACCGTGTTGT
	Mut:	AACAGGTCTCACTGACACATGATTTGGCGCATTGAA
bp-9	WT :	AACAGGTCTCAGGCTCAATGGGAAGAGCTCCATGCT
	Mut:	AACAGGTCTCACTGAAACACTGTGGTAGCTCATCTGAG
myb68-2-4	WT :	AACAGGTCTCAGGCTCAATGGCCACAAGAGCTTCTA
	Mut:	AACAGGTCTCACTGATCACATATCTCTAAGTTTGC
myb87-3		GGTTAGAGGTGCATGGTGGA
		AAATAGCTCGGCCTGGAAAT
	Seq.	TCATTGCCTTTTTCTCACCA

References

Afgan E, Baker D, Batut B, van den Beek M, Bouvier D, Cech M, Chilton J, Clements D, Coraor N, Grüning BA, Guerler A, Hillman-Jackson J, Hiltemann S, Jalili V, Rasche H, Soranzo N, Goecks J, Taylor J, Nekrutenko A, Blankenberg D. 2018. The Galaxy platform for accessible, reproducible and collaborative biomedical analyses: 2018 update. Nucleic Acids Res **46**, W537-w544.

Almeida T, Pinto G, Correia B, Santos C, Goncalves S. 2013. QsMYB1 expression is modulated in response to heat and drought stresses and during plant recovery in Quercus suber. Plant Physiol Biochem **73**, 274-281.

Andersen TG, Molina D, Kilian J, Franke RB, Ragni L, Geldner N. 2021. Tissue-Autonomous Phenylpropanoid Production Is Essential for Establishment of Root Barriers. Curr. Biol. **31**, 965-977.e965.

Barberon M, Vermeer JE, De Bellis D, Wang P, Naseer S, Andersen TG, Humbel BM, Nawrath C, Takano J, Salt DE, Geldner N. 2016. Adaptation of Root Function by Nutrient-Induced Plasticity of Endodermal Differentiation. Cell **164**, 447-459.

Binenbaum J, Wulff N, Camut L, Kiradjiev K, Anfang M, Tal I, Vasuki H, Zhang Y, Sakvarelidze-Achard L, Davière JM, Ripper D, Carrera E, Manasherova E, Ben Yaakov S, Lazary S, Hua C, Novak V, Crocoll C, Weinstain R, Cohen H, Ragni L, Aharoni A, Band LR, Achard P, Nour-Eldin HH, Shani E. 2023. Gibberellin and abscisic acid transporters facilitate endodermal suberin formation in Arabidopsis. Nat Plants.

Campilho A, Nieminen K, Ragni L. 2020. The development of the periderm: the final frontier between a plant and its environment. Curr Opin Plant Biol **53**, 10-14.

Cantó-Pastor A, Kajala K, Shaar-Moshe L, Manzano C, Timilsena P, De Bellis D, Gray S, Holbein J, Yang H, Mohammad S, Nirmal N, Suresh K, Ursache R, Mason GA, Gouran M, West DA, Borowsky AT, Shackel KA, Sinha N, Bailey-Serres J, Geldner N, Li S, Franke RB, Brady SM. 2022. A suberized exodermis is required for tomato drought tolerance. bioRxiv, 2022.2010.2010.511665.

Capote T, Barbosa P, Usie A, Ramos AM, Inacio V, Ordas R, Goncalves S, Morais-Cecilio L. 2018. ChIP-Seq reveals that QsMYB1 directly targets genes involved in lignin and suberin biosynthesis pathways in cork oak (Quercus suber). BMC Plant Biol. **18**, 198.

Cohen H, Fedyuk V, Wang C, Wu S, Aharoni A. 2020. SUBERMAN regulates developmental suberization of the Arabidopsis root endodermis. The Plant Journal **102**, 431-447.

de Reuille PB, Ragni L. 2017. Vascular morphodynamics during secondary growth. *Xylem*: Humana Press, New York, NY, 103-125.

Doblas VG, Geldner N, Barberon M. 2017. The endodermis, a tightly controlled barrier for nutrients. Curr. Opin. Plant Biol. **39**, 136-143.

Duan L, Sebastian J, Dinneny JR. 2015. Salt-stress regulation of root system growth and architecture in Arabidopsis seedlings. Methods Mol Biol **1242**, 105-122.

Dubos C, Stracke R, Grotewold E, Weisshaar B, Martin C, Lepiniec L. 2010. MYB transcription factors in Arabidopsis. Trends in plant science **15**, 573-581.

Enstone DE, Peterson CA, Ma F. 2002. Root Endodermis and Exodermis: Structure, Function, and Responses to the Environment. J. Plant Growth Regul. **21**, 335-351.

Evert RF. 2006. *Esau's Plant Anatomy: meristems, cells, and tissues of the plant body: their structure, function, and development*. Hoboken, NJ, USA: John Wiley & Sons, Inc.

Fauser F, Schiml S, Puchta H. 2014. Both CRISPR/Cas-based nucleases and nickases can be used efficiently for genome engineering in Arabidopsis thaliana. Plant J **79**, 348-359.

Graves SJ, Rifai SW, Putz FE. 2014. Outer bark thickness decreases more with height on stems of fire-resistant than fire-sensitive Floridian oaks (Quercus spp.; Fagaceae). Am J Bot **101**, 2183-2188.
Harman-Ware AE, Sparks S, Addison B, Kalluri UC. 2021. Importance of suberin biopolymer in plant function, contributions to soil organic carbon and in the production of bio-derived energy and materials. Biotechnol. Biofuels **14**, 75.
Julkowska MM, Hoefsloot HCJ, Mol S, Feron R, de Boer G-J, Haring MA, Testerink C. 2014. Capturing Arabidopsis Root Architecture Dynamics with root-fit Reveals Diversity in Responses to Salinity Plant Physiology **166**, 1387-1402.
Kamiya T, Borghi M, Wang P, Danku JM, Kalmbach L, Hosmani PS, Naseer S, Fujiwara T, Geldner N, Salt DE. 2015. The MYB36 transcription factor orchestrates Casparian strip formation. Proc Natl Acad Sci U S A **112**, 10533-10538.
Khakhar A, Starker CG, Chamness JC, Lee N, Stokke S, Wang C, Swanson R, Rizvi F, Imaizumi T, Voytas DF. 2020. Building customizable auto-luminescent luciferase-based reporters in plants. eLife **9**, e52786.
Kosma DK, Murmu J, Razeq FM, Santos P, Bourgault R, Molina I, Rowland O. 2014. AtMYB41 activates ectopic suberin synthesis and assembly in multiple plant species and cell types. Plant J **80**, 216-229.
Kosma DK, Rice A, Pollard M. 2015. Analysis of aliphatic waxes associated with root periderm or exodermis from eleven plant species. Phytochemistry **117**, 351-362.
Lampropoulos A, Sutikovic Z, Wenzl C, Maegele I, Lohmann JU, Forner J. 2013. GreenGate - A Novel, Versatile, and Efficient Cloning System for Plant Transgenesis. PLoS One **8**, e83043.
Lashbrooke J, Cohen H, Levy-Samocha D, Tzfadia O, Panizel I, Zeisler V, Massalha H, Stern A, Trainotti L, Schreiber L, Costa F, Aharoni A. 2016. MYB107 and MYB9 Homologs Regulate Suberin Deposition in Angiosperms. The Plant Cell **28**, 2097-2116.
Leal AR, Barros PM, Parizot B, Sapeta H, Vangheluwe N, Andersen TG, Beeckman T, Oliveira MM. 2022. Translational profile of developing phellem cells in Arabidopsis thaliana roots. The Plant Journal **110**, 899-915.
Liberman LM, Sparks EE, Moreno-Risueno MA, Petricka JJ, Benfey PN. 2015. MYB36 regulates the transition from proliferation to differentiation in the Arabidopsis root. Proc Natl Acad Sci U S A **112**, 12099-12104.
Lux A, Morita S, Abe J, Ito K. 2005. An improved method for clearing and staining free-hand sections and whole-mount samples. Ann Bot **96**, 989-996.
Manzano C, Morimoto KW, Shaar-Moshe L, Mason GA, Cantó-Pastor A, Gouran M, Bellis DD, Ursache R, Kajala K, Sinha N, Bailey-Serres J, Geldner N, Pozo JCd, Brady SM. 2022. Regulation and Function of a Polarly Localized Lignin Barrier in the Exodermis. bioRxiv, 2022.2010.2020.513117.
Naseer S, Lee Y, Lapierre C, Franke R, Nawrath C, Geldner N. 2012. Casparian strip diffusion barrier in Arabidopsis is made of a lignin polymer without suberin. Proceedings of the National Academy of Sciences **109**, 10101-10106.
Pattanaik S, Patra B, Singh SK, Yuan L. 2014. An overview of the gene regulatory network controlling trichome development in the model plant, Arabidopsis. Front Plant Sci **5**, 259.
Salas-González I, Reyt G, Flis P, Custódio V, Gopaulchan D, Bakhoum N, Dew TP, Suresh K, Franke RB, Dangl JL, Salt DE, Castrillo G. 2021. Coordination between microbiota and root endodermis supports plant mineral nutrient homeostasis. Science **371**.
Serra O, Geldner N. 2022. The making of suberin. New Phytologist **235**, 848-866.

Serra O, Mähönen AP, Hetherington AJ, Ragni L. 2022a. The Making of Plant Armor: The Periderm. Annu Rev Plant Biol.
Serra O, Mähönen AP, Hetherington AJ, Ragni L. 2022b. The making of plant armor: The periderm. Annu Rev Plant Biol **73**, 405-432.
Shukla V, Han J-P, Cléard F, Lefebvre-Legendre L, Gully K, Flis P, Berhin A, Andersen Tonni G, Salt David E, Nawrath C, Barberon M. 2021. Suberin plasticity to developmental and exogenous cues is regulated by a set of MYB transcription factors. Proceedings of the National Academy of Sciences **118**, e2101730118.
Thangavel T, Tegg RS, Wilson CR. 2016. Toughing It Out--Disease-Resistant Potato Mutants Have Enhanced Tuber Skin Defenses. Phytopathology **106**, 474-483.
Ursache R, Andersen TG, Marhavy P, Geldner N. 2018. A protocol for combining fluorescent proteins with histological stains for diverse cell wall components. The Plant Journal **93**, 399-412.
Ursache R, De Jesus Vieira Teixeira C, Dénervaud Tendon V, Gully K, De Bellis D, Schmid-Siegert E, Grube Andersen T, Shekhar V, Calderon S, Pradervand S, Nawrath C, Geldner N, Vermeer JEM. 2021. GDSL-domain proteins have key roles in suberin polymerization and degradation. Nat Plants **7**, 353-364.
Wang C, Wang H, Li P, Li H, Xu C, Cohen H, Aharoni A, Wu S. 2020. Developmental programs interact with abscisic acid to coordinate root suberization in Arabidopsis. The Plant Journal **104**, 241-251.
Wang Z, Zhang B, Chen Z, Wu M, Chao D, Wei Q, Xin Y, Li L, Ming Z, Xia J. 2022. Three OsMYB36 members redundantly regulate Casparian strip formation at the root endodermis. The Plant Cell **34**, 2948-2968.
Wei X, Mao L, Lu W, Wei X, Han X, Guan W, Yang Y, Zha M, Xu C, Luo Z. 2019. Three Transcription Activators of ABA Signaling Positively Regulate Suberin Monomer Synthesis by Activating Cytochrome P450 CYP86A1 in Kiwifruit. Front Plant Sci **10**, 1650.
Wunderling A, Ripper D, Barra-Jimenez A, Mahn S, Sajak K, Targem MB, Ragni L. 2018. A molecular framework to study periderm formation in Arabidopsis. New Phytol. **219**, 216-229.
Xiao W, Molina D, Wunderling A, Ripper D, Vermeer JEM, Ragni L. 2020. Pluripotent Pericycle Cells Trigger Different Growth Outputs by Integrating Developmental Cues into Distinct Regulatory Modules. Curr. Biol. **30**, 4384-4398.e4385.
Xu H, Liu P, Wang C, Wu S, Dong C, Lin Q, Sun W, Huang B, Xu M, Tauqeer A, Wu S. 2022. Transcriptional networks regulating suberin and lignin in endodermis link development and ABA response. Plant Physiology **190**, 1165-1181.
Xu X, Guerriero G, Domergue F, Beine-Golovchuk O, Cocco E, Berni R, Sergeant K, Hausman JF, Legay S. 2023. Characterization of MdMYB68, a suberin master regulator in russeted apples. Front Plant Sci **14**, 1143961.
Zhang J, Eswaran G, Alonso-Serra J, Kucukoglu M, Xiang J, Yang W, Elo A, Nieminen K, Damén T, Joung JG, Yun JY, Lee JH, Ragni L, Barbier de Reuille P, Ahnert SE, Lee JY, Mähönen AP, Helariutta Y. 2019. Transcriptional regulatory framework for vascular cambium development in Arabidopsis roots. Nat. Plants **5**, 1033-1042.

5.2 Draft manuscript 2: The SCHENGEN Pathway Orchestrates the Protective Capacity of the Periderm

D.M. and L.R. planned and conducted the majority of the experiments. N.R conducted preliminary experiments. D.M. and L.R acquired the confocal images. D.M. and N.R. conducted the Fluorol Yellow (FY) experiments. D.M., and N.R. conduct the peptide treatments for qPCR. D.M obtained the RNA material for RNAseq. L.R. and D.M analyse the data. D.R. helped in generating the T3 lines. D.M. wrote the paper.

The SCHENGEN Pathway Orchestrates the Protective Layer of the Periderm

Authors: Molina David[1], Xiao Wei [1,3]Ragab Noah[1] and Laura Ragni[1,2*]

Affiliations:
[1] ZMBP- Center for Plant Molecular Biology, University of Tübingen, Auf der Morgenstelle 32, D-72076 Tübingen, Germany
[2] University of Freiburg, Institute of Biology II, Schänzlerstr 1, 79104 Freiburg, Germany.
[3] Ghent University, Department of Plant Biotechnology and Bioinformatics, 9052 Ghent, Belgium; VIB Center for Plant Systems Biology, 9052 Ghent, Belgium.

David Molina: 0000-0001-5858-3331; david.molina@zmbp.uni-tuebingen.de

Wei Xiao: 0000-0002-6392-5866;wei.xiao@psb.vib-ugent.be

Laura Ragni: 0000-0002-3651-8966; laura.ragni@zmbp.uni-tuebngen.de

* Corresponding author: laura.ragni@zmbp.uni-tuebingen.de +49 (0)7071 - 29 76677

Summary

Apoplastic barriers play a vital role in plant homeostasis, growth, and development. The proper function of these barriers is monitored by surveillance mechanisms that ensure plant protection. Until now, the only well-documented example is the SCHENGEN pathway. It regulates and monitors Casparian strip formation, guarantees the proper embryonic cuticle formation during seed development and, orchestrates modifications of pollen wall components within the anther locule. The activation of this pathway involves the perception of peptide ligands released into the plant apoplast by leucine-rich repeat receptor-like kinases (LRR-RLKs) and a cytoplasmic kinase specifically localized. Altogether this leads to the proper deposition of suberin, lignin, or cutin, depending on the developmental contexts. In Arabidopsis lines with impaired suberin or lignin deposition, such as pELTP:MYB and *gelp22 gelp38 gelp51 gelp49 gelp9* mutants, we observed a compensation mechanism that includes an increase in apoplastic barrier production and the upregulation of several suberin and lignin related genes. To understand this better, we identified the specific expression pattern for Schengen pathway components in the periderm. For example, SGN3/GSO1 and GSO2 receptor kinases are specifically expressed in the periderm, while certain peptide ligands, such as TWS1 or CIF4, are expressed in the surrounding tissues, including the phellogen. Additionally, in the *gso1gso2* double receptor mutant and *tws1* ligand mutant, we observed a delay in phellem differentiation. Furthermore, the Arabidopsis periderm exhibits a response to the exogenous application of CIF2 and TWS1 ligand peptides. This response involves the upregulation of suberin and lignin-related genes, indicating an active state of the surveillance system after the initial establishment of phellem apoplastic barriers. In conclusion, we propose that the continuous monitoring of the phellem by the SCHENGEN pathway ensures the periderm's role as armor by maintaining its protective capacity during development and in emergency situations. This discovery provides researchers with new tools for the study of apoplastic barrier establishment and new strategies to generate more resistant plants

Keywords: Schengen pathway, suberin, lignin, periderm, phellem

Introduction

Apoplastic barriers such as suberin or lignin, are identified as evolutionary adaptations which help plants in surviving and thriving in demanding environments (Nawrath et al., 2013). For example, phylogenetic analysis of 18 representative species show that suberin related genes evolved through the duplication of genes functioning in other processes, and that suberin lamella is exclusive of seed plants (Su et al., 2023). Suberin is an aromatic and aliphatic polymeric material that consists of oxygenated long-chain fatty acids (C16-C24), glycerol, and aromatic monomers such as ferulic acid (Bernards, 2002; Kolattukudy, 1980; Pollard et al., 2008; Serra and Geldner, 2022). The biosynthesis and regulation of suberin deposition in Arabidopsis are relatively well understood (Nomberg et al., 2022). On the other hand, lignin is composed of p-hydroxyphenyl (H), guaiacyl (G), and syringyl (S) units derived from the polymerization of monolignols originating in the phenylpropanoid pathway, especially hydroxycinnamyl alcohols, with p-coumaryl, coniferyl, and sinapyl alcohols being the most common (Vanholme et al., 2019; Weng & Chapple, 2010). The final polymerization of lignin in the cell walls involves the activation of cell-wall-localized oxidation systems, such as laccase/O2 and/or peroxidase/H2O2, for combinatorial radical coupling to form the final lignin polymers. (Tobimatsu & Schuetz, 2019). Lignin and suberin accumulate in the cell walls of many organs and plant species, with the endodermis being one of the most common and well-studied examples. For instance, Casparian strips (CS) are made by lignin and in the endodermis block apoplastic spaces, preventing the diffusion of solutes between outer and inner tissues and forcing them to pass through the symplast of endodermal cells (Geldner, 2013; Naseer et al., 2012a). The integrity of the apoplastic barrier is essential for its protective capacity. In the past years, it was discovered that in Arabidopsis, the Schengen pathway, in cooperation of MYB36, controls precise lignification of Casparian strip, in the endodermis while also serving as a surveillance system to monitor the integrity of the barrier. This pathway in the endodermis comprises the interaction of CASPARIAN STRIP INTEGRITY FACTORS 2 peptides (CIF1 and CIF2), SCHENGEN3 (SGN1) kinase protein and a leucine-rich repeat receptor-like kinase SCHENGEN3 (SGN3/GSO1). This triggers a signaling pathway that increases ROS (Reactive Oxygen Species) production, which is necessary for lignin polymerization (Alassimone et al., 2016; Doblas et al., 2017; Fujita et al., 2020b). In Arabidopsis, CIF1, CIF2, CIF3, CIF4, and TWS1 are ligands that interact with two Shengen kinase receptors, SGN3 (GSO1) and GSO2 (Doblas et al., 2017; Doll et al., 2020; Fujita et al., 2020b; Nakayama et al., 2017; Truskina, Brück B, et al.,

2022). Today, we know that this pathway regulates and monitors the integrity of the Casparian strips formation, guarantees the proper embryonic cuticle formation during seed development, and orchestrates modifications of pollen wall components to ensure proper tapetum within the anther locule. (Truskina et al., 2022; Doll et al., 2020). In secondary growth, apoplastic barriers reinforce the periderm in both roots and shoots. The periderm is the outermost tissue in secondary growth, serving as a barrier that protects the plant against various stresses to keep homeostasis. It is composed of three layers: the phellogen, phellem (also known as cork), and phelloderm. The phellogen is a meristematic tissue that divides bidirectionally to form the phelloderm inward and the phellem outward. The phelloderm is thought to store nutrients, while the phellem is characterized by the significant presence of suberin and lignin, which make up a substantial portion of the periderm's mass (Serra et al., 2022). Despite this, in contrast to the endodermis, there is limited information available on how these diffusion barriers are specifically produced and accumulated during periderm development. Previous research using ribosome affinity purification followed by mRNA sequencing (TRAP-SEQ) has shown that the early onset of phellem suberization takes place following phellogen division and involves the upregulation of suberin and lignin related genes, WOX, NAC, and MYB transcription factors and other putative regulators (Leal et al., 2022). We postulate that, in addition to other regulators, the Schengen pathway plays a pivotal role in orchestrating the deposition of both suberin and lignin in phellem. We found that the components of the Schengen pathway are expressed in the periderm with a little difference with those described in the endodermis. TWS1 and CIF4 emerge as the most promising ligand peptide candidates for activating both receptors, SGN3 and GSO2, expressed in the phellem. We show that periderm development in the Schengen loss-of-function mutants is delayed, and the apoplastic barriers are not properly established. Furthermore, our findings suggest that the Schengen pathway can activate periderm specific downstream enzymes, such as peroxidases, potentially influencing lignin polymerization in the onset of phellem differentiation. However, certain questions, including those related to peptide processing and movement, necessitate further investigation. This work uncovers a novel role of the Schengen pathway in establishing the apoplastic barrier in the periderm.

Results:

As a Compensatory Surveillance Response, Periderm Increases Apoplastic Barriers Deposition.

To investigate the periderm response resulting from compromised apoplastic barrier integrity, we examined two plant lines with deficient apoplastic barrier establishment. Previous research has shown that pELTP:MYB4 leads to a collapsed phellem due to decreased suberin and lignin deposition (Andersen et al., 2021b). This line, in combination with the suberin reporter pGPAT5: mCitrine-SYP122, allowed us to assess both the quality of the barrier and the expression of GPAT5, which correlates with suberin deposition (Barberon et al., 2016). As reported, the phellem in pELTP:MYB4 exhibits a disrupted layer with poorly defined cell walls (Figure 1b). Interestingly, our analysis of GPAT5 expression revealed a marked upregulation in pELTP:MYB4 (Figure 1b). This suggests that despite the challenges and limitations in the production of suberin and lignin monomers in pELTP:MYB4, the plant is able to upregulate suberin genes probably to compensate the barrier issues.

In addition, we examined *gelp22 gelp38 gelp51 gelp49 gelp9* quintuple mutant, which has been shown to be incapable of suberin polymerization in cell walls (Ursache et al., 2021). In this mutant, biosynthesis is not affected, and only the last step of suberin polymerization is compromised, in contrast to the situation observed in pELTP:MYB4. The periderm of *gelp22 gelp38 gelp51 gelp49 gelp9* quintuple mutant showed a strong reduction of suberin deposition as we expected. Interestingly, it appears that lignin deposition in this mutant is much higher in comparison with WT plants (Figure 1c). This could be interpreted as an expected Schengen response, which could be found in similar scenarios in the endodermis (Reyt et al., 2021). Further analysis using other approaches, especially analytical methods, is needed in order to confirm the overproduction of lignin in the tissues.

It was shown that Piperonylic Acid (PA) suppresses the phenylpropanoid pathway by inactivating CYP73A cytochrome P450 enzyme. This inactivation reduces dramatically the cinnamic acid accumulation in the beginning of the phenylpropanoid pathway affecting the final monolignol production (Schalk et al., 1998). PA was previously used to diminish the establishment of Casparian strips (Naseer et al., 2012a). Then, we decided to block the phenylpropanoid pathway in the periderm of Col-0 (WT) using PA, and we checked the expression of suberin and lignin related genes. Our analysis revealed a significant upregulation of suberin and lignin related genes in the

plants treated with PA (Figure 1d). This reinforces the idea of the existence of a surveillance system in the periderm that senses and triggers the upregulation of genes to repair or establish the phellem.

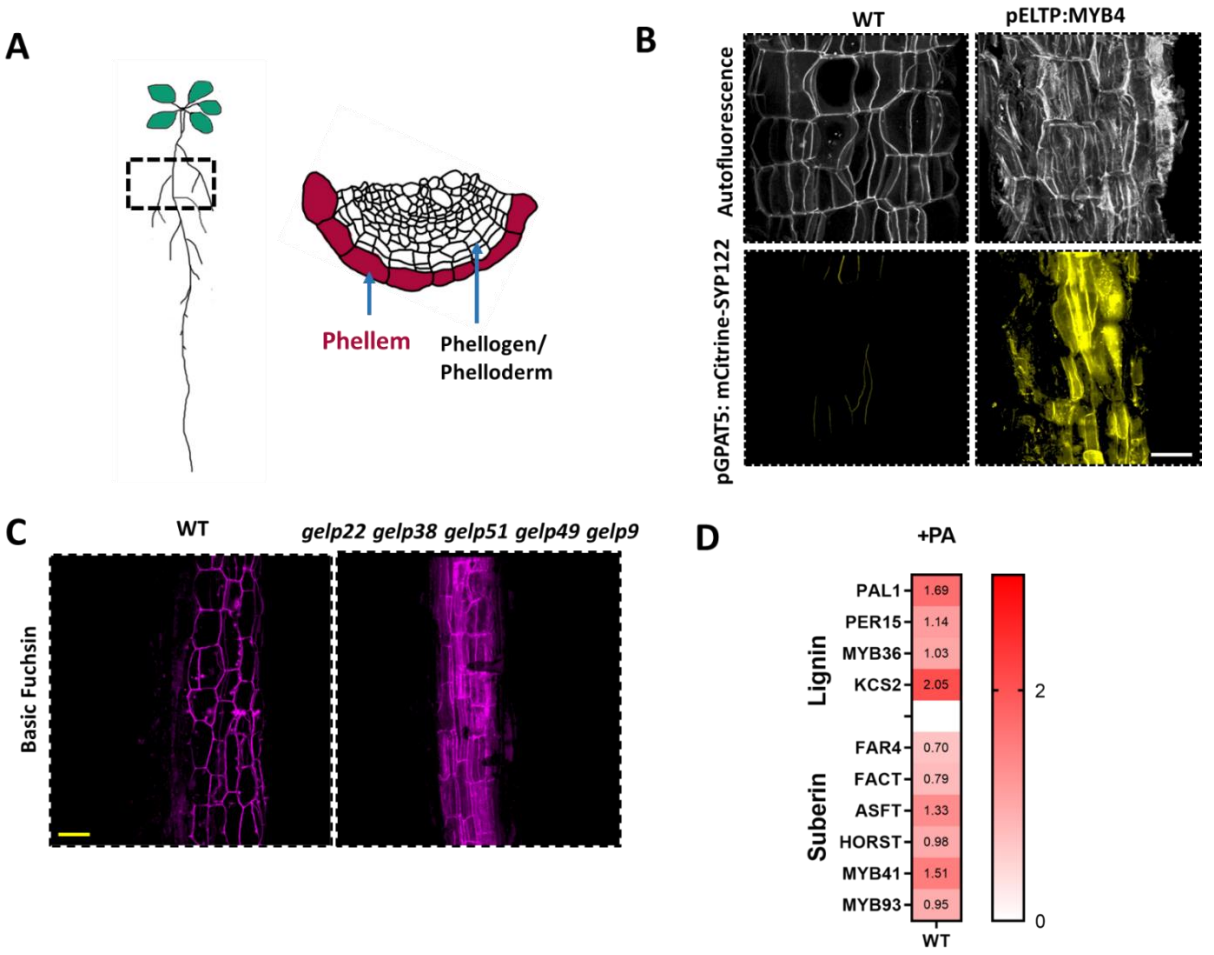

Figure 1: Compensatory Surveillance Response in the periderm. (A) Schematics drown of a periderm, it shows the position of the differentiated phellem along the root and includes a cross-section highlighting the phellem layer where suberin and lignin accumulate. (B) Representative images showing the GPAT5:mCitrine signal in the cork indicate a much stronger signal in the pELTP:MYB4 line. (C) Representative images illustrating lignin deposition in both WT and the *gelp22 gelp38 gelp51 gelp49 gelp9* quintuple mutant, the mutant plant shows a stronger signal. (D) Log2 Fold Change of relative expression of selected suberin and lignin related genes, upon induction of 10 µM PA for 24h.). Data were obtained by qPCR as described in the methods section. Yellow scale bars: 50µm. White scale bars: 60µm.

Suberin and Lignin do not Exhibit the Same Deposition Pattern During Phellem Differentiation.

To understand how lignification occurs during phellem differentiation, we analysed the lignin deposition at different stages of phellem differentiation. Based on the developmental stages defined by Wunderling et al. (2018), we analyzed stages 1/2, 3/4, and 4/5. We observed that lignification occurs in a gradient manner, with the major zone of lignification being the upper part close to the hypocotyl. As we descend in the root, our analysis shows that lignification is reduced, especially in the early stages of development (Stage 1/2) (Fig. Supl. 1). Interestingly, we observed that lignification in the early stages is polarly localized in the new undifferentiated phellem cell. This suggests that lignification is not random and may require molecular specifiers for polar deposition. Next, we were curious about whether suberin deposition follows the same pattern as lignin. To explore this, we employed a combination of suberin and lignin staining, as demonstrated in (Sexauer et al., 2021). By simultaneously using Basic Fuchsin and Fluorol Yellow, we observed that suberin is deposited uniformly around the cell, displaying a non-polarized pattern (Fig. Supl, 2). These findings suggest that, unlike suberization, lignification within the phellem cells during the initial steps of differentiation is achieve gradually.

Schengen Pathway Components, and Suberin and Lignin Related Genes are Expressed in the Periderm at Different Steps of Differentiation.

To identify possible genes that may elucidate this barrier compensation response, we analysed and compared transcriptomic datasets from two sources: one by Leal et al. (2022) and another from a cork trans-differentiation system developed in our group by Xiao et al. (unpublished). This system enables the study of phellem differentiation in an elegant and controllable manner, enhancing phellem differentiation in a spatial-temporal manner. In our analysis, we initially looked for well-known suberin and lignin-related genes. The phellem differentiation in the cork trans-differentiation was previously done by Xiao et al. (unpublished) at two time points, 24h and 48h. After comparing the dataset, we identified a significant number of lignin-related genes such as PAL4, RBOH2, PER (Fujita et al., 2020b; Kamiya et al., 2015b; Vanholme et al., 2019), suberin genes involved in biosynthesis such as HORST and GPAT5 (Belsson et al., 2007; Höfer et al., 2008), suberin transcription factors like MYB41, MYB93, MYB53 (Shukla et al., 2021), and genes involved in the polarization of suberin within the cell walls like GDSLs genes (Nomberg et al., 2022; Ursache et al., 2021). Interestingly, this analysis also displayed the upregulation of GSO1/SGN3 receptor (Figure 2a). GSO1/SGN3 is a kinase receptor that in collaboration of SGN1

kinase protein, together with MYB36, controls the specific formation of Casparian strips (CS). Briefly, SGN1 facilitates the transmission of the activation signal from the CIF2 secreted peptide to the SGN3 receptor. SGN1 induces localized production of reactive oxygen species (ROS) at the Casparian strip by directly phosphorylating NADPH oxidases (Doblas et al., 2017; Fujita et al., 2020b; Kamiya et al., 2015b; Nakayama et al., 2017). These observations suggest that the Schengen pathway may also play a role in the periderm by regulating suberin and lignin deposition.

Then, we wondered whether we could confirm the presence of the Schengen pathway components in the periderm. By employing fluorescent reporter lines, we confirmed that the components express in the periderm, and we could define the expression pattern of both receptors, GSO1/SGN3 and GSO2, along with the expression of the kinase protein SGN1. Additionally, ligands TWS1 and CIF4 (Doll et al., 2020; Okuda et al., 2020) were also expressed in the periderm (Figure 2b). Interestingly, both receptors GSO1/SGN3 and GSO2 were expressed mostly in the phellem of the periderm, although GSO2 was also present in the vasculature. Regarding the ligand peptides, CIF4 was observed in periderm and cortex. On the other hand, TWS1 was mostly expressed in the phellogen, phelloderm, and vasculature. It was not possible to identify expression in the phellem. It seems that both ligand peptides and the receptors partially share a pattern of expression, but it is also clear that each may have specificities. Finally, SGN1 kinase protein was also found in the periderm (Figure 2b). The expression of nearly all known components of the Schengen pathway strongly suggests that it could play a role in the establishment of apoplastic barriers in the periderm.

Next, as in the endodermis SGN3 protein polarly localized, we explored the localization of GSO1/SGN3 protein using the SGN3:SGN3-VENUS reporter line in the periderm. We analyzed the protein localization at two developmental stages, as defined by Wunderling et al. (2018): stages 2/3 and 4/5. The first one shows a partial differentiation, while in the other, the phellem is completely differentiated. We observed a specific polar localization of GSO1/SGN3 (Figure 2c). In the younger stages, this receptor was situated perpendicular to the phellogen's long axis in between the new phellem cells, which are not yet differentiated and still covered by the cortex and epidermis. In the older stage, GSO1/SGN3 maintained this specific localization (Figure 2b) although it was not possible to see expression in fully differentiated phellem. It is important to mention that GSO1/SGN3 is expressed at low levels, and the signal could be mask by the intrinsic strong autofluorescence displayed by the phellem. Furthermore, we observed that in the undifferentiated phellem, lignin shared the same localization pattern as GSO1/SGN3. This strongly suggests that the Schengen pathway can precisely define the site of lignification during phellem

differentiation in the first stages of differentiation.

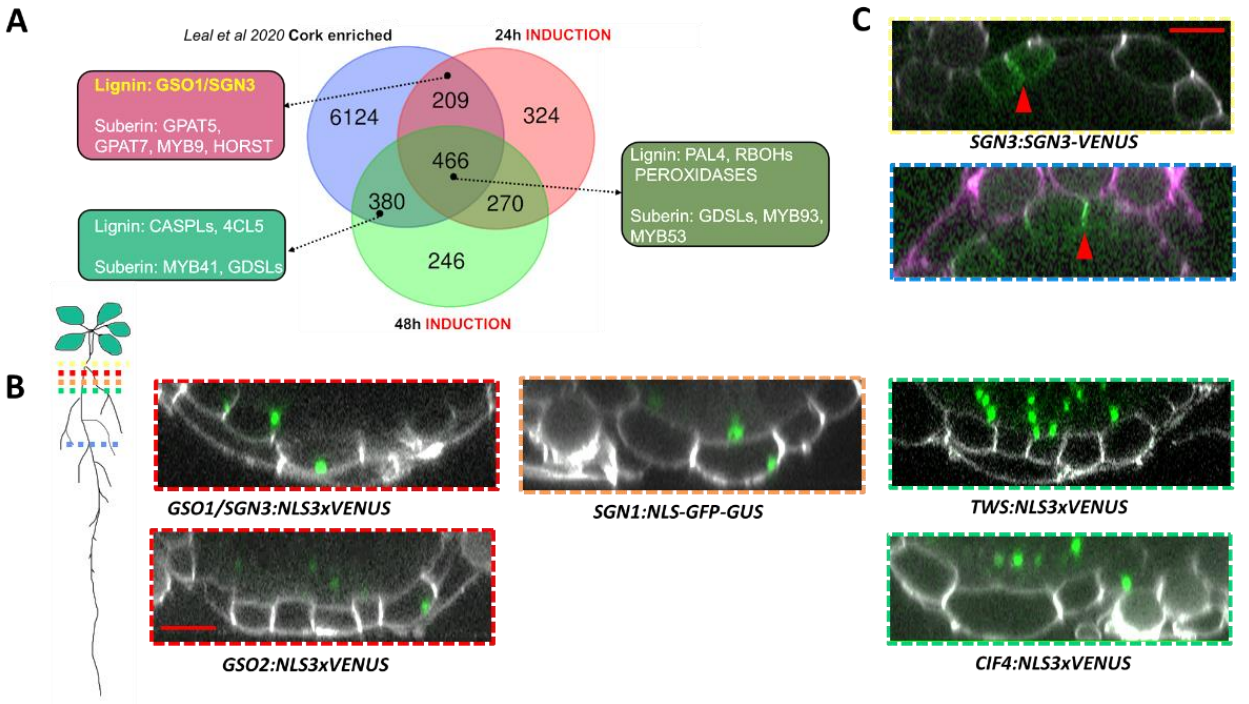

Figure 2: Schengen components are present in the periderm (A) Venn diagram showing suberin/lignin-related genes expressed in the phellem induced in the cork trans-differentiation system, at two times of induction (Xiao et al. unpublished), and the cork-enriched analysis by Leal et al. 2020. (B) Orthogonal view of z stacks showing the expression of GSO1/SGN3 (pGSO1/SGN3:NLS-3xVenus), GSO2 (pGSO2:NLS-3xVenus), SGN1(pSGN1:NLS-GFP-GUS), TWS1 (pTWS1:NLS-3xVenus), and CIF4 (pCIF4:NLS-3xVenus) (14 day- old plants). (C) Orthogonal view of z stacks showing the protein localization of SGN3 (pSGN3:SGN3-Venus). Red scale bars: 20µm.

Mutants in the Schengen Pathway Show Altered Phellem Differentiation.

To confirm a possible role of the Schengen pathway in phellem differentiation, we analyzed how the phellem is established in loss-of-function mutants of the Schengen pathway components. First, using Basic Fuchsin staining, we analyzed how lignin is deposited in the phellem of 14-day-old WT (Col-0) and the *gso1/sgn3 gso2* double mutant plants. The *gso1/sgn3 gso2* double mutant showed irregular deposition of lignin in comparison with WT. Additionally, based on the signal intensity, we could also infer that lignin is deposited in very small amounts compared with WT plants, although further analytical analysis is needed. Then, we wondered if the onset of phellem differentiation is delayed in *gso1/sgn3 gso2* double mutant and *tws1* ligand peptide mutants, so we

decided to analyse the suberin deposition phellem differentiation along the root, which correlates with the phellem differentiation. We used a similar approach shown in (Andersen et al., 2021b). Using Fluorol Yellow (FY), a classic suberin staining, we could distinguish two developmental stages of the phellem: the mature phellem and the developing phellem. When we compared Col-0 plants against the *gso1/sgn3 gso2* and *tws1* mutant plants, we could see a significant reduction in the total phellem area in both mutant lines (Figure 3b). It means that indeed the onset of phellem differentiation in the mutants is delayed in comparison with Col-0. In addition, we could observe that both developmental stages were proportionally reduced. It could mean that the differentiation program of the phellem cells is delayed but not abolished.

Previously, it was shown that the external treatment of Arabidopsis roots with the CIF2 peptide can induce early suberization and upregulation of suberin and lignin genes in the endodermis (Fujita et al., 2020b; Reyt et al., 2021). Thus, we wondered if it is possible to induce in the periderm suberin accumulation and upregulation of genes of interest by the external treatment with CIF2 or TWS1. In order to address this question, we used two different approaches. First, we treated 11-day-old Arabidopsis WT plants with 450 nM TWS1 peptide for 96 hours, and we analyzed the onset of phellem differentiation. We found that the treatment with TWS1 significantly increased both periderm areas, the mature phellem and the developing phellem (Figure 3c). It could mean that the peptide by itself can active downstream signallers to enhance phellem differentiation. Then, we used a similar set-up to analyze this induction at the transcriptional level using qPCR. The main difference here was that we treated 13-day-old plants for 24 hours with CIF2 peptide. We collected the periderm sections without lateral roots and analyzed it using qPCR. We found that in WT plants, there was a notable upregulation of suberin and lignin-related genes (Figure 3d). These results suggest that the periderm in Arabidopsis can respond to several inputs, including the application of synthetic peptides. All this suggests the presence or absence of some components in the periderm will alter the phellem differentiation rate suggesting a pivotal role of the Schengen pathway in phellem differentiation.

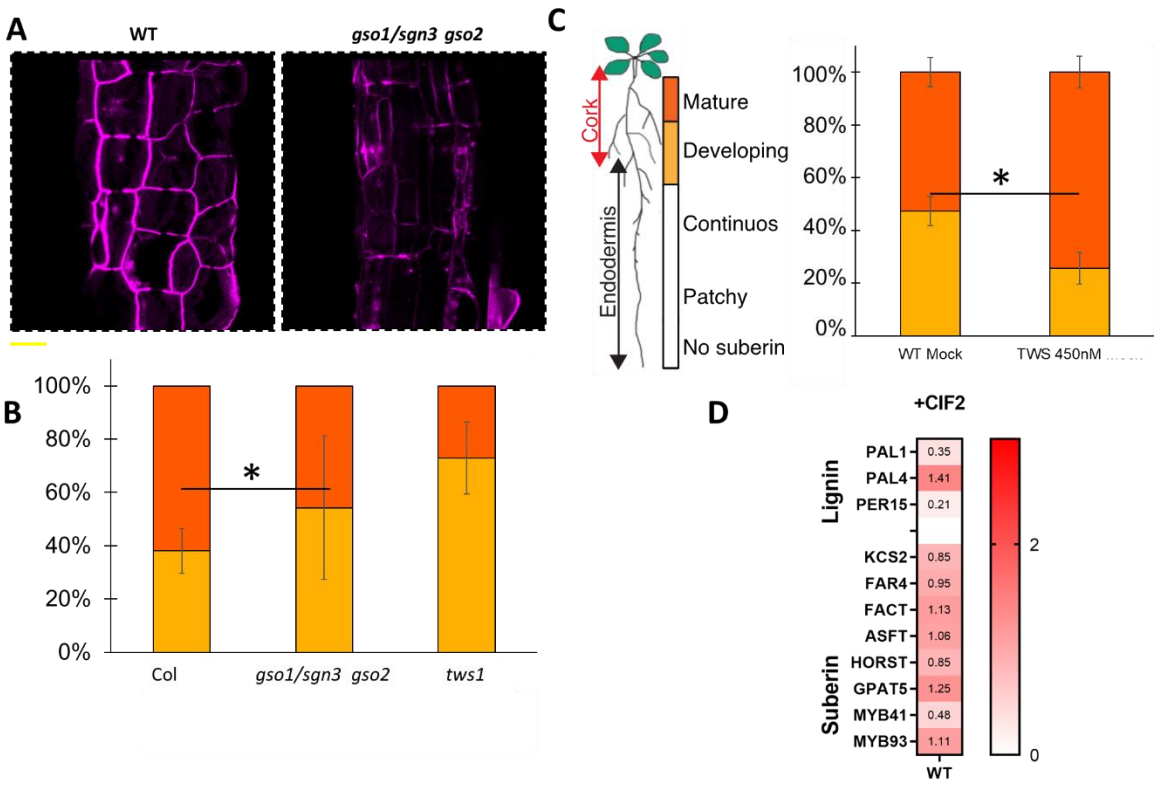

Figure 3: Apoplastic barriers in phellem are defective in Schengen loss-of-function mutants. (A) Representative images illustrate lignin deposition in both WT and the gso1/sgn3 gso2 double mutant receptor, where lignin deposition is reduced and irregular. (B and C) Suberin deposition in the phellem, showing developing phellem (light orange) and mature phellem (dark orange). (B) Relative quantification of developing and mature phellem in WT, *gso1/sgn3 gso2*, and tws1 mutants, mutants display a marked reduction. (C) Relative quantification of developing and mature phellem in WT plants treated with 450nM of TWS1, inducing phellem differentiation. (D) Log2 Fold Change of relative expression of selected suberin and lignin related genes upon induction of 450nM of CIF2 for 24h, measured by qPCR. (B and C) Students T-Test (*: P<0.05, n:10-15) Yellow scale bars: 40µm.

A Set of Periderm Peroxidases is Induced by TWS1 Ligand Peptide

Then we wondered whether the Schengen pathway response shares similarities between the endodermis and the periderm. To address this question, we performed RNA-seq using periderm and endodermis root material. We treated 13-day-old WT plants for 24 hours with 450nM TWS1 and collected periderm and endodermis root regions without lateral roots (Figure 4a). Comparison of the differentially expressed genes (DEGs) from both showed that the most strongly induced

genes are peroxidases and laccases, both necessary for the final step of the polymerization of lignin. Additionally, we found that some of these genes were exclusively induced in the endodermis (270), phellem (799), and some were present in both tissues (234) (Figure 4b). It has been shown that the formation of Casparian strips requires exclusively the participation of peroxidases, with a minor role of laccases (Rojas-Murcia et al., 2020). In our analysis, similarly to the endodermis, a significant number of peroxidases were much more induced than laccases. Interestingly, we found that the number of peroxidases was higher in the periderm than in the endodermis (Figure 4c). In addition, we could see that some of the peroxidases found in the periderm were not found previously in the endodermis. All this could mean two things: first, that the lignin deposited in the phellem could share a similar chemical nature with the ones that build the Casparian strips, and second, that the final polymerization requires specific enzymes for both tissues

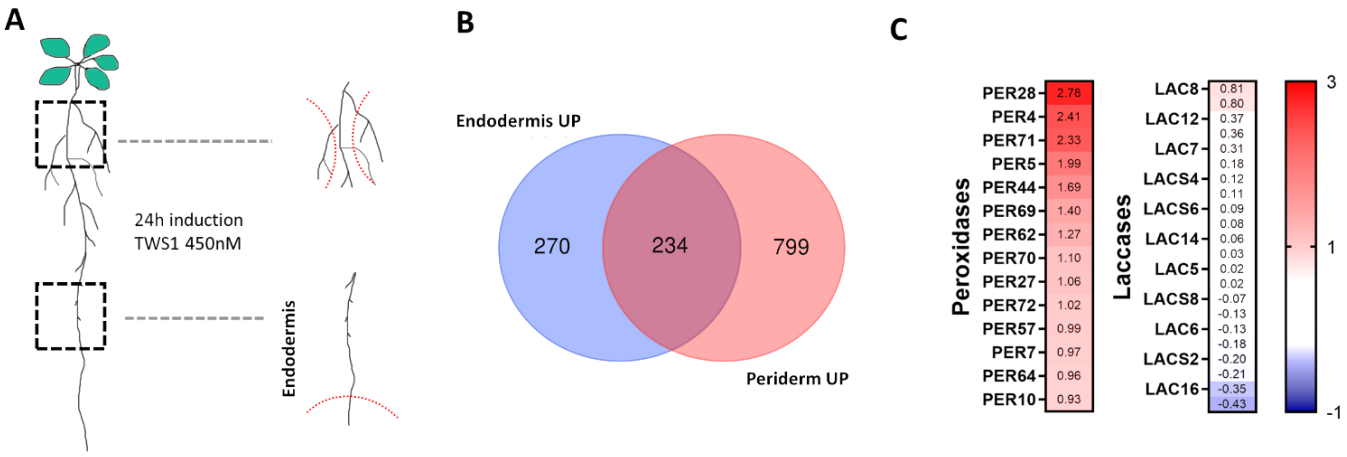

Figure 4: RNAseq analysis of TWS1 induction in Arabidopsis root: (A) Schematic diagram of the setup used for TWS1 induction. (B) A Venn diagram illustrating genes upregulated in the endodermis (270), periderm (799), and genes commonly upregulated in both tissues (234). (C) Fold change of selected peroxidases (PER) and laccases (LAC) ($P < 0.05$ and log2(fold change)) after TWS1 treatment in the periderm. The degree of fold changes is shown in a color code as indicated.

Discussion

Phellem establishment is a crucial process in plants. The protection capacity of the phellem relies on the integrity of apoplastic barriers. Issues in the deposition of suberin and lignin could lead to limitations in plant growth or, in extreme cases, lethality (Andersen et al., 2021b). While the

understanding of how apoplastic barriers are formed in the endodermis is better established, information regarding this process in the periderm is very limited. Recently, Arabidopsis has provided new research opportunities to understand secondary growth including the periderm. For example, it is now known that the phellogen requires auxin for its formation and maintenance (Xiao et al., 2020). The study of apoplastic barrier establishment in Arabidopsis root during secondary growth also has been facilitated. Combining lignin and suberin stainings and analyzing different developmental stages of phellem differentiation, we found that suberin and lignin do not follow the same pattern. Lignin is mostly polarized to specific positions within the phellem cell walls. Additionally, the development of new molecular tools has greatly increased the identification of candidates for phellem differentiation. For example, the cork trans-differentiation system has provided us with an advantage in studying phellem differentiation, as it enhances phellem differentiation without directly influencing the expression of suberin or lignin-related genes. It operates by reducing the meristematic capacity of the phellogen, allowing us to study apoplastic barrier deposition independently (Xiao, unplublished). Moreover, the use of mutant lines or specific engineering approaches that reduce or block the deposition of suberin and lignin in the periderm has helped us identify the constant monitoring of barrier integrity by the plant and the consequences when it is exposed to stresses.

Furthermore, the phellem can differentiate under two scenarios: as part of the normal developmental program or as a response in case of an emergency, for instance, in the case of wounding (Evert, 2006; Serra et al., 2022a). We show that when the apoplastic barrier is deficient, the periderm can increase the production of suberin or lignin as a compensatory mechanism. In addition, we found that lignification in the early steps of phellem differentiation follows a specific pattern. It has been shown that the Schengen pathway plays a dual role in the endodermis. First, it defines precise lignification for the formation of Casparian strips, and second, it acts as a surveillance system to monitor the integrity of the barrier and induce the production of suberin or lignin polymerization. (Fujita et al., 2020b). Interestingly, we found that both receptors GSO1/SGN3 and GSO2, SGN1 kinase proteins and the two ligand peptides TWS1 and CIF4 express in the periderm. Our results also show that in some Schengen loss-of-function mutants, phellem differentiation is delayed, and the deposition of the apoplastic barrier is partially diminished. Together with other evidence, we suggest that the Schengen Pathway regulates and specifies both lignification and suberization in the phellem.

The ectodomain of GSO1/SGN3 and GSO2 influences the affinity of CIF peptides (including TWS1). These peptides require a tyrosine sulfation by the tyrosyl-protein sulfotransferase (TPST/SGN2), important posttranlational modification to become active (Komori et al., 2009; Okuda et al., 2020). These modifications occur in distinct tissues depending on the developmental process (Doblas et al., 2017; Doll et al., 2020; Komori et al., 2009). In this context, post-translational modifications of peptides, which we did not analyze in this work, are a priority in research to outline how the Schengen pathway specifically functions in the periderm. Recent research, both public and unpublished, (Michael Hothorn personal communication), highlights that the ectodomain of receptors can impact peptide affinity, subsequently defining specific signaling cascades (Doll et al., 2020; Truskina, et al., 2022). For instance, GSO2 exhibits high affinity for TWS1 and CIF3, while GSO1 has an affinity for CIF2 and CIF4. This suggests that, even though both receptors can detect the five described ligand peptides (Doblas et al., 2017; Doll et al., 2020; Nakayama et al., 2017; Okuda et al., 2020), the receptor's high affinity for a specific ligand may influence the signaling cascade. In the periderm, this could explain lignification and suberization in both the normal phellem developmental program and the emergency establishment of barriers. In this context, although further analysis is necessary to provide a robust explanation, we can speculate that TWS1, together with GSO2, might act in parallel to CIF4 and GSO1/SGN3, defining different developmental responses.

In addition, it is important to highlight the fact that periderm and endodermis could have differences regarding the downstream signaling molecules they trigger. In comparison with the endodermis, the periderm triggers the expression of a higher number of peroxidases and laccases. It suggests that the mechanism could be conserved between both tissues, but with specifications. Furthermore, this new characterization of the Schengen pathway in the periderm, along with recent discoveries, suggests a Schengen well-conserved mechanism to specifically establish apoplastic barriers depending on the plant necessities. Recently, new specific roles of the Schengen pathway have been proposed. For example, it is involved in the formation of the plant embryonic cuticle (Doll et al., 2020) and the formation of the pollen wall to ensure proper tapetum function (Truskina, Brück, et al., 2022). Nevertheless, the potential of the Schengen pathway in defining specific polymerization of apoplastic barriers could also help us understand some other plant processes. For example, it has been shown that floral organ abscission requires the activation of HAESA (HAE)

and HAESA-LIKE2 (HSL2) receptors by the IDA ligand peptide (Butenko et al., 2003; Jinn et al., 2000; Ki Cho et al., 2008). Later on, it was demonstrated that abscission requires the specific formation of a cuticle layer and a lignin mechanical brace to localize cell wall breakdown and limit abscising cells in the receptacle as residuum cells (RECs) and the separated organs as secession cells (SECs). This lignin brace acts as an apoplastic barrier, restricting the diffusion of cell wall enzymes. (Lee et al., 2018b). How this precise lignification occurs is not yet described. Interestingly, the transcriptional analysis of SECs and RECs shows that in addition to other receptors, GSO1/SGN3 is strongly upregulated together with an important number of peroxidases, laccases, and transcription factors involved in cuticle and lignin polymerization.

We can extend our analysis to more bigger contexts, for example the conservation among plant species. Very recently it has been shown by Su et al. (2023) that genes necessary for suberin formation are highly conserved among seed plants. On the other hand, there is very little information about the role of the Schengen Pathway in other plant species. Recently, the rice homologs of Arabidopsis CIF1, CIF2, and GSO1/SGN3 were characterized, named OsCIF1, OsCIF2, OsSGN3a, and OsSGN3b (B. Zhang et al., 2023). They reported that these genes also participate in the formation and monitoring of the Casparian strip in rice. Furthermore, the ectopic expression of OsCIF2 could induce suberin deposition and the formation of Casparian strips in cortical cells. This reinforces the idea that the Schengen pathway can adapt their mechanism to control multiple specific lignification processes, and that the downstream signalling molecules could be conserved, for example, among seed plants. Newly, it is suggested that the role of the Schengen pathway is not limited to apoplastic barrier formation. It has been shown that the GSO1/SGN3 receptor is involved in cellular Na+ regulation. Under salt stress, GSO1 accumulates specifically in endodermal cells without fully established Casparian strips, activating defence mechanisms. The Schengen pathway promotes Casparian strip establishment, while GSO1 activates the SOS2-SOS1 module, part of the SOS pathway, for salt extrusion. Additionally, an uncharacterized family of peptides, the Salt-Induced Factors (SIF), is postulated to play a role (Chen et al., 2023). In the context of the periderm, it is very likely that, in addition to the establishment of apoplastic barriers in the phellem, more mechanisms could be involved. Further investigation and evidence are required to understand and provide additional roles of the Schengen pathway in the periderm.

These previous and new studies, together with our work, strongly suggest a conserved mechanism of apoplastic barrier formation in different plant organs and plant species. This does not rule out the specialization of this pathway for specific organs, although it seems that the outputs, such as the upregulation of suberin-related genes, are highly conserved among plants. For example, it appears that suberization is highly conserved among angiosperms and gymnosperms, with conserved molecular regulators. (Nomberg et al., 2022; Su et al., 2023). Understanding this pathway in different developmental and environmental contexts will shed light on a very influential process of plant growth. The elegant and versatile manner in which the Schengen pathway operates and adapts can contribute to engineering new biotechnological tools and new strategies for plant breeding.

Author contributions

D.M. and L.R. planned and conducted the majority of the experiments. N.R conducted preliminary experiments. D.M. and L.R acquired the confocal images. D.M. and N.R. conducted the Fluorol Yellow (FY) experiments. D.M., and N.R. conduct the peptide treatments for qPCR. D.M obtained the RNA material for RNAseq. L.R. and D.M analyse the data. D.M. wrote the paper.

Acknowledgement

We thank Gwyneth C Ingram and Nico Geldner and for sharing the seeds. We thank everyone involved in this project.

Conflict of Interest

The authors declare no conflict of interest.

Method details

Plant Material and Growth.

Unless stated otherwise, plants were grown in vitro in 1/2MS media at 22C in continuous light. All Arabidopsis lines are in the Columbia background. Details of mutant alleles and transgenic lines are described in Supl file S1. For TWS1 (PEPMIC, China) and CIF2 (PEPMIC, China) induction, plants were initially grown and then, after either 9 or 13 days, transferred to 1/2MS media supplemented with 450nM TWS1 or CIF2. For PA (Sigma Aldrich, Cat# P49805-5G) treatments, plants were grown for 9 days on 1/2MS and then transferred to 1/2MS media supplemented with 10μM PA. For all pharmacological treatments, unless specified otherwise, plants were treated for 5 days.

Histological Techniques.

For the analysis of root suberin, Fluorol Yellow (Santa Cruz Cat# sc-215052) was employed. Complete roots (for assessing root suberin coverage) were first collected and placed in water. Subsequently, they were incubated in a solution of Fluorol Yellow 088 (0.01% dissolved in lactic acid) for 30 minutes at 70°C in the dark. The stained material was washed with water and incubated in a solution of aniline blue (0.5% in water) for counterstaining. After staining, plant material was mounted with 10% glycerol on glass slides for analysis using epifluorescence.

For periderm lignin studies, roots were collected in water and then stained in a solution of Basic Fuchsin (Sigma, 857343-100G) (0.5% in water) for 5 minutes. Afterward, they were washed with water, mounted with water on glass slides, and observed under the microscope.

For gene lignin pattern analysis, either vibratome cross-sections or whole-mounts were utilized. In the case of vibratome sections, 1 cm root samples from the root junction were first collected in water and then fixed using a 4% PFA solution (in 1xPBS) as is indicated in Ursache et al., 2018. The fixation took 1 hour, and after this, the seedlings were rinsed twice for 1 min in 1xPBS and subsequently transferred to the clearing solution (ClearSee) as described in (Ursache et al., 2018). Vibratome cross-sections were prepared following the protocol described in (Wunderling et al., 2018). The sections were collected in water and stained with Basic Fuchsin or Fluorol Yellow for subsequent examination following (Ursache et al., 2018). For whole-mounts, root sections were directly mounted on glass slides for analysis.

Confocal Laser Scanning Microscopy Imaging.

Confocal pictures were obtained using a Zeiss LSM 880 CLS microscope. Whole mount roots and roots virbratome sections were imaged with a Zeiss LSM880 with the following settings: cork autofluorescence (ex.405 nm; em. 420-460 nm), Basic Fuchsin (ex.566 nm; em.570-630 nm). FY (ex.488nm, em. 490- 540 nm), GFP (488nm, 490 -510 nm), Venus and Citrine: (ex. 514 nm; em. 520–540 nm) and Calcofluor white (ex.475 nm, em 405-425nm). 3D reconstructions and Orthogonal views of a Z stack were obtained using the ZEN Black software.

Sample preparation for RNA-seq and qPCR experiments.

RNA was extracted from root sections of approximately 2 cm from the root junction. Lateral roots were excised, and the samples were promptly collected in a tube submerged in liquid nitrogen to preserve RNA integrity. To create one single RNA sample, between 40 and 50 root sections were pooled together. The RNA extraction was done using using the Universal RNA Purification Kit (Roboklon, E3598-02) according to the manufacturer protocol.

RNAseq data processing and analysis.

RNA sequencing (pair end 150bp) was performed at Novogene. Raw data sequences will be available at after publisching. Data processing and data analysis was performed using the Galaxy platform (https://usegalaxy.eu/)(Afgan et al., 2018). Adaptors were removed with Trim Galore using default parameters, read quality was assesed with FastQC. Reads were aligned to TAIR10 genome using HISAT2 using default parameters. Reads were counted using featureCounts and differential gene expression analysis was performed using DESeq2 and can be query in DataS6.

qPCR analysis.

C-DNA was synthetized using AMV Reverse Transcriptase Native (Roboklon, E1372-01). qPCR was performed using MESA blue (Eurogentec, RT-SYS2X-03- +NRWOUB) in a CFX96 Real-Time System machine (BIO-RAD). Primers used for qPCR are listed in Table S2. The relative expression was calculated using CFX Maestro software (BIO-RAD) and the sample were normalized against EF1.

Quantitative Analysis.

No statistical methods were used to predetermine sample size. The experiments were not randomized. IBM SPSS Statistics version 24-25-26 (IBM) were used to make statistical analysis. The root suberin coverage was determined using imageJ / Fiji5. The Root length and Root Suberin Coverage was done according (Andersen et al., 2021). For the suberin root coverage quantification in old roots that comprised the periderm, statistic was performed separately for each root zone.

Supplemental material

Figure S1: Lignification deposition during phellem differentiation. A schematic diagram of the three analysed developmental stages of periderm. In yellow, stage 4/5 is shown; in blue, stage 3/4; and in red, stage 2. Stage 2 exhibits lower lignification in comparison with the other stages. White scale bar: 60µm.

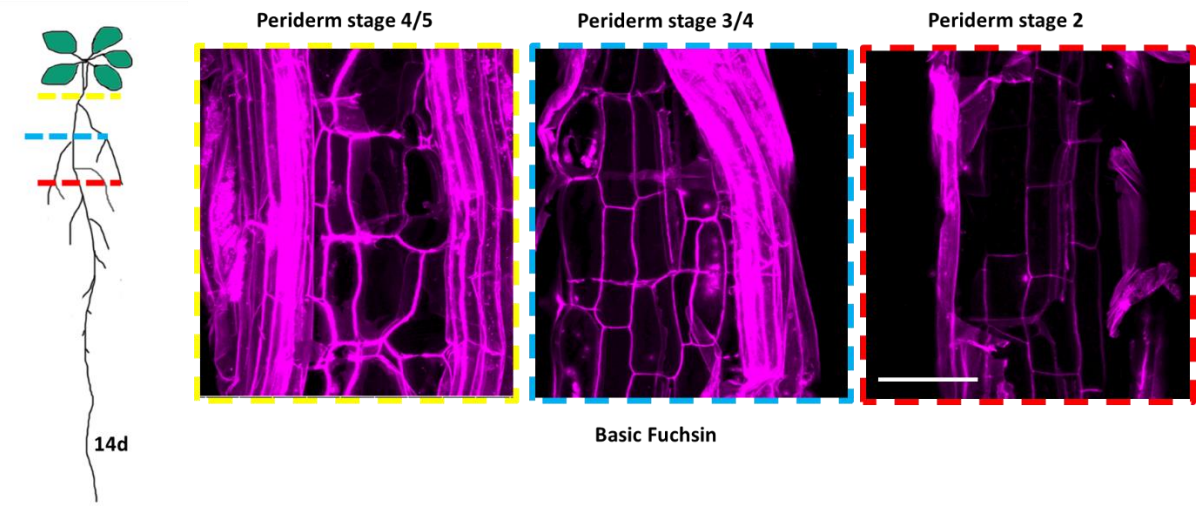

Figure S2: Basic Fuchsin and Fluorol Yellow do not share a deposition pattern in the initial stages of differentiation. The left image displays the Fluorol Yellow signal (suberin) in the phellem, while the middle image shows the Basic Fuchsin signal (lignin), comparison with differentiated phellem, lignin is polarly localized in the undifferentiated phellem (red arrows). On the right, Fluorol Yellow, Basic Fuchsin, and bright-field pictures are merged together. This composite image illustrates differentiated and undifferentiated phellem, characterized by the continued coverage of cortex and epidermis:

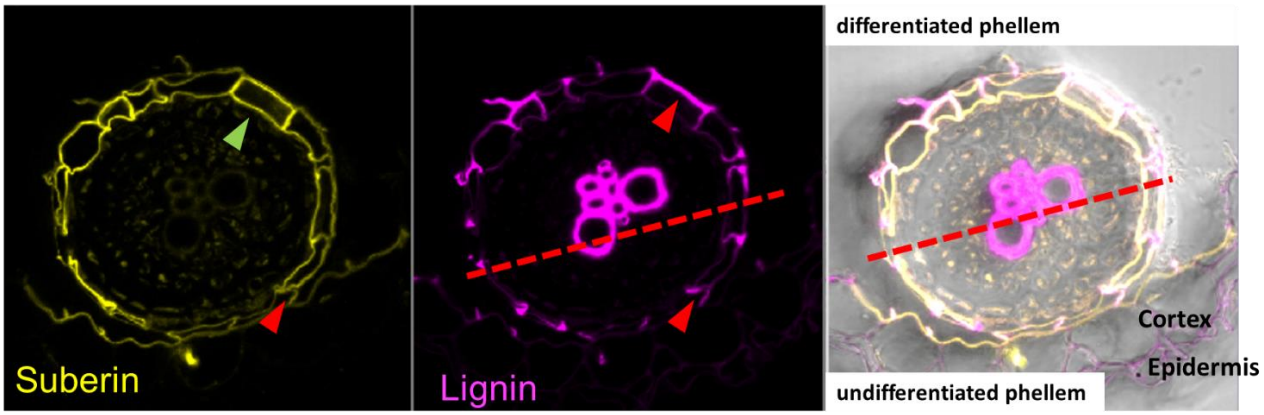

Table S1: Lines used in the research

Arabidopsis Lines	**Obtained from/by**	**Described in**
ELTP.MYB4 in pGPAT4:mCitine-SYP122	Andersen Tonni	(Andersen et al., 2021b)
gso1gso2	Ingram, G. / Gelder, N.	(Doll et al., 2020)
tws1	Ingram, G. / Gelder, N.	(Doll et al., 2020)
pGSO1/SGN3:NLS-3xVenus	Niko Geldner	Doll et al., 2020)
pGSO2:NLS-3xVenus	Ingram, G.	(Truskina, Brück, et al., 2022)
pSGN1:NLS-GFP-GUS	Niko Geldner	
pTWS1:NLS-3xVenus	Ingram, G.	Doll et al., 2020)
pCIF4:NLS-3xVenus	Ingram, G.	(Truskina, Brück, et al., 2022)
pSGN3:SGN3-Venus	Ingram, G.	Doll et al., 2020)
gelp22 gelp38 gelp51 gelp49 gelp9	Ursache R / Geldner N	(Ursache et al., 2021)

Table S2: Primers used in the research

Element	**Primer**	**Sequence**
PAL1	PAL1 qPCR F	aagtggctgcgatctcaactattgg
	PAL1 qPCR R	gtggcttgtttctttcgtgcttcc
PAL4	PAL4 qPCR F	ccgaggaacggacagttatggag
	PAL4 qPCR R	gcacggagtgatttcgtggttg
PER15	PER15 qPCR F3	gacgacgacgagagtaacta
	PER15 qPCR R4	cagtaactatactcccactggt
MYB36	MYB36 qPCR F	ccaagcttcatccattgctc
	MYB36 qPCR R	tgatgatcaacgttaactcctaaag
KCS2	KCS2 qPCR F	ccttcgttatcggctatgatcgtga
	KCS2 qPCR R	tgcagtttgagagaagcattgatcg
FAR4	FAR4 qPCR F	catgcaacggtttcacagtgaggt
	FAR4 qPCR R	tgagcggtccaaatgtgttgacg
FACT	FACT qPCR F	cagtcctgaaggaaagatcgctgtg
	FACT qPCR R	ctcggcccaagagttgaggaac
ASFT	ASFT qPCR F	cccgatcctgaaactctagggaagc
	ASFT qPCR R	ccgagaacaaaccctccacatttga
HORST	HORST qPCR F	ggagacacgtggcaatgatcagga
	HORST qPCR R	gtcgagcctcttggcacgaaagt
GPAT5	GPAT5 qPCR F	accgtgtcgctaatttgtttgttgg
	GPAT5 qPCR R	ccgtcgtgaaatatcaccggaagt
MYB41	MYB41qPCR F	gtacgctccccaaaaatgctggac
	MYB41 qPCR R	gcggctattgctgaccacttgtttc
MYB93	MYB93 qPCR F	gctcgcagatttgaataggtgtgga
	MYB93 qPCR R	tgcgtcgcaatagctgaccattt

References

Alassimone, J., Fujita, S., Doblas, V. G., Van Dop, M., Barberon, M., Kalmbach, L., Vermeer, J. E. M., Rojas-Murcia, N., Santuari, L., Hardtke, C. S., & Geldner, N. (2016). Polarly localized kinase SGN1 is required for Casparian strip integrity and positioning. *Nature Plants*, *2*(8). https://doi.org/10.1038/NPLANTS.2016.113

Andersen, T. G., Molina, D., Kilian, J., Franke, R. B., Ragni, L., & Geldner, N. (2021). Tissue-Autonomous Phenylpropanoid Production Is Essential for Establishment of Root Barriers. *Current Biology*, *31*(5), 965-977.e5. https://doi.org/10.1016/j.cub.2020.11.070

Barberon, M., Vermeer, J. E. M., De Bellis, D., Wang, P., Naseer, S., Andersen, T. G., Humbel, B. M., Nawrath, C., Takano, J., Salt, D. E., & Geldner, N. (2016). Adaptation of Root Function by Nutrient-Induced Plasticity of Endodermal Differentiation. *Cell*, *164*(3), 447–459. https://doi.org/10.1016/j.cell.2015.12.021

Belsson, F., Li, Y., Bonaventura, G., Pollard, M., & Ohlrogge, J. B. (2007). The acyltransferase GPAT5 is required for the synthesis of suberin in seed coat and root of Arabidopsis. *Plant Cell*, *19*(1), 351–368. https://doi.org/10.1105/tpc.106.048033

Bernards, M. A. (2002). Demystifying suberin. In *Canadian Journal of Botany* (Vol. 80, Issue 3, pp. 227–240). https://doi.org/10.1139/b02-017

Butenko, M. A., Patterson, S. E., Grini, P. E., Stenvik, G. E., Amundsen, S. S., Mandal, A., & Aalen, R. B. (2003). INFLORESCENCE DEFICIENT in ABSCISSION Controls Floral Organ Abscission in Arabidopsis and Identifies a Novel Family of Putative Ligands in Plants. *Plant Cell*, *15*(10), 2296–2307. https://doi.org/10.1105/tpc.014365

Chen, C., He, G., Li, J., Perez-Hormaeche, J., Becker, T., Luo, M., Wallrad, L., Gao, J., Li, J., Pardo, J. M., Kudla, J., & Guo, Y. (2023). A salt stress-activated GSO1-SOS2-SOS1 module protects the Arabidopsis root stem cell niche by enhancing sodium ion extrusion . *The EMBO Journal*, *42*(13). https://doi.org/10.15252/embj.2022113004

Doblas, V. G., Smakowska-Luzan, E., Fujita, S., Alassimone, J., Barberon, M., Madalinski, M., Belkhadir, Y., & Geldner, N. (2017). Root diffusion barrier control by a vasculature-derived peptide binding to the SGN3 receptor. *Science*, *355*(6322), 280–284. https://www.science.org

Doll, N. M., Royek, S., Fujita, S., Okuda, S., Chamot, S., Stintzi, A., Widiez, T., Hothorn, M., Schaller, A., Geldner, N., & Ingram, G. (2020). A two-way molecular dialogue between embryo and endosperm is required for seed development. *Science*, *367*(6476), 431–435. https://www.science.org

Evert, R. (2006). Chapter Fifteen - Periderm. In *Esau's Plant Anatomy: Meristems, Cells, and Tissues of the Plant Body: Their Structure, Function, and Development* (Vol. 1, pp. 427–446).

Fujita, S., De Bellis, D., Edel, K. H., Köster, P., Andersen, T. G., Schmid-Siegert, E., Dénervaud Tendon, V., Pfister, A., Marhavý, P., Ursache, R., Doblas, V. G., Barberon, M., Daraspe, J., Creff, A., Ingram, G., Kudla, J., & Geldner, N. (2020). SCHENGEN receptor module drives localized ROS production and lignification in plant roots . *The EMBO Journal*, *39*(9). https://doi.org/10.15252/embj.2019103894

Geldner, N. (2013). The endodermis. In *Annual Review of Plant Biology* (Vol. 64, pp. 531–558). https://doi.org/10.1146/annurev-arplant-050312-120050

Höfer, R., Briesen, I., Beck, M., Pinot, F., Schreiber, L., & Franke, R. (2008). The Arabidopsis cytochrome P450 CYP86A1 encodes a fatty acid ω-hydroxylase involved in suberin monomer biosynthesis. *Journal of Experimental Botany*, *59*(9), 2347–2360. https://doi.org/10.1093/jxb/ern101

Jinn, T.-L., Stone, J. M., & Walker, J. C. (2000). HAESA, an Arabidopsis leucine-rich repeat receptor kinase, controls floral organ abscission. *Genes & Development*, *14*, 108–117. www.genesdev.org

Kamiya, T., Borghi, M., Wang, P., Danku, J. M. C., Kalmbach, L., Hosmani, P. S., Naseer, S., Fujiwara, T., Geldner, N., & Salt, D. E. (2015). The MYB36 transcription factor orchestrates Casparian strip formation. *Proceedings of the National Academy of Sciences of the United States of America*, *112*(33), 10533–10538. https://doi.org/10.1073/pnas.1507691112

Ki Cho, S., Larue, C. T., Chevalier, D., Wang, H., Jinn, T.-L., Zhang, S., & Walker, J. C. (2008). Regulation of floral organ abscission in Arabidopsis thaliana. In *PLANT BIOLOGY* (Vol. 105).

Kolattukudy, P. E. (1980). Biopolyester Membranes of Plants:Cutin and Suberin. *Science*, *30*(30), 990–1000.

Komori, R., Amano, Y., Ogawa-Ohnishi, M., & Matsubayashi, Y. (2009). Identification of tyrosylprotein sulfotransferase in Arabidopsis. *Proceedings of the National Academy of Sciences (PNAS)*, *106*(35), 15067–15072. www.pnas.org/cgi/content/full/

Leal, A. R., Barros, P. M., Parizot, B., Sapeta, H., Vangheluwe, N., Andersen, T. G., Beeckman, T., & Oliveira, M. M. (2022). Translational profile of developing phellem cells in Arabidopsis thaliana roots. *Plant Journal*, *110*(3), 899–915. https://doi.org/10.1111/tpj.15691

Lee, Y., Yoon, T. H., Lee, J., Jeon, S. Y., Lee, J. H., Lee, M. K., Chen, H., Yun, J., Oh, S. Y., Wen, X., Cho, H. K., Mang, H., & Kwak, J. M. (2018). A Lignin Molecular Brace Controls Precision Processing of Cell Walls Critical for Surface Integrity in Arabidopsis. *Cell*, *173*(6), 1468-1480.e9. https://doi.org/10.1016/j.cell.2018.03.060

Nakayama, T., Shinohara, H., Tanaka, M., Baba, K., Ogawa-Ohnishi, M., & Matsubayashi, Y. (2017). A peptide hormone required for Casparian strip diffusion barrier formation in Arabidopsis roots. *Science*, *355*(6322), 284–286. https://doi.org/10.1126/science.aai9057

Naseer, S., Lee, Y., Lapierre, C., Franke, R., Nawrath, C., & Geldner, N. (2012). Casparian strip diffusion barrier in Arabidopsis is made of a lignin polymer without suberin. *Proceedings of the National Academy of Sciences of the United States of America*, *109*(25), 10101–10106. https://doi.org/10.1073/pnas.1205726109

Nawrath, C., Schreiber, L., Franke, R. B., Geldner, N., Reina-Pinto, J. J., & Kunst, L. (2013). Apoplastic Diffusion Barriers in Arabidopsis. *The Arabidopsis Book*, *11*, e0167. https://doi.org/10.1199/tab.0167

Nomberg, G., Marinov, O., Arya, G. C., Manasherova, E., & Cohen, H. (2022). The Key Enzymes in the Suberin Biosynthetic Pathway in Plants: An Update. In *Plants* (Vol. 11, Issue 3). MDPI. https://doi.org/10.3390/plants11030392

Okuda, S., Fujita, S., Moretti, A., Hohmann, U., Doblas, V. G., Ma, Y., Pfister, A., Brandt, B., Geldner, N., & Hothorn, M. (2020). Molecular mechanism for the recognition of sequence-divergent CIF peptides by the plant receptor kinases GSO1/SGN3 and GSO2. *Proceedings of the National Academy of Sciences (PNAS)*, *117*(5), 2693–2703. https://doi.org/10.1073/pnas.1911553117/-/DCSupplemental

Pollard, M., Beisson, F., Li, Y., & Ohlrogge, J. B. (2008). Building lipid barriers: biosynthesis of cutin and suberin. In *Trends in Plant Science* (Vol. 13, Issue 5, pp. 236–246). https://doi.org/10.1016/j.tplants.2008.03.003

Reyt, G., Ramakrishna, P., Salas-González, I., Fujita, S., Love, A., Tiemessen, D., Lapierre, C., Morreel, K., Calvo-Polanco, M., Flis, P., Geldner, N., Boursiac, Y., Boerjan, W., George, M. W., Castrillo, G., & Salt, D. E. (2021). Two chemically distinct root lignin barriers control solute and water balance. *Nature Communications*, *12*(1). https://doi.org/10.1038/s41467-021-22550-0

Rojas-Murcia, N., Hématy, K., Lee, Y., Emonet, A., Ursache, R., Fujita, S., De Bellis, D., & Geldner, N. (2020). High-order mutants reveal an essential requirement for peroxidases but not laccases in Casparian strip lignification. *Proceedings of the National Academy of Sciences of the United States of America*, *117*(46), 29166–29177. https://doi.org/10.1073/pnas.2012728117/-/DCSupplemental

Schalk, M., Cabello-Hurtado, F., Pierrel, M.-A., Atanossova, R., Saindrenan, P., & Werck-Reichhart, D. (1998). Piperonylic Acid, a Selective, Mechanism-Based Inactivator of the trans-Cinnamate 4-Hydroxylase: A New Tool to Control the Flux of Metabolites in the Phenylpropanoid Pathway 1. *Plant Physiology*, *118*, 209–218. https://academic.oup.com/plphys/article/118/1/209/6085572

Serra, O., & Geldner, N. (2022). The making of suberin. In *New Phytologist* (Vol. 235, Issue 3, pp. 848–866). John Wiley and Sons Inc. https://doi.org/10.1111/nph.18202

Serra, O., Mähönen, A. P., Hetherington, A. J., & Ragni, L. (2022). The Making of Plant Armor: The Periderm. *Annual Review of Plant Biology*, *73*, 405–432. https://doi.org/10.1146/annurev-arplant-102720

Sexauer, M., Shen, D., Schön, M., Andersen, T. G., & Markmann, K. (2021). Visualizing polymeric components that define distinct root barriers across plant lineages. *Development (Cambridge)*, *148*(23). https://doi.org/10.1242/dev.199820

Shukla, V., Han, J.-P., Cléard, F., Lefebvre-Legendre, L., Gully, K., Flis, P., Berhin, A., Andersen, T. G., Salt, D. E., Nawrath, C., & Barberon, M. (2021). Suberin plasticity to developmental and exogenous cues is regulated by a set of MYB transcription factors. *Proceedings of the National Academy of Sciences of the United States of America*, *118*(39), 1–10. https://doi.org/10.1073/pnas.2101730118/-/DCSupplemental

Tobimatsu, Y., & Schuetz, M. (2019). Lignin polymerization: how do plants manage the chemistry so well? In *Current Opinion in Biotechnology* (Vol. 56, pp. 75–81). Elsevier Ltd. https://doi.org/10.1016/j.copbio.2018.10.001

Truskina, J., Brück B, S., Stintzi, A., Boeuf, S., Doll, N. M., Fujita, S., Geldner, N., Schaller, A., & Ingram, G. C. (2022). A peptide-mediated, multilateral molecular dialogue for the coordination of pollen wall formation. *Proceedings of the National Academy of Sciences of the United States of America*, *119*(22), 1–10. https://doi.org/10.1073/pnas

Ursache, R., Andersen, T. G., Marhavý, P., & Geldner, N. (2018). A protocol for combining fluorescent proteins with histological stains for diverse cell wall components. *Plant Journal*, *93*(2), 399–412. https://doi.org/10.1111/tpj.13784

Ursache, R., De Jesus Vieira Teixeira, C., Dénervaud Tendon, V., Gully, K., De Bellis, D., Schmid-Siegert, E., Grube Andersen, T., Shekhar, V., Calderon, S., Pradervand, S., Nawrath, C., Geldner, N., & Vermeer, J. E. M. (2021). GDSL-domain proteins have key roles in suberin polymerization and degradation. *Nature Plants*, *7*(3), 353–364. https://doi.org/10.1038/s41477-021-00862-9

Vanholme, R., De Meester, B., Ralph, J., & Boerjan, W. (2019). Lignin biosynthesis and its integration into metabolism. In *Current Opinion in Biotechnology* (Vol. 56, pp. 230–239). Elsevier Ltd. https://doi.org/10.1016/j.copbio.2019.02.018

Weng, J. K., & Chapple, C. (2010). The origin and evolution of lignin biosynthesis. In *New Phytologist* (Vol. 187, Issue 2, pp. 273–285). https://doi.org/10.1111/j.1469-8137.2010.03327.x

Xiao, W., Molina, D., Wunderling, A., Ripper, D., Vermeer, J. E. M., & Ragni, L. (2020). Pluripotent Pericycle Cells Trigger Different Growth Outputs by Integrating Developmental Cues into Distinct Regulatory Modules. *Current Biology*, *30*(22), 4384-4398.e5. https://doi.org/10.1016/j.cub.2020.08.053

Zhang, B., Xin, B., Sun, X., Chao, D., Zheng, H., Peng, L., Chen, X., Zhang, L., Yu, J., Ma, D., & Xia, J. (2023). Small peptide signaling via OsCIF1/2 mediates Casparian strip formation at the root endodermal and nonendodermal cell layers in rice. *The Plant Cell*. https://doi.org/10.1093/plcell/koad269

5.3 Publish manuscript 1: Tissue-Autonomous Phenylpropanoid Production Is Essential for Establishment of Root Barriers

T.G.A. acquired and interpreted data, conceived the research, and wrote the manuscript. D.M. conducted and analyzed GC-MS data together with J.K. R.B.F. interpreted data and contributed to writing the manuscript. D.M. and L.R. acquired the cork data. L.R. conceived the research, acquired and interpreted data, and contributed to writing the manuscript. N.G. conceived the research and contributed to writing the manuscript. All authors have approved the final manuscript and agree to be personally accountable for the individual contributions

Article

Current Biology

Tissue-Autonomous Phenylpropanoid Production Is Essential for Establishment of Root Barriers

Graphical Abstract

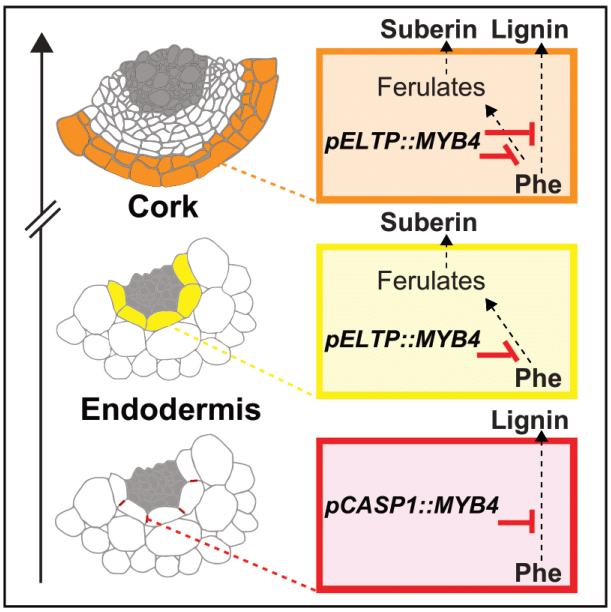

Highlights

- Autonomous production of phenylpropanoids is required for Casparian strip formation
- Phenylpropanoids are essential for suberin deposition in endodermis and cork
- Cork differentiation requires autonomous production of phenylpropanoids
- Spatiotemporal repression of phenylpropanoids can dissect barrier functions

Authors

Tonni Grube Andersen, David Molina, Joachim Kilian, Rochus B. Franke, Laura Ragni, Niko Geldner

Correspondence

tandersen@mpipz.mpg.de (T.G.A.), laura.ragni@zmbp.uni-tuebingen.de (L.R.), niko.geldner@unil.ch (N.G.)

In Brief

Andersen et al. show here that cell-autonomous phenylpropanoid production is required for root barrier formation and integrity.

Andersen et al., 2021, Current Biology *31*, 965–977
March 8, 2021
https://doi.org/10.1016/j.cub.2020.11.070

CellPress

Current Biology

CellPress

Article

Tissue-Autonomous Phenylpropanoid Production Is Essential for Establishment of Root Barriers

Tonni Grube Andersen,[1,5,4,*] David Molina,[2] Joachim Kilian,[2] Rochus B. Franke,[3] Laura Ragni,[2,*] and Niko Geldner[1,*]
[1]Department of Plant Molecular Biology, University of Lausanne, 1015 Lausanne, Switzerland
[2]ZMBP—Center for Plant Molecular Biology, University of Tuebingen, Auf der Morgenstelle 32, 72076 Tuebingen, Germany
[3]Institute of Cellular and Molecular Botany, Rheinische Friedrich-Wilhelms-University of Bonn, Kirschallee 1, 53115 Bonn, Germany
[4]Present address: Max Planck Institute for Plant Breeding Research, Carl-Von-Linné-weg 10, 50829 Cologne, Germany
[5]Lead Contact
*Correspondence: tandersen@mpipz.mpg.de (T.G.A.), laura.ragni@zmbp.uni-tuebingen.de (L.R.), niko.geldner@unil.ch (N.G.)
https://doi.org/10.1016/j.cub.2020.11.070

SUMMARY

Plants deposit hydrophobic polymers, such as lignin or suberin, in their root cell walls to protect inner tissues and facilitate selective uptake of solutes. Insights into how individual root tissues contribute to polymer formation are important for elucidation of ultrastructure, function, and development of these protective barriers. Although the pathways responsible for production of the barrier constituents are established, our models lack spatiotemporal resolution—especially in roots—thus, the source of monomeric barrier components is not clear. This is mainly due to our restricted ability to manipulate synthesis of the broadly important phenylpropanoid pathway, as mutants in this pathway display lethal or pleiotropic phenotypes. Here, we overcome this challenge by exploiting highly controlled *in vivo* repression systems. We provide strong evidence that autonomous production of phenylpropanoids is essential for establishment of the endodermal Casparian strip as well as adherence of the suberin matrix to the cell wall of endodermis and cork. Our work highlights that, in roots, the phenylpropanoid pathway is under tight spatiotemporal control and serves distinct roles in barrier formation across tissues and developmental zones. This becomes evident in the late endodermis, where repression of phenylpropanoid production leads to active removal of suberin in pre-suberized cells, indicating that endodermal suberin depositions might embody a steady state between continuous synthesis and degradation.

INTRODUCTION

Among the diffusion barriers in root cell walls, the best characterized is, arguably, the Casparian strip (CS). The CS consists of precisely localized oxidatively coupled lignin-polymer depositions between the newly differentiated endodermal cells.[1,2] As development progresses, the surface of most endodermal cells becomes covered by hydrophobic suberin (Figure 1A).[3] In contrast to the CS, the suberin barrier consists of lamellae-like structures below the primary cell wall,[4,5] constituting a transmembrane rather than an apoplastic barrier,[6–8] i.e., blocking uptake into cells. The exact lamellae structure remains enigmatic but consists of a crosslinked matrix of fatty acids, glycerol, and aromatic monomers joined through a variety of ester and oxidative couplings.[9,10] Establishment and function of endodermal barriers is tightly controlled by a surveillance system.[11] This consists of an elegant, localized multi-component pathway,[12] which requires diffusion of Casparian strip integrity factor (CIF) peptides from the stele to the surface of the endodermis. Here, CIF peptides activate the leucine rich repeat (LRR)-family receptor SCHENGEN 3 (SGN3)[13] (also called GSO1).[14] This creates a self-regulating system, as formation of a tight CS inhibits CIF diffusion. In the case of a non-functional CS, excess activation of this pathway serves to initiate endodermal "sealing" through ectopic non-CS localized lignification and suberin depositions in the younger, normally unsuberized endodermal cells.[15]

In the older part of the root, radial cell divisions in the stele lead to thickening of the root (secondary growth). As a consequence, the endodermis undergoes programmed cell death, the outer cell layers are shed, and the barrier function is overtaken by the periderm.[17] The periderm consists of the meristematic phellogen (originating from the pericycle), which divides bifacially and gives rise to cork (toward the soil) and phelloderm layers (toward the vasculature).[18] Cork cell walls are highly suberized and lignified, which is essential for their barrier role. In line with this, elevated number of cork layers and suberin content have been associated with increased tolerance to stresses.[18–21]

Common to the polymeric root barriers across these developmental stages and tissues is that their building blocks are derived from the fatty acid (aliphatic) and phenylpropanoid (PP) (aromatic) pathways. For production of aliphatic suberin constituents, fatty acids are oxidized[22,23] and conjugated to glycerol moieties via glycerol-3-phosphate acyltransferases (GPATs)[24–26] before export to the apoplast. Suberin biosynthetic gene expression correlates with suberin deposition,[17,27] and *GPAT5* has been established as a marker for endodermal cells undergoing suberization.[28] Therefore, combined with the hydrophobic nature of fatty acids, it is reasonable to assume that aliphatic constituents of

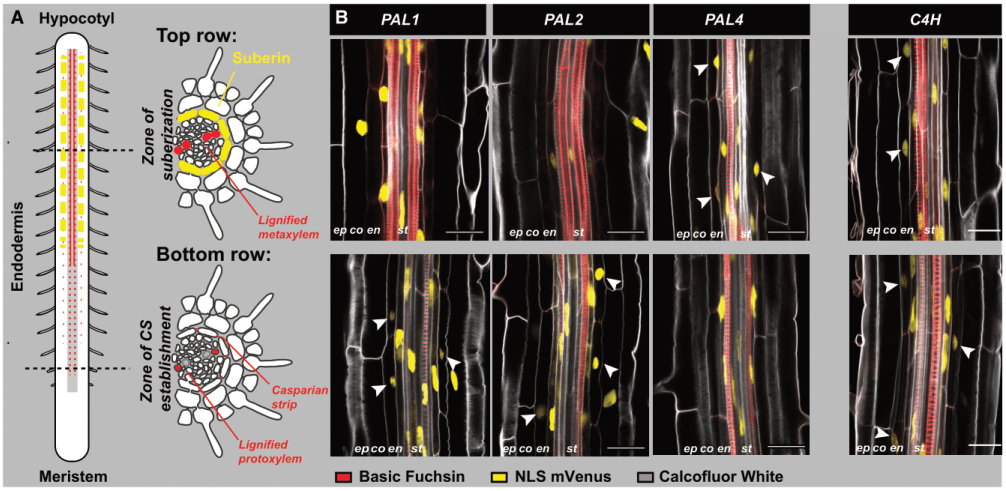

Figure 1. Essential Phenylpropanoid Pathway Genes Are Expressed in the Root Endodermis

(A) Endodermis differentiation can be divided in two successive steps: first, Casparian strips (CSs) are deposited (zone of CS establishment) concomitantly with protoxylem lignification. Second, the suberin lamella is formed (zone of suberization) alongside metaxylem lignification.

(B) Activity of nuclear localized (NLS) 3× mVenus fusion reporters driven by promoter regions of root-expressed *phenylalanine ammonia lyase* (*PAL*) and *cinnamate 4-hydroxylase* (*C4H*) homologs in *Arabidopsis* roots. Expression in 5-day-old roots in the zone of CS establishment (bottom) and suberization (top) of the endodermis is shown. All roots were fixed using a previously established ClearSee protocol.[16] Cell walls were highlighted using Calcofluor White, whereas basic fuchsin was used to highlight lignin depositions in the xylem and in the CSs. Arrowheads point to endodermis cells with reporter activity. co, cortex; en, endodermis; ep, epidermis; st, stele. Scale bars represent 25 μm.

suberin are produced by the depositing tissues themselves.[3] In contrast, the source tissue for PP-derived barrier constituents is less clear, as these have the physio-chemical properties for diffusion across tissues.[29] Besides acting as structural constituents, such as coniferyl alcohol (lignin) and ferulic acid (FA) (suberin), the PP pathway gives rise to a bouquet of metabolites that function in different chemical systems. These include defenses, chelators, colorants, and/or pollinator attractors.[30] Phenylalanine is the major precursor for PPs in most plants, and the initial two committing steps of the PP pathway are catalyzed by the phenylalanine ammonia lyase (PAL)[31] and cinnamate-4-hydroxylase (C4H) enzymes, respectively.[32–34] However, a large degree of redundancy, multi-gene families, and promiscuous branch-point enzymes make it difficult to pinpoint the exact origin of a given PP metabolite. An additional issue is that barrier precursors needed for polymerization and deposition in the cell walls must be transported across the plasma membrane to reach the apoplast. Therefore, the origin of these metabolites is even more enigmatic, as they can be produced and employed cell autonomously or originate from distal cells. Indeed, in the xylem, both cell-autonomous and distal PP production for lignin monomers occurs.[35] Despite the importance of PP metabolites for barriers, and the close proximity of the barrier-containing tissues to the xylem, the tissue-specific coordination of the PP synthesis remains unclear.

Here, we address this question in the roots of *Arabidopsis*. By employing transcriptional repressors in a tissue- and time-dependent manner, we created plants with controllable reduction in PP synthesis within discrete, tissue-specific subzones of the root. This allowed us to investigate the origin of PP precursors and the functional role in different root barriers across root development. We show that both endodermis and cork have the capacity to synthesize PP-derived metabolites. Moreover, our controlled manipulations allowed us to establish that the PP metabolites serve distinct, overlooked functions in barrier dynamics and adherence to the cell wall, especially with regards to endodermal suberin.

RESULTS

Endodermal Cells Have the Capacity for PP Synthesis

To establish whether the endodermis has the capacity to synthesize PP-derived metabolites, we investigated the expression of the PP pathway in *Arabidopsis* roots. *Arabidopsis* has 4 homologs of the *PAL* genes,[36] where only *PAL1*, *PAL2*, and *PAL4* transcripts can be detected in roots.[37] In contrast, only one *C4H* locus exists.[36] As publicly available datasets do not provide sufficient resolution for our analysis, we constructed fluorescent, transcriptional reporters based on promoter regions of *PAL1*, *PAL2*, *PAL4*, and *C4H* driving expression of a nuclear-localized triple mVenus reporter (NLS 3× mVenus). We investigated expression of these reporters at two critical endodermal developmental stages: (1) during CS establishment, which occurs simultaneously to protoxylem lignification (Figure 1A, bottom panel) and (2) during suberization, which happens concomitantly to metaxylem lignification (Figure 1A, top panel). Expectedly, in

roots of 5-day-old seedlings, activity of all promoters was found within the vasculature/stele at both developmental stages (Figure 1B) where the PP pathway is presumably responsible for synthesis of lignin monomers for xylem formation. We also found evidence for expression of PP genes in the cortex (Figure 1B), which might be due to the formation of other PP-derived metabolites, such as coumarins,[38] in this tissue. *PAL1* and *PAL2* promoters were additionally active in the zone of CS establishment (Figure 1B, bottom panel). Interestingly, *PAL4* was only found to be endodermis expressed in the zone of suberization (Figure 1B, top panel). *C4H* expression was broader and encompassed the cortex, endodermis, and stele at both investigated stages (Figure 1B). Thus, the endodermis expresses key genes of the PP pathway, which makes it plausible that this layer can produce PP metabolites.

Lignification of CS and Xylem after Inhibition Recovers with Similar Dynamics

Lignification of the CS and xylem starts at a similar developmental point in the root, which suggests that these processes share a common source of PP substrates. Our next step was therefore to address whether lignin deposition in the CS and xylem is coordinated. As previously described, treating 5-day-old *Arabidopsis* seedlings for 24 h with the C4H-inhibitor piperonylic acid (PA)[39] leads to a non-lignified zone where developing xylem and CS would normally have initiated lignification (Figure 2A).[40] To investigate the ability of the tissues to recover lignification after inhibition, we transferred PA-inhibited seedlings to recovery plates (without PA), in presence or absence of the lignin monomer coniferyl alcohol (G-OH) and measured recovery of lignification over time. Lignin deposition without exogenous monomer supply—dependent on endogenous PP synthesis—reoccurred surprisingly fast, as we observed a significant ($p < 0.01$; two-tailed Student's t test versus untreated) lignin-specific fluorescence (basic fuchsin stain) for both the xylem and CS in the PA-induced non-lignified zone after only 4 h of transfer to plates without G-OH (Figures 2B and S1A). This was further decreased by at least 2 h for both CS and xylem in presence of 20 μM G-OH (Figures 2B and S1A). Thus, PA interferes with endogenous monolignol availability, but not apoplastic polymerization capacity, for lignin. Only in the presence of externally supplied G-OH did both xylem and CS fully recover within the tested time frame (Figure 2B). We conclud that lignin polymerization capacity in both the CS and xylem can be uncoupled from substrate availability and that these tissues show similar lignification dynamics (Figures 2B and S1A).

Inhibition of PP Synthesis Leads to Aberrant Suberin Deposition

Disruption of the CS promotes ectopic suberization in young parts of the endodermis due to stimulation of the SCHENGEN (SGN) pathway.[11–13] With this in mind, our PA-inhibited plants must show SGN-dependent responses, such as ectopic suberization (Figure 2A). On a gene expression level, this was indeed the case, as the PA treatment led to a strong upregulation of genes related to suberin biosynthesis in a SGN3-dependent manner (Figure 2C). We realized that we could use this setup to address whether *de novo* deposition of endodermal suberin can occur without the ability to locally produce PP-derived metabolites. Under standard growth conditions, endodermal suberization is initiated in a "patchy" manner (Figures 2A and S1D) as cells at the xylem pole show delay in suberin onset.[28] Intriguingly, in contrast to the normal "smooth" signal observed when staining the endodermal cells with Fluorol Yellow (FY),[40] PA-treated roots showed a "droplet-like" FY signal specifically in the non-lignified zone (Figures 2F, 2G, and S1E). This signal depends on a stimulated SGN pathway, because we did not observe this in PA-treated *sgn3* roots (Figures 2D and 2F). Moreover, in PA-treated roots, suberin depositions already established before the treatment start were strongly reduced in a SGN-independent manner (Figures 2D and 2F) and not due to growth-related changes in the proportions of suberized root zones (Figure S1F). This observation is remarkable and suggests that already established endodermal suberin lamellae are unstable without active PP synthesis. We attempted to identify the specific metabolite involved in this by complementing the PA treatment with PP metabolites typical for lignin and suberin. Intriguingly, only FA and not G-OH in the media led to complementation of the droplet-like ectopic suberin deposition and prevented suberin disappearance in the pre-established zone (Figure 2E). This complementation could not be observed with other FA-related PP acids (Figure S1B). FA is a well-described constituent of suberin, and we therefore investigated a mutant with a non-functional version of the ALIPHATIC SUBERIN FERULOYL TRANSFERASE (ASFT), involved in the incorporation of ferulates into suberin.[27] Transfer DNA (T-DNA) knockout (KO) alleles of this mutant also showed droplet-like suberin depositions in the endodermis, even under normal growth conditions (Figures 2E and S1C). Moreover, FA-dependent complementation was absent in the *asft-1* mutant (Figure 2E). We therefore conclude that a tight coordination of aromatic (in particular FA) and aliphatic monomer synthesis is necessary for correct establishment of the endodermal suberin barrier.

Monolignol Production in the Endodermis Is Required for CS Formation

PA treatment indiscriminately inhibits the PP pathway in all cell types. Thus, we sought to create a genetic tool that would allow tissue-specific repression of PP synthesis, avoiding pleiotropic effects due to disruption of xylem formation, for example. Transcriptional regulation of PP synthesis includes the ethylene-responsive element binding factor-associated amphiphilic repression (EAR) domain-containing subgroup 4 MYB transcription factors.[41] All members in *Arabidopsis* (MYB3, MYB4, MYB7, and MYB32) repress genes of the PP pathway and could in theory work as genetic PP-synthesis repressors through ectopic expression. Although MYB7 represses mainly flavanol biosynthesis,[42] MYB3, MYB4, and MYB32 target expression of *C4H*. It is not clear whether these factors directly repress PP genes, so we focused on MYB4, as its DNA-binding domain has been shown to be required for repression of *C4H*[41] and has recently been shown to additionally repress the final step of phenyl alanine synthesis.[43] We established plant lines containing *MYB4* driven by the promoters of the Casparian strip membrane protein 1 (p*CASP1*)[44] or endodermal lipid transfer protein (p*ELTP*)[7] active specifically in the zone of CS establishment or suberization, respectively (Figure 3A). Consistent with expectations, only plants with p*CASP1*-driven expression of *MYB4* showed CS dysfunction. This was manifested as a "discontinuous" CS with

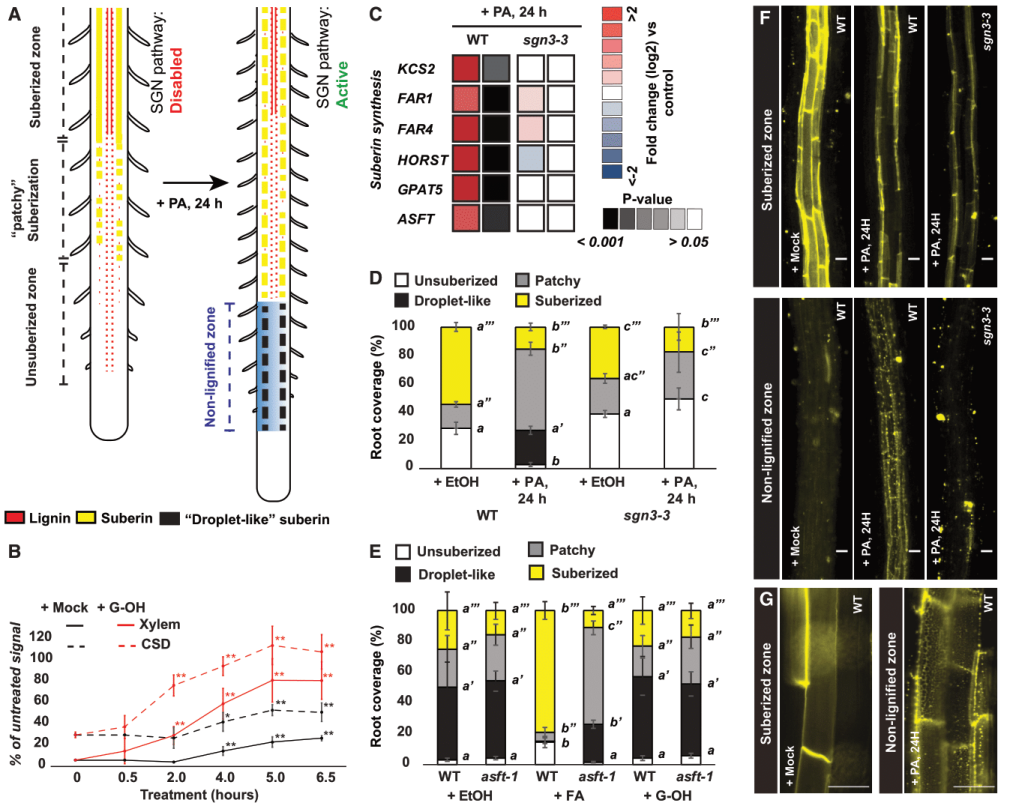

Figure 2. Endodermal Suberin Deposition Is Disrupted by Inhibition of PP Synthesis and Specifically Complemented by Ferulic Acid

(A) Scheme explaining the effects of piperonylic acid (PA) treatment on roots. Roots continue growth during PA treatment, which leads to establishment of a non-lignified zone where the xylem and Casparian strip (CS) are normally lignified in mock conditions. Absence of lignification in the CS domain (CSD) leads to diffusion of CS integrity factor peptides (CIFs) and consecutive activation of the Schengen (SGN) pathway. Activation of the SGN pathway is known to induce ectopic suberization of the otherwise non-lignified endodermal cells.[15] Our experimental setup therefore allowed us to study the effect of inhibited PP-metabolite production on ectopic suberin deposition.

(B) Time course analysis of basic fuchsin signal recovery in the PA-induced non-lignified zone of xylem or CSD. 5-day-old plants were treated for 24 h with PA and then moved to recovery plates with either a mock solution or 20 μM coniferyl alcohol (G-OH) at the indicated time points. The signals were normalized to identically grown non-PA-treated plants. n = 5; *p < 0.05; **p < 0.01; two-tailed Student's t test versus 0 h treatment.

(C) Relative expression of suberin biosynthesis genes in WT and *sgn3-3* roots treated with mock or PA for 24 h. Data were obtained by qPCR as described in the STAR Methods section. For primer and gene information, see Table S1. p values are based on a two-tailed Student's t test versus non-PA-treated control plants of the same genotype.

(D) Quantification of suberin root coverage by Fluorol Yellow (FY) staining of suberin in the endodermis of 5-day-old WT and *sgn3-3* roots treated with mock (EtOH) or PA for 24 h before staining. In the non-lignified zone of PA-treated roots, FY staining gave rise to "droplet-like" structures as seen in (F) and (G); n = 6.

(E) Quantification of suberin root coverage by FY staining in the endodermis of 5-day-old PA-treated WT and *asft-1* mutant roots co-treated with mock (EtOH) or 20 μM ferulic acid (FA) or 20 μM G-OH for 24 h; n = 6.

(F) Representative images of FY staining of the experiment shown in (D). Upper panels correspond to images taken at the level of the suberized zone, whereas lower panels correspond to images taken in non-lignified zone.

(G) Magnification of FY-staining images of a WT mock and PA-treated root in the suberin zone to highlight the suberin droplet-like phenotype shown in (F).

All error bars are SD; letters refer to individual groups/treatments in a one-way ANOVA analysis with a post hoc multiple group t test (Tukey) ($p < 0.05$). Scale bars represent 25 μm. See also Figure S1.

irregular patches (Figure 3A) and by increased propidium iodide (PI) permeability (Figure 3B). MYB3 and MYB32 showed similar effects, whereas no effects on CS formation was seen when MYB7 was employed in a similar manner (Figure S2D). Importantly, the MYB4-dependent CS disruption could be complemented by addition of G-OH to the media or through expression

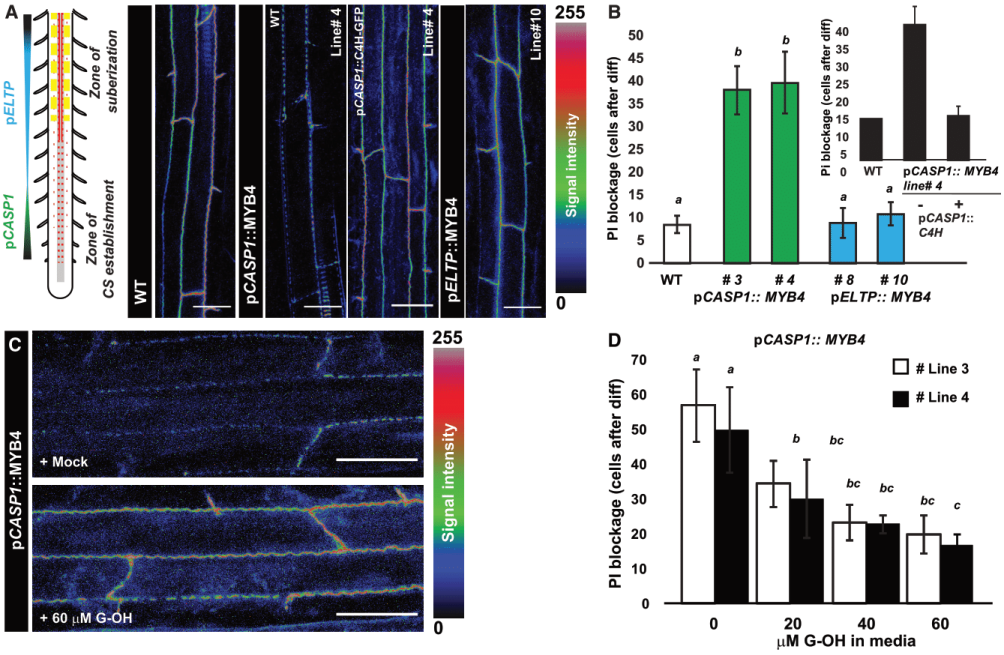

Figure 3. Endodermis-Specific Expression of MYB4 Alters Lignin Deposition and CS Formation

(A) The phenylpropanoid-repressive transcription factor MYB4[41] or cinnamate-4-hydroxylase (C4H) was expressed using the promoter from the CS membrane domain protein 1 (p*CASP1*)[44] active in the endodermis during CS establishment. MYB4 was additionally expressed under the promoter from the endodermal lipid transfer protein (p*ELTP*)[7] active in the zone of suberization. The panels show longitudinal surface projections of lignin depositions in the endodermis stained by basic fuchsin using an established ClearSee-based protocol.[16]

(B) Functional analysis of CS by measuring onset of propidium iodide (PI) diffusion blockage into the stele;[40] n = 6.

(C) Surface view of endodermal CS stained by basic fuchsin in p*CASP1*::MYB4 plants treated with either ethanol (mock) or G-OH upon germination.

(D) Blockage of PI in p*CASP1*::MYB4 roots under increasing amount of G-OH. Plants were germinated and grown for 5 days in presence of the indicated substrate before measurement of PI penetration. n = 6.

All error bars are SD; letters refer to individual groups in a one-way ANOVA analysis with a post hoc multiple group t test (Tukey) ($p < 0.05$). Scale bars represent 10 μm. See also Figure S2.

of *C4H* under the p*CASP1* promoter in p*CASP1*::MYB4-expressing plants (Figures 3B–3D). Together, this strongly suggests that the effect of MYB4 is due to PP synthesis inhibition and not due to a more general interruption of endodermal differentiation, e.g., interference with MYB36 activity.[45,46] Furthermore, plants with ectopic MYB4 expression in the differentiating endodermis showed correct localization of the CS protein CASP1 (Figure S2C).[2] We did not find differences in root length for all lines compared to wild type (WT), even though we did observe a trend toward shorter roots in plants with ectopic MYB expression (Figure S2B). As the employed promoters are not active in the meristematic zone of roots, this probably reflects physiological effects of disrupted barrier formation. None of the investigated lines led to decreased lignin signal in the xylem (Figure S2E).

The remaining CS-associated lignin observed in p*CASP1*::MYB4 plants could be explained by PP synthesis in adjacent tissues and/or by ectopic lignification activated by the SGN surveillance system.[15] To address this, we created plants with p*CASP1*-driven MYB4 expression in the *sgn3-3* background.[13] Interestingly, only this background led to a significant decrease of *C4H* expression (Figure 4A), suggesting that activation of *C4H* by the SGN pathway might overshadow the relatively restricted tissue-specific repression caused by MYB4 under the *CASP1* promoter. To test this, we combined expression of the p*CASP1*::MYB4 construct with the p*C4H*::NLS 3× mVenus reporter. In these plants, *C4H* reporter activity was strongly decreased in the endodermis, although at least the cortex showed significantly increased *C4H* activity ($p < 0.05$) when normalized to WT (Figures 4B and S2F). Moreover, we found that externally applied CIF2 peptide, which is a ligand for the SGN3 receptor,[11] could induce activity of the *C4H* transcriptional reporter across all tissue layers, but only in plants with an active SGN pathway (Figures 4C and S2G). Taking together, SGN-activated lignin production/secretion from the endodermis-adjacent tissues appears to contribute to ectopic endodermis lignification. To substantiate this, we expressed a p*CASP1*::MYB4-GFP construct in a *cif1cif2*

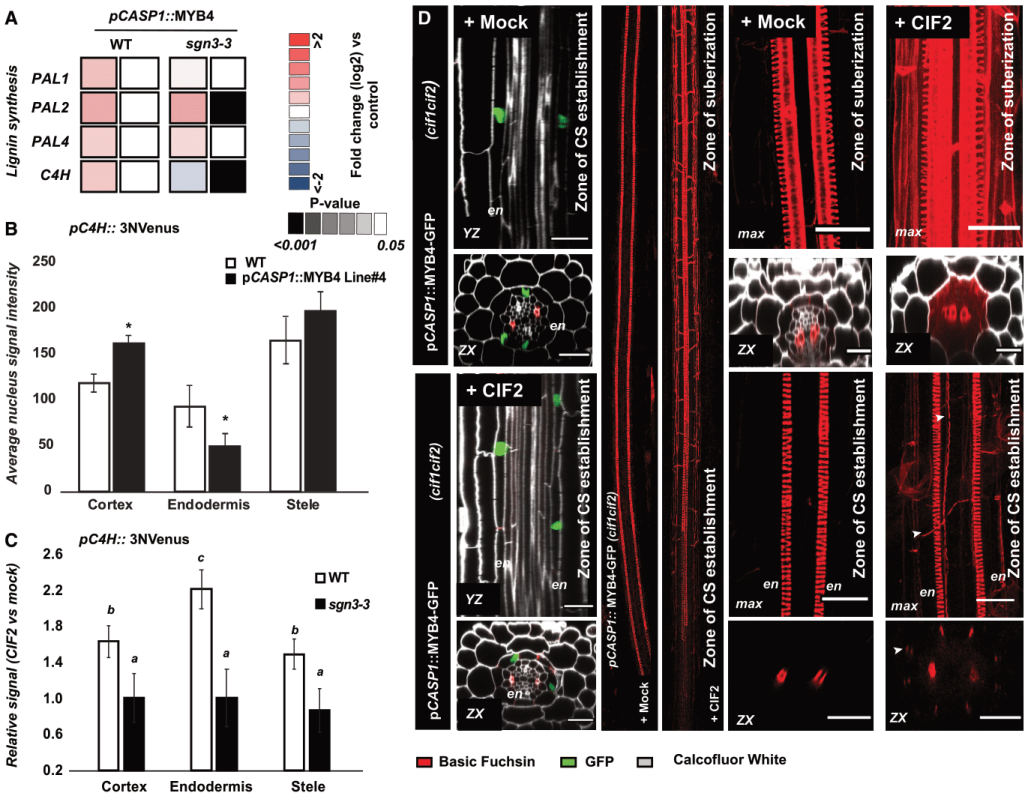

Figure 4. Compensatory SGN3-Dependent Lignification Is Activated upon MYB4 Expression in the Endodermis

(A) Relative expression of genes involved in the phenylpropanoid (PP) pathway in 5-day-old WT and *sgn3-3* roots expressing p*CASP1*::MYB4 measured by qPCR. Expression was normalized to each genotype without MYB4 expression. n = 3; p values are based on a two-tailed Student's t test (PA versus mock treated). For primer and gene information, see Table S1.

(B) Average fluorescence signal of *C4H* activity (p*C4H*::3NVenus) in 5-day-old WT and p*CASP1*::MYB4 roots. n = 5.

(C) Relative quantification of *C4H* activity (p*C4H*::3NVenus) in the zone of CS establishment in WT and *sgn3-3* mutants treated with CIF2 peptide. Fluorescent intensity signals were normalized to mock-treated roots of the same line. All treatments were 24 h. n = 8.

(D) Longitudinal YZ, XZ, or maximum projections of lignin deposition (basic fuchsin staining) in the endodermis (both CS establishment and suberization zones) and vasculature of 5-day-old seedlings p*CASP1*::MYB4-GFP *cif1cif2* roots upon treatment with mock or 1 μM CIF2 peptide for 24 h. Roots were fixed and stained with Calcofluor White and basic fuchsin.[16] Arrowheads point to non-connected lignification; max, maximum projection.

All error bars are SD; scale bars represent 10 μm. Letters refer to individual groups in a one-way ANOVA analysis with a post hoc multiple group t test (Tukey) ($p < 0.05$).

double mutant, which knocks out root ligands for the SGN pathway and phenocopies *sgn3* but allows the activation by addition of CIF peptides to the media.[11] When grown under mock conditions, these lines lacked lignin across the entire endodermis, although CIF2 treatment led to non-connected endodermal lignin depositions in both the zone of CS establishment and in the suberizing zone (Figure 4D). Thus, under normal conditions, the endodermis autonomously produces lignin monomers required for CS formation without dependency on synthesis from surrounding tissues. Upon barrier disruption, ectopic lignification is likely to be coordinated with the adjacent tissues through SGN-dependent activation of monolignol production.

Continuous PP Synthesis in the Endodermis Is Essential for Suberization

Besides the defective CS, all the p*CASP1*::MYBs lines had suberin deposition patterns similar to those of WT plants (Figures 5A, 5B, S2A, S2D, and S3B). This is intriguing, as the endodermis in the CS-establishing zone should undergo suberization due to activation of the SGN pathway. These plants also displayed a reduced suberin deposition response to the CIF2 peptide (Figure S3B). One explanation for this is that the presence of MYB4 in the endodermis represses suberin deposition. In line with this, plants expressing MYB4 in the zone of suberization (p*ELTP* promoter) had normal CSs (Figure 3A) but displayed an almost complete

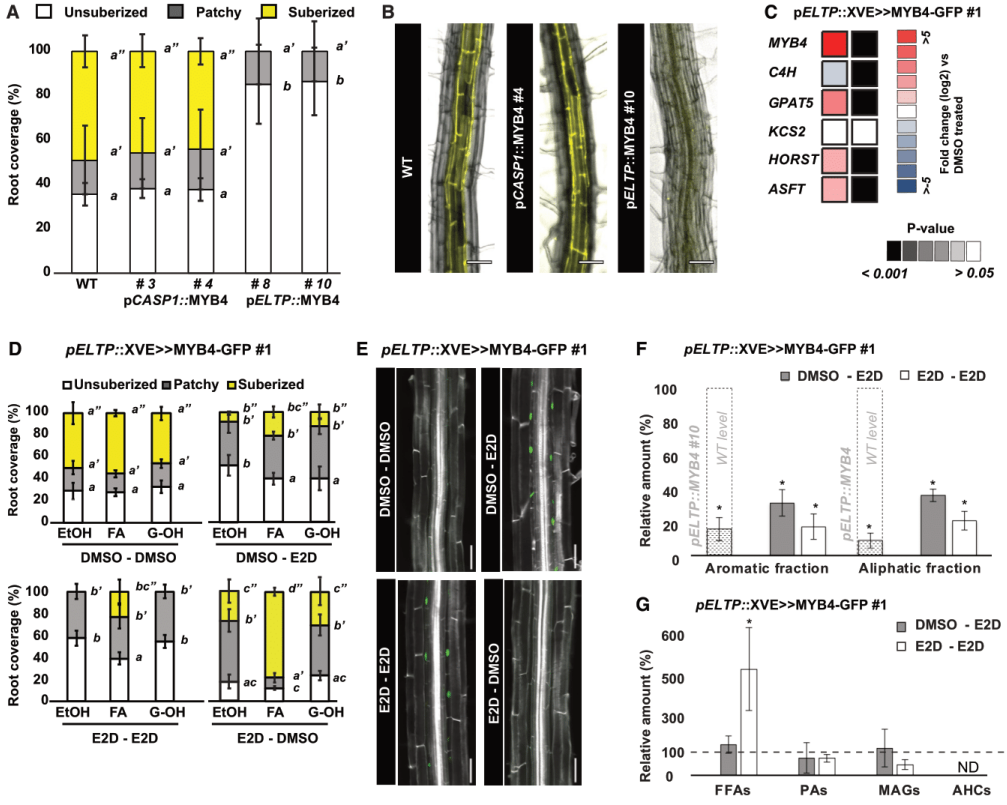

Figure 5. Repression of PP Synthesis in the Mature Endodermis Leads to Suberin Detachment

(A) Quantification of relative suberin root coverage by FY staining in the endodermis of 5-day-old roots; n = 6.

(B) Representative images of FY-stained, 5-day-old root quantified in (A). Scale bars represent 25 μm.

(C) Relative expression of suberin biosynthetic genes in the endodermis upon induction of p*ELTP::*XVE>>MYB4-GFP measured by qPCR. Expression was normalized to DMSO-treated plants. n = 3; p values are based on a two-tailed Student's t test (PA versus mock treated). For primer and gene information, see Table S1.

(D) Quantification of suberin root coverage by FY staining. p*ELTP::*XVE>>MYB4-GFP plants were grown for 4 days on either DMSO- (upper graphs) or 5 μM E2D (lower graphs)-containing media and then transferred to plates containing E2D or DMSO, respectively, in combination with ethanol (EtOH), 20 μM FA, or 20 μM G-OH for 2 days before suberin quantification by FY staining.

(E) GFP signal in 6-day-old p*ELTP::*XVE>>MYB4-GFP plants grown on plates containing DMSO or 5 μM E2D. Scale bars represent 50 μm.

(F) Relative amount (%) of suberin aromatic and aliphatic fractions from 8-day-old p*ELTP::*MYB4 or p*ELTP::*XVE>>MYB4-GFP roots grown under E2D regimens (6 days mock + 2 days E2D: "DMSO-E2D" or 6 days E2D + 2 days E2D: "E2D-E2D"). Levels were normalized to WT plants of identical age for p*ELTP::*MYB4 (white with stripes) and to DMSO-DMSO-treated plants for p*ELTP::*XVE>>MYB4-GFP (gray, white), respectively; n = 3–5; *p < 0.05; two-tailed t test versus WT or mock.

(G) Relative amount (%) of chloroform extractives of the endodermis of 18-day-old p*ELTP::*XVE>>MYB4-GFP-expressing roots under different E2D treatments (2-day, DMSO-E2D or 18-day, E2D-E2D); n = 3–4; *p < 0.05; two-tailed t test versus mock.

AHCs, alkyl hydroxycinnamates; FFAs, free fatty acids; MAGs, monoacylglycerol conjugates; ND, not detected; PAs, primary alcohols; WT, wild type. All error bars are SD. Letters refer to individual groups in a one-way ANOVA analysis with a post hoc multiple group t test (Tukey) (p < 0.05). See also Figures S2–S4.

loss of FY-stained endodermal cells (Figures 5A and 5B). MYB3 or MYB32 had a similar effect, whereas no decrease in suberin signal was seen in p*ELTP::*MYB7-expressing plants (Figures S2A and S2D). p*ELTP::*MYB4 roots showed a strong decrease in all major aromatic and aliphatic suberin constituents compared to WT (Figures 5F and S4A), confirming that ectopic MYB4 expression indeed represses suberin in the endodermis. Next, we investigated whether the negative effects of MYB4 on suberin deposition can be explained by repression of suberin biosynthesis genes. To address this, we employed an estradiol (E2D)-inducible chimeric transcription activator based on fusion of the DNA-binding domain of the bacterial repressor LexA (X), the acidic transactivating domain of VP16 (V), and the regulatory region of the human estrogen receptor (E; ER) (XVE) containing the p*ELTP*[47] promoter

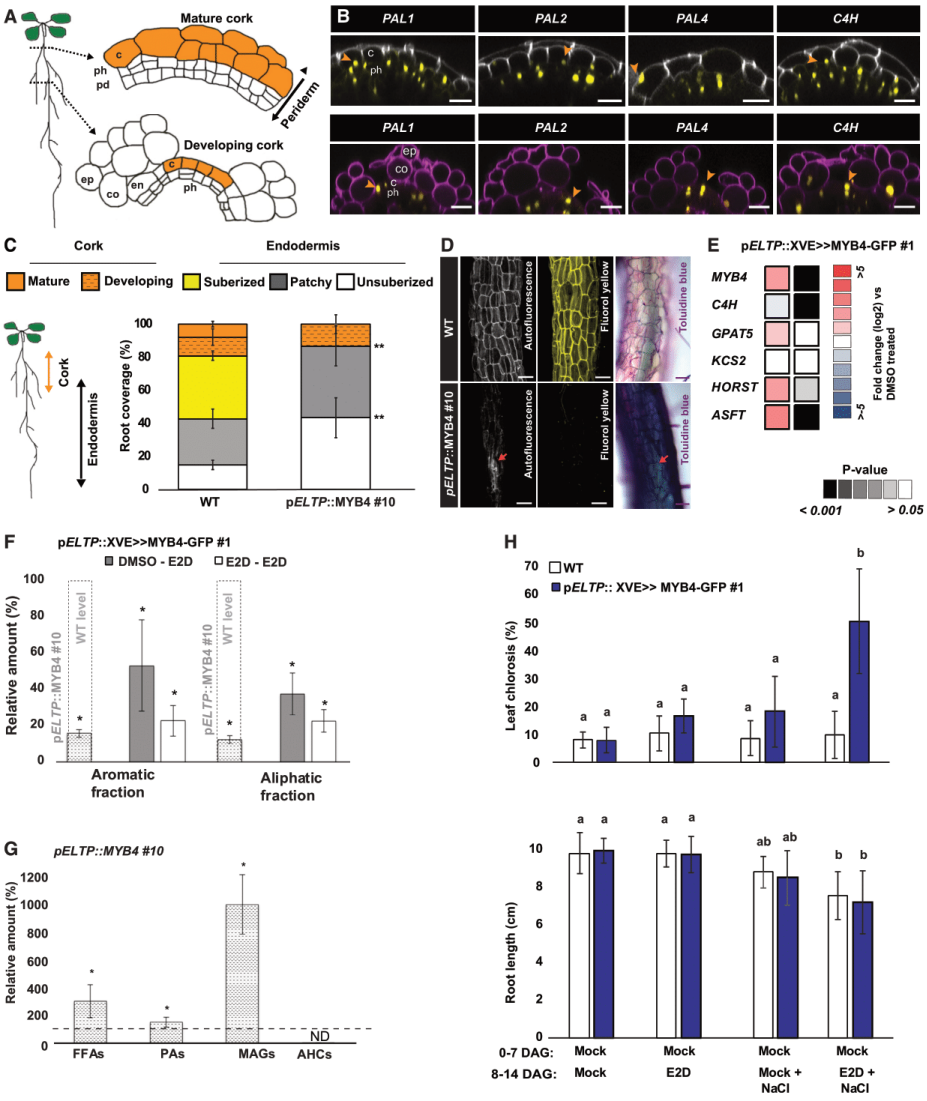

Figure 6. Collapse of Cork Formation by Ectopic Expression of MYB4 in the Periderm

(A) A simplified scheme of periderm development in the *Arabidopsis* root. During secondary growth, the root increases in girth, the endodermis undergoes programmed cell death, and its barrier function is eventually replaced by the periderm.[17,18] This is a developmental process, and zones of "developing" and "mature" cork formation can be identified along the root.

(B) Activity of nuclear localized (NLS) 3× mVenus fusion reporters driven by promoter regions of root-expressed *PAL* and *C4H* homologs in 21-day-old *Arabidopsis* roots at the different cork developmental stages (orange arrowheads). Cell walls were highlighted using the intrinsic autofluorescence of cork cells (gray) in the mature cork zone or PI (magenta) for "patchy" cork zones. Orange arrowheads point toward cork cells with positive marker expression.

(C) Quantification of suberin root coverage in 12-day-old WT and p*ELTP*::MYB4 roots using FY staining[28] (n = 6; *p < 0.05; **p < 0.01; two-tailed Student's t test versus WT).

(D) Autofluorescence (left panel), FY staining (middle panel), and toluidine blue (right panel) of cork cells in WT and p*ELTP*::MYB4 19-day-old roots.

(legend continued on next page)

to add temporal control to the MYB4 expression. We used this system to drive a MYB4-GFP fusion (p*ELTP::*XVE>>MYB4-GFP). The fusion of MYB4 to GFP had no effect on the repressive effect of MYB4 on suberin (Figure S3C). Interestingly, when roots were subject to 48 h of E2D exposure, we saw a significant increase in expression of several key genes for aliphatic suberin constituent synthesis as well as a concomitant repression of *C4H* (Figure 5C). Thus, the repressive effects of MYB4 on suberin deposition are not due to direct transcriptional repression of the underlying biosynthesis of aliphatic monomers. To further establish whether the disappearance of suberin can be complemented by PP-derived metabolites, seedlings were grown for 4 days on mock- or E2D-containing plates and transferred to similar plates with or without PP metabolites for 2 days. After a total of 6 days E2D induction, in control treatments (2 days of EtOH), the suberized zone was strongly reduced when compared to similar non-induced plants (Figure 5D). We could partially complement this by adding FA or other PP-derived acids, but not G-OH, to the media for the last 2 days (Figures 5D and S3A), supporting that active endodermal PP synthesis is necessary to establish a suberized barrier. We then grew plants for 4 days on mock-containing plates to allow a suberized zone to be established (Figure S1F) and transferred to E2D plates (suppressing further PP-metabolite synthesis) for 2 days with or without PP-derived metabolites. Remarkably, and in line with our observations for PA-treated roots (Figures 2D, 2F, and S1F), the proportion of root containing a suberized zone of the root was significantly ($p < 0.05$) reduced when compared to mock-treated plants but was again partially complemented by PP-derived acids (Figures 5D and S3A). The lack of complete complementation by PP acids could be explained by the fact that MYB4 also represses genes of the PP pathway involved in FA-coenzyme A (CoA) conjugation.[41] To further probe this, we reversed the experimental setup and allowed plants to grow for 4 days on E2D-containing plates with 2 additional days on mock-containing plates with or without PP-derived metabolites. This recovery phase allowed complete MYB4-GFP degradation (Figure 5E). Interestingly, after the treatments, roots regained a suberized zone, even in mock treatments (Figure 5D), which was strongly increased by the specific addition of FA to recovery plates (Figures 5D and S3A). In conclusion, the p*ELTP*::XVE>>MYB4-GFP line on suberin deposition recapitulates the effect of both PA treatment and the p*ELTP*::MYB4 line. Therefore, these experiments strongly indicate that suberin is incorrectly attached to the cell wall and removed from the endodermal cell wall matrix upon repression of PP production in the endodermis.

Unbound Aliphatic Suberin Constituents Accumulate in Absence of Aromatics

Constitutive expression (p*ELTP::*MYB4) or short (2-day) or constitutive MYB4 induction using the p*ELTP::*XVE>>MYB4-GFP system led to comparable reductions of both extractable aromatic and aliphatic suberin components when compared to WT or mock treatment, respectively (Figures 5F and S4B). As the suberin biosynthetic machinery was not repressed by MYB4 (Figure 5C), aliphatic constituents were probably not incorporated in the final suberin structure without PP-derived metabolites. To clarify the fate of these metabolites, we performed a chloroform-based extraction[48] of the endodermis-containing root parts during MYB4-GFP induction. Surprisingly, only in continuously induced or constitutive MYB4-expressing plants did the reduction of suberin-associated aromatic components co-occur with a significant overaccumulation of free aliphatic constituents, such as very-long-chain free fatty acids (FFAs), characteristic for suberin ($p < 0.01$; two-tailed Student's t test versus mock; Figures 5G and S4C). Based on this, we propose that, in absence of PP metabolites, aliphatic constituents, meant to be incorporated into the suberin matrix, accumulate as unpolymerized constituents in the apoplast and/or are funneled into other FFA-related pathways.

Repression of PP Synthesis in Periderm Leads to Collapse of the Cork Barrier

To analyze whether suberin depositions in the barrier layers of the periderm behave in a similar manner to the endodermis with regards to PP biosynthesis, we grew plants for up to 21 days to allow secondary growth. The periderm can be divided into a "developing" and a "mature" cork stage dependent on the distance from the meristematic zone (Figure 6A). In both of these zones, we observed activity of all analyzed PP expression reporters in the cork and phellogen layers (Figure 6B), suggesting that the periderm also functions autonomously to produce monomers for construction of the cork barrier. As the *ELTP* promoter is active in the periderm during secondary growth (Figure S5A), we investigated the specific role of PP production in the periderm using our MYB4-based repressor tools. Similar to the endodermis, p*ELTP*::MYB4-expressing plants showed a reduction of lignin and suberin staining of cork cells when compared to WT (Figures 6C, 6D, S5B, and S5C). The reduced suberin content was maintained through periderm development (Figures 6C, 6D, and S5C), indicating that the periderm is dependent on tissue-autonomous PP production in a similar manner to the endodermis. Interestingly, p*ELTP::*MYB4-expressing plants had collapsed cork cells, which compromised the barrier function as visualized

(E) Relative expression of suberin biosynthetic genes in the periderm upon induction of p*ELTP::*XVE>>MYB4-GFP measured by qPCR. Expression was normalized to DMSO-treated plants. n = 3; p values are based on a two-tailed Student's t test (PA versus mock treated). For primer and gene information, see Table S1.

(F) Relative amount (%) of suberin aromatic and aliphatic fractions form the cork of 20-day-old WT, p*ELTP::*MYB4, and p*ELTP::*XVE>>MYB4-GFP roots. Levels were normalized to WT and mock-treated plants of identical age for p*ELTP::*MYB4 and p*ELTP::*XVE>>MYB4-GFP, respectively. n = 3–4; *p < 0.05; two-tailed t test versus WT or mock.

(G) Relative amounts (%) of chloroform extractives of 20-day-old p*ELTP::* MYB4-expressing roots. Normalization was to WT plants of identical age; n = 3; *p < 0.05; two-tailed t test versus WT.

(H) Leaf chlorosis (%) and primary root length quantification of WT or p*ELTP::*XVE>>MYB4-GFP plants 7 days after germination (0–7 DAGs) under standard conditions (mock) and transferred for 7 days to plates with combinations of mock, 5 μM E2D, and 100 mM NaCl treatments for an additional 7 days (8–14 DAGs). All error bars are SD. *p < 0.05; **p < 0.01 in a two-tailed Student's t test versus WT. Letters refer to individual groups in a one-way ANOVA analysis with a post hoc multiple group t test (Tukey) (p < 0.05).

c, cork; DAG, days after germination; pd, phelloderm; ph, phellogen. Scale bars represent 20 μm. See also Figures S5–S7.

by increased toluidine-blue penetration (Figure 6D). We therefore employed the p*ELTP::*XVE>>MYB4-GFP system to investigate whether suberin in cork cell layers are dependent on continuous PP synthesis. To ensure onset of cork differentiation, we let the plants grow for 12 days on plates containing either mock or 5 μM E2D and then cross-transferred them to mock or E2D for an additional 8 days to allow constant or induced expression of MYB4-GFP in pre-formed periderm cells. In both cases, we observed cork cell collapse similar to the p*ELTP::*MYB4 plants; however, this appeared to be stronger in plants with constant induction (Figure S5D), which likely reflects that the suberin pre-established in the initial 12 days mock treatment might not be degraded in the periderm. Also in this tissue, we observed that MYB4 led to a transcriptional repression of *C4H* and activation of some of suberin biosynthesis genes (Figure 6E), further indicating that the repressive effect of MYB4 does not affect suberin synthesis directly. To determine the fate of the suberin constituents in the periderm, we isolated the cork-containing root parts and subjected them to the same gas chromatography-mass spectrometry (GC-MS)-based pipeline as the endodermis samples. All lines (including constitutive p*ELTP::*MYB4 plants) displayed a strong reduction in suberin constituents when compared to the respective controls (Figures 6F, S5E, and S6A), supporting that ectopic MYB4 expression prevents *de novo* suberin deposition. Both constant and short-term-induced MYB4-GFP (and constitutive p*ELTP::*MYB4-expressing plants) showed a reduced content of the extractable aliphatic-aromatic conjugated alkyl hydroxycinnamates (AHCs) (Figures 6G, S6B, and S6C). This observation suggests that the detected AHCs originate from the cork. In contrast to the endodermis inductions, where aromatic-conjugated aliphatic compounds are typically found in low levels using the employed extraction method,[48] repression in the periderm led to increased accumulation of aliphatic suberin constituents in the chloroform fractions (Figures 6G, S6B, and S6C). Surprisingly, continuous repression using the XVE system led to a decrease in these components (Figure S6C), which is most likely related to physiological effects of the repressed periderm barrier formation on all plant processes. Finally, to substantiate that ectopic MYB4-GFP expression in the cork and the consequential cell collapse give rise to a non-functional periderm barrier, we grew plants on mock-containing plates for 7 days followed by transfer to mock or 5 μM E2D-containing plates with or without 100 mM NaCl for an additional 7 days. Only the combination of E2D (and the resulting MYB4-GFP expression) and NaCl led to a significant ($p < 0.01$; pairwise t test) increase in leaf chlorosis (Figures 6H and S7A). This supports a role for the periderm in salt stress protection and emphasizes the defective barriers in our analysis. In all cases, NaCl stress led to reduced root lengths, without significant difference between the mock and E2D-treated plants (Figure 6H). In summary, our periderm analysis indicates that, similar to the endodermis, suberin cannot be incorporated correctly into the cork barrier upon ectopic MYB4 expression. Moreover, this highlights our temporally controlled MYB4 expression as a model to study physiological roles of the periderm barrier.

DISCUSSION

Plant apoplastic barriers help to control nutrient uptake, gas exchange, and water availability and confer protection to biotic and abiotic stresses. These structures are therefore traits of crucial agronomical importance. In roots, CSs represent the first apoplastic barrier established after germination. In *Arabidopsis*, polymerization of lignin in the CS occurs few cells after the onset of elongation and simultaneously to xylem differentiation.[2,40] In the xylem, polymerization of lignin can continue after cell death,[49] which indicates that monolignols can diffuse from surrounding cells. Most PPs have the physio-chemical properties to passively diffuse across membranes,[29] which suggests that defining elements of CS lignin originates from xylem, given such a diffusion path already exists for barrier surveillance CIF peptides that are produced in the stele but perceived in the CS domain.[11] In line with this, it is interesting that all of the PP-synthesis genes investigated here showed strong expression in the pericycle (Figure 1B), hinting that this cell layer, situated in between the endodermis and the xylem, may contribute PP metabolites for lignification in both tissues. Moreover, the tight developmental association of lignification dynamics in the xylem and endodermis (Figures 2B and S1A) supports a model where lignification of the distinct, adjacent tissues shares a common biosynthetic framework. Yet, our work clearly demonstrates that, under normal conditions, production of lignin monomers in the endodermis is required for CS formation. Upon CS disruption, the root deposits ectopic non-CS localized lignin in the endodermis through activation of the SGN pathway. Our findings reveal that the PP pathway is responsive to CIF2 treatment in the cortex and stele (Figure 4C). Thus, it is likely that, upon CS disruption, the surrounding tissues aid in ectopic lignification of the endodermis. Indeed, *C4H* was upregulated in these tissues upon MYB4-dependent disruption of the CS (Figure 4B). Although the monolignol-specific ABCG29/PDR1 transporter is expressed in both the vasculature and endodermis,[50] the role of active monolignol transport between root cell types and especially upon SGN activation is still unclear. However, due to the broad range of PP metabolites, tissue-specific compartmentalization—such as production PP metabolites for CS in the endodermis—might add spatial control over metabolites synthesis in a given cell and serve to avoid bottlenecks for compounds produced from a common pool of substrates. In support of this, we observed *PAL4* activity only in the suberizing zone of the endodermis (Figure 1B, top panel), suggesting that this isoform acts in the production of ferulates earmarked for suberin production (Figure 7). Future studies that include careful high-resolution multi-level localization and metabolite analysis of the PP pathway are therefore likely to reveal currently unappreciated regulatory mechanisms that drive tissue and developmental-stage-specific PP metabolic pathways within the root.

Besides the analysis of monolignol production for CS formation, our work reveals an interesting new aspect of suberin behavior, namely that PP-derived metabolites components of the suberin matrix serve to somehow stabilize and anchor the polymers to the cell wall and regulate active turnover of suberin in the endodermis. The length of the suberized endodermal zone is increased or decreased under certain abiotic stresses in an abscisic acid (ABA)- and ethylene-dependent manner, respectively.[7] An active mechanism for turnover of suberin based on regulation of PP metabolism in the endodermis would therefore allow the plant to quickly adjust its diffusion barrier to abiotic changes in the external environment. The PP pathway is responsive to abiotic stress,[51] and further root-specific investigations will

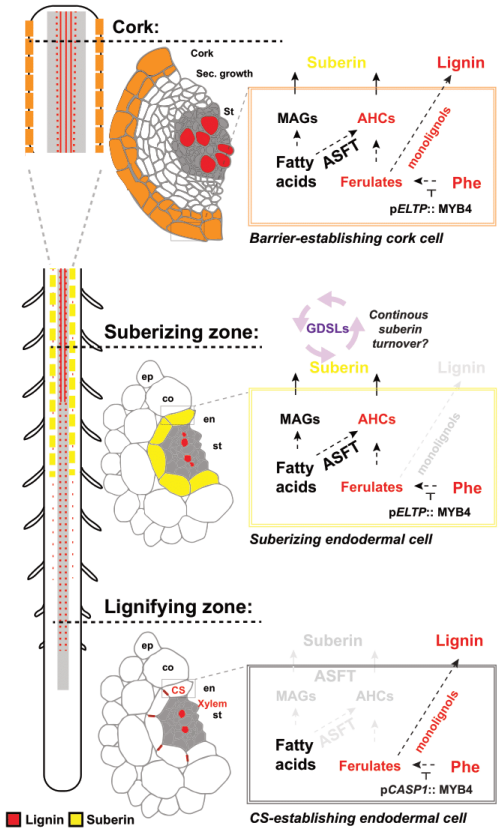

Figure 7. Spatiotemporal Coordination of Barrier-Constituent Synthesis in the Root

Synthesis of monomers necessary for root barrier construction requires the PP and fatty acid biosynthetic pathways for production of aromatic and aliphatic constituents, respectively. Based on our results, we propose a model in which, in the lignifying endodermis, the PP pathway is active and is responsible for synthesizing lignin monomers required for CS formation, whereas lignification of the xylem occurs independent via stele (St)-synthesized PP metabolites. In the suberizing zone of the endodermis, the PP pathway produces mainly ferulates, possibly through *PAL4*, which is incorporated with fatty acid metabolites via the aliphatic suberin feruloyl transferase (ASFT) into AHCs, secreted to the cell wall, and polymerized with MAGs into suberin lamellae. GDSL lipases in the cell wall degrade suberin, making the suberin depositions reflect a steady state of continuous synthesis and degradation. After secondary growth, the barrier functions of the endodermis are replaced by the cork layers. Here, the barrier consists of a complex mixture of lignin and suberin depositions that appear to be stable and represent a non-dynamic endpoint barrier, which is reflected in the role of this tissue in protecting against abiotic stresses.

likely shed light on a putative suberin-related regulatory function. Suberin constituents appear to accumulate as fatty-acid-derived constituents (Figures 5G, 6G, S4C, and S6C). Intriguingly, symbiotic associations with, for example, arbuscular mycorrhiza-forming fungi exchange photosynthates from the plant in the form of sugars and fatty acids for assimilated phosphate.[51] Because suberin deposition is decreased upon phosphate starvation,[28] it is tempting to speculate that exchange of fatty acids might correlate with suberin dynamics, and it would be interesting to explore the role of PP-derived metabolites in this communication. The GDSL motif-containing lipase cuticle destruction factor 1 (CDEF1) involved in degradation of cutin[52] has been employed as a tool to remove suberin in the endodermis,[7,13,28,40] and very recently, a range of GDSL motif-containing lipases were found to be involved in suberin dynamics.[53] This illustrates the capacity of plants for suberin catabolism by a rather simple mechanism and emphasizes that this function is likely facilitated by GDSL motif-containing lipase enzymes. Our setup with inducible repression of PP synthesis and the corresponding turnover of suberin provides an excellent platform to further unravel aspects of GDSL motif-containing lipases and suberin function in inter-species associations.

Repression of PP in the periderm leads to barrier failure, collapse of cork cells, and reduced salt tolerance, a more severe phenotype compared to any of the characterized suberin biosynthesis mutants,[22,27,54,55] emphasizing the role of the cork during abiotic stresses. Short-term repression of PP in the periderm led to release of multiple different classes of aliphatic compounds from the cork (Figure S6C). Similarly, in the endodermis, only in constitutive MYB4 expression conditions did we see specifically a release of FAs. This is not due to a different relative suberin composition of these tissues (Figure S7B) but supports that suberin dynamics are different in cork and endodermal tissues.

In conclusion, our work illustrates that genetic repressors can be used as a tool to elucidate PP pathway function in a cell-type- and tissue-specific manner. Our work provides a novel approach to affect root barrier formation and function with an unprecedented resolution and has provided intriguing insights into the complex association between PP and FA synthesis required for suberin deposition (Figure 7). The ability to control barrier formation with high resolution within tissues will help to dissect the distinct contributions of root barriers during development and in the context of specialized stress situations.

STAR★METHODS

Detailed methods are provided in the online version of this paper and include the following:

- KEY RESOURCES TABLE
- RESOURCE AVAILABILITY
  - Lead Contact
  - Materials Availability
  - Data and Code Availability
- EXPERIMENTAL MODEL AND SUBJECT DETAILS
- METHOD DETAILS
  - Molecular Cloning
  - GC-MS
  - Stainings
  - Confocal Microscopy
  - Root Suberin Coverage
  - q-PCR

- QUANTIFICATION AND STATISTICAL ANALYSIS
  - Gene List

SUPPLEMENTAL INFORMATION

Supplemental Information can be found online at https://doi.org/10.1016/j.cub.2020.11.070.

ACKNOWLEDGMENTS

We wish to thank Magdalena Marek and Colleen Drapek for their readthrough and insightful comments to the manuscript. We thank Dagmar Ripper for helping in the cork staining, as well as Robertas Ursache and Joop Vermeer for insightful discussions. The authors are grateful to the central imaging facility (CIF) at University of Lausanne for aid in image quantification and analysis. Work in the Geldner lab was supported by an ERC Consolidator grant (GA-N: 616228–ENDOFUN) and Swiss National Science Foundation grant (310030B_176399). Work in the Ragni lab is supported by the Deutsche Forschungsgemeinschaft (DFG grant RA-2590/1-2). The ORCIDs for the authors are as follows: 0000-0002-8905-0850 (T.G.A.); 0000-0001-5858-3331 (D.M.); 0000-0001-5711-3688 (J.K.); 0000-0003-2269-7390 (R.B.F.); 0000-0002-3651-8966 (L.R.); and 0000-0002-2300-9644 (N.G.).

AUTHOR CONTRIBUTIONS

T.G.A. acquired and interpreted data, conceived the research, and wrote the manuscript. D.M. conducted and analyzed GC-MS data together with J.K. R.B.F. interpreted data and contributed to writing the manuscript. D.M. and L.R. acquired the cork data. L.R. conceived the research, acquired and interpreted data, and contributed to writing the manuscript. N.G. conceived the research and contributed to writing the manuscript. All authors have approved the final manuscript and agree to be personally accountable for the individual contributions.

DECLARATION OF INTERESTS

The authors declare no competing interests.

Received: July 31, 2020
Revised: October 30, 2020
Accepted: November 30, 2020
Published: February 1, 2021

REFERENCES

1. Geldner, N. (2013). The endodermis. Annu. Rev. Plant Biol. *64*, 531–558.
2. Lee, Y., Rubio, M.C., Alassimone, J., and Geldner, N. (2013). A mechanism for localized lignin deposition in the endodermis. Cell *153*, 402–412.
3. Andersen, T.G., Barberon, M., and Geldner, N. (2015). Suberization - the second life of an endodermal cell. Curr. Opin. Plant Biol. *28*, 9–15.
4. Sitte, P. (1959). Mischkörperdoppelbrechung der Kork-Zellwände. Naturwissenschaften *46*, 260–261. https://doi.org/10.1007/BF00632301.
5. Franke, R., Briesen, I., Wojciechowski, T., Faust, A., Yephremov, A., Nawrath, C., and Schreiber, L. (2005). Apoplastic polyesters in Arabidopsis surface tissues–a typical suberin and a particular cutin. Phytochemistry *66*, 2643–2658.
6. Barberon, M., and Geldner, N. (2014). Radial transport of nutrients: the plant root as a polarized epithelium. Plant Physiol. *166*, 528–537.
7. Barberon, M., Vermeer, J.E., De Bellis, D., Wang, P., Naseer, S., Andersen, T.G., Humbel, B.M., Nawrath, C., Takano, J., Salt, D.E., and Geldner, N. (2016). Adaptation of root function by nutrient-induced plasticity of endodermal differentiation. Cell *164*, 447–459.
8. Schreiber, L. (2010). Transport barriers made of cutin, suberin and associated waxes. Trends Plant Sci. *15*, 546–553.
9. Riley, R.G., and Kolattukudy, P.E. (1975). Evidence for covalently attached p-coumaric acid and ferulic acid in cutins and suberins. Plant Physiol. *56*, 650–654.
10. Schreiber, L., Franke, R., and Hartmann, K. (2005). Wax and suberin development of native and wound periderm of potato (Solanum tuberosum L.) and its relation to peridermal transpiration. Planta *220*, 520–530.
11. Doblas, V.G., Smakowska-Luzan, E., Fujita, S., Alassimone, J., Barberon, M., Madalinski, M., Belkhadir, Y., and Geldner, N. (2017). Root diffusion barrier control by a vasculature-derived peptide binding to the SGN3 receptor. Science *355*, 280–284.
12. Fujita, S., De Bellis, D., Edel, K.H., Köster, P., Andersen, T.G., Schmid-Siegert, E., Dénervaud Tendon, V., Pfister, A., Marhavý, P., Ursache, R., et al. (2020). SCHENGEN receptor module drives localized ROS production and lignification in plant roots. EMBO J. *39*, e103894.
13. Pfister, A., Barberon, M., Alassimone, J., Kalmbach, L., Lee, Y., Vermeer, J.E., Yamazaki, M., Li, G., Maurel, C., Takano, J., et al. (2014). A receptor-like kinase mutant with absent endodermal diffusion barrier displays selective nutrient homeostasis defects. eLife *3*, e03115.
14. Racolta, A., Bryan, A.C., and Tax, F.E. (2014). The receptor-like kinases GSO1 and GSO2 together regulate root growth in Arabidopsis through control of cell division and cell fate specification. Dev. Dyn. *243*, 257–278.
15. Doblas, V.G., Geldner, N., and Barberon, M. (2017). The endodermis, a tightly controlled barrier for nutrients. Curr. Opin. Plant Biol. *39*, 136–143.
16. Ursache, R., Andersen, T.G., Marhavý, P., and Geldner, N. (2018). A protocol for combining fluorescent proteins with histological stains for diverse cell wall components. Plant J. *93*, 399–412.
17. Wunderling, A., Ripper, D., Barra-Jimenez, A., Mahn, S., Sajak, K., Targem, M.B., and Ragni, L. (2018). A molecular framework to study periderm formation in Arabidopsis. New Phytol. *219*, 216–229.
18. Campilho, A., Nieminen, K., and Ragni, L. (2020). The development of the periderm: the final frontier between a plant and its environment. Curr. Opin. Plant Biol. *53*, 10–14.
19. Almeida, T., Pinto, G., Correia, B., Santos, C., and Gonçalves, S. (2013). QsMYB1 expression is modulated in response to heat and drought stresses and during plant recovery in Quercus suber. Plant Physiol. Biochem. *73*, 274–281.
20. Thangavel, T., Tegg, R.S., and Wilson, C.R. (2016). Toughing it out–disease-resistant potato mutants have enhanced tuber skin defenses. Phytopathology *106*, 474–483.
21. Du, Y.-P., Wang, Z.-S., and Zhai, H. (2011). Grape root cell features related to phylloxera resistance and changes of anatomy and endogenous hormones during nodosity and tuberosity formation. Aust. J. Grape Wine Res. *17*, 291–297.
22. Compagnon, V., Diehl, P., Benveniste, I., Meyer, D., Schaller, H., Schreiber, L., Franke, R., and Pinot, F. (2009). CYP86B1 is required for very long chain ω-hydroxyacid and α, ω -dicarboxylic acid synthesis in root and seed suberin polyester. Plant Physiol. *150*, 1831–1843.
23. Höfer, R., Briesen, I., Beck, M., Pinot, F., Schreiber, L., and Franke, R. (2008). The Arabidopsis cytochrome P450 CYP86A1 encodes a fatty acid ω-hydroxylase involved in suberin monomer biosynthesis. J. Exp. Bot. *59*, 2347–2360.
24. Li, Y., Beisson, F., Koo, A.J., Molina, I., Pollard, M., and Ohlrogge, J. (2007). Identification of acyltransferases required for cutin biosynthesis and production of cutin with suberin-like monomers. Proc. Natl. Acad. Sci. USA *104*, 18339–18344.
25. Yang, W., Pollard, M., Li-Beisson, Y., Beisson, F., Feig, M., and Ohlrogge, J. (2010). A distinct type of glycerol-3-phosphate acyltransferase with sn-2 preference and phosphatase activity producing 2-monoacylglycerol. Proc. Natl. Acad. Sci. USA *107*, 12040–12045.
26. Yang, W., Simpson, J.P., Li-Beisson, Y., Beisson, F., Pollard, M., and Ohlrogge, J.B. (2012). A land-plant-specific glycerol-3-phosphate acyltransferase family in Arabidopsis: substrate specificity, sn-2 preference, and evolution. Plant Physiol. *160*, 638–652.

27. Molina, I., Li-Beisson, Y., Beisson, F., Ohlrogge, J.B., and Pollard, M. (2009). Identification of an Arabidopsis feruloyl-coenzyme A transferase required for suberin synthesis. Plant Physiol. *151*, 1317–1328.

28. Andersen, T.G., Naseer, S., Ursache, R., Wybouw, B., Smet, W., De Rybel, B., Vermeer, J.E.M., and Geldner, N. (2018). Diffusible repression of cytokinin signalling produces endodermal symmetry and passage cells. Nature *555*, 529–533.

29. Vermaas, J.V., Dixon, R.A., Chen, F., Mansfield, S.D., Boerjan, W., Ralph, J., Crowley, M.F., and Beckham, G.T. (2019). Passive membrane transport of lignin-related compounds. Proc. Natl. Acad. Sci. USA *116*, 23117–23123.

30. Vogt, T. (2010). Phenylpropanoid biosynthesis. Mol. Plant *3*, 2–20.

31. Koukol, J., and Conn, E.E. (1961). The metabolism of aromatic compounds in higher plants. IV. Purification and properties of the phenylalanine deaminase of Hordeum vulgare. J. Biol. Chem. *236*, 2692–2698.

32. Fahrendorf, T., and Dixon, R.A. (1993). Stress responses in alfalfa (Medicago sativa L.). XVIII: Molecular cloning and expression of the elicitor-inducible cinnamic acid 4-hydroxylase cytochrome P450. Arch. Biochem. Biophys. *305*, 509–515.

33. Mizutani, M., Ward, E., DiMaio, J., Ohta, D., Ryals, J., and Sato, R. (1993). Molecular cloning and sequencing of a cDNA encoding mung bean cytochrome P450 (P450C4H) possessing cinnamate 4-hydroxylase activity. Biochem. Biophys. Res. Commun. *190*, 875–880.

34. Teutsch, H.G., Hasenfratz, M.P., Lesot, A., Stoltz, C., Garnier, J.M., Jeltsch, J.M., Durst, F., and Werck-Reichhart, D. (1993). Isolation and sequence of a cDNA encoding the Jerusalem artichoke cinnamate 4-hydroxylase, a major plant cytochrome P450 involved in the general phenylpropanoid pathway. Proc. Natl. Acad. Sci. USA *90*, 4102–4106.

35. Smith, R.A., Schuetz, M., Roach, M., Mansfield, S.D., Ellis, B., and Samuels, L. (2013). Neighboring parenchyma cells contribute to Arabidopsis xylem lignification, while lignification of interfascicular fibers is cell autonomous. Plant Cell *25*, 3988–3999.

36. Hamberger, B., Ellis, M., Friedmann, M., de Azevedo Souza, C., Barbazuk, B., and Douglas, C.J. (2007). Genome-wide analyses of phenylpropanoid-related genes in Populus trichocarpa, Arabidopsis thaliana, and Oryza sativa: the Populus lignin toolbox and conservation and diversification of angiosperm gene families. Can. J. Bot. *85*, 1182–1201.

37. Hruz, T., Laule, O., Szabo, G., Wessendorp, F., Bleuler, S., Oertle, L., Widmayer, P., Gruissem, W., and Zimmermann, P. (2008). Genevestigator v3: a reference expression database for the meta-analysis of transcriptomes. Adv. Bioinforma. *2008*, 420747.

38. Schmid, N.B., Giehl, R.F., Döll, S., Mock, H.P., Strehmel, N., Scheel, D., Kong, X., Hider, R.C., and von Wirén, N. (2014). Feruloyl-CoA 6′-hydroxylase1-dependent coumarins mediate iron acquisition from alkaline substrates in Arabidopsis. Plant Physiol. *164*, 160–172.

39. Schalk, M., Cabello-Hurtado, F., Pierrel, M.A., Atanossova, R., Saindrenan, P., and Werck-Reichhart, D. (1998). Piperonylic acid, a selective, mechanism-based inactivator of the trans-cinnamate 4-hydroxylase: A new tool to control the flux of metabolites in the phenylpropanoid pathway. Plant Physiol. *118*, 209–218.

40. Naseer, S., Lee, Y., Lapierre, C., Franke, R., Nawrath, C., and Geldner, N. (2012). Casparian strip diffusion barrier in Arabidopsis is made of a lignin polymer without suberin. Proc. Natl. Acad. Sci. USA *109*, 10101–10106.

41. Jin, H., Cominelli, E., Bailey, P., Parr, A., Mehrtens, F., Jones, J., Tonelli, C., Weisshaar, B., and Martin, C. (2000). Transcriptional repression by AtMYB4 controls production of UV-protecting sunscreens in Arabidopsis. EMBO J. *19*, 6150–6161.

42. Fornalé, S., Lopez, E., Salazar-Henao, J.E., Fernández-Nohales, P., Rigau, J., and Caparros-Ruiz, D. (2014). AtMYB7, a new player in the regulation of UV-sunscreens in Arabidopsis thaliana. Plant Cell Physiol. *55*, 507–516.

43. Wang, X.-C., Wu, J., Guan, M.L., Zhao, C.H., Geng, P., and Zhao, Q. (2020). Arabidopsis MYB4 plays dual roles in flavonoid biosynthesis. Plant J. *101*, 637–652.

44. Roppolo, D., De Rybel, B., Dénervaud Tendon, V., Pfister, A., Alassimone, J., Vermeer, J.E., Yamazaki, M., Stierhof, Y.D., Beeckman, T., and Geldner, N. (2011). A novel protein family mediates Casparian strip formation in the endodermis. Nature *473*, 380–383.

45. Kamiya, T., Borghi, M., Wang, P., Danku, J.M., Kalmbach, L., Hosmani, P.S., Naseer, S., Fujiwara, T., Geldner, N., and Salt, D.E. (2015). The MYB36 transcription factor orchestrates Casparian strip formation. Proc. Natl. Acad. Sci. USA *112*, 10533–10538.

46. Liberman, L.M., Sparks, E.E., Moreno-Risueno, M.A., Petricka, J.J., and Benfey, P.N. (2015). MYB36 regulates the transition from proliferation to differentiation in the Arabidopsis root. Proc. Natl. Acad. Sci. USA *112*, 12099–12104.

47. Siligato, R., Wang, X., Yadav, S.R., Lehesranta, S., Ma, G., Ursache, R., Sevilem, I., Zhang, J., Gorte, M., Prasad, K., et al. (2016). MultiSite gateway-compatible cell type-specific gene-inducible system for plants. Plant Physiol. *170*, 627–641.

48. Delude, C., Fouillen, L., Bhar, P., Cardinal, M.J., Pascal, S., Santos, P., Kosma, D.K., Joubès, J., Rowland, O., and Domergue, F. (2016). Primary fatty alcohols are major components of suberized root tissues of Arabidopsis in the form of alkyl hydroxycinnamates. Plant Physiol. *171*, 1934–1950.

49. Hosokawa, M., Suzuki, S., Umezawa, T., and Sato, Y. (2001). Progress of lignification mediated by intercellular transportation of monolignols during tracheary element differentiation of isolated Zinnia mesophyll cells. Plant Cell Physiol. *42*, 959–968.

50. Alejandro, S., Lee, Y., Tohge, T., Sudre, D., Osorio, S., Park, J., Bovet, L., Lee, Y., Geldner, N., Fernie, A.R., and Martinoia, E. (2012). AtABCG29 is a monolignol transporter involved in lignin biosynthesis. Curr. Biol. *22*, 1207–1212.

51. Keymer, A., Pimprikar, P., Wewer, V., Huber, C., Brands, M., Bucerius, S.L., Delaux, P.M., Klingl, V., Röpenack-Lahaye, E.V., Wang, T.L., et al. (2017). Lipid transfer from plants to arbuscular mycorrhiza fungi. eLife *6*, e29107.

52. Takahashi, K., Shimada, T., Kondo, M., Tamai, A., Mori, M., Nishimura, M., and Hara-Nishimura, I. (2010). Ectopic expression of an esterase, which is a candidate for the unidentified plant cutinase, causes cuticular defects in Arabidopsis thaliana. Plant Cell Physiol. *51*, 123–131.

53. Ursache, R., Vieira-Teixeira, C.D.J., Tendon, V.D., Gully, K., De Bellis, D., Schmid-Siegert, E., Andersen, T.G., Shekhar, V., Calderon, S., Pradervand, S., et al. (2020). GDSL-domain containing proteins mediate suberin biosynthesis and degradation, enabling developmental plasticity of the endodermis during lateral root emergence. bioRxiv. https://doi.org/10.1101/2020.06.25.171389.

54. Domergue, F., Vishwanath, S.J., Joubès, J., Ono, J., Lee, J.A., Bourdon, M., Alhattab, R., Lowe, C., Pascal, S., Lessire, R., and Rowland, O. (2010). Three Arabidopsis fatty acyl-coenzyme A reductases, FAR1, FAR4, and FAR5, generate primary fatty alcohols associated with suberin deposition. Plant Physiol. *153*, 1539–1554.

55. Beisson, F., Li, Y., Bonaventure, G., Pollard, M., and Ohlrogge, J.B. (2007). The acyltransferase GPAT5 is required for the synthesis of suberin in seed coat and root of Arabidopsis. Plant Cell *19*, 351–368.

56. Laflamme, B., Middleton, M., Lo, T., Desveaux, D., and Guttman, D.S. (2016). Image-based quantification of plant immunity and disease. Mol. Plant Microbe Interact. *29*, 919–924.

57. Kurihara, D., Mizuta, Y., Sato, Y., and Higashiyama, T. (2015). ClearSee: a rapid optical clearing reagent for whole-plant fluorescence imaging. Development *142*, 4168–4179.

58. Berhin, A., de Bellis, D., Franke, R.B., Buono, R.A., Nowack, M.K., and Nawrath, C. (2019). The root cap cuticle: a cell wall structure for seedling establishment and lateral root formation. Cell *176*, 1367–1378.e8.

59. Schindelin, J., Arganda-Carreras, I., Frise, E., Kaynig, V., Longair, M., Pietzsch, T., Preibisch, S., Rueden, C., Saalfeld, S., Schmid, B., et al. (2012). Fiji: an open-source platform for biological-image analysis. Nat. Methods *9*, 676–682.

STAR★METHODS

KEY RESOURCES TABLE

REAGENT or RESOURCE	SOURCE	IDENTIFIER
Bacterial and Virus Strains		
Escherichia coli DH5alfa	Widely distributed	N/A
Agrobacterium tumefaciens GV3101	Widely distributed	N/A
Chemicals, Peptides, and Recombinant Proteins		
β-Estradiol (E2D.)	Sigma	Cat# E8875
Propidium Iodide (PI)	Sigma	Cat# P4864
Murashige and Skoog Basal Medium (MS)	Duchefa	Cat# M0255
Plant Agar	Duchefa	Cat# P1001.1000
CIF2	[11]	N/A
DMSO	Sigma	Cat#D8418
Xylitol (for preparing ClearSee solution)	Sigma	Cat# 87-99-0
Sodium Deoxycholate (for preparing ClearSee solution)	Sigma	Cat# D6750
Urea (for preparing ClearSee solution)	Sigma	Cat# U5378
Fluorol yellow (FY)	Santa Cruz	Cat# sc-215052
Acid lactic	VWR	Cat# 20366293
Calcofluor White	Sigma	Cat# F3543
Basic Fuchsin	Sigma	Cat# 47860
p-formaldehyde	Sigma	Cat# P6148
Piperonylic acid (PA)	Sigma	Cat# P49805
Coniferyl alcohol	Sigma	Cat# 223735
Ferulic acid	Sigma	Cat# 1270311
p-coumaric acid	Sigma	Cat# C9008
NaCl	Sigma	Cat# S3014
Cellulase,	Sigma	Cat# C2605
Pectinase	Sigma	Cat#P4716
Chloroform	Fischer Chemical	Cat#C14960/17
Methanol	Sigma	Cat#34885-M
BSTFA (bis-(N,O-trimethylsilyl)-tri-fluoroacetamide	Macherey-Nagel	Cat# 701220.110
Pyridin	Roth	Cat# CP07.1
C32 alkane	Sigma	Cat#D223107
C15 alkane	Sigma Aldrich	Cat# P3406
Critical Commercial Assays		
The Universal RNA Purification Kit	Roboklon	Cat# E3598-02
BP clonase II	Invitrogen	Cat# 11789100
LR-clonase II	Invitrogen	Cat# 11791043
ReliaPrep RNA Tissue Miniprep Kit	Promega	Cat# Z6112
PrimeScript RT Master Mix	Takara	Cat# RR036B
AMV Reverse Transcriptase Native	Roboklon	Cat# E1372-01
MESA blue	Eurogentec	Cat# RT-SYS2X-03+NRWOUB
Experimental Models: Organisms/Strains		
Arabidopsis: Col-0	Widely distributed	N/A
Arabidopsis: *pPAL1::NLS-3xVenus*	This manuscript	N/A
Arabidopsis: *pPAL2::NLS-3xVenus*	This manuscript	N/A
Arabidopsis: *pPAL4::NLS-3xVenus*	This manuscript	N/A
Arabidopsis: *pCH4::NLS-3xVenus*	This manuscript	N/A
Arabidopsis: *sgn3-3*	[11,13]	N/A

(*Continued on next page*)

Continued

REAGENT or RESOURCE	SOURCE	IDENTIFIER
Arabidopsis: *pGPAT5::mCitrin-SYP122*	[28]	N/A
Arabidopsis: *pCASP1::MYB4* in *pGPAT5::mCitrin-SYP122*	This manuscript	N/A
Arabidopsis: *pELTP::MYB4* in *pGPAT5::mCitrin-SYP122*	This manuscript	N/A
Arabidopsis: *pELTP::XVE>> MYB4-GFP* in Col-0	This manuscript	N/A
Arabidopsis: *pELTP::XVE>> MYB4* in Col-0	This manuscript	N/A
Arabidopsis: *asft-1*	[27]	N/A
Arabidopsis: *asft-2*	[27]	N/A
Arabidopsis: *pCASP1::CASP1-GFP* in Col-0	[43]	N/A
Arabidopsis: *pCASP1::MYB4* in *pCASP1::CASP1-GFP*	This manuscript	N/A
Arabidopsis: *pCASP1::MYB4* in *sgn3-3*	This manuscript	N/A
Arabidopsis: *cif1cif2* in Col-0	[11]	N/A
Arabidopsis: *pCASP1::MYB4* in *cif1cif2*	This manuscript	N/A
Arabidopsis: *pCASP1::MYB3* in *pGPAT5::mCitrin-SYP122*	This manuscript	N/A
Arabidopsis: *pCASP1::MYB7* in *pGPAT5::mCitrin-SYP122*	This manuscript	N/A
Arabidopsis: *pCASP1::MYB32* in *pGPAT5::mCitrin-SYP122*	This manuscript	N/A
Arabidopsis: *pELTP::MYB3* in *pGPAT5::mCitrin-SYP122*	This manuscript	N/A
Arabidopsis: *pELTP::MYB7* in *pGPAT5::mCitrin-SYP122*	This manuscript	N/A
Arabidopsis: *pELTP::MYB32* in *pGPAT5::mCitrin-SYP122*	This manuscript	N/A
Arabidopsis:	This manuscript	N/A
Oligonucleotides		
See Document S1	Sigma	N/A
Recombinant DNA		
P4L1r pDONR	Takara	N/A
pDONR 221	Invitrogen	Cat# 12536017
pDONR 221-MYB4	This manuscript	See Method details
pDONR 221-MYB7	This manuscript	See Method details
pDONR 221-MYB32	This manuscript	See Method details
pDONR 221-MYB3	This manuscript	See Method details
P4L1r pDONR-pELTP	[28]	N/A
P4L1r pDONR- pELTP::XVE>>	[28]	N/A
P4L1r pDONR-pCASP1	[28]	N/A
pDONR 221-gMYB4-GFP	This manuscript	See STAR Methods
P4L1r pDONR-pPAL1	This manuscript	See STAR Methods
P4L1r pDONR-pPAL2	This manuscript	See STAR Methods
P4L1r pDONR-pCH4	This manuscript	See STAR Methods
pED97	[28]	N/A
Software and Algorithms		
ZEN Black (Zen 2.3 SP1)	Zeiss	https://www.zeiss.de/corporate/home.html
Fiji/ImageJ	[56]	https://fiji.sc/)
IBM SPSS Statistics version 24-25-26	IBM	https://www.ibm.com/products/spss-statistics
CFX Maestro	BIO-RAD	https://www.bio-rad.com

RESOURCE AVAILABILITY

Lead Contact

Further information and requests for resources should be directed to and will be fulfilled by the Lead Contact, Tonni Grube Andersen (tandersen@mpipz.mpg.de).

Materials Availability

There are no restrictions to the availability of the newly generated resources except for the CIF2 peptide, which will be provided if available.

Data and Code Availability

This study did not generate any unique code. This study did not produce any unique NGS sequencing/ protein structure/microarray data.

EXPERIMENTAL MODEL AND SUBJECT DETAILS

Arabidopsis thaliana transgenic and mutant lines were used to performed experiments. For all experiments, *Arabidopsis thaliana* (ecotype Columbia 0) was used. The background and the details of each line/mutant are specified in the Key Resources Table. Seeds were kept for 2 days at 4°C in the dark for stratification, then grown at 22°C under 16 h light/8 h dark vertically on solid half-strength Murashige–Skoog (MS) medium without sucrose for all experiments except. for periderm and GC-MS analysis, in which plants were grown at 22°C under continuous light conditions.

METHOD DETAILS

Molecular Cloning

To generate endodermis specific expression constructs the genomic region of MYB3, 4 7 or 32 were amplified using specific primers (Data S1) and Gateway cloned into a pDONR221 entry vector using BP clonase II (Invitrogen) according to manufactures description. In case of MYB4-GFP, the genomic region was directly fused to GFP by overlapping PCR and inserted as one into the pDONR 221 vector. Together with previously generated P4L1r pDONR entry vectors containing either p*CASP1*, p*ELTP* or p*ELTP::*XVE>>[28], the MYB entry vectors were recombined using LR-clonase II (Invitrogen) into a fastred selection-contain destination vector (pED97). For promoter constructs p*PAL1* (4038bp) p*PAL2* (3456bp), p*PAL4* (2332 bp) and p*C4H* (2450bp) were cloned using specific primers (Data S1) into a modified gateway vector containing an attL4 R1r cassette cut with XbaI using Infusion cloning (Takara). The Promoter entry vectors were recombined using LR-clonase II (Invitrogen) into a fastred selection-contain destination vector. The final constructs were transformed into Col-0 or other backgrounds using the floral dip method[54] and selected using FastRed selection.

GC-MS

For periderm analysis, sections of ~2 cm of periderm from 20-day-old plants were collected directly from plates. Most lateral roots were cut off from the samples. For endodermis analysis, the whole root was collected if no periderm was already formed, or if the periderm was already present, only the lower portion of the root was collected. In both cases, the samples were washed by submerging three times in deionized water and carefully dried on paper towel before subsequent analysis. For suberin analysis, we followed a previously established protocol[5]. Briefly, the roots were treated with an enzymatic solution (Cellulase, Pectinase- Sigma-Aldrich, Germany) for 7 days. The solution was exchanged four times. After enzymatic treatment, unbound lipids were extracted from the roots by Soxhlet extraction with chloroform: methanol (1:1; v/v) for 2 days. The samples were dried and weighed. Consecutively, suberin was depolymerized using a 10% BF3/MeOH-based procedure[5]. In order to quantify (μg/mg sample) the suberin monomers detected by gas chromatography-coupled mass spectrometry (GC-MS), after the depolymerization, 25 μl of C32 alkane internal standard (13,5 mg/50 ml) was added in each sample. After the extraction, samples were concentrated by evaporation with N_2 until ~50 μl and posteriorly derivatized with 20 μL of BSTFA (bis-(N,O-trimethylsilyl)-tri-fluoroacetamide, Macherey-Nagel, Germany) and 20 μL Pyridin for 40 min at 70°C. For chloroform-extraction analysis, fresh samples were used. After washing with deionized-water samples were carefully weighed. In order to quantify chloroform extracts (μg/g fresh weight), 22 μL of C15 (20 μl /50 ml) was added to each sample. following this, samples were submerged in chloroform for 90 s[48]. The chloroform extracts were then evaporated with N_2 until ~50 μl. Finally, before GC-MS analysis, samples were derivatized with 20 μL of BSTFA (bis-(N,O-trimethylsilyl)-tri-fluoroacetamide, Macherey-Nagel, Germany) and 20 μL Pyridin for 40 min at 70°C. All extracts were measured using a Shimadzu TQ8040 GC-MS setup using splitless injection mode on a SH-Rxi-5SIL-MS column (30 m, 0.25 mm internal diameter, 0.25 μm film, Shimadzu Cooperation). The starting temperature was 50°C for two minutes, with an increase of 10°C per minute until 150°C, 150°C for one minute, with an increase of 3°C per minute until 310°C, and 310°C for 15 minutes. Helium was used as carrier gas with a flow rate of 0.86 mL min^{-1}. The mass spectrometer was operated in electron impact ionization (EI) scan mode. The analyses were conducted with three or five replicates. In the chloroform extractive analyses the blank was subtracted from C16 and C18 acids (all the other compounds were not detected in the blank). As C16 acid after blank subtraction was below detection it was not included in the analyses.

Stainings

For the endodermis: ClearSee staining coupled to cell wall stainings was performed as recently described in[16,57]. Briefly, plants were fixed in 3 mL 1 x PBS containing 4% *p*-formaldehyde for 1 hour at room temperature in 12-well plates and washed twice with 3 mL 1 x PBS. Following fixation, the seedlings were cleared in 3 mL ClearSee solution (10% Xylitol, 15% Sodium Deoxycholate and 25% Urea in water) under gentle shaking. After overnight clearing, the solution was exchanged to new ClearSee solution containing 0.2% Basic Fuchsin and 0.1% Calcofluor White for lignin and cell wall staining respectively. The dye solution was removed after overnight staining and rinsed once with fresh ClearSee solution. The samples were washed in new ClearSee solution for 30 min with gentle shaking and washed again in another fresh ClearSee solution for at least one overnight before observation. For quantification of Basic Fuchsin signal, recovering roots were normalized to signals from identically stained, non-PA treated Col-0 plants and plants taken directly from PA-containing plates (time point 0). For Fluorol Yellow staining of *Arabidopsis* root suberin vertically grown 5-day old seedlings

were incubated solution of Fluorol Yellow 088 (0.01%, in lactic acid) and incubated for 30 min at 70 degrees. The stained seedlings were rinsed shortly in water and transferred to a freshly prepared solution of aniline blue (0.5%, in water) for counterstaining. Following this, seedlings were washed for 2-3 min in water and transferred to a chambered cover glass (Thermo Scientific), and imaged either using Confocal laser scanning (CLSM) microscopy or a Leica DM5500 wide field microscope (GFP filtercube ex: 470 nm/40 em:525/50 bs: 500). For CLSM fluorescence, Fluorol Yellow was detected using 488 nm as excitation wavelength, and collection of emission from 500-550nm. PI assays were done as described[2] shortly, seedlings were incubated in water containing 10 μg /mL PI for 10 min and transferred into fresh water. The number of endodermal cells were scored using a Leica DM5500 wide field microscope (TX2 filtercube ex: 560 nm/40 em:645/75 bs: 595) from onset of cell elongation (defined as endodermal cell length being more than two times than width in the median, longitudinal section) until PI could not penetrate into the stele.

For the periderm: For Fluorol Yellow staining was performed as described for the endodermis except that the samples were mounted on a slide in 10% Glycerol and sample were imaged with a CLSM (Zeiss LSM880) for 3D pictures of Cork cells and with a Zeiss Axiophot epifluorescence microscope with GFP filter cube to measure the length of the different suberized zones. ClearSee coupled to Basich Fuchsin staining was performed as in the endodermis, except that after Basic Fuchsin staining, roots were washed with ClearSee solution 3times for 10 minutes and then mounted on a slide in ClearSee solution and imaged with a CLSM (Zeiss LSM880). Toluidine Blue penetration assay in the cork was performed as described for analysis in the lateral root cap[58]. Briefly, plants were collected in water in a 6-well plate, transferred in a 6-well plate containing 0.05% Toluidine Blue, incubate for 2 min and washed twice with water prior mounting then them in water on a slide. Imaging was performed straight after mounting with a Zeiss Axiophot microscope.

For the leaf: Chlorosis of leaves was measured in ImageJ[59] by measuring green channel values images as previously described[56].

Confocal Microscopy

Confocal pictures were obtained using Leica SP8 or Zeiss LSM 880 CLS microscopes.

The excitation and detection window settings to obtain signal when using a Leica SP8 were as follows: GFP (ex.488 nm, em.500–550 nm), mVenus, (ex.514 nm, em.518–560 nm). All periderm pictures were acquired with a Zeiss LSM880 with the following settings: cork autofluorescence (ex.405 nm; em. 420-460 nm), PI and Basic Fuchsin (ex.566 nm; em.570-630 nm). FY (ex.488nm, em. 490-540 nm), GFP (488nm, 490-510 nm), Venus and Citrine: (ex. 514 nm; em. 520–540 nm). 3D reconstructions and Orthogonal views of a Z stack were obtained using the ZEN Black software.

Root Suberin Coverage

Quantification of Root suberin coverage in 5-8d old root was performed as described in[7,28] Briefly, after FY stainings, the whole root is analyzed, first we measured the length of the root from the root tip to the first endodermis suberized cell (no suberin), then the distance from the first suberized cell to the point in which all endodermal cells (excluding passage cells are suberized) are suberized (patchy suberin) and then we measured the root length from that point to the hypocotyl (continuous suberin). Total root length is measured summing all 3 distances, and the relative distance of every zone is obtained dividing the distance of each zone by the total length. In the graph the mean distance of the 3 zones is plotted. The mean distance of the patchy zone is plotted on the top of the no suberin zone, and the mean distance of the continuous zones on the top of the previous developmental zone.

For older roots (from 12-old), which comprise also the periderm, the quantification is performed similarly, the only difference is that endodermis continuous suberin zone finishes at the point of the first cork cell is stained by FY, then we measure the distance from the first stained cork cell to the point in which the whole root is covered by the cork (developing periderm/cork). Finally we measure the distance from that point to the hypocotyl root junction (mature cork/periderm). Total root length is measured summing all 5 distances, and the relative distance of every zone is obtained dividing the distance of each zone by the total length. In the graph the mean distance of the 5 zones is plotted. The number of roots analyzed per genotype/treatment is mentioned in the figure legend.

q-PCR

For the *pCASP1::*MYB4 experiment: seedlings were grown on half MS without sucrose for 5 days. Only root parts (around 100 mg) were collected from each genotype and total RNA was extracted using a Trizol-adapted ReliaPrep RNA Tissue Miniprep Kit (Promega). Reverse transcription was carried out with PrimeScript RT Master Mix (Takara). All steps were done in at least triplicates and as indicated in manufactures' protocols. The qPCR reaction was performed on an Applied Biosystems QuantStudio3 thermocycler using a MESA BLUE SYBR Green kit (Eurogentech). For the *pELTP::XVE*>>MYB4-GFP experiment: plants were grown on half MS without sucrose for 19 days and then transferred in Mock or E2D supplemented half MS liquid for 48h. For the periderm: the 2 uppermost cm of the root were collected, whereas for the endodermis the lower half of the roots (without the root tip and the first 3 cm) was collected. RNA was extracted using the Universal RNA Purification Kit (Roboklon) according to the manufacturer protocol. C-DNA was synthetized using AMV Reverse Transcriptase Native (Roboklon) according to manufacturer protocol. qPCR was performed using MESA blue (Eurogentec, RT-SYS2X-03+NRWOUB) in a CFX96 Real-Time System machine (BIO-RAD). All transcripts are normalized to Clathrin adaptor complexes medium subunit family protein (AT4G24550) expression. For periderm and suberized endodermis experiments, the relative expression was calculated using CFX Maestro software (BIO-RAD) and the sample were normalized against *EF1*.Primers and gene names used for qPCR are listed in Table S1.

QUANTIFICATION AND STATISTICAL ANALYSIS

No statistical methods were used to predetermine sample size. The experiments were not randomized. Root length and the length of suberized zone was measured using imageJ / Fiji[56].

Quantification of the Propidium Iodide blockage was performed as described in[40]. All quantitative fluorescence intensities were measured using imageJ/Fiji[56] in identical optical sections of either 8- or 16-bit images with no overexposed pixels. For endodermis suberin coverage experiments, statistical analyses were performed in R-studio (ver 1.1.463) For multiple sample comparisons, a one-way ANOVA with Tukeys's post hoc (equal variance not assumed) test was performed unless otherwise stated. For the suberin root coverage quantification, statistic was performed separately for each root zone (indicate by the absence or presence of ';'';' or '' adjacent to the letters) but across all plants within one subfigure. For GC-MS and periderm experiments, statistical analyses were performed with IBM SPSS Statistics version 25 (IBM). First, the datasets were tested for the homogeneity of variances using the Levene's Test. The significant differences between two datasets were calculated using a Welch's two-tailed t test in case of a non-homogeneous variance or a Student's two-tailed t test if the variance was homogeneous. For multiple sample comparisons, a one-way ANOVA with Tamhane's post hoc (equal variance not assumed) or a Bonferroni correction (equal variance assumed) was performed unless otherwise stated. For the detailed suberin quantification of each compound/category of compound via GC-MS, statistic was performed separately for each compound/category (indicate by the absence or presence of ';''; close to letter). For the suberin root coverage quantification in old roots that comprised the periderm, statistic was performed separately for each root zone.

Gene List

The gene number of all genes mentioned in this study is presented in Table S1.

Current Biology, Volume *31*

Supplemental Information

Tissue-Autonomous Phenylpropanoid Production Is Essential for Establishment of Root Barriers

Tonni Grube Andersen, David Molina, Joachim Kilian, Rochus B. Franke, Laura Ragni, and Niko Geldner

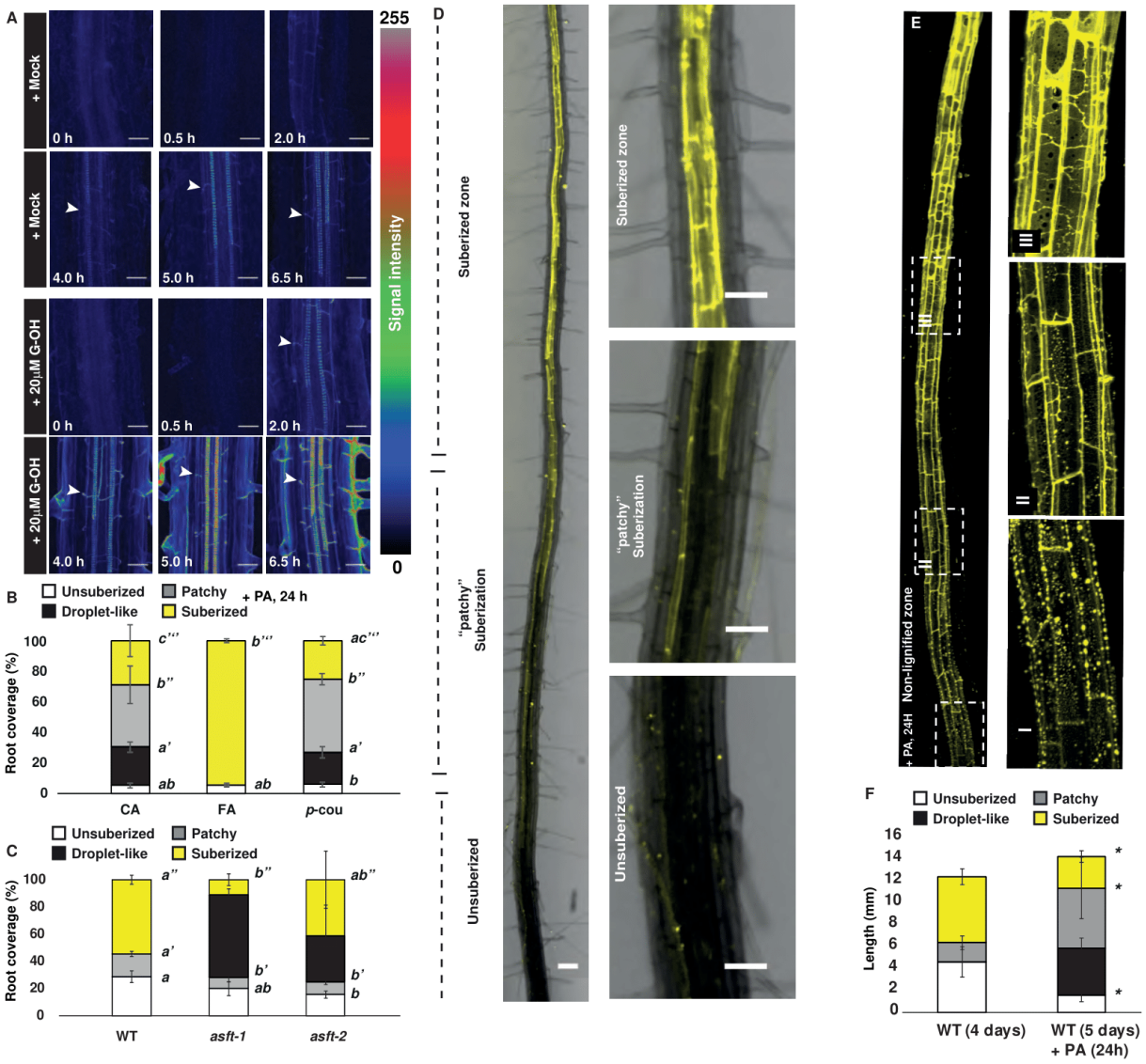

Figure S1 | Behavior of lignin and suberin in roots upon PA treatment. Related to Figure 2

(A) Time course analysis of Basic fuchsin signal recovery in the non-lignified zone of xylem or Casparian Strip Domain (CSD) after 24 h of piperonylic acid (PA) pre-treatment. 6-day-old plants were moved from PA-containing plates to recovery plates with either a mock solution or 20 μM coniferyl alcohol (G-OH) at the indicated timepoints. Lignin deposition highlighted by Basic fuchsin signal in the endodermis and vasculature using an established ClearSee-based protocol[55]. Arrowheads point towards lignifying Casparian strips (CS). (B) Quantification of suberin root coverage by Fluorol Yellow (FY) staining of suberin in the endodermis of 6-day-old WT roots. 4-day-old plants treated with PA for 24 h and then transferred for to plates containing 20 μM p-Caffeic Acid (CA) or 20 μM ferulic acid (FA) or 20 μM para-coumaric acid (*p*-cou) for an additional 24 hours. N=6. (C) Quantification of suberin root coverage by Fluorol Yellow (FY) staining of suberin in the endodermis of 5-day-old WT, *asft-1* and *asft-2* roots, N=6. (D) FY stained endodermis of a 5-day-old root illustrating the different zones of suberization along the developmental stages of the endodermis. (E) Deposition of "droplet-like" suberin visualized by Fluorol yellow (FY) in the non-lignified zone of a 5-day-old plant previously treated with 1 μM PA for 24 hours. (F) Quantification of absolute suberin root coverage by Fluorol Yellow (FY) staining of suberin in the endodermis, N=6). All error bars are SD. *: P< 0.05, **, P<0.01 in a two-tailed Students T-test vs WT. Letters refer to individual groups in a one-way ANOVA analysis with a post-hoc multiple group T-test (Tukey). Scalebars are 50 μm.

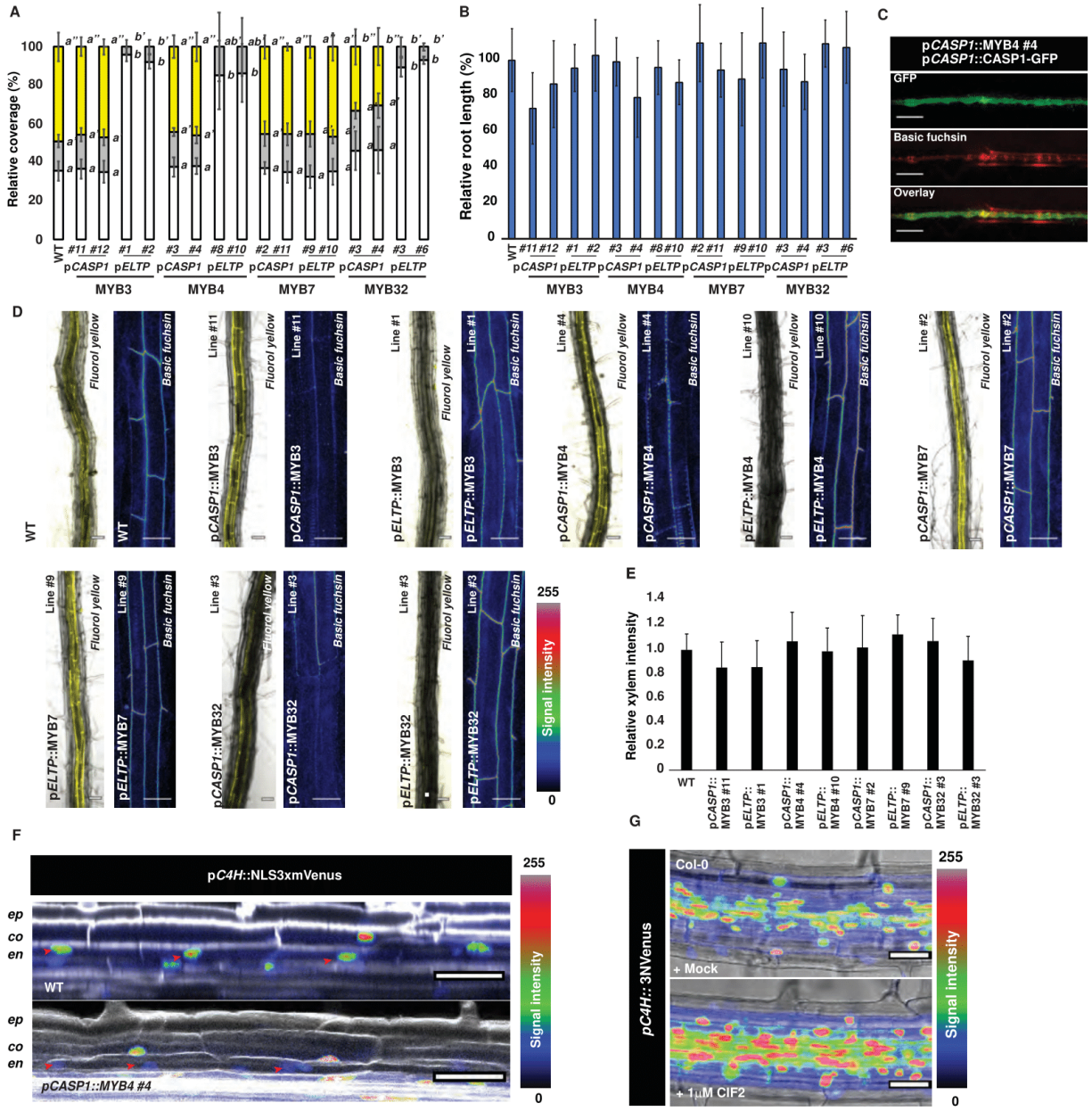

Figure S2 | Lignin and suberin analysis upon ectopic expression of MYB-repressors. Related to Figure 3 and Figure 5.

(A) Quantification of suberin by Fluorol yellow (FY) staining (Root suberin coverage) in 5-day-old roots of lines with pCASP1- or pELTP-driven MYB repressor expression, N=6. (B) Root length relative to Wildtype (WT) plants subject to FY staining. N=6, *: P< 0.05, **, P<0.01 in a two-tailed Students T-test vs WT. (C) Projected surface view of an endodermal cell with highlighted Casparian strip domain by CASP1-GFP and lignin deposition by Basic Fuchsin (BF) staining in 5-day-old pCASP1::MYB4 expressing plants Scalebars are 10 μm. (D) Suberin and lignin deposition highlighted by FY and BF respectively, in the endodermis of 5-day-old seedlings. Scale bars are 20 μm. (E) Quantification of fluorescence intensity of BF staining in the xylem of lines from (D). The signal was normalized to signal obtained from identically grown WT plants, N=8. *: P< 0.05, **, P<0.01 in a two-tailed Students T-test vs WT. (F) Representative images of C4H activity (pC4H::3NVenus) in the zone of Casparian strip establishment of 5-day-old plants. (G) Representative images of C4H activity (pC4H::3NVenus) in the zone of Casparian strip establishment of 5-day-old plants upon treatment with mock or 1 μM CIF2 peptide for 24 h. in both F and G 5-day-old roots were fixed and stained with calcofluor white and Basic Fuchsin using a previously established ClearSee-based protocol[55]. Scalebars are 25 μm. All error bars are SD. Letters refer to individual groups in a one-way ANOVA analysis with a post-hoc multiple group T-test (Tukey).

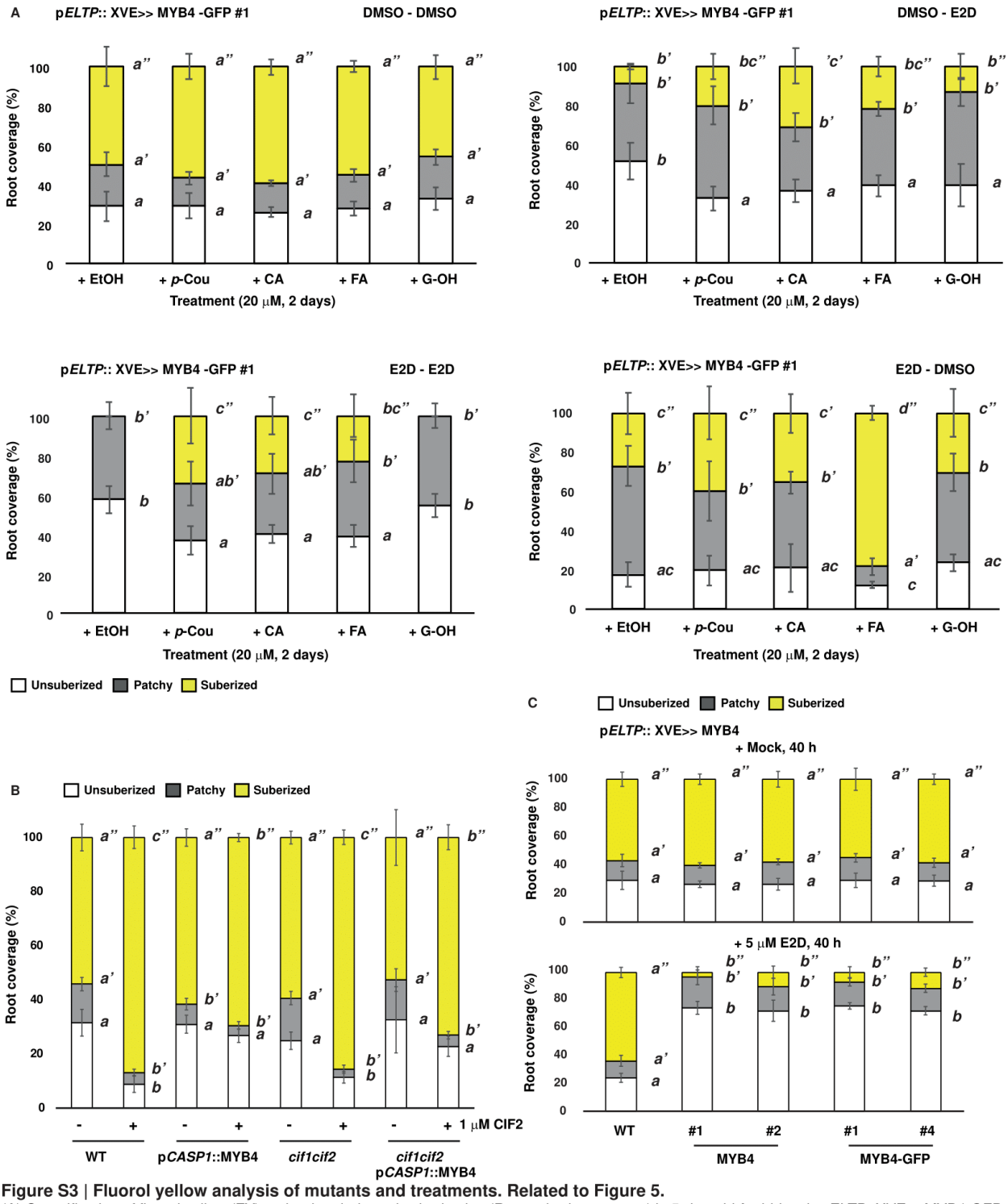

Figure S3 | Fluorol yellow analysis of mutants and treatments. Related to Figure 5.
(A) Quantification of fluorol yellow (FY)-stained endodermal suberization (Root suberin coverage) in 5-day-old Arabidopsis pELTP::XVE>>MYB4-GFP seedlings treated with either DMSO or 5 μM beta-estradiol (E2D) in combination-regimes with mock (EtOH), 20 μM p-coumaric acid (p-Cou) 20 μM caffeic acid (CA), 20 μM ferulic acid (FA), or 20 μM coniferyl alcohol (G-OH) for 48 h. (B) Quantification of FY-stained endodermal suberization (Root suberin coverage) in 5-day-old WT, or *cif1cif2* dKO Arabidopsis plants with or without pCASP1::MYB4 expression. Plants were treated for 24 h with wither mock (H2O) or 1 μM CIF2 peptide. (C) Quantification of FY stained endodermal suberization (Root suberin coverage) in 5-day-old Arabidopsis pELTP::XVE>>MYB4-GFP or MYB4 seedlings treated with either DMSO or 5 μM E2D. For all experiments, N=6. All error bars are SD, Letters refer to individual groups in a one-way ANOVA analysis with a post-hoc multiple group T-test (Tukey).

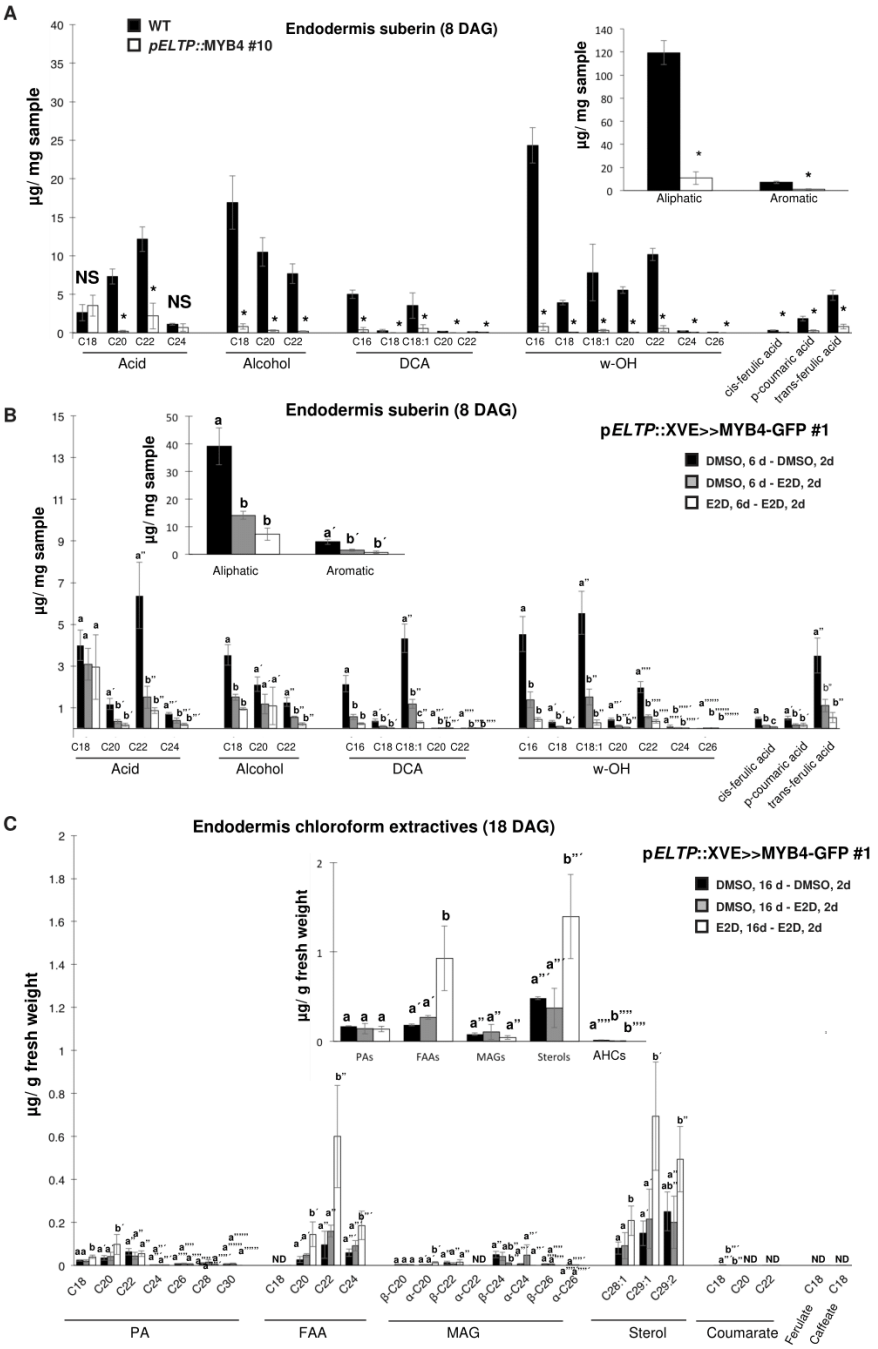

Figure S4 | Suberin and chloroform extractives quantification in the endodermis. Related to Figure 5.

(A) Suberin quantification by Gas chromatography-coupled mass spectroscopy (GC-MS)-based analysis from the endodermis of 8-days-old wildtype (WT) and pELTP::MYB4 expressing roots (N=4-5; T-Test *: P<0.05. (B) Suberin quantification by GC-MS-based analysis from the endodermis of 8-days-old pELTP::XVE>>MYB4-GFP expressing roots under different beta-estradiol (E2D) treatments (One-way ANOVA (CI95%, N=3-4). (C) Chloroform extractives quantification by GC-MS-based analysis from the endodermis of 18-day-old pELTP::MYB4 expressing roots under different E2D treatment regimens (One-way ANOVA (CI95%, N=3). For the comparison of the suberin fractions, each compound was normalized to the total aliphatic or aromatic respectively. Numbers refer to carbon chain lengths of aliphatic fatty acid derivatives. DCA: $\alpha-\omega$-dicarboxylic acid, ND: Not detected, NS: Not significant. All error bars are SD.

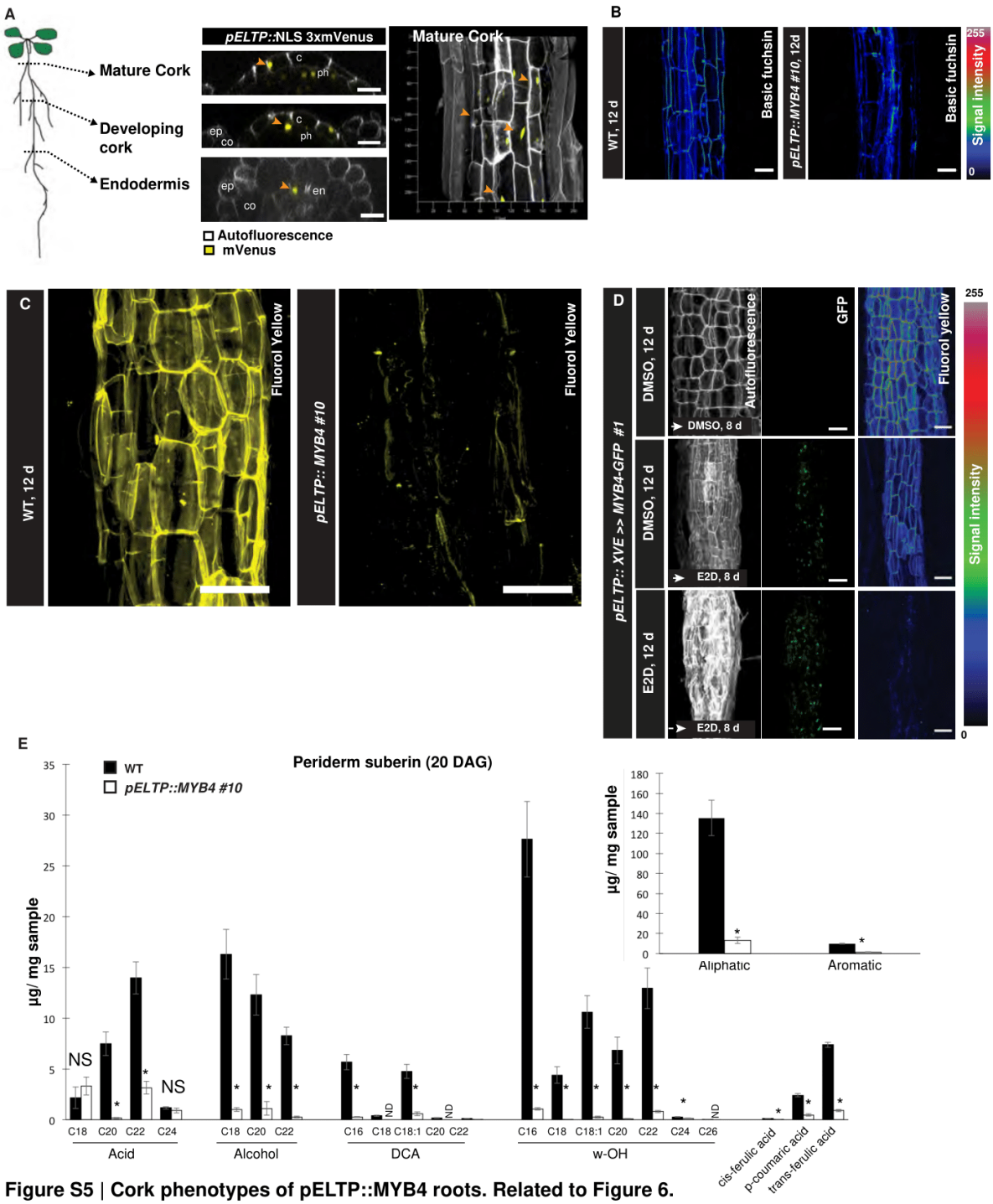

Figure S5 | Cork phenotypes of pELTP::MYB4 roots. Related to Figure 6.

(A) Representative images of pELTP-driven nuclear-localized (NLS) 3x mVenus reporter in the developing and mature cork as well as endodermis of 14-day-old roots. Orange arrowheads highlight cells with pELTP activity. (B) Visualization of lignin in the cork cells of 12-day-old roots of wildtype (WT) and pELTP::MYB4 expressing plants were fixed and stained with Basic Fuchsin using a previously established ClearSee-based protocol[57]. (C) Fluorol yellow (FY) staining of suberin in the cork of 12-day-old roots of WT and pELTP::MYB4 expressing plants. (D) Autofluorescence (left panel), GFP (middle panel) or Fluorol Yellow (FY) (right panel) signal in the cork of 20-day-old pELTP::XVE>>MYB4-GFP roots under different mock and 5 uM estradiol (E2D) treatment regimes. Plants were grown for 12 days on DMSO or E2D and transferred to plates containing either DMSO or E2D to allow induction of MYB4 in pre-suberized and lignified cork cells. E) Suberin quantification by Gas chromatography-coupled mass spectroscopy (GC-MS)-based analysis from the cork of 20-day-old wildtype (WT) and pELTP::MYB4 expressing roots (N=3-4; Two-tailed Students T-Test *: P<0.05). Numbers refer to carbon chain lengths of aliphatic fatty acid derivatives., c: cork, co: cortex DCA: α–ω -dicarboxylic acid, ep: epidermis, NS: Not significant, ph: phellogen. All error bars are SD. Scalebars are 20 µm.

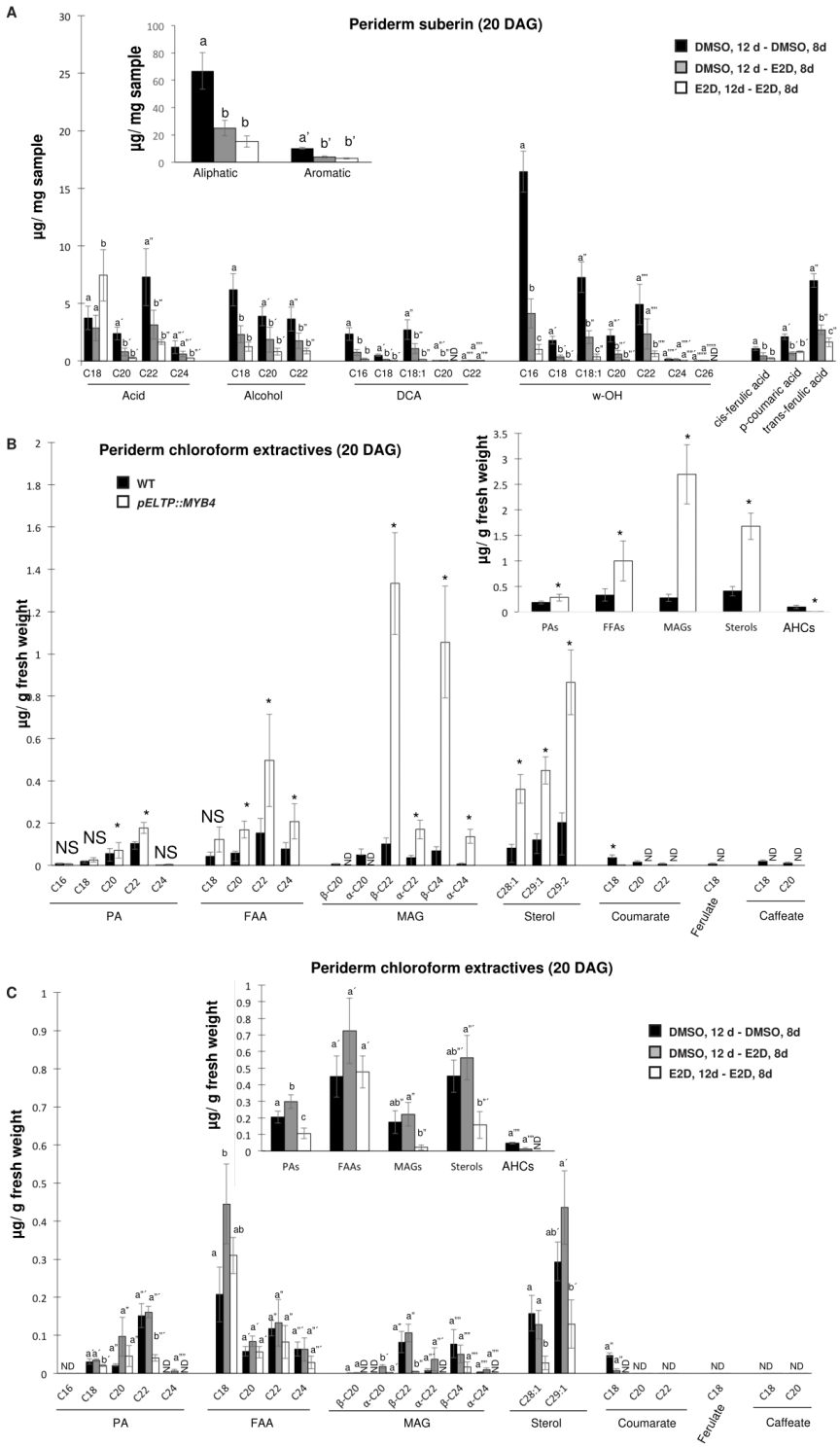

Figure S6 | Suberin and Chloroform extractives quantification in the cork. Related to Figure 6.

(A) Suberin quantification by Gas Chromatography coupled Mass Spectroscopy (GC-MS)-based analysis from the cork of pELTP::XVE>>MYB4-GFP expressing roots under different estradiol (E2D) treatments (One-way ANOVA, CI95%, N=3-4). (B) Chloroform extractives quantification by GC-MS-based analysis from the cork of 20-day-old WT and pELTP::MYB4 expressing roots (N=3-4; Two-tailed Students T-Test *: P<0.05). (C) Chloroform extractives quantification by GC-MS-based analysis from the cork of pELTP::XVE>>MYB4-GFP expressing roots under different E2D treatments (One-way ANOVA, CI95%, N=3). For the comparison of the suberin fractions, each compound was normalized to the total aliphatic or aromatic respectively. Numbers refer to carbon chain lengths of aliphatic fatty acid derivatives. AHCs: Alkyl hydroxycinnamates, DCA: α–ω-dicarboxylic acid, FFAs: Free fatty acids, MAGs: Mono-acyl glycerol conjugates, ND: Not detected, NS: Not significant, PAs: Primary alcohols, all error bars are SD, letters refer to individual groups in a one-way ANOVA analysis.

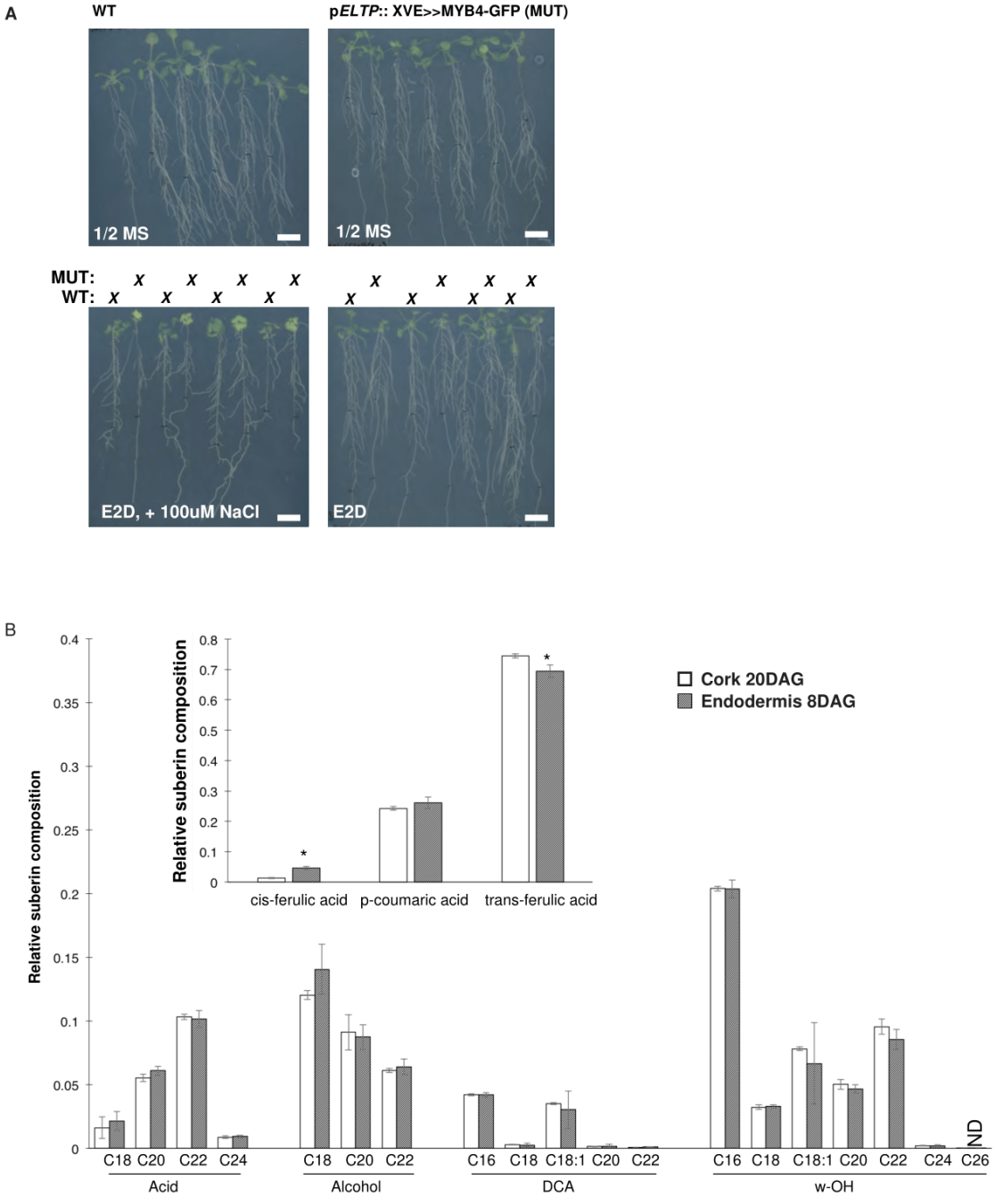

Figure S7 | Phenotypes of pELTP::XVE>>MYB4-GFP roots under stress. Related to Figure 6.

(A) Images depicting pELTP::XVE>>MYB4-GFP plants grown for 14 days under different regimes of the experiment shown in Figure 6H. Scale bars: 1cm. (B) Relative composition of suberin of the cork of 20-day-old roots and the endodermis of 8-day-old roots. For the comparison, each compound was normalized to the total aliphatic or aromatic respectively. Numbers refer to carbon chain lengths of aliphatic fatty acid derivatives. DCA: α–ω-dicarboxylic acid, (N=3-5; T-Test *: P<0,05). All error bars are SD.

Primer Name	Gene Name	Purpose	Sequence	AGI	Description
MYB3_F	MYB3	Cloning	aaaaagcaggcttaatgggaagatcaccatgctgc	AT1G22640	MYB3
MYB3_R	MYB3	Cloning	agaaagctgggtctaatgagtctaacatcagaaaccc	AT4G38620	MYB4
MYB4_F	MYB4	Cloning	aaaaagcaggcttaatgggaaggtcaccgtgctg	AT2G16720	MYB7
MYB4_R	MYB4	Cloning	agaaagctgggtttatttcatctccaagcttcg	AT4G34990	MYB32
MYB4-GFP_F	MYB4	Cloning	gctttcgaagcttggagatgaaaatggtgagcaagggc	AT2G48140	Endodermis lipid tranfer protein (ELTP)
MYB4-GFP_R	GFP	Cloning	cgcccttgctcaccattttcatctccaagcttcgaaac	AT2G36100	Casparian strip membrane domain protein 1 (CASP1)
GFP_R	GFP	Cloning	agaaagctgggttcacttgtacagctcgtccatgccg	AT2G16385	Casparian strip integrety factor 1(CIF1)
MYB7_F	MYB7	Cloning	aaaaagcaggcttaatgggaagatctccttgctgcg	AT4G34600	Casparian strip integrety factor 2(CIF2)
MYB7_R	MYB7	Cloning	agaaagctgggtttatttcatttccaagcttcg	AT5G41040	Aliphatic suberin feruloyl-transferase (ASFT)
MYB32_F	MYB32	Cloning	aaaaagcaggcttaatgggaaggtctccttgct	AT2G37040	Phenyl alanine Lyase 1 (PAL1)
MYB32_R	MYB32	Cloning	agaaagctgggttcatttcatttccaaagtgc	AT3G53260	Phenyl alanine Lyase 2 (PAL2)
pPAL1_F	Phenyl alanine Lyase 1 (PAL1)	Cloning	gaaaagttgggtactaaagagtaggaaaaactattaaa	AT3G10340	Phenyl alanine Lyase 4 (PAL4)
pPAL1_R	Phenyl alanine Lyase 1 (PAL1)	Cloning	acaaacttgcccgggttagacttttgatcttagttttt	AT2G30490	Cinnamate 4-Hydroxylase (C4H)
pPAL2_F	Phenyl alanine Lyase 2 (PAL2)	Cloning	gaaaagttgggtactgttgtgctaaaactatcaagaaa	AT5G22500	Fatty acid reductase 1 (FAR1)
pPAL2_R	Phenyl alanine Lyase 2 (PAL2)	Cloning	acaaacttgcccgggtggttttcaagaagttgtg	AT3G44540	Fatty acid reductase 4 (FAR4)
pPAL4_F	Phenyl alanine Lyase 4 (PAL4)	Cloning	gaaaagttgggtacaaagagattaatttgtaatgttc	AT1G04220	3-Ketoacyl-coa synthase 2 (KCS2)
pPAL4_R	Phenyl alanine Lyase 4 (PAL4)	Cloning	acaaacttgcccgggcgcgccgactcggttaaag	AT5G58860	CYP86A1, Hydroxylase of root suberized tissue (HORST)
pC4H_F	Cinnamate 4-Hydroxylase (C4H)	Cloning	gaaaagttgggtaccttatggttaaaaatttgg	AT3G11430	Glycerol-3-phosphate SN-2-acyltransferase 5 (GPAT5)
pC4H_R	Cinnamate 4-Hydroxylase (C4H)	Cloning	acaaacttgcccgggtatagtttgtgtatccgc	AT4G24550	Adaptor protein-4-MU-adaptin (Clathrin)
KCS2_F	3-Ketoacyl-coa synthase 2 (KCS2)	q-PCR	ccttcgttatcggctatgatcgtga	AT5G60390	EF1alpha (EF1)
KCS2_R	3-Ketoacyl-coa synthase 2 (KCS2)	q-PCR	tgcagtttgagagaagcattgatcg		
FAR1_F	Fatty acid reductase 1 (FAR1)	q-PCR	ggagccctgaatgttctcaacttcg		
FAR1_R	Fatty acid reductase 1 (FAR1)	q-PCR	gagagtctcccccatcttgaatggt		
FAR4_F	Fatty acid reductase 4 (FAR4)	q-PCR	catgcaacggtttcacagtgaggt		
FAR4_R	Fatty acid reductase 4 (FAR4)	q-PCR	tgagcggtccaaatgtgttgacg		
HORST_F	CYP86A1, Hydroxylase of root suberized tissue (HORST)	q-PCR	ggagacacgtggcaatgatcagga		
HORST_R	CYP86A1, Hydroxylase of root suberized tissue (HORST)	q-PCR	gtcgagcctcttggcacgaaagt		
GPAT5_F	Glycerol-3-phosphate SN-2-acyltransferase 5 (GPAT5)	q-PCR	accgtgtcgctaatttgtttgttgg		
GPAT5_R	Glycerol-3-phosphate SN-2-acyltransferase 5 (GPAT5)	q-PCR	ccgtcgtgaaatatcaccggaagt		
ASFT_F	Aliphatic suberin feruloyl-transferase (ASFT)	q-PCR	cccgatcctgaaactctagggaagc		
ASFT_R	Aliphatic suberin feruloyl-transferase (ASFT)	q-PCR	ccgagaacaaaccctccacatttga		
PAL1_F	Phenyl alanine Lyase 1 (PAL1)	q-PCR	aagtggctgcgatctcaactattgg		
PAL1_R	Phenyl alanine Lyase 1 (PAL1)	q-PCR	gtggcttgtttctttcgtgcttcc		
PAL2_F	Phenyl alanine Lyase 2 (PAL2)	q-PCR	aacactgacgatcggacaagttgc		
PAL2_R	Phenyl alanine Lyase 2 (PAL2)	q-PCR	ccgaatattccggcgttcaaaaatc		
PAL4_F	Phenyl alanine Lyase 4 (PAL4)	q-PCR	ccgaggaacggacagttatggag		
PAL4_R	Phenyl alanine Lyase 4 (PAL4)	q-PCR	gcacggagtgatttcgtggttg		
C4H_F	Cinnamate 4-Hydroxylase (C4H)	q-PCR	gtgccattgatcacatccttgaagc		
C4H_R	Cinnamate 4-Hydroxylase (C4H)	q-PCR	aatcgccattctcagacgaagagtc		
EF1 F	EF1	q-PCR	AGCATACACTGCGTGCAAAG		
EF1 R	EF1	q-PCR	TCGCCTGTGTCACATATCTC		
Clathrin_F	Clathrin adaptor complexes medium subunit family protein (CHLATHRIN)	q-PCR	AGCATACACTGCGTGCAAAG		
Clathrin_R	Clathrin adaptor complexes medium subunit family protein (CHLATHRIN)	q-PCR	TCGCCTGTGTCACATATCTC		

Table S1. Primer and gene information used in this study. Related to Figure 2, Figure 4, Figure 5 and Figure 6.

6. Conclusion and Discussion

The coordinated expression and interaction of genes under specific biological contexts regulate growth and development. In Arabidopsis, approximately 6% of genes are transcription factors, with 9% being MYBs, playing a pivotal role in plant development, including secondary growth (Riechmann et al., 2000). Secondary growth involves the increase of plant thickness, as well as the presence of specialized cell types. This process is facilitated by two meristematic rings: the vascular cambium and the phellogen, also known as cork cambium. The study of secondary growth in trees is complex for several reasons such as the very long period of growth, the difficulty in creating transgenic lines, and the limited bioinformatic background. In this context, Arabidopsis has played a crucial role in advancing our understanding of secondary growth, including periderm development. Arabidopsis is an annual herbaceous plant that was previously considered not very comparable to long-lived woody perennial plants, such as forest trees (Wilkins et al., 2009). The main differences postulated between trees and herbaceous plants include the fact that Arabidopsis lacks a self-supporting structure, has a short lifespan, and exhibits general differences in secondary growth. Today, we know that Arabidopsis undergoes secondary growth and develops a well-organized and conserved periderm in hypocotyls, stems, and roots. The periderm in Arabidopsis roots exhibits the three characteristic layers of the periderm, which include an active phellogen layer in the middle, phellem inward, and a fully functional phellem with high deposition of suberin, lignin, and waxes. Despite the reduced number of periderm layers found in Arabidopsis, its anatomical structure is comparable to trees, making Arabidopsis a suitable model for studying periderm development. Additionally, in Arabidopsis roots, we can observe, with relative ease, the multiple stages of phellem differentiation, including cell wall suberization, cell expansion, and programmed cell death. We know, based on molecular evidence, that the early onset of phellem suberization takes place following phellogen (cork cambium) division (Leal et al., 2022). In our research, we extended this analysis by investigating suberin deposition along the Arabidopsis roots. During secondary growth, the upper part of the root shows more differentiation, and close to the endodermis, it is common to observe few or even a single differentiated cell, suggesting a gradual differentiation process. In this context, we suggest that phellem differentiation could be understood as both an increase in the amount of apoplastic barriers in the phellem cells and the rise of newly differentiated phellem cells along the periderm. This understanding would be useful in applying

this knowledge to specific plants of interest, where it is crucial to increase not only suberin in the phellem but also the rate of phellem differentiation.

Recent research has suggested that periderm regulators could be highly conserved among plant species, including Arabidopsis and tress. For instance, QsMYB1 in cork oak is homologue of MYB84 and MYB68 in Arabidopsis, and it has been proposed as a putative regulator of the periderm (Capote et al., 2018). Furthermore, in the study by Leal et al., 2022, a TRAP-SEQ study identified novel putative phellem regulators, including a significant number of MYB transcription factors, some of which were previously associated with suberin regulation. Interestingly, the dataset includes MYB84, MYB37, and MYB87, although specific roles were not suggested for any of them. These MYBs, along with MYB38, MYB68, and MYB36, constitute the MYB clade 14. In our research, we demonstrate that MYB68 and other MYBs from this clade regulate division by modulating the rate of phellem differentiation. This means that phellogen cells are capable of dividing until key regulators activate the phellem differentiation process. In our research, we identified MYB68 and other MYBs as central regulators of phellem differentiation, particularly associated with the establishment of the diffusion barriers. Surprisingly, we did not find evidence indicating a crucial role for the Casparian strip master regulator, MYB36, in phellem differentiation. Phellem differentiation is highly regulated, and any disruption in this equilibrium will change the balance of the periderm cells, resulting in a non-functional periderm. For instance, the specific overexpression of MYB68 in the phellogen and phellem using pPER15:MYB68-GR leads to a formation of a second or third layer of phellem. It's worth noting that the phenotypic changes in this line depend on when and how long this overexpression occurs. Early expression of MYB68 in the first periderm cells leads to more dramatic phenotypes and a reduction in the number of phellogen cells, which limits plant expansion. It appears that production of new potential phellem cells and the maturation of them are two independent processes. For example, in *myb37 myb38 myb68 myb84* quadruple mutants, the formation of the new phellem cells is not altered, but maturation in this line is delayed or, in some cases, not achieved at all. This suggests that both processes are independent but coordinated upstream by MYB68. For instance, MYB68, by itself, can induce over-suberization by the expression of suberin biosynthesis genes such as GPAT5, FAR4, HORST, and a significant number of suberin polymerizing enzymes, (GDSL/GELPs) (Ursache et al., 2021). Furthermore, in other plant species such as *Malus* x *domestica* cv. “Cox Orange Pippin,” it was shown that MdMYB68 can trigger the expression of gene clusters

associated with cell wall modification, including phenylpropanoid and suberin biosynthesis regulators. Interestingly, MdMYB68, in Nicotiana leaves, also induces the expression of a large number of orthologous GELP genes in Arabidopsis such as GELP38, GELP51, GELP72, and GELP96 (Xu et al., 2023). This clearly demonstrates the regulatory capacity of MYB68 in suberin regulation. The substantial increase in suberization resulting from the overexpression of MYB68 becomes evident when combining suberin-specific staining, such as fluorol yellow, with fluorescent and confocal microscopy. Furthermore, this process involves the rearrangement of the cell wall, leading to an increase in the size and a change in the shape of phellem cells. This suggests that MYB68 regulates not only suberin deposition in the phellem but also its expansion, potentially influencing two different developmental outcomes.

In addition to genes related to suberin and lignin, our research suggests that MYB68 regulation may extend to both the activation and repression of genes associated with meristematic activity. This regulatory mechanism aims to reduce the division capacity following phellogen division. Previously, WOX4 and BP were identified as phellogen regulators; the loss-of-function mutants of both showed a reduced number of phellogen cells (Xiao et al., 2020). In our research, it is evident that in the *myb68 myb84* double mutant, the number of phellogen cells increased, indicating a lack of differentiation. Interestingly, in *bp myb68 myb84* and *wox4 myb68 myb84* triple mutants, this increase was diminished. This implies that MYB68 and others from this clade might inhibit phellogen meristematic activity, possibly by reducing WOX4 and BP activity. Surprinsigly, MYB68 and MYB84 were not able to repress the expression of WOX and BP significantly. This could mean that MYB68 does not regulate directly WOX4 or BP, and there could be another player that, together with MYB68, regulates the reduction of meristematic activity. Moreover, we demonstrate that MYB68 is capable of promoting cell differentiation in other tissues. For example, when we overexpress MYB68 or MYB87 using a specific vascular cambium promoter (pPXY:MYB68-GR or pPXY:MYB87-GR), we observed a significant increase in the number of xylem vessels. It is important to mention that the increase in suberin can lead to changes in cell identity. For instance, MYB41 ectopic overexpression can induce suberization and changes in cell size and shape in Nicotiana leaves (Kosma et al., 2014). In the case of MYB68, we demonstrate that MYB68 is capable of promoting cell differentiation not only by increasing suberin deposition. For example, in the *myb41 myb53 myb92 myb93* quadruple mutant, which lacks suberin in the endodermis (Shukla et al., 2021), we observed contrasting effects compared to the *myb37 myb38*

myb68 myb84 mutant. The *myb41 myb53 myb92 myb93* quadruple mutant shows a similar phellem differentiation rate to Col-0; this is opposite to what happens in *myb37 myb38 myb68 myb84*, which exhibited a significant increase in phellogen and periderm cells, along with a notable reduction in phellem differentiation.

Furthermore, the regulation of meristematic activity by MYB68 and other members of this clade has not been elucidated yet. One explanation that we propose is the regulation of plant hormone concentrations within the cells by MYB68. Recent unpublished data from our lab suggests the possible role of hormones such as cytokinins in phellem differentiation. In addition, the specific expression of MYB68 in the phellogen and phellem using pPER15:MYB68-GR results in a significant downregulation of enzymes involved in cytokinin biosynthesis. Interestingly, we could observe this only when MYB68 is expressed in both phellem and phellogen. When MYB68 is overexpressed only in the phellem, we do not see a downregulation of any genes related to plant hormones. This suggests that the modulation of cytokinin levels might play a crucial role in phellem differentiation. Although the role of cytokinin in the periderm is not elucidated yet, it is known that in vascular development, it plays a pivotal role. Cytokinin in this context has two identified roles. First, it represses the formation of protoxylem, which is the part of the primary xylem that develops first, consisting of narrow, thin-walled cells and characterized by high auxin but also by low cytokinin responses. Second, it promotes periclinal division (De Rybel et al., 2016; Mähönen et al., 2006; Nieminen et al., 2015) The modulation of cytokinins by MYB68 could also explain the significant increase in the number of xylem vessels in pPXY:MYB68-GR or pPXY:MYB87-GR. In our context, it is highly plausible that a reduction in hormone biosynthesis might be necessary as a component of the differentiation program for the phellem, although further investigation is required to clarify this process.

On the other hand, the Arabidopsis root, as a periderm model, also facilitates the study of plant apoplastic barriers and its regulation in response to stresses or environmental cues. Recent data from our lab suggest that the Arabidopsis root periderm can respond to NaCl by increasing the rate of phellem differentiation and suberin deposition. Furthermore, it has been shown in Quercus that heat and drought stress lead to an upregulation of QsMYB1, enhaicing phellem differentiation (Almeida et al., 2013). This suggests that the phellem differentiation regulatory network may incorporate abiotic stress as triggering factors. This could imply that early phellem differentiation

serves as an emergency mechanism employed by plants to establish a barrier in response to stress. Previous research was mostly focused on how the alteration of periderm functionality, principally related to the capacity of suberin deposition, affects plant stability. This research was predominantly focused on potatoes. For example, in the phellem of potato tubers, the silencing of StCYP86A33, a suberin biosynthetic enzyme, leads to a significant reduction in suberin, mainly C18:1 diacids and ω-hydroxyacids monomers, increasing the water permeability due to changes is suberin deposition, and affecting the tuber resistance (Serra et al., 2009). In our research, we observed that overexpression of MYB4 under the ELTP promoter resulted in the collapse of the phellem barrier, increasing its permeability. MYB4 negatively regulates the expression of CINNAMATE 4-HYDROXYLASE (C4H), which is involved in the transformation of cinnamate into p-coumarate, the second step in the phenylpropanoid pathway. The specific overexpression of MYB4 leads to a dramatic reduction in aromatic monomers produced in the phenylpropanoid pathway, consequently reducing lignin and suberin monomers, which ultimately affects the establishment of the barrier (Andersen et al., 2021). This also highlights the pivotal participation of aromatic monomers produced in the phenylpropanoid pathway, which seems to be structurally necessary for the polymerization and accumulation of apoplastic barriers within cell walls. Furthermore, we demonstrate that both lignin and suberin are necessary for maintaining the functionality of the phellem. We propose that blocking the polymerization of either of them will impact phellem stability. For instance, in the *gelp22 gelp38 gelp51 gelp49 gelp9* quintuple mutant (Ursache et al., 2021), the drastic reduction in suberin deposition in the periderm significantly increases its permeability, affecting plant homeostasis. These findings also raise new questions, particularly regarding the sensing of environmental cues and the early activation of the phellem differentiation program in response to streses.

Finally, our research also focuses on understanding how apoplastic barriers are specifically formed in the phellem and the regulators that control this process. This process has been extensively studied in other plant organs, for example, the comprehension of the formation of Casparian strips in the endodermis. On the contrary, the precise lignification and suberization in the phellem remain a mystery. In Arabidopsis, the formation of Casparian strips, orchestrated by MYB36, involves the activation of the Schengen pathway, with key components including CIF2, SGN1, and SGN3 (Alassimone et al., 2016; Doblas et al., 2017; Fujita et al., 2020; Kamiya et al., 2015; Naseer et al., 2012). The analysis of how the Schengen components interact and coordinate the formation of

diffusion barriers in plant organs presents some complexity. In Arabidopsis, the presence of five ligand peptides (CIF1, CIF2, CIF3, CIF4, and TWS1), two receptor kinases (GSO1/SGN3 and GSO2), along with other participants in this pathway increases the possible scenarios about the specific roles and mechanisms in determined plant organs (Doblas et al., 2017; Doll et al., 2020; Fujita et al., 2020b; Nakayama et al., 2017; Truskina, Brück B, et al., 2022). Through extensive efforts in Arabidopsis, it is now relatively clear where the components of the Schengen pathway are expressed and how they interact and collaborate in the precise formation of Casparian strips, plant embryonic cuticle, and pollen grain cell walls. In our research, we propose that, in addition to the previously described processes, the Schengen pathway plays a role in the periderm. We show that the kinase receptors GSO1/SGN3 and GSO2, the protein kinase SGN1, and the ligand peptides CIF4 and TWS1 are expressed during secondary growth. Surprisingly, in the periderm context, the production of these ligands is not limited to one face of the periderm. For instance, TWS1 shows strong expression in the vasculature and the phellogen, while CIF4 expresses in the vasculature and cortex. Although both ligand peptides are expressed during secondary growth, it might not imply a redundant function. Furthermore, it is thought that RR-RKs GSO1/SGN3 and GSO2 have evolved specific peptide binding properties that allow them to specifically control several developmental processes in different plant organs. For example, in the endodermis, the exogenous application of TWS1 can induce early suberization in the endodermis, but with much lower efficiency than the one induced by CIF2 (Doll et al., 2020; Okuda et al., 2020; Truskina, Brück, et al., 2022). This could be the case for the periderm, in which both receptors and two ligands are present. In our research, we propose that the establishment of apoplastic barriers in the phellem could occur under two scenarios: first, in the onset of phellem differentiation, and second, as a surveillance mechanism to maintain the integrity of the barrier. We suggest that the establishment of a functional phellem involves a fine-tuned coordination between primary and secondary growth. This coordination is probably focused on a few specific cells in the onset of phellem differentiation and is coordinated by the Schengen pathway. Indeed, this was evident in the *gso1/sgn3 gso2* mutants, which could not establish regular apoplastic barriers and showed a delay in phellem differentiation. Additionally, Arabidopsis lines with defective production and polymerization of apoplastic barriers clearly show a specific phellem response. We observe similar responses to those triggered by the Schengen pathway in the endodermis. This reinforces the idea of an active surveillance system that monitors the phellem and is able to trigger responses to correct any issues.

In our analysis, we mostly focused on the role of GSO1 and GSO2 for diffusion barriers establishment, but we did not do a deep analysis in other aspects that could be involved in the plant defense. For instance, it has been recently shown that the GSO1/SGN3 receptor is also involved in cellular Na^+ extrusion. Salt stress enhances the specific accumulation of GSO1 in endodermal cells where the Casparian strip is either not formed or not completely established, mostly in the differentiation zone and in the meristematic zone (Chen et al., 2023). This accumulation activates two defense mechanisms. First, the Schengen pathway promotes the rapid establishment of Casparian strips. Second, GSO1 directly activates the SOS2-SOS1 module, a part of the Salt Overly Sensitive (SOS) pathway, to induce salt extrusion. It is believed that GSO1 triggers a cascade, including the phosphorylation of SOS2 and SOS1, facilitating cellular Na^+ detoxification. Interestingly, it is postulated that under this scenario, another uncharacterized family of peptides plays a role. These are the Salt-Induced Factors (SIF) peptides, and there is limited information about them (Chen et al., 2023). We can speculate that the periderm, as a barrier, probably not only regulates its apoplastic barriers as a defense mechanism but also other undescribed processes, such as salt extrusion, in order to maintain the homeostasis of the plant. This new perspectives open new questions regarding the capacity of the periderm to sense and respond. Understanding what influences and controls phellem differentiation is essential not only for plant breeding and enhancing plant resistance to stresses but also for exploring numerous biotechnological applications. These applications extend beyond conventional concerns to include opportunities for generating raw materials in a more intelligent and sustainable manner, or storing CO_2 in complex biopolymers such as suberin. For example, the Salk's Ideal Plants initiative aims to create bigger and more robust root systems capable of significantly storing CO_2 as suberin for much longer periods of time.

7. References

Alassimone, J., Fujita, S., Doblas, V. G., Van Dop, M., Barberon, M., Kalmbach, L., Vermeer, J. E. M., Rojas-Murcia, N., Santuari, L., Hardtke, C. S., & Geldner, N. (2016). Polarly localized kinase SGN1 is required for Casparian strip integrity and positioning. *Nature Plants*, *2*(8). https://doi.org/10.1038/NPLANTS.2016.113

Almeida, T., Pinto, G., Correia, B., Santos, C., & Gonçalves, S. (2013). QsMYB1 expression is modulated in response to heat and drought stresses and during plant recovery in Quercus suber. *Plant Physiology and Biochemistry*, *73*, 274–281. https://doi.org/10.1016/j.plaphy.2013.10.007

Andersen, T. G., Molina, D., Kilian, J., Franke, R. B., Ragni, L., & Geldner, N. (2021a). Tissue-Autonomous Phenylpropanoid Production Is Essential for Establishment of Root Barriers. *Current Biology*, *31*(5), 965-977.e5. https://doi.org/10.1016/j.cub.2020.11.070

Andersen, T. G., Molina, D., Kilian, J., Franke, R. B., Ragni, L., & Geldner, N. (2021b). Tissue-Autonomous Phenylpropanoid Production Is Essential for Establishment of Root Barriers. *Current Biology*, *31*(5), 965-977.e5. https://doi.org/10.1016/j.cub.2020.11.070

Barberon, M., & Geldner, N. (2014). Radial transport of nutrients: The plant root as a polarized epithelium1. *Plant Physiology*, *166*(2), 528–537. https://doi.org/10.1104/pp.114.246124

Barberon, M., Vermeer, J. E. M., De Bellis, D., Wang, P., Naseer, S., Andersen, T. G., Humbel, B. M., Nawrath, C., Takano, J., Salt, D. E., & Geldner, N. (2016). Adaptation of Root Function by Nutrient-Induced Plasticity of Endodermal Differentiation. *Cell*, *164*(3), 447–459. https://doi.org/10.1016/j.cell.2015.12.021

Barra-Jiménez, A., & Ragni, L. (2017). Secondary development in the stem: when Arabidopsis and trees are closer than it seems. In *Current Opinion in Plant Biology* (Vol. 35, pp. 145–151). Elsevier Ltd. https://doi.org/10.1016/j.pbi.2016.12.002

Beeckman, T., & De Smet, I. (2014, May 19). Pericycle. *Current Biology*, *24*(10). https://doi.org/10.1016/j.cub.2014.03.031

Belsson, F., Li, Y., Bonaventura, G., Pollard, M., & Ohlrogge, J. B. (2007). The acyltransferase GPAT5 is required for the synthesis of suberin in seed coat and root of Arabidopsis. *Plant Cell*, *19*(1), 351–368. https://doi.org/10.1105/tpc.106.048033

Bernards, M. A. (2002). Demystifying suberin. In *Canadian Journal of Botany* (Vol. 80, Issue 3, pp. 227–240). https://doi.org/10.1139/b02-017

Boerjan, W., Ralph, J., & Baucher, M. (2003). Lignin Biosynthesis. In *Annual Review of Plant Biology* (Vol. 54, pp. 519–546). https://doi.org/10.1146/annurev.arplant.54.031902.134938

Boher, P., Serra, O., Soler, M., Molinas, M., & Figueras, M. (2013). The potato suberin feruloyl transferase FHT which accumulates in the phellogen is induced by wounding and regulated by abscisic and salicylic acids. *Journal of Experimental Botany*, *64*(11), 3225–3236. https://doi.org/10.1093/jxb/ert163

Butenko, M. A., Patterson, S. E., Grini, P. E., Stenvik, G. E., Amundsen, S. S., Mandal, A., & Aalen, R. B. (2003). INFLORESCENCE DEFICIENT in ABSCISSION Controls Floral Organ Abscission in Arabidopsis and Identifies a Novel Family of Putative Ligands in Plants. *Plant Cell*, *15*(10), 2296–2307. https://doi.org/10.1105/tpc.014365

Campilho, A., Nieminen, K., & Ragni, L. (2020). The development of the periderm: the final frontier between a plant and its environment. In *Current Opinion in Plant Biology* (Vol. 53, pp. 10–14). Elsevier Ltd. https://doi.org/10.1016/j.pbi.2019.08.008

Capote, T., Barbosa, P., Usié, A., Ramos, A. M., Inácio, V., Ordás, R., Gonçalves, S., & Morais-Cecílio, L. (2018). ChIP-Seq reveals that QsMYB1 directly targets genes involved in lignin and suberin biosynthesis pathways in cork oak (Quercus suber). *BMC Plant Biology*, *18*(1). https://doi.org/10.1186/s12870-018-1403-5

Chen, C., He, G., Li, J., Perez-Hormaeche, J., Becker, T., Luo, M., Wallrad, L., Gao, J., Li, J., Pardo, J. M., Kudla, J., & Guo, Y. (2023). A salt stress-activated GSO1-SOS2-SOS1 module protects the

Arabidopsis root stem cell niche by enhancing sodium ion extrusion . *The EMBO Journal*, *42*(13). https://doi.org/10.15252/embj.2022113004
Coen, O., Lu, J., Xu, W., De Vos, D., Péchoux, C., Domergue, F., Grain, D., Lepiniec, L., & Magnani, E. (2019). Deposition of a cutin apoplastic barrier separating seed maternal and zygotic tissues. *BMC Plant Biology*, *19*(1). https://doi.org/10.1186/s12870-019-1877-9
Cohen, H., Fedyuk, V., Wang, C., Wu, S., & Aharon, A. (2020). An MYB-family transcription factor with suber powers. *Plant Journal*, *102*(3), 429–430. https://doi.org/10.1111/tpj.14785
Cominelli, E., Sala, T., Calvi, D., Gusmaroli, G., & Tonelli, C. (2008). Over-expression of the Arabidopsis AtMYB41 gene alters cell expansion and leaf surface permeability. *Plant Journal*, *53*(1), 53–64. https://doi.org/10.1111/j.1365-313X.2007.03310.x
Creff, A., Brocard, L., Joubès, J., Taconnat, L., Doll, N. M., Marsollier, A. C., Pascal, S., Galletti, R., Boeuf, S., Moussu, S., Widiez, T., Domergue, F., & Ingram, G. (2019). A stress-response-related inter-compartmental signalling pathway regulates embryonic cuticle integrity in Arabidopsis. *PLoS Genetics*, *15*(4). https://doi.org/10.1371/journal.pgen.1007847
De Rybel, B., Mähönen, A. P., Helariutta, Y., & Weijers, D. (2016). Plant vascular development: From early specification to differentiation. In *Nature Reviews Molecular Cell Biology* (Vol. 17, Issue 1, pp. 30–40). Nature Publishing Group. https://doi.org/10.1038/nrm.2015.6
Doblas, V. G., Smakowska-Luzan, E., Fujita, S., Alassimone, J., Barberon, M., Madalinski, M., Belkhadir, Y., & Geldner, N. (2017). Root diffusion barrier control by a vasculature-derived peptide binding to the SGN3 receptor. *Science*, *355*(6322), 280–284. https://www.science.org
Doll, N. M., Royek, S., Fujita, S., Okuda, S., Chamot, S., Stintzi, A., Widiez, T., Hothorn, M., Schaller, A., Geldner, N., & Ingram, G. (2020). A two-way molecular dialogue between embryo and endosperm is required for seed development. *Science*, *367*(6476), 431–435. https://www.science.org
Dubos, C., Stracke, R., Grotewold, E., Weisshaar, B., Martin, C., & Lepiniec, L. (2010). MYB transcription factors in Arabidopsis. In *Trends in Plant Science* (Vol. 15, Issue 10, pp. 573–581). https://doi.org/10.1016/j.tplants.2010.06.005
Evert, R. (2006). Chapter Fifteen - Periderm. In *Esau's Plant Anatomy: Meristems, Cells, and Tissues of the Plant Body: Their Structure, Function, and Development* (Vol. 1, pp. 427–446).
Fagerstedt, K. V., Saranpää, P., Tapanila, T., Immanen, J., Serra, J. A. A., & Nieminen, K. (2015). Determining the composition of lignins in different tissues of silver birch. *Plants*, *4*(2), 183–195. https://doi.org/10.3390/plants4020183
Farvardin, A., González-hernández, A. I., Llorens, E., García-agustín, P., Scalschi, L., & Vicedo, B. (2020). The apoplast: A key player in plant survival. In *Antioxidants* (Vol. 9, Issue 7, pp. 1–26). MDPI. https://doi.org/10.3390/antiox9070604
Feng, C., Andreasson, E., Maslak, A., Mock, H. P., Mattsson, O., & Mundy, J. (2004). Arabidopsis MYB68 in development and responses to environmental cues. *Plant Science*, *167*(5), 1099–1107. https://doi.org/10.1016/j.plantsci.2004.06.014
Fischer, U., Kucukoglu, M., Helariutta, Y., & Bhalerao, R. P. (2019). The Dynamics of Cambial Stem Cell Activity. *Annu. Rev. Plant Biol*, *70*, 293–319. https://doi.org/10.1146/annurev-arplant-050718
Fiume, E., Guyon, V., Remoué, C., Magnani, E., Miquel, M., Grain, D., & Lepiniec, L. (2016). TWS1, a novel small protein, regulates various aspects of seed and plant development. *Plant Physiology*, *172*(3), 1732–1745. https://doi.org/10.1104/pp.16.00915
Franke, R., & Schreiber, L. (2007). Suberin - a biopolyester forming apoplastic plant interfaces. In *Current Opinion in Plant Biology* (Vol. 10, Issue 3, pp. 252–259). https://doi.org/10.1016/j.pbi.2007.04.004
Fraser, C. M., & Chapple, C. (2011). The Phenylpropanoid Pathway in Arabidopsis. *The Arabidopsis Book*, *9*, e0152. https://doi.org/10.1199/tab.0152
Fujita, S., De Bellis, D., Edel, K. H., Köster, P., Andersen, T. G., Schmid-Siegert, E., Dénervaud Tendon, V., Pfister, A., Marhavý, P., Ursache, R., Doblas, V. G., Barberon, M., Daraspe, J., Creff, A., Ingram, G., Kudla, J., & Geldner, N. (2020a). SCHENGEN receptor module drives localized ROS production and lignification in plant roots . *The EMBO Journal*, *39*(9). https://doi.org/10.15252/embj.2019103894

Fujita, S., De Bellis, D., Edel, K. H., Köster, P., Andersen, T. G., Schmid-Siegert, E., Dénervaud Tendon, V., Pfister, A., Marhavý, P., Ursache, R., Doblas, V. G., Barberon, M., Daraspe, J., Creff, A., Ingram, G., Kudla, J., & Geldner, N. (2020b). SCHENGEN receptor module drives localized ROS production and lignification in plant roots . *The EMBO Journal*, *39*(9). https://doi.org/10.15252/embj.2019103894

Gao, Y.-Q., Huang, J.-Q., Reyt, G., Song, T., Love, A., Tiemessen, D., Xue, P.-Y., Wu, W.-K., George, M. W., Chen, X.-Y., Chao, D.-Y., Castrillo, G., & Salt, D. E. (2023). A dirigent protein complex directs lignin polymerization and assembly of the root diffusion barrier. *Science*, *382*, 464–471. https://www.science.org

Geldner, N. (2013). The endodermis. In *Annual Review of Plant Biology* (Vol. 64, pp. 531–558). https://doi.org/10.1146/annurev-arplant-050312-120050

Gou, M., Hou, G., Yang, H., Zhang, X., Cai, Y., Kai, G., & Liu, C. J. (2017). The MYB107 transcription factor positively regulates suberin biosynthesis. *Plant Physiology*, *173*(2), 1045–1058. https://doi.org/10.1104/pp.16.01614

Graça, J. (2015). Suberin: The biopolyester at the frontier of plants. In *Frontiers in Chemistry* (Vol. 3, Issue OCT). Frontiers Media S. A. https://doi.org/10.3389/fchem.2015.00062

Höfer, R., Briesen, I., Beck, M., Pinot, F., Schreiber, L., & Franke, R. (2008). The Arabidopsis cytochrome P450 CYP86A1 encodes a fatty acid ω-hydroxylase involved in suberin monomer biosynthesis. *Journal of Experimental Botany*, *59*(9), 2347–2360. https://doi.org/10.1093/jxb/ern101

Inácio, V., Lobato, C., Graça, J., & Morais-Cecílio, L. (2021). Cork cells in cork oak periderms undergo programmed cell death and proanthocyanidin deposition. *Tree Physiology*, *41*(9), 1701–1713. https://doi.org/10.1093/treephys/tpab031

Inácio, V., Martins, M. T., Graça, J., & Morais-Cecílio, L. (2018). Cork oak young and traumatic periderms show pcd typical chromatin patterns but different chromatin-modifying genes expression. *Frontiers in Plant Science*, *9*. https://doi.org/10.3389/fpls.2018.01194

Jiang, C., Gu, X., & Peterson, T. (2004). Identification of conserved gene structures and carboxy-terminal motifs in the Myb gene family of Arabidopsis and Oryza sativa L. ssp. indica. *Genome Biology*, *5*(7), 46. http://genomebiology.com/2004/5/7/R46

Jia, T., Zhang, K., Li, F., Huang, Y., Fan, M., & Huang, T. (2020). The AtMYB2 inhibits the formation of axillary meristem in Arabidopsis by repressing RAX1 gene under environmental stresses. *Plant Cell Reports*, *39*(12), 1755–1765. https://doi.org/10.1007/s00299-020-02602-3

Jinn, T.-L., Stone, J. M., & Walker, J. C. (2000). HAESA, an Arabidopsis leucine-rich repeat receptor kinase, controls floral organ abscission. *Genes & Development*, *14*, 108–117. www.genesdev.org

Kamiya, T., Borghi, M., Wang, P., Danku, J. M. C., Kalmbach, L., Hosmani, P. S., Naseer, S., Fujiwara, T., Geldner, N., & Salt, D. E. (2015a). The MYB36 transcription factor orchestrates Casparian strip formation. *Proceedings of the National Academy of Sciences of the United States of America*, *112*(33), 10533–10538. https://doi.org/10.1073/pnas.1507691112

Keller, T., Abbott, J., Moritz, T., & Doerner, P. (2006). Arabidopsis REGULATOR OF AXILLARY MERISTEMS1 controls a leaf axil stem cell niche and modulates vegetative development. *Plant Cell*, *18*(3), 598–611. https://doi.org/10.1105/tpc.105.038588

Ki Cho, S., Larue, C. T., Chevalier, D., Wang, H., Jinn, T.-L., Zhang, S., & Walker, J. C. (2008). Regulation of floral organ abscission in Arabidopsis thaliana. In *PLANT BIOLOGY* (Vol. 105).

Kolattukudy, P. E. (1980). Biopolyester Membranes of Plants:Cutin and Suberin. *Science*, *30*(30), 990–1000.

Komori, R., Amano, Y., Ogawa-Ohnishi, M., & Matsubayashi, Y. (2009). Identification of tyrosylprotein sulfotransferase in Arabidopsis. *Proceedings of the National Academy of Sciences (PNAS)*, *106*(35), 15067–15072. www.pnas.org/cgi/content/full/

Kosma, D. K., Murmu, J., Razeq, F. M., Santos, P., Bourgault, R., Molina, I., & Rowland, O. (2014). AtMYB41 activates ectopic suberin synthesis and assembly in multiple plant species and cell types. *Plant Journal*, *80*(2), 216–229. https://doi.org/10.1111/tpj.12624

Kranz, H. D., Denekamp, M., Greco, R., Jin, H., Leyva, A., Meissner, R. C., Petroni, K., Urzainqui, A., Bevan, M., Martin, C., Smeekens, S., Tonelli, C., Paz-Ares, J., & Weisshaar, B. (1998). Towards

functional characterisation of the members of the R2R3-MYB gene family from Arabidopsis thaliana. *Plant Journal*, *16*(2), 263–276. https://doi.org/10.1046/j.1365-313X.1998.00278.x

Lashbrooke, J., Cohen, H., Levy-Samocha, D., Tzfadia, O., Panizel, I., Zeisler, V., Massalha, H., Stern, A., Trainotti, L., Schreiber, L., Costa, F., & Aharoni, A. (2016). MYB107 and MYB9 homologs regulate suberin deposition in angiosperms. *Plant Cell*, *28*(9), 2097–2116. https://doi.org/10.1105/tpc.16.00490

Leal, A. R., Barros, P. M., Parizot, B., Sapeta, H., Vangheluwe, N., Andersen, T. G., Beeckman, T., & Oliveira, M. M. (2022). Translational profile of developing phellem cells in Arabidopsis thaliana roots. *Plant Journal*, *110*(3), 899–915. https://doi.org/10.1111/tpj.15691

Lee, Y., Yoon, T. H., Lee, J., Jeon, S. Y., Lee, J. H., Lee, M. K., Chen, H., Yun, J., Oh, S. Y., Wen, X., Cho, H. K., Mang, H., & Kwak, J. M. (2018a). A Lignin Molecular Brace Controls Precision Processing of Cell Walls Critical for Surface Integrity in Arabidopsis. *Cell*, *173*(6), 1468-1480.e9. https://doi.org/10.1016/j.cell.2018.03.060

Lee, Y., Yoon, T. H., Lee, J., Jeon, S. Y., Lee, J. H., Lee, M. K., Chen, H., Yun, J., Oh, S. Y., Wen, X., Cho, H. K., Mang, H., & Kwak, J. M. (2018b). A Lignin Molecular Brace Controls Precision Processing of Cell Walls Critical for Surface Integrity in Arabidopsis. *Cell*, *173*(6), 1468-1480.e9. https://doi.org/10.1016/j.cell.2018.03.060

Liberman, L. M., Sparks, E. E., Moreno-Risueno, M. A., Petricka, J. J., & Benfey, P. N. (2015). MYB36 regulates the transition from proliferation to differentiation in the Arabidopsis root. *Proceedings of the National Academy of Sciences of the United States of America*, *112*(39), 12099–12104. https://doi.org/10.1073/pnas.1515576112

Li, P., Yu, Q., Gu, X., Xu, C., Qi, S., Wang, H., Zhong, F., Baskin, T. I., Rahman, A., & Wu, S. (2018). Construction of a Functional Casparian Strip in Non-endodermal Lineages Is Orchestrated by Two Parallel Signaling Systems in Arabidopsis thaliana. *Current Biology*, *28*(17), 2777-2786.e2. https://doi.org/10.1016/j.cub.2018.07.028

Liu, J., Osbourn, A., & Ma, P. (2015). MYB transcription factors as regulators of phenylpropanoid metabolism in plants. In *Molecular Plant* (Vol. 8, Issue 5, pp. 689–708). Cell Press. https://doi.org/10.1016/j.molp.2015.03.012

Mahmood, K., Zeisler-Diehl, V. V., Schreiber, L., Bi, Y. M., Rothstein, S. J., & Ranathunge, K. (2019). Overexpression of ANAC046 promotes suberin biosynthesis in roots of arabidopsis Thaliana. *International Journal of Molecular Sciences*, *20*(24). https://doi.org/10.3390/ijms20246117

Mähönen, A. P., Higuchi, M., Törmäkangas, K., Miyawaki, K., Pischke, M. S., Sussman, M. R., Helariutta, Y., & Kakimoto, T. (2006). Cytokinins Regulate a Bidirectional Phosphorelay Network in Arabidopsis. *Current Biology*, *16*(11), 1116–1122. https://doi.org/10.1016/j.cub.2006.04.030

Mattinen, M. L., Filpponen, I., Järvinen, R., Li, B., Kallio, H., Lektinen, P., & Argyropoulos, D. (2009). Structure of the polyphenolic component of suberin isolated from potato (Solanum tuberosum war. Nikola). *Journal of Agricultural and Food Chemistry*, *57*(20), 9747–9753. https://doi.org/10.1021/jf9020834

Molina, I., Li-Beisson, Y., Beisson, F., Ohlrogge, J. B., & Pollard, M. (2009). Identification of an Arabidopsis feruloyl-coenzyme a transferase required for suberin synthesis. *Plant Physiology*, *151*(3), 1317–1328. https://doi.org/10.1104/pp.109.144907

Müller, D., Schmitz, G., & Theres, K. (2006). Blind homologous R2R3 Myb genes control the pattern of lateral meristem initiation in Arabidopsis. *Plant Cell*, *18*(3), 586–597. https://doi.org/10.1105/tpc.105.038745

Nakayama, T., Shinohara, H., Tanaka, M., Baba, K., Ogawa-Ohnishi, M., & Matsubayashi, Y. (2017). A peptide hormone required for Casparian strip diffusion barrier formation in Arabidopsis roots. *Science*, *355*(6322), 284–286. https://doi.org/10.1126/science.aai9057

Naseer, S., Lee, Y., Lapierre, C., Franke, R., Nawrath, C., & Geldner, N. (2012). Casparian strip diffusion barrier in Arabidopsis is made of a lignin polymer without suberin. *Proceedings of the National Academy of Sciences of the United States of America*, *109*(25), 10101–10106. https://doi.org/10.1073/pnas.1205726109

Nawrath, C., Schreiber, L., Franke, R. B., Geldner, N., Reina-Pinto, J. J., & Kunst, L. (2013). Apoplastic

Diffusion Barriers in Arabidopsis. *The Arabidopsis Book*, *11*, e0167. https://doi.org/10.1199/tab.0167

Nieminen, K., Blomster, T., Helariutta, Y., & Mähönen, A. P. (2015). Vascular Cambium Development. *The Arabidopsis Book*, *13*, e0177. https://doi.org/10.1199/tab.0177

Nomberg, G., Marinov, O., Arya, G. C., Manasherova, E., & Cohen, H. (2022). The Key Enzymes in the Suberin Biosynthetic Pathway in Plants: An Update. In *Plants* (Vol. 11, Issue 3). MDPI. https://doi.org/10.3390/plants11030392

Okuda, S., Fujita, S., Moretti, A., Hohmann, U., Doblas, V. G., Ma, Y., Pfister, A., Brandt, B., Geldner, N., & Hothorn, M. (2020). Molecular mechanism for the recognition of sequence-divergent CIF peptides by the plant receptor kinases GSO1/SGN3 and GSO2. *Proceedings of the National Academy of Sciences (PNAS)*, *117*(5), 2693–2703. https://doi.org/10.1073/pnas.1911553117/-/DCSupplemental

Pfister, A., Barberon, M., Alassimone, J., Kalmbach, L., Lee, Y., Vermeer, J. E. M., Yamazaki, M., Li, G., Maurel, C., Takano, J., Kamiya, T., Salt, D. E., Roppolo, D., & Geldner, N. (2014). A receptor-like kinase mutant with absent endodermal diffusion barrier displays selective nutrient homeostasis defects. *ELife*, *3*, e03115. https://doi.org/10.7554/eLife.03115

Pollard, M., Beisson, F., Li, Y., & Ohlrogge, J. B. (2008). Building lipid barriers: biosynthesis of cutin and suberin. In *Trends in Plant Science* (Vol. 13, Issue 5, pp. 236–246). https://doi.org/10.1016/j.tplants.2008.03.003

Raes, J., Rohde, A., Christensen, J. H., Van De Peer, Y., & Boerjan, W. (2003). Genome-Wide Characterization of the Lignification Toolbox in Arabidopsis. *Plant Physiology*, *133*(3), 1051–1071. https://doi.org/10.1104/pp.103.026484

Ragni, L., & Greb, T. (2018). Secondary growth as a determinant of plant shape and form. In *Seminars in Cell and Developmental Biology* (Vol. 79, pp. 58–67). Elsevier Ltd. https://doi.org/10.1016/j.semcdb.2017.08.050

Reyt, G., Ramakrishna, P., Salas-González, I., Fujita, S., Love, A., Tiemessen, D., Lapierre, C., Morreel, K., Calvo-Polanco, M., Flis, P., Geldner, N., Boursiac, Y., Boerjan, W., George, M. W., Castrillo, G., & Salt, D. E. (2021). Two chemically distinct root lignin barriers control solute and water balance. *Nature Communications*, *12*(1). https://doi.org/10.1038/s41467-021-22550-0

Riechmann, J. L., Heard, J., Martin, G., Reuber, L., Jiang, C.-Z., Keddie, J., Adam, L., Pineda, O., Ratcliffe, O. J., Samaha, R. R., Creelman, R., Pilgrim, M., Broun, P., Zhang, J. Z., Ghandehari, D., Sherman, B. K., & Yu, G.-L. (2000). Arabidopsis Transcription Factors: Genome-Wide Comparative Analysis Among Eukaryotes. *Science*, *290*, 2105–2110. https://www.science.org

Rohde, A., Morreel, K., Ralph, J., Goeminne, G., Hostyn, V., De Rycke, R., Kushnir, S., Van Doorsselaere, J., Joseleau, J. P., Vuylsteke, M., Van Driessche, G., Van Beeumen, J., Messens, E., & Boerjan, W. (2004). Molecular phenotyping of the pal1 and pal2 mutants of Arabidopsis thaliana reveals far-reaching consequences on phenylpropanoid, amino acid, and carbohydrate metabolism. *Plant Cell*, *16*(10), 2749–2771. https://doi.org/10.1105/tpc.104.023705

Rojas-Murcia, N., Hématy, K., Lee, Y., Emonet, A., Ursache, R., Fujita, S., De Bellis, D., & Geldner, N. (2020). High-order mutants reveal an essential requirement for peroxidases but not laccases in Casparian strip lignification. *Proceedings of the National Academy of Sciences of the United States of America*, *117*(46), 29166–29177. https://doi.org/10.1073/pnas.2012728117/-/DCSupplemental

Sangha, A. K., Parks, J. M., Standaert, R. F., Ziebell, A., Davis, M., & Smith, J. C. (2012). Radical coupling reactions in lignin synthesis: A density functional theory study. *Journal of Physical Chemistry B*, *116*(16), 4760–4768. https://doi.org/10.1021/jp2122449

Schalk, M., Cabello-Hurtado, F., Pierrel, M.-A., Atanossova, R., Saindrenan, P., & Werck-Reichhart, D. (1998). Piperonylic Acid, a Selective, Mechanism-Based Inactivator of the trans-Cinnamate 4-Hydroxylase: A New Tool to Control the Flux of Metabolites in the Phenylpropanoid Pathway 1. *Plant Physiology*, *118*, 209–218. https://academic.oup.com/plphys/article/118/1/209/6085572

Schreiber, L., Franke, R., & Hartmann, K. (2005). Wax and suberin development of native and wound periderm of potato (Solanum tuberosum L.) and its relation to peridermal transpiration. *Planta*, *220*(4), 520–530. https://doi.org/10.1007/s00425-004-1364-9

Serra, O., & Geldner, N. (2022). The making of suberin. In *New Phytologist* (Vol. 235, Issue 3, pp. 848–866). John Wiley and Sons Inc. https://doi.org/10.1111/nph.18202

Serra, O., Mähönen, A. P., Hetherington, A. J., & Ragni, L. (2022a). The Making of Plant Armor: The Periderm. *Annual Review of Plant Biology*, *73*, 405–432. https://doi.org/10.1146/annurev-arplant-102720

Serra, O., Mähönen, A. P., Hetherington, A. J., & Ragni, L. (2022b). The Making of Plant Armor: The Periderm. *Annual Review OfPlant Biology*, *73*, 405–432. https://doi.org/10.1146/annurev-arplant-102720

Serra, O., Soler, M., Hohn, C., Sauveplane, V., Pinot, F., Franke, R., Schreiber, L., Prat, S., Molinas, M., & Figueras, M. (2009). CYP86A33-targeted gene silencing in potato tuber alters suberin composition, distorts suberin lamellae, and impairs the periderm's water barrier function. *Plant Physiology*, *149*(2), 1050–1060. https://doi.org/10.1104/pp.108.127183

Sexauer, M., Shen, D., Schön, M., Andersen, T. G., & Markmann, K. (2021). Visualizing polymeric components that define distinct root barriers across plant lineages. *Development (Cambridge)*, *148*(23). https://doi.org/10.1242/dev.199820

Shukla, V., Han, J.-P., Cléard, F., Lefebvre-Legendre, L., Gully, K., Flis, P., Berhin, A., Andersen, T. G., Salt, D. E., Nawrath, C., & Barberon, M. (2021). Suberin plasticity to developmental and exogenous cues is regulated by a set of MYB transcription factors. *Proceedings of the National Academy of Sciences of the United States of America*, *118*(39), 1–10. https://doi.org/10.1073/pnas.2101730118/-/DCSupplemental

Stracke, R., Werber, M., & Weisshaar, B. (2001). The R2R3-MYB gene family in Arabidopsis thaliana. *Current Opinion in Plant Biology*, *4*, 447–456.

Thangave, T., Tegg, R. S., & Wilson, C. R. (2016). Toughing it out-disease-resistant potato mutants have enhanced tuber skin defenses. *Phytopathology*, *106*(5), 474–483. https://doi.org/10.1094/PHYTO-08-15-0191-R

To, A., Joubès, J., Thueux, J., Kazaz, S., Lepiniec, L., & Baud, S. (2020). AtMYB92 enhances fatty acid synthesis and suberin deposition in leaves of Nicotiana benthamiana. *Plant Journal*, *103*(2), 660–676. https://doi.org/10.1111/tpj.14759

Tobimatsu, Y., & Schuetz, M. (2019). Lignin polymerization: how do plants manage the chemistry so well? In *Current Opinion in Biotechnology* (Vol. 56, pp. 75–81). Elsevier Ltd. https://doi.org/10.1016/j.copbio.2018.10.001

Truskina, J., Bruck B, S., Stintzi, A., Boeuf, S., Doll, N. M., Fujita, S., Geldner, N., Schaller, A., & Ingram, G. C. (2022). A peptide-mediated, multilateral molecular dialogue for the coordination of pollen wall formation. *Proceedings of the National Academy of Sciences* , *119*(22), 1–10. https://doi.org/10.1073/pnas

Ursache, R., Andersen, T. G., Marhavý, P., & Geldner, N. (2018). A protocol for combining fluorescent proteins with histological stains for diverse cell wall components. *Plant Journal*, *93*(2), 399–412. https://doi.org/10.1111/tpj.13784

Ursache, R., De Jesus Vieira Teixeira, C., Dénervaud Tendon, V., Gully, K., De Bellis, D., Schmid-Siegert, E., Grube Andersen, T., Shekhar, V., Calderon, S., Pradervand, S., Nawrath, C., Geldner, N., & Vermeer, J. E. M. (2021). GDSL-domain proteins have key roles in suberin polymerization and degradation. *Nature Plants*, *7*(3), 353–364. https://doi.org/10.1038/s41477-021-00862-9

Vanholme, R., De Meester, B., Ralph, J., & Boerjan, W. (2019). Lignin biosynthesis and its integration into metabolism. In *Current Opinion in Biotechnology* (Vol. 56, pp. 230–239). Elsevier Ltd. https://doi.org/10.1016/j.copbio.2019.02.018

Vishwanath, S. J., Delude, C., Domergue, F., & Rowland, O. (2015). Suberin: biosynthesis, regulation, and polymer assembly of a protective extracellular barrier. In *Plant Cell Reports* (Vol. 34, Issue 4, pp. 573–586). Springer Verlag. https://doi.org/10.1007/s00299-014-1727-z

Vogt, T. (2010). Phenylpropanoid biosynthesis. In *Molecular Plant* (Vol. 3, Issue 1, pp. 2–20). Oxford University Press. https://doi.org/10.1093/mp/ssp106

Weijers, D., Nemhauser J., & Yang Z. (2018). Auxin: small molecule, big impact. *Journal of Experimental Botany*, *69*(2), 133–136. https://academic.oup.com/jxb/article/69/2/133/4788745

Weng, J. K., & Chapple, C. (2010). The origin and evolution of lignin biosynthesis. In *New Phytologist* (Vol. 187, Issue 2, pp. 273–285). https://doi.org/10.1111/j.1469-8137.2010.03327.x

Wilkins, O., Nahal, H., Foong, J., Provart, N. J., & Campbell, M. M. (2009a). Expansion and diversification of the Populus R2R3-MYB family of transcription factors. *Plant Physiology*, *149*(2), 981–993. https://doi.org/10.1104/pp.108.132795

Wilkins, O., Nahal, H., Foong, J., Provart, N. J., & Campbell, M. M. (2009b). Expansion and diversification of the Populus R2R3-MYB family of transcription factors. *Plant Physiology*, *149*(2), 981–993. https://doi.org/10.1104/pp.108.132795

Wunderling, A., Ripper, D., Barra-Jimenez, A., Mahn, S., Sajak, K., Targem, M. Ben, & Ragni, L. (2018). A molecular framework to study periderm formation in Arabidopsis. *New Phytologist*, *219*(1), 216–229. https://doi.org/10.1111/nph.15128

Wu, Y., Wen, J., Xia, Y., Zhang, L., & Du, H. (2022). Evolution and functional diversification of R2R3-MYB transcription factors in plants. In *Horticulture Research* (Vol. 9). Oxford University Press. https://doi.org/10.1093/hr/uhac058

Xiao, W., Molina, D., Wunderling, A., Ripper, D., Vermeer, J. E. M., & Ragni, L. (2020). Pluripotent Pericycle Cells Trigger Different Growth Outputs by Integrating Developmental Cues into Distinct Regulatory Modules. *Current Biology*, *30*(22), 4384-4398.e5. https://doi.org/10.1016/j.cub.2020.08.053

Xu, X., Guerriero, G., Domergue, F., Beine-Golovchuk, O., Cocco, E., Berni, R., Sergeant, K., Hausman, J. F., & Legay, S. (2023). Characterization of MdMYB68, a suberin master regulator in russeted apples. *Frontiers in Plant Science*, *14*. https://doi.org/10.3389/fpls.2023.1143961

Yonghua Li, Fred Beisson, Abraham J. K. Koo, Isabel Molina, Mike Pollard, & John Ohlrogge. (2007). Identification of acyltransferases required for cutin biosynthesis and production of cutin with suberin-like monomers. *Proceedings of the National Academy of Sciences*, *104*(46), 18339–18344.

Zhang, B., Xin, B., Sun, X., Chao, D., Zheng, H., Peng, L., Chen, X., Zhang, L., Yu, J., Ma, D., & Xia, J. (2023). Small peptide signaling via OsCIF1/2 mediates Casparian strip formation at the root endodermal and nonendodermal cell layers in rice. *The Plant Cell*. https://doi.org/10.1093/plcell/koad269

Zhang, J., Eswaran, G., Alonso-Serra, J., Kucukoglu, M., Xiang, J., Yang, W., Elo, A., Nieminen, K., Damén, T., Joung, J. G., Yun, J. Y., Lee, J. H., Ragni, L., Barbier de Reuille, P., Ahnert, S. E., Lee, J. Y., Mähönen, A. P., & Helariutta, Y. (2019). Transcriptional regulatory framework for vascular cambium development in Arabidopsis roots. *Nature Plants*, *5*(10), 1033–1042. https://doi.org/10.1038/s41477-019-0522-9

8. Acknowledgements

I would like to extend my heartfelt gratitude to all the individuals who played a significant role in this project, with special recognition to Prof. Laura Ragni for offering me the opportunity to be a part of her group. I am also deeply thankful for the valuable contributions, discussions, and assistance provided by Dagmar, Wei, Sara, Hengqi, Noah, and every member of the group. I also would like to thank my TAQ members Prof. Marja Timmermans and Prof. Chang Liu. I would like to extend my thanks to all the members of ZMBP for their invaluable assistance and support. I am especially grateful to Dr. Rochus Franke for introducing me to the fascinating world of apoplastic barriers

My appreciation also extends to my family and friends for their unwavering support throughout this endeavor. Last but certainly not least, I want to express my profound gratitude to my wife, Gaby, for her constant support, invaluable help, and engaging discussions.